



Holtec Center, 555 Lincoln Drive West, Marlton, NJ 08053

Telephone (856) 797-0900

Fax (856) 797-0909

TOPICAL REPORT ON HI-STAR AND HI-STORM 100 SYSTEM DEPLOYMENT

AT HIGH ZPA ISFSI SITES

Holtec Report No. HI-982004

Holtec Project No. 71178

Report Category: A

Report Class: Safety Related

NON-PROPRIETARY VERSION

COMPANY PRIVATE

This document has all proprietary information removed and has replaced those sections, figures, and tables with highlighting and/or notes to designate the removal of such information. This document is the property of Holtec International and its Client. It is to be used only in connection with the performance of work by Holtec International or its designated subcontractors. Reproduction, publication, or presentation, in whole or in part, for any other purpose by any party other than the Client is expressly forbidden.



Holtec Center, 555 Lincoln Drive West, Marlton, NJ 08053
 Telephone (609) 797- 090
 Fax (609) 797 - 090

QA AND ADMINISTRATIVE INFORMATION LOC

(To Be Filled In By the Principal Author of the Document and Placed After the Title Page)

Document No HI-982004	CATEGORY: <input type="checkbox"/> Generic <input checked="" type="checkbox"/> Project Specific						
Holtec Project No 71178							
<p>In accordance with the Holtec Quality Assurance Manual, and associated Holtec Quality Procedures (HQPs), this document is categorized as a :</p> <table style="width: 100%; border: none;"> <tr> <td style="width: 50%; padding: 5px;"><input type="checkbox"/> Calculation Package * (Per HQP 3.2)</td> <td style="width: 50%; padding: 5px;"><input type="checkbox"/> Technical Report (Per HQP 3.2) (Such as a Licensing report)</td> </tr> <tr> <td style="padding: 5px;"><input type="checkbox"/> Design Criterion Document</td> <td style="padding: 5px;"><input type="checkbox"/> Design Specification (Per HQP 3.4)</td> </tr> <tr> <td colspan="2" style="padding: 5px;"><input checked="" type="checkbox"/> Other (Specify): _____</td> </tr> </table>		<input type="checkbox"/> Calculation Package * (Per HQP 3.2)	<input type="checkbox"/> Technical Report (Per HQP 3.2) (Such as a Licensing report)	<input type="checkbox"/> Design Criterion Document	<input type="checkbox"/> Design Specification (Per HQP 3.4)	<input checked="" type="checkbox"/> Other (Specify): _____	
<input type="checkbox"/> Calculation Package * (Per HQP 3.2)	<input type="checkbox"/> Technical Report (Per HQP 3.2) (Such as a Licensing report)						
<input type="checkbox"/> Design Criterion Document	<input type="checkbox"/> Design Specification (Per HQP 3.4)						
<input checked="" type="checkbox"/> Other (Specify): _____							
<p>The formatting of the contents of this document is in accordance with the instructions of HQP 3.2 or 3.4 except as noted below:</p> <p>_____</p> <p>_____</p> <p>_____</p>							
<p>This document is labelled :</p> <p><input checked="" type="checkbox"/> Nonproprietary <input type="checkbox"/> Holtec Proprietary <input type="checkbox"/> Privileged Intellectual Property (PIP)</p> <p>Documents labelled Privileged Intellectual Property contains extremely valuable intellectual/commercial property of Holtec International. They can not be released to external organizations or entites without explicit approval of a company corporate officer. The recipient of Holtec's proprietary or Privileged Intellectual Property (PIP) document bears full and undivided responsibility to safeguard it against loss or duplication.</p>							
<p>* Revisions to the calculation Packages may be made by adding supplements to the document and replacing the "Table of Contents", the "Review and Certification" page and the "Revision Log".</p>							



Holtec Center, 555 Lincoln Drive West, Marlton, NJ 08053

Telephone (609) 797- 0900

Fax (609) 797 - 0909

REVIEW AND CERTIFICATION LOG

DOCUMENT NAME :	TOPICAL REPORT ON HI-STAR 100 AND HI-STORM 100 SYSTEM DEPLOYMENT AT HIGH ZPA ISFSI SITES
HOLTEC DOCUMENT I.D. NUMBER :	982004
HOLTEC PROJECT NUMBER :	71178
CUSTOMER/CLIENT:	PG&E

REVISION BLOCK

REVISION NUMBER *	AUTHOR & DATE	REVIEWER & DATE	QA & DATE	APPROVED & [!] DATE	DIST. ^x
ORIGINAL	<i>A.S. 12/10/98</i>	<i>K.P. 12/10/98</i>	<i>J. Gupta 12-16-98</i>	<i>Ben [Signature] 12/10/98</i>	C, NRC
REVISION 1					
REVISION 2					
REVISION 3					
REVISION 4					
REVISION 5					
REVISION 6					

This document conforms to the requirements of the design specification and the applicable sections of the governing codes.

Note : Signatures and printed names required in the review block.

* A revision of this document will be ordered by the Project Manager and carried out if any of its contents is materially affected during evolution of this project. The determination as to the need for revision will be made by the Project Manager with input from others, as deemed necessary by him.

! Must be Project Manager or his designee.

x Distribution : C : Client
M : Designated Manufacturer
F : Florida Office

*** Report category on the cover page indicates the contractual status of this document as ***
A = to be submitted to client for approval I = for client's information N = not submitted externally

THE REVISION CONTROL OF THIS DOCUMENT IS BY A "SUMMARY OF REVISIONS LOG" PLACED BEFORE THE TEXT OF THE REPORT.

 TABLE OF CONTENTS

GLOSSARY	
PREFACE	
1.0 INTRODUCTION AND SCOPE	1-1
2.0 STRUCTURAL DEFINITION OF HI-STAR AND HI-STORM	2-1
3.0 DESIGN AND CONSTRUCTION OF THE ISFSI PAD	3-1
3.1 General Comments	3-1
3.2 General Requirements for ISFSI Pad	3-2
4.0 STRUCTURAL DESIGN OF THE CONCRETE SLAB	4-1
5.0 DESIGN BASIS LOADINGS	5-1
5.1 Seismic Loadings	5-1
5.2 Bounding Hydraulic, Wind and Missile Loads	5-4
5.3 Other Loadings	5-4
6.0 FACTORED LOADS	6-1
6.1 Definitions	6-1
6.2 Load Combinations for the Concrete Pad	6-2
6.3 Load Combinations for the Attachment Structure	6-3
6.4 Load Combinations for the Connection Between HI-STAR and the Interface Structure	6-4
7.0 HI-STAR ANCHOR SYSTEM	7-1
8.0 HI-STORM ANCHOR SYSTEM	8-1
9.0 STRUCTURAL MATERIALS AND STRESS LIMITS	9-1
9.1 HI-STAR Clevis Support Blocks and HI-STORM Sector Lugs	9-1
9.2 Fasteners	9-1
9.3 Allowable Stresses	9-2

10.0	DYNAMIC ANALYSIS OF THE CASK	10-1
10.1	Dynamic Analysis of HI-STAR 100	10-2
10.2	Dynamic Analysis of HI-STORM 100	10-9
10.3	Confirmatory Static Analysis	10-13
11.0	STRUCTURAL ANALYSIS	11-1
11.1	Structural Qualification of the HI-STAR Clevis Support	11-1
11.2	Structural Analysis of the HI-STORM Sector Lugs	11-16
11.3	Structural Integrity Analysis of the Local Cask Region	11-17
	Due to Attachments Loads	
11.4	Structural Considerations Setting Upper Bounds	
	on the Hydrological Loads	11-20
11.5	ISFSI Concrete Slab Evaluation.....	11-22
12.0	ACCEPTABLE CARRY HEIGHTS FOR HI-STAR AND HI-STORM	12-1
13.0	TECHNICAL SPECIFICATION	13-1
13.1	Scope	13-1
13.2	Pad	1
13.3	Anchorage System	13-1
13.4	Maintenance and Design Life	13-1
14.0	INSTALLATION PROCEDURES.....	14-1
14.1	Introduction.....	14-1
14.2	Responsibilities.....	14-2
14.3	Procedure.....	14-2
15.0	REFERENCES	15-1

APPENDICES

- Appendix A: Dynamic Analysis Procedure
- Appendix B: HI-STAR 100 High Seismic Attachment
- Appendix C: Calculation of Cask Mass and Inertia Properties for High Seismic Dynamic Analysis
- Appendix D: Static Analysis for Maximum Cask Attachment Bolt Forces in HI-STAR 100
- Appendix F: HI-STORM Cask Mass and Inertia Properties
- Appendix G: Calculation of Spring Constants for HI-STORM 100 Dynamic Analysis
- Appendix H: HI-STORM Anchor System Stress Analysis

- Appendix I: Static Calculation of Anchor Bolt Forces in HI-STORM 100
- Appendix J: Hydrological Load Considerations
- Appendix K: Structural Evaluation of ISFSI Slab Supporting HI-STAR 100 Cask
- Appendix L: Structural Evaluation of ISFSI Slab Supporting HI-STORM 100 Cask
- Appendix M: Clevis-to-Baseplate Weld Qualification for HI-STAR 100 High Seismic Attachment

Total Number of Figures in Sections 1-15: 37

Supplementary Information:

We note that most of the appendices that contain actual calculations have been written using the MATHCAD commercially available computer code. This code has the capability of creating a complete text document with embedded calculations. The mathematical notation used within MATHCAD is program specific and some comment is warranted. Specifically, the notation “:=” is the designator for an assignment operation separating two sides of an equation, while the notation “=” is used to produce a numerical result. The appearance of a filled solid rectangular after an equation (e.g. $x := y+z$ ■) means that the equation is part of the text and is “not live”(i.e. does not participate in the flow of the calculations).

Archive Information: Location of computer files on Holtec’s Server

Projects\971178\ais\hi982004\982004.zip (report plus appendices)
Projects\971178\ais\hi982004\dynamics*.* (results of dynamic analyses)

Computer Environment: Pentium 266 - Windows 95

GLOSSARY

ACI: American Concrete Institute

ANCHOR BOLT THREADED COUPLING: The item that connects the two threaded ends of the anchor bolts in the HI-STORM 100 attachment system (see Figure 8.4).

CASK: Generic term to indicate HI-STAR or HI-STORM Systems (overpack and MPC assemblage)

CLEVIS: Attachment device for HI-STAR (Figure 7.1). This consists of many parts (the stud, the support blocks, and the clevis pins) that are shown in the assemblage of figures in section 7.

DBE: Acronym for "Design Basis Earthquake," defined as the seismic event applicable to the ISFSI, which is of extremely low probability (Service Level D in the ASME Code Section III).

HI-STAR: Holtec International Storage, Transport, and Repository Cask System

HI-STORM: Holtec International Storage and Transfer Operation Reinforced Module Cask System

ISFSI: Independent Spent Fuel Storage Installation

ITS: Important to Safety

MPC: Multi-Purpose Canister

MRS: Monitored Retrievable Storage

NOAA: National Oceanographic and Atmospheric Administration

NRC: Nuclear Regulatory Commission

OVERPACK: The radiation shielding barrier which surrounds the MPC

OWNER: The entity which owns or operates the ISFSI

PAD: Reinforced concrete slab on which the casks are positioned

971178

PSD: Power Spectral Density

SECTOR LUG: Attachment device for HI-STORM (Figure 8.1)

SLAB: Another term for the cask pad

SNF: Spent Nuclear Fuel

SRP: Standard Review Plan

TSAR: Topical Safety Analysis Report

ZPA: Zero Period Acceleration

PREFACE

Continuing uncertainty in establishing a central federal or a private MRS facility will soon force several nuclear utilities with sites located in high seismic regions to undertake the development of an ISFSI within or adjacent to their reactor facilities. Current certification requests for HI-STAR 100 and HI-STORM 100, however, are for quite modest ground acceleration levels, computed using a static equilibrium procedure. The objective of this topical report is to extend the application of HI-STAR 100 and HI-STORM 100 to sites with "high" seismic levels using a carefully engineered interface structure to attach the cask to the ISFSI pad. Attaching the cask to the pad, however, converts the pad into a structure essential to maintaining the cask's stability. Therefore, the structural configuration of the pad must be prescribed in an unambiguous manner, and the integrity of the pad/cask assemblage under the postulated seismic event must be established for the prescribed cask pad geometry. Toward this end, a bounding seismic spectrum is defined at the top of the ISFSI pad with the intent to envelope virtually *all* potential sites around the world. Based on dynamic simulations of the cask incorporating the interface structure to the pad and using appropriate time history seismic inputs derived from the bounding spectra, the loads on the interface structure are defined for both HI-STAR and HI-STORM casks as a function of time. Using the resulting peak loads from the dynamic analyses, the cask/pad interface structure is analyzed for structural integrity and is shown to meet appropriate structural acceptance criteria. The design parameters of the pad and interface loads to the pad from the structural simulations are specified and the pad and underlying foundation analyzed to demonstrate that its integrity can be maintained under the bounding DBE seismic event. Finally, a vertical handling accident on a bounding (stiff) pad/foundation is considered to demonstrate that the casks can be safely carried over the strongest proposed pad/foundation configuration without exceeding the design basis decelerations set forth in the appropriate TSARs for HI-STAR 100 and for HI-STORM 100. The capacity of the anchored systems to withstand later loadings from environmental effects (such as flood water, tsunami, wind, and missile impact) is also established by defining bounding values for these loadings that insure the same positive safety factors that are established for the seismic loads.

The design and supporting analyses presented in this topical report are readily implemented in a HI-STAR 100 or HI-STORM 100 overpack; no new penetration in the overpack is required. The maximum permissible seismic acceleration set at the top surface of the ISFSI pad is the 1.5g ZPA Reg. Guide 1.60 spectrum in three orthogonal directions. It is expected that the permissible earthquake level assumed in this topical report for sizing the cask anchoring system envelopes the DBE values at all candidate ISFSI sites. The anchoring system has been sized such that the stresses are well below the applicable Code (Section III Subsection NF, or AISC, as applicable) limits at the maximum stipulated seismic excitation levels. At a specific candidate site, the seismic inputs are apt to be smaller, resulting in even greater structural margins.

Likewise, the key parameters in the ISFSI pad design (viz., pad thickness, rebar size and grid spacing, and soil subgrade modulus, etc.), have been set down such that the ISFSI pad will comply with NUREG-1567 specifications. Sufficient range of variation in the key parameters (e.g., pad thickness, concrete compressive strength) is permitted to enable practical construction of the pad.

Evaluation of the system loads has been carried out using three independent methods, namely (i) the time-history method (most rigorous), (ii) the response spectrum method (less rigorous), and (iii) the static method. The analyses show that the time-history method gives larger interface loads than the less comprehensive simulations; however, the predictions of all three methods are in reasonable accord. The results from the time-history solution are used in subsequent stress evaluations to determine the minimum factors of safety.

It is evident that the fastening of the loaded cask to the ISFSI pad must be carried out with minimum exposure to the plant personnel. The HI-STAR 100 and HI-STORM 100 attachment systems have been designed to be installation-friendly with full consideration of factors such as tolerance variations and heavy load handling logistics which can subvert the efficiency of the cask installation effort. Chapter 14 of this topical report addresses the practical considerations in HI-STAR 100 and HI-STORM 100 installation to

realize ALARA. Procedural guidance to install the HI-STORM 100 and HI-STAR 100 Systems on their respective anchor systems is provided to assure simple and accurate first-time alignment of the components.

This topical report expands upon the "Topical Report Outline", Holtec Report Number HI-981905 that was submitted to the USNRC on May 1, 1998 to solicit the Commission's comments on the structure and content of the topical report. The main body of this report contains 15 sections that provide complete information on the system design, analysis, material selection, practical considerations, applicable codes/standards, permissible seismic/hydrological loadings, permissible cask carry height, conditions of use (Technical Specification), and installation procedures. In addition, a number of appendices are included that, while not necessary for reading and understanding the content of the main report, provide supplemental calculations for completeness. In other words, the appendices serve merely to lend complete transparency to the underlying calculations; they are not needed for a seamless reading of the main body of the report.

The Pacific Gas and Electric Company has provided technical and financial support in the preparation, review, and QA acceptance of this report.

In conclusion, a structurally rugged and ALARA-compliant anchoring system has been designed and qualified for anchored installation of HI-STAR 100 and HI-STORM 100 systems. The supporting analyses demonstrate positive safety factors under postulated bounding loads.

1.0 INTRODUCTION AND SCOPE

In compliance with 10CFR72, Subpart F, "General Design Criteria," the HI-STAR and HI-STORM cask systems are classified as "important to safety" (ITS) [1,2]. The topical safety analysis reports (TSARs) for Holtec International's dry storage systems [3,4] explicitly recognize HI-STAR 100 and HI-STORM 100 as equipment containing numerous ITS components. The reinforced concrete pad on which the cask is situated, however, is designated as a non-ITS structure. This is principally because, in most cases, cask systems for storing spent nuclear fuel on reinforced concrete pads have been installed as free-standing structures. The lack of a physical connection between the cask and the pad has allowed the NRC to specify a clear regulatory position with respect to storage casks, i.e., the storage pads are not important to safety. This permits the holder of a Part 50 license to deploy an NRC-certified storage cask on its storage pad without further site-specific reviews, using the provisions of Subpart K of 10CFR72.

Even though the casks are installed as free-standing structures in relative close proximity to each other, their kinematic stability under earthquake loadings has not been a matter of in-depth assessment and inquiry on the part of the cask designers or the NRC. This is partly because the casks are relatively stubby structures, which makes them reasonably stable under moderate seismic events. In addition, the ISFSI installations to date have been located primarily in regions of the country that have low "design basis earthquakes" (DBE). However, this condition is about to change as utilities in the western United States consider siting ISFSIs at their plants to meet their fuel storage needs as a prerequisite to decommissioning. Utilities with ISFSIs located on sites with the potential for high seismic ground motions must consider the consequences of DBEs as an important part of their safety evaluation.

In a recent paper, Singh, Soler, and Smith [6] present a method for dynamic qualification of a free-standing HI-STAR cask that indicates accelerations considerably in excess of the static "g-limit" provided in the TSAR [3] can be applied to a free-standing loaded HI-STAR system without jeopardizing the kinematic stability of the system. Dynamic evaluation procedures for free-standing casks have not yet been certified by the NRC; while regulatory action is needed on this matter, this topical report does not address free standing casks under high seismic loadings except for the brief discussion below.

The dynamic evaluation procedure for nonlinear structures such as a fuel storage cask is typically performed using a time-history approach [7,8]. This approach essentially consists of integrating the dynamic equations of motion, which are second-order differential equations with the time coordinate as the independent variable, over the duration of the postulated seismic event. Holtec's computer code DYNAMO [9], based on the methodology given in Reference [7], has been utilized in time-history analysis of many free-standing structures in nuclear plants over the past two decades.

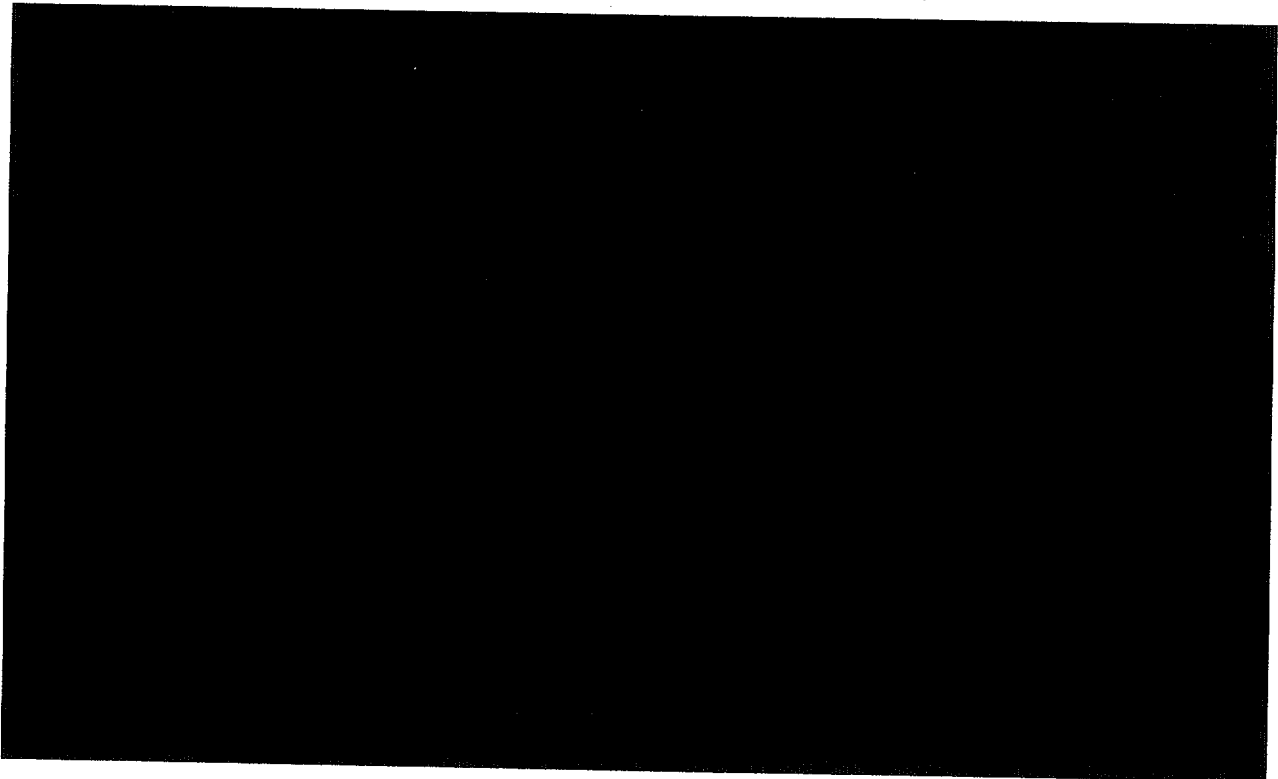
The dynamic evaluation technique extends the range of acceptable seismic levels to somewhat higher values than those predicted by purely static evaluation, but does not yield results that would permit the employment of free standing casks in extremely high ground motion level sites. For an extremely high ground motion level ($ZPA^{\dagger} \geq 1.0g$), such as those postulated for certain regions in East Asia and in the western United States, a free-standing cask cannot be demonstrated to be safe from overturning during a postulated design basis seismic event. For such sites, it is essential to constrain the cask on the ISFSI pad. In contrast to an ISFSI containing free-standing casks, a constrained-cask installation relies on the structural capacity of the pad to ensure structural safety. The regulatory position with respect to such structures is clearly specified in Paragraph 72.122, Subpart F of CFR Part 72 [10]:

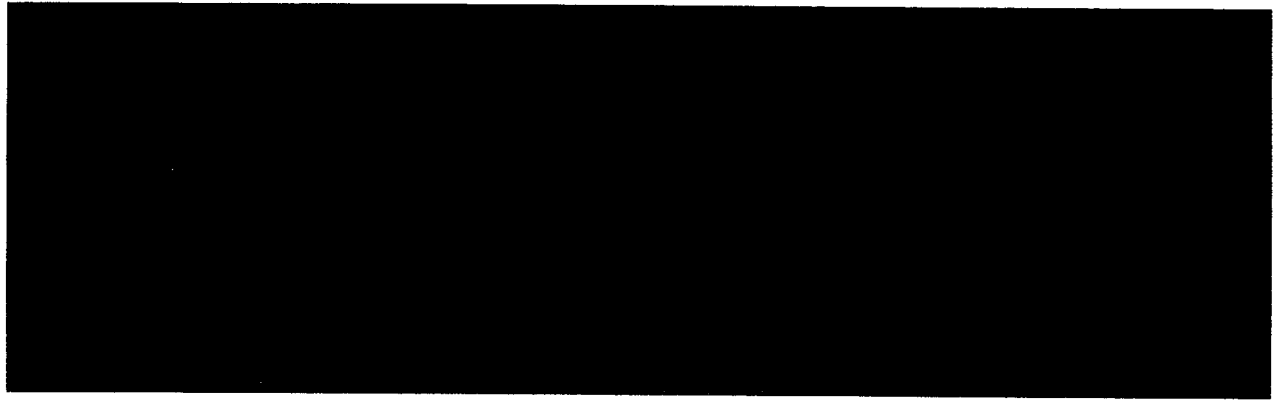
[†] ZPA is the acronym for Zero Period Acceleration.

"(2) Structures, systems, and components important to safety must be designed to withstand the effects of natural phenomena such as earthquakes, tornadoes, lightning [sic], hurricanes, floods, tsunami, and seiches, without impairing their capability to perform safety functions. The design bases for these structures, systems, and components must reflect:

- (i) Appropriate consideration of the most severe of the natural phenomena reported for the site and surrounding area, with appropriate margins to take into account the limitations of the data and the period of time in which the data have accumulated, and
- (ii) Appropriate combinations of the effects of normal and accident conditions and the effects of natural phenomena."

Since an ISFSI pad in a constrained cask installation participates in maintaining the stability of the cask during "natural phenomena" on the cask and pad, it is an ITS structure. The procedure suggested in Regulatory Guide 7.10 [2] and the associated NUREG [1] indicates that an ISFSI pad used to secure anchored casks should be classified as a Category C ITS structure.





Because the environmental conditions at potential ISFSI sites vary widely across the continental United States, ranging from dry and arid to extremely humid and marine, some latitude in the selection of the material of construction for the attachment structure should be permitted. Accordingly, this topical report provides for a limited menu of acceptable attachment materials.

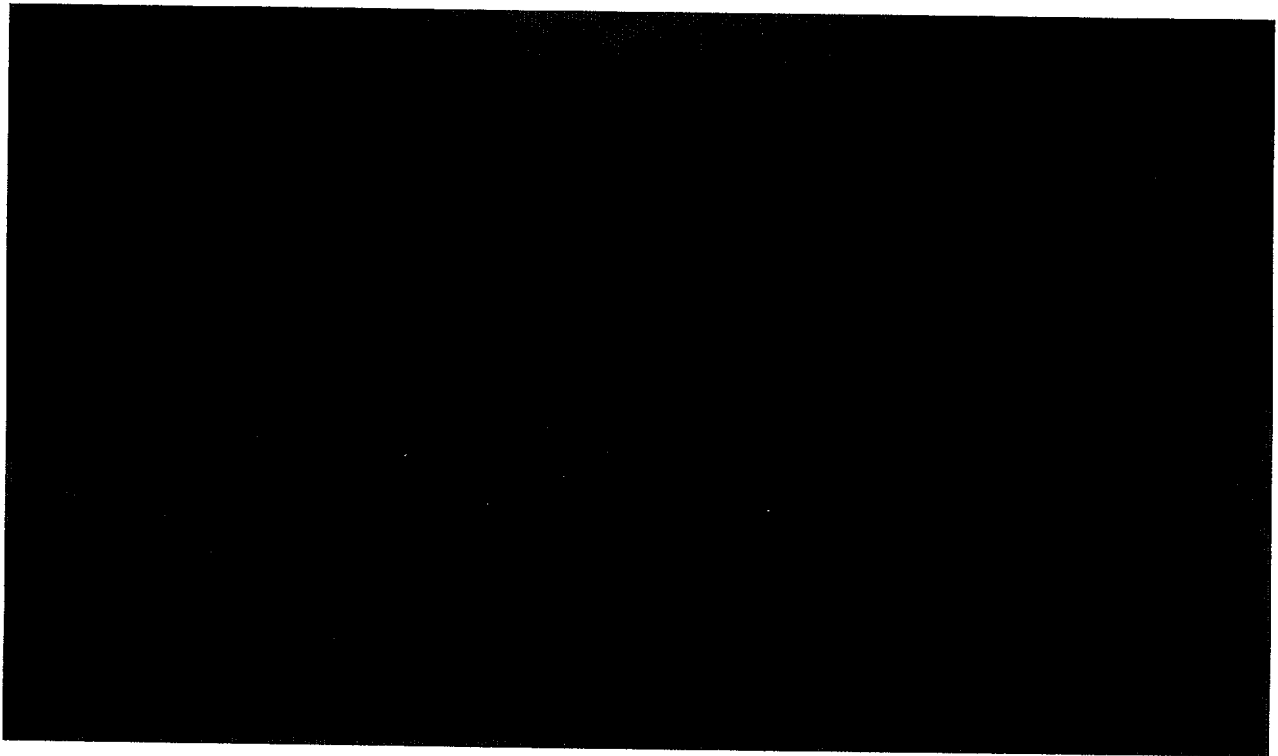
In this report, the essential design parameters of the ISFSI pad required to establish its ability to secure the HI-STAR 100 and HI-STORM 100 overpacks under the postulated seismic events are set down. Design characteristics not necessary for the strength characterization of the pad are left unprescribed to permit the individual ISFSI design to be best synchronized to the characteristics of a specific site. A common ISFSI pad design (which we will henceforth refer to as the “reference pad”) is proposed for both HI-STAR 100 and HI-STORM 100 Systems. The essential pad design parameters which are needed to be specified to set down the fixity of attachment between the cask and the ISFSI consist of the geometric characteristics of the pad (thickness, rebar, etc.), strength properties of its constituent materials (concrete and rebars), anchor system geometry, and equivalent elastostatic characteristics of the underlying foundation, including the subgrade. The values (or range of permissible values, where appropriate) for all of the above ISFSI pad design data are set forth for the reference pad design in this topical report.

The reference pad design proposed and qualified in this document is restricted to installing HI-STAR 100 and HI-STORM 100 systems. It has not been analyzed for storing other cask systems certified

by the USNRC.

Finally, the allowable “carry height” for both HI-STAR 100 and HI-STORM 100 are established for the reference pad design.

As stated in the Technical Specification in Section 13 of this report, to deploy a constrained HI-STAR 100 or HI-STORM 100 under the provisions of this topical report, the ISFSI owner must ensure that:



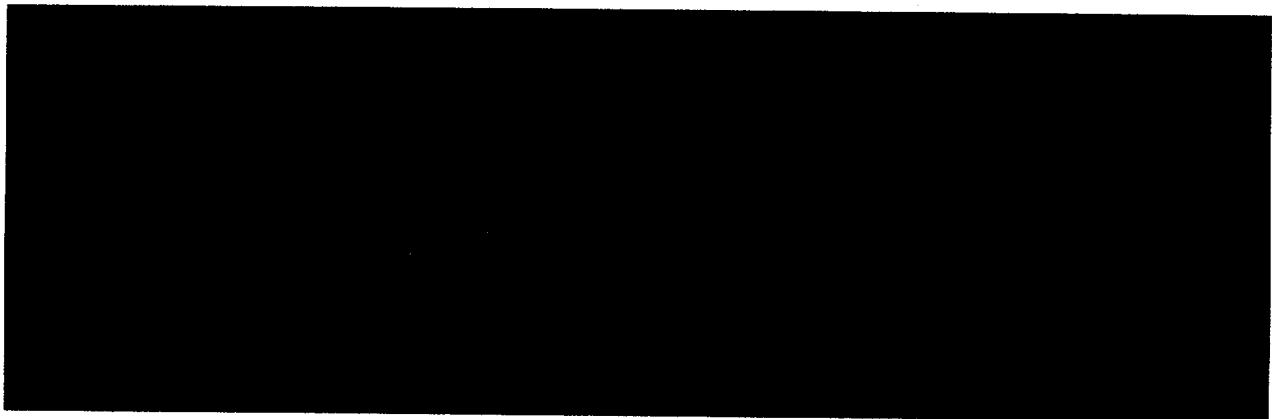
This topical report relies on the HI-STAR 100 and HI-STORM 100 TSARs [3,4] to qualify these cask systems for all other safety criteria (e.g., criticality, shielding, and heat dissipation). The cask attachment system design does not invalidate any safety analyses contained in the topical reports of HI-STAR 100 or HI-STORM. 100.

This topical report extends the application of the HI-STAR 100 and HI-STORM 100 systems for deployment as constrained structures at relatively high seismic sites. To realize this objective

under a general certification, the structural design of the pad/cask attachment system, and the input loading from the cask to the ISFSI pad have to be rigorously prescribed. The information presented in this report quantifies the safety factors that exist in the anchored HI-STAR 100 or HI-STORM 100 system and the anchoring system when subjected to a bounding set of inertial loads.

The seismic-related resultant loadings on the anchoring system are established using three discrete approaches, namely:

- time-history analysis
- response spectrum analysis
- static analysis



Because the response spectrum analysis presupposes a linear structure; the cask structure is linearized by lumping the fuel, fuel basket, and MPC masses with the overpack. The elastic properties of the attachment structure, are simulated by linearly elastic springs. The results provide cask/pad interface loads, which are compared with the time-history solution for design verification purposes.

Finally, static equilibrium calculations are performed assuming that the cask tends to rotate about a single point to provide a simple estimate of the maximum bolt load in tension for additional

design verification to show that the time history solution does indeed provide reasonable results.

This document does not deal with SNF fragility issues (acceptable g-load to preserve cladding integrity). Rather, the 60g limit adopted in the HI-STAR 100 TSAR and the 45g limit adopted in the HI-STORM 100 TSAR (the different design basis deceleration limits set in the HI-STORM 100 TSAR are due to differences in the geometry and extent of lateral support provided to the MPC by the enclosing HI-STORM 100 overpack) are used as the upper bound limit. Similarly, environmental events such as lightning, etc., are covered in the respective system TSAR and, as such, are not dealt with in this document[†]. It should be emphasized, however, that should the rattling loads (between fuel assemblies and the storage cavity walls) computed by the time-history analysis be deemed to be excessive for a particular ISFSI site, then measures to protect the fuel from impact damage (such as lateral spacers to reduce rattling) may be considered by the owner and appropriate amendments to the HI-STORM 100 and HI-STAR 100 TSARs may be required. This topical report does not preclude the use of devices to protect the SNF in the storage mode from intense seismic events.

The applicable load combinations for structural evaluation of the ISFSI pad/cask system have been extracted from NUREG-1567 [12].

[†]Permissible limits on missile impact load, flood water velocity, and other kinematically destabilizing environmental loadings for the constrained cask configuration are defined within this topical report.

2.0 STRUCTURAL DEFINITION OF HI-STAR 100 AND HI-STORM 100

HI-STAR 100 and HI-STORM 100, pictorially illustrated in Figures 2.1 through 2.4, are essentially thick-walled stubby structures. The length-to-diameter ratio (aspect ratio) and thickness-to-diameter ratio of HI-STAR 100 and HI-STORM 100 are shown in Table 2.1. These ratios show that the structures will, if anchored at the bottom, simulate a very stiff beam-like structure cantilevered from the pad. It is therefore reasonable to treat the overpack as a rigid body (six degrees of freedom) in the seismic simulations.

Table 2.1		
HI-STAR 100 AND HI-STORM 100 OVERPACK PRINCIPAL GEOMETRIC DATA		
ITEM	HI-STAR	HI-STORM
Height, inch	203-1/8	231-1/4
Diameter at mid-height, inch	96	132-1/2
Wall thickness at mid-height, inch	13-5/8	29-1/2
Aspect ratio	2.12	1.75
Wall Thickness-to-diameter ratio at mid-height	0.14	0.22
Diameter at contact surface with ISFSI, inch	83.25	132-1/2

The contents of the cask, however, are not rigidly connected to the overpack. The MPC is installed in the cask with an annular clearance, which renders it an unsecured mass (which can rattle) during an earthquake event. Moreover, the fuel assemblies are free to rattle within the basket cells and the basket itself can also rattle within the MPC enclosure vessel during a seismic event. The clearances between the fuel assembly and storage cells, between the basket and the MPC, and between the MPC and the overpack, are unavoidable in a cask system. These gaps, however, have the effect of modifying the seismic response of the cask system and, therefore,

are factored into the seismic model. Were it not for these inter-body gaps, an anchored cask system would behave as a nearly linear structure[†] wholly appropriate for seismic analysis by a quasi-dynamic method such as the response spectrum method [12]. Because of the non-linear effects inherent in a cask system, the principal vehicle for seismic evaluation used in this topical report is the time-history method.

The HI-STAR 100 and HI-STORM 100 topical reports [3,4] contain complete drawings for these cask systems. In Table 2.2, necessary data to create the dynamic analysis models are extracted from References [3] and [4]. The data presented in Table 2.2 have been compiled with two guiding considerations, which are stated below for clarity:

- Since an increase in mass increases inertia loads, the heaviest loaded MPC weight is used in the analyses.
- All geometric dimensions are cited as "nominal" values. Variation in gaps, to the extent permitted by the design drawings, are considered by sensitivity studies to demonstrate that a large change in a cask response does not occur due to a small change in the gap sizes (arising from the fabrication of weldments). Results from the sensitivity studies are given in Table 10.2 for HI-STAR 100 and in Table 10.6 for HI-STORM 100.

[†] We say nearly linear because the interface connection structure will still have different stiffness in tension than in compression.

Table 2.2
 REPRESENTATIVE GEOMETRIC AND INERTIA DATA FOR HI-STAR 100
 AND HI-STORM 100

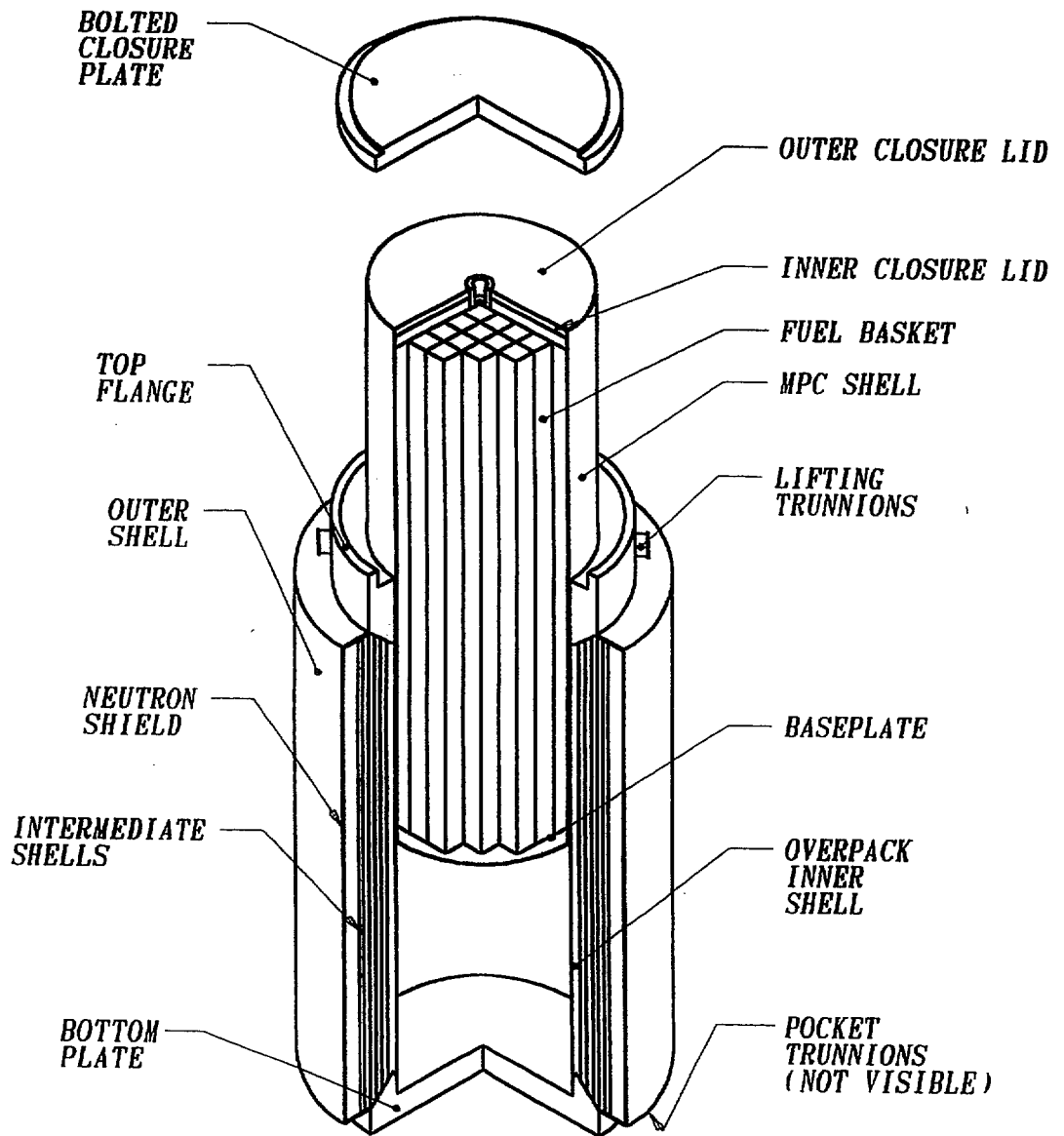
ITEM	HI-STAR 100 (Reference 3) [†]	HI-STORM 100 (Reference 4) [†]
Empty overpack weight, lb	153,710 (Table 3.2.1)	269,003 (Table 3.2.1)
Loaded MPC bounding weight, lb	90,000 (Table 3.2.4)	90,000
Bounding weight of fuel basket, lb	13,000	13,000
Weight of MPC canister, lb	21,502	21,502
Bounding weight of empty MPC, lb	36,000 (Table 3.2.4)	36,000
Bounding total weight of stored SNF, lb	54,000 (PWR assemblies)	54,000 (PWR assemblies)
Bounding Weight of Overpack with fully loaded MPC, lb	250,000 (Table 3.2.4)	360,000
Basket-to-MPC axial gap, inch	2	2
Overpack-to-MPC radial gap (width of annulus available for rattling) ^{††} , inch	0.1875	0.2825
SNF-to-Basket cell half gap ^{†††} (for heaviest SNF case), inch	0.105 (B&W 15x15)	0.105 (B&W 15x15)
Height of C.G. of empty overpack above datum surface ^{††††} , inch	99.7 (Table 3.2.2)	116.8 (Table 3.2.3)
Height of C.G. of empty MPC above datum surface, inch	109.9 (Table 3.2.2)	132.5 (Dwg. 1397, Sht.1)
Height of C.G. of fuel basket above datum surface, inch	95.5	113.5

[†] Location of the data in the cited reference is provided adjacent to the data in this table.

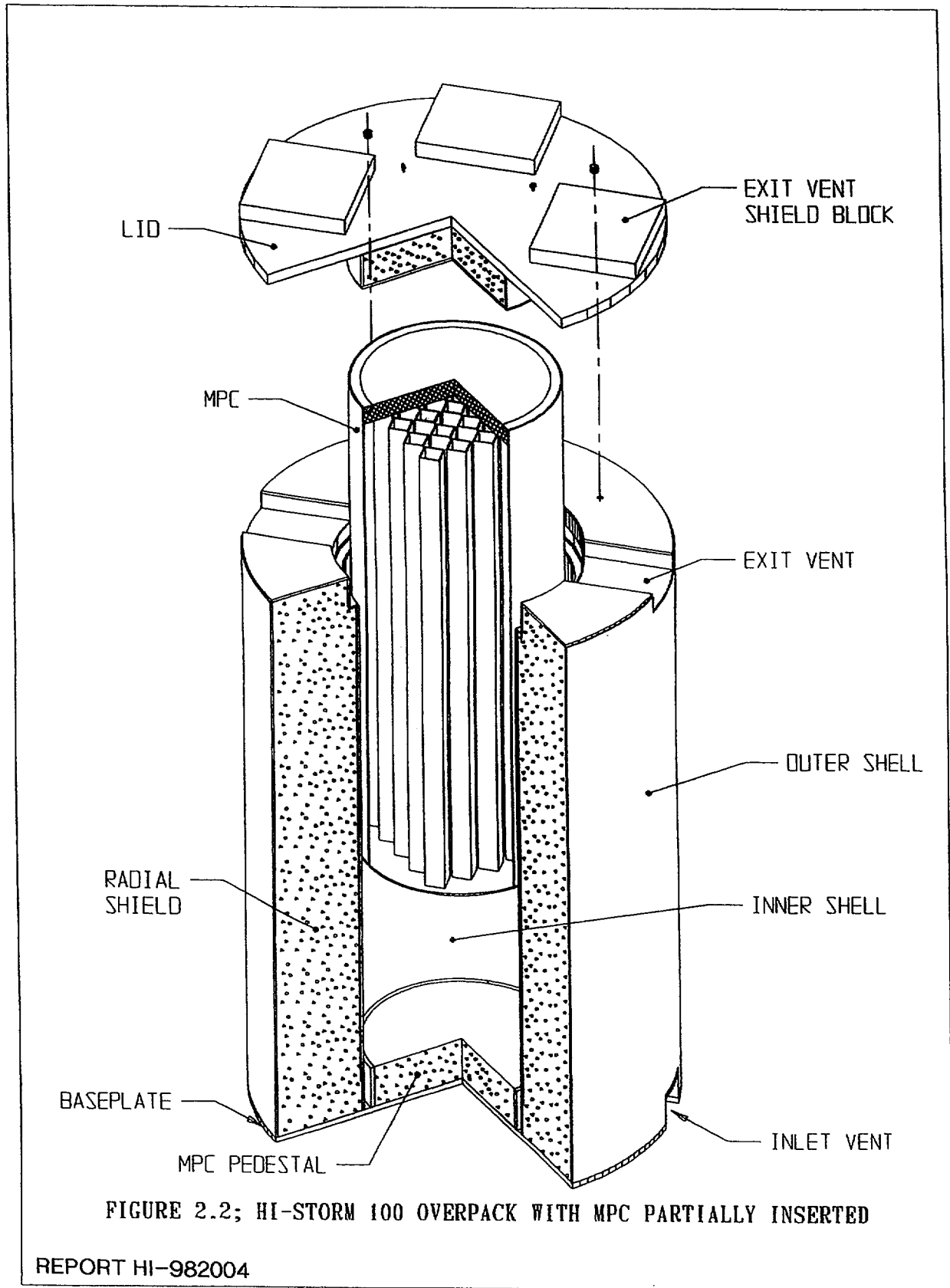
^{††} Sensitivity analysis for different gap case (i.e., MPC OD tolerance) is also performed.

^{†††} Sensitivity analysis for different gap case (i.e., different fuel size) is also performed (see Tables 10.2 and 10.6).

^{††††} Datum surface is indicated from the bottom surface of the cask (Figures 2.3 and 2.4).



**FIGURE 2.1; HI-STAR 100 OVERPACK
WITH MPC PARTIALLY INSERTED**



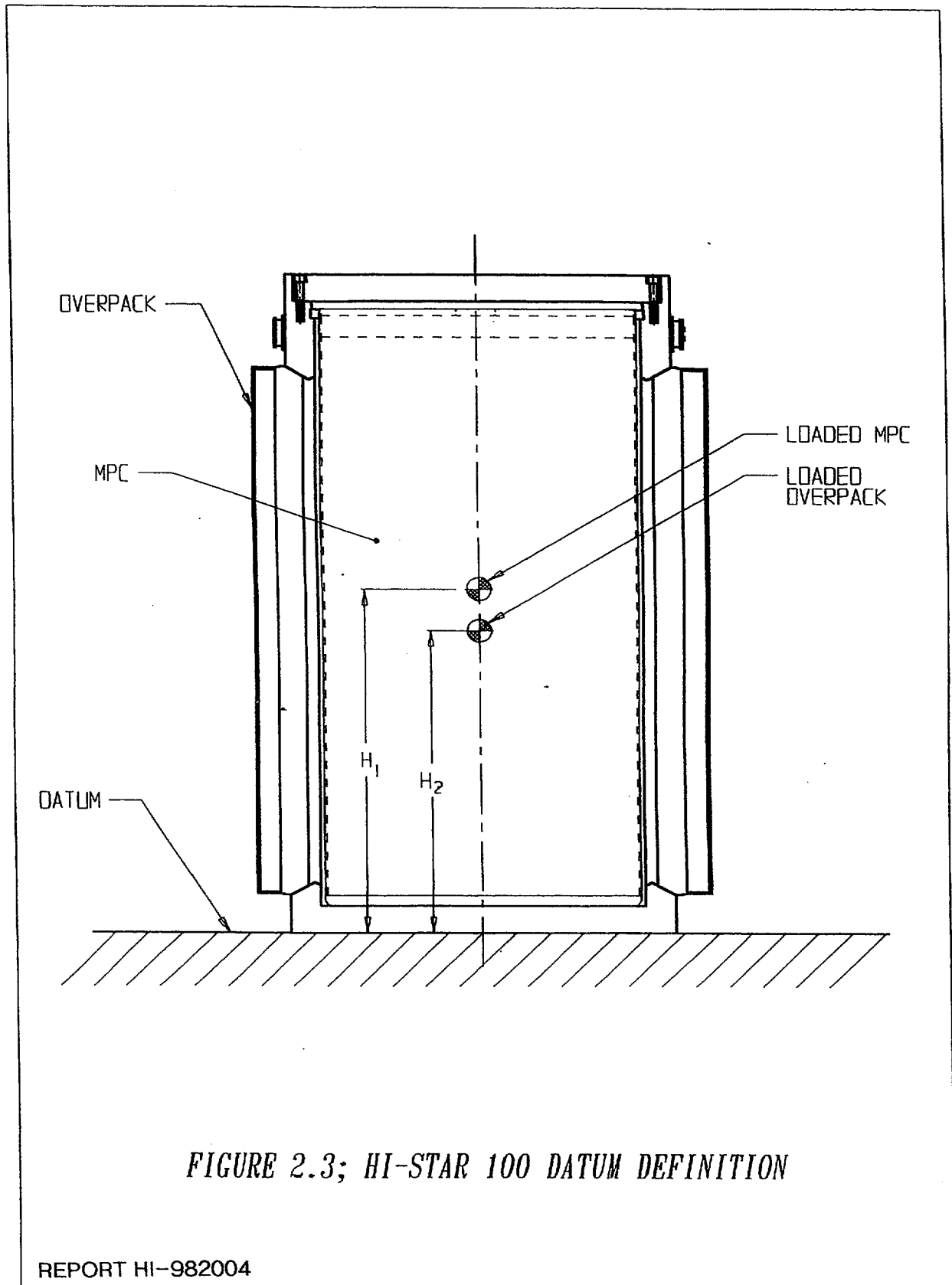


FIGURE 2.3; HI-STAR 100 DATUM DEFINITION

REPORT HI-982004

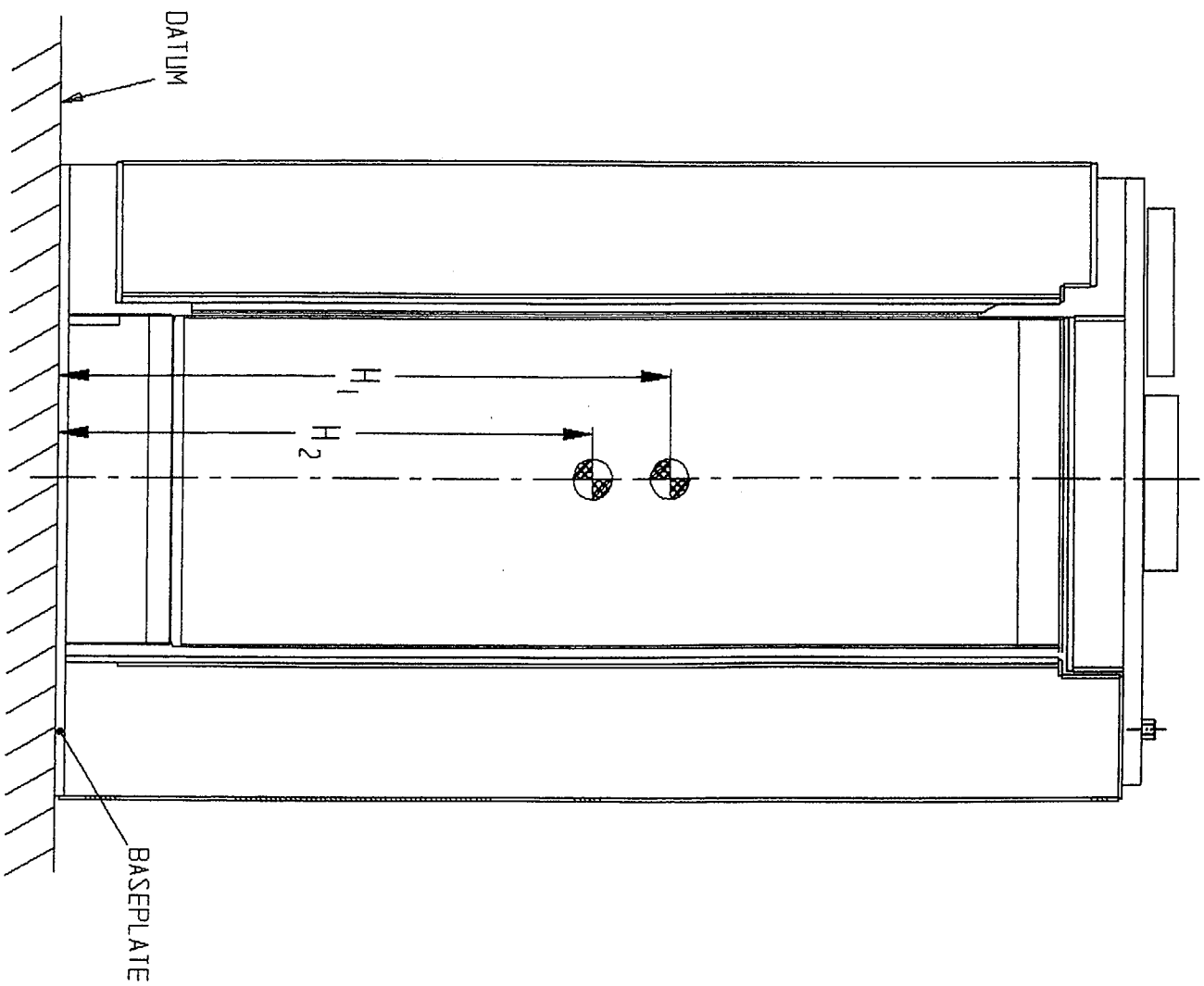


FIGURE 2.4: HI-STORM 100 CROSS SECTION
SHOWING DATUM DEFINITION

REPORT HI-982004

PROJECTS\971178\A1S\HI982004\FIGURES\FIG 2.4

3.0 GENERAL DESIGN AND CONSTRUCTION REQUIREMENTS FOR THE PAD

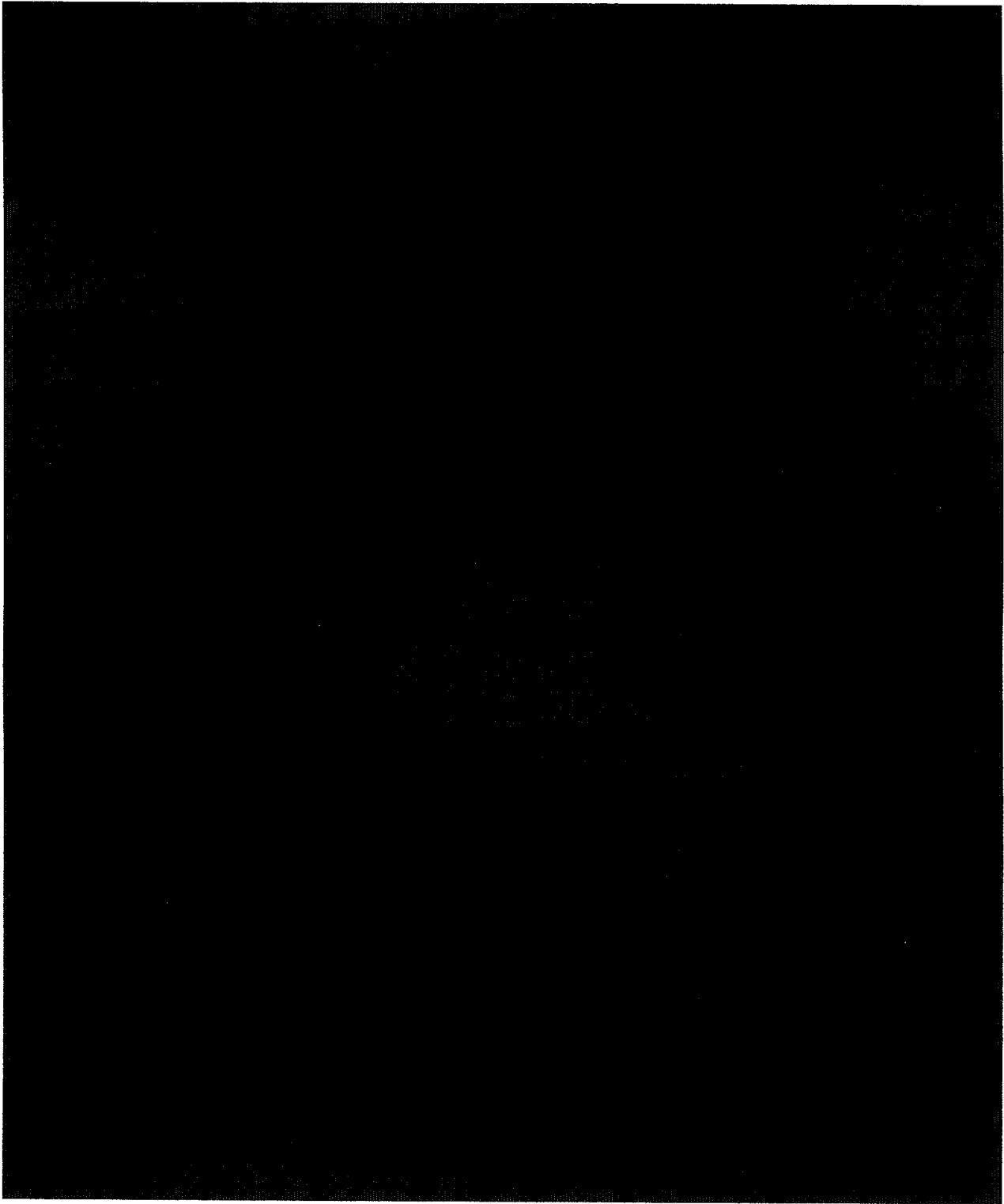
3.1 General Comments

As stated in Chapter 1, an ISFSI slab that anchors a spent fuel storage cask should be classified as "important to safety." This classification of the slab follows from the provisions of 10CFR72 [10] which requires that the cask system retains its capacity to store spent nuclear fuel in a safe configuration subsequent to a seismic or other environmental event. Since the cask slab is designated as ITS, the licensee is required to determine whether the reactor site parameters, including analysis of earthquake intensity and tornado missiles, are enveloped by the cask design bases. The intent of the regulatory criteria is to ensure that the slab meets all interface requirements of the cask design and the site characteristics.

Recent NRC guidance for evaluating handling accidents and tipover of the cask system has enabled Holtec International to establish a simulation model that incorporates the cask and the target (slab) energy absorbing properties [17]. This requires that the ISFSI designer demonstrate that the final slab design has energy absorption characteristics equal to or better than the characteristics used for the handling accidents considered to be credible during the cask deployment operations. Results have been presented in the TSAR's [3,4] to demonstrate that the specified design bases decelerations are bounding.

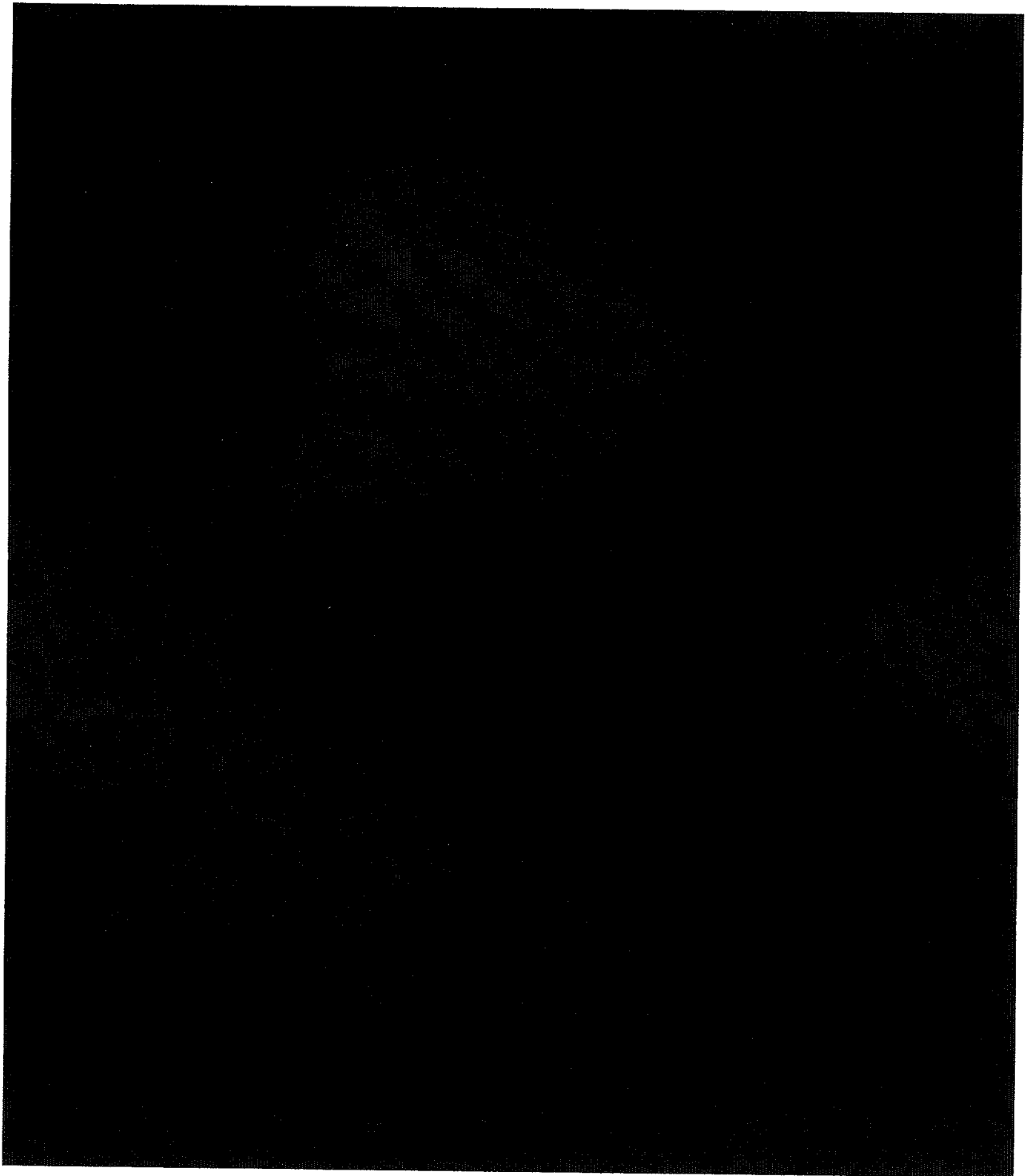
This chapter provides general requirements for design and construction of the ISFSI concrete pad as an ITS structure, and also establishes the framework for ensuring that the ISFSI design bases are clearly articulated. In Chapter 4, additional requirements for the pad structural design/analysis are set down to insure that the loaded ISFSI (cask plus attachment structure plus ISFSI pad plus pad foundation) meets all structural integrity and stability requirements.

3.2 General Requirements for ISFSI Pad





4.0 STRUCTURAL DESIGN REQUIREMENTS FOR THE CONCRETE SLAB



c.

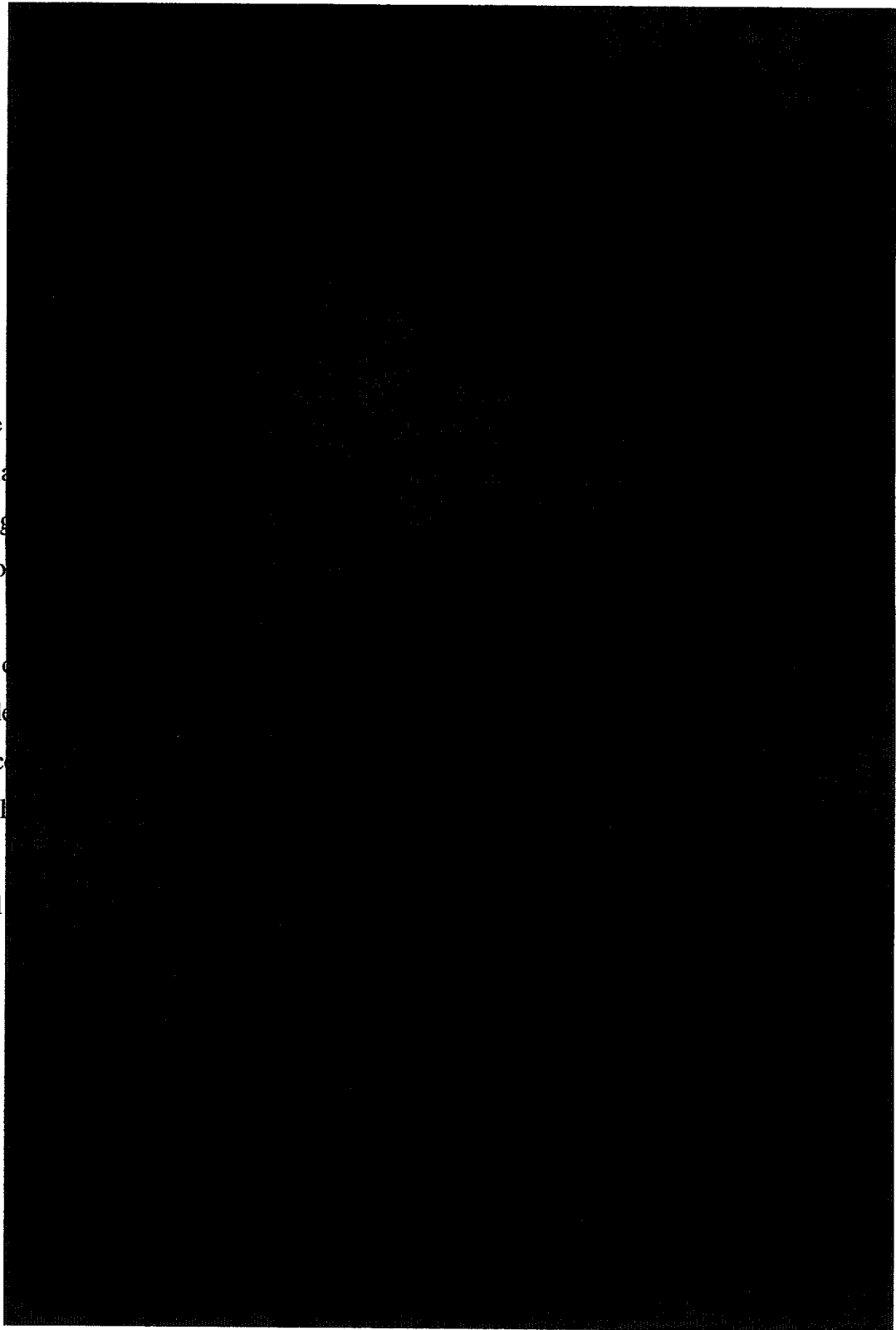
d.

Increasing the
against external
concrete strength
which leads to
handling over
concrete (and
that the pad de
properties of c
to bracket such

The ISFSI pad
criteria:

i.

ii



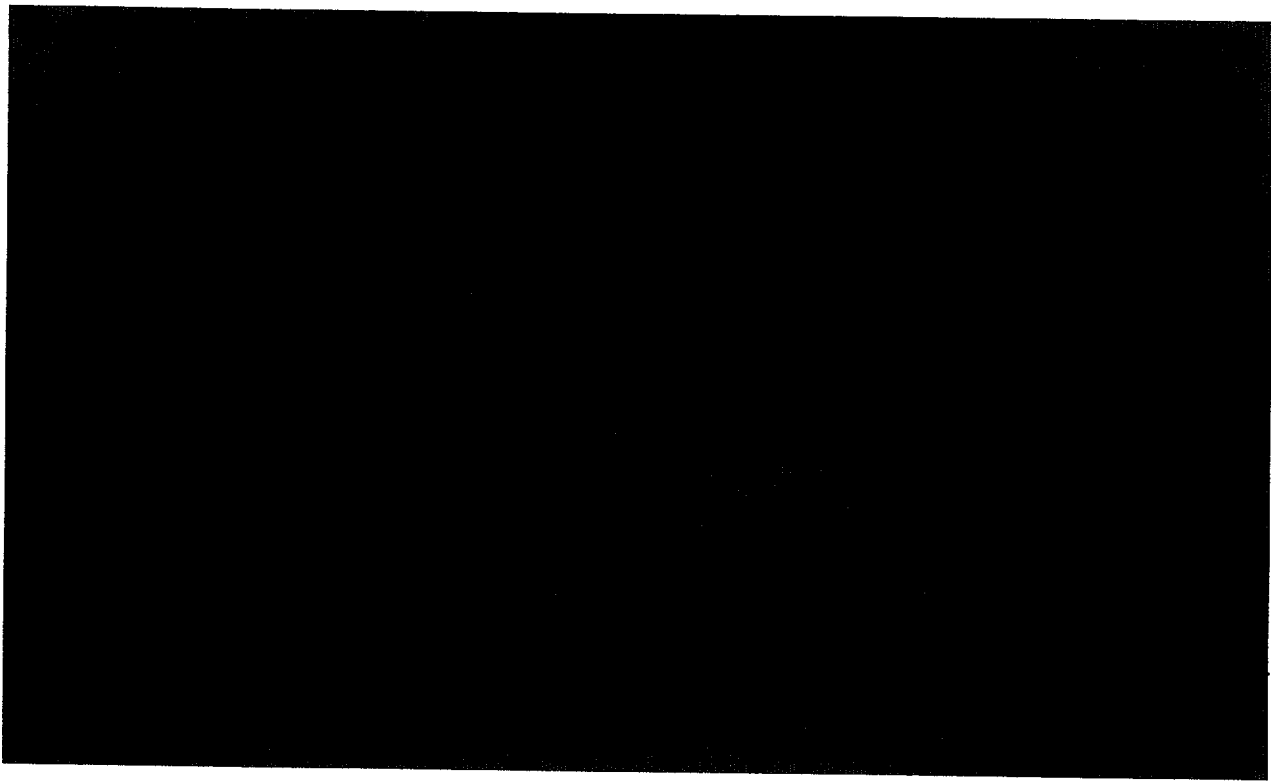


Table 4.1		
BOUNDING DESIGN DATA FOR THE ISFSI PAD		
	Maximum	Minimum
Concrete pad thickness, inch	60	54
Concrete compression strength, [†] psi	6,000	4,000
Re-bar arrangement	#11 bars @ 8" (see Figure 4.1)	
Characteristic Standard Subgrade Modulus ^{††} , pci	3,000	200
Minimum Soil Bearing Pressure for Sustained Loading (psi)	-----	Greater than 25
Characteristic Shear Modulus of Sub-Base Below Subgrade, psi	3,000,000	30,000

† At 28 days.

†† The Standard Subgrade Modulus is defined as the pressure applied to the lateral surface of a 30 inch diameter rigid circular plate divided by the measured deformation of the rigid plate into the subgrade. Using the Boussinesq solution from the linear theory of elasticity, this measured ratio can be related to the Young's Modulus and the Poisson's Ratio of a homogeneous soil.

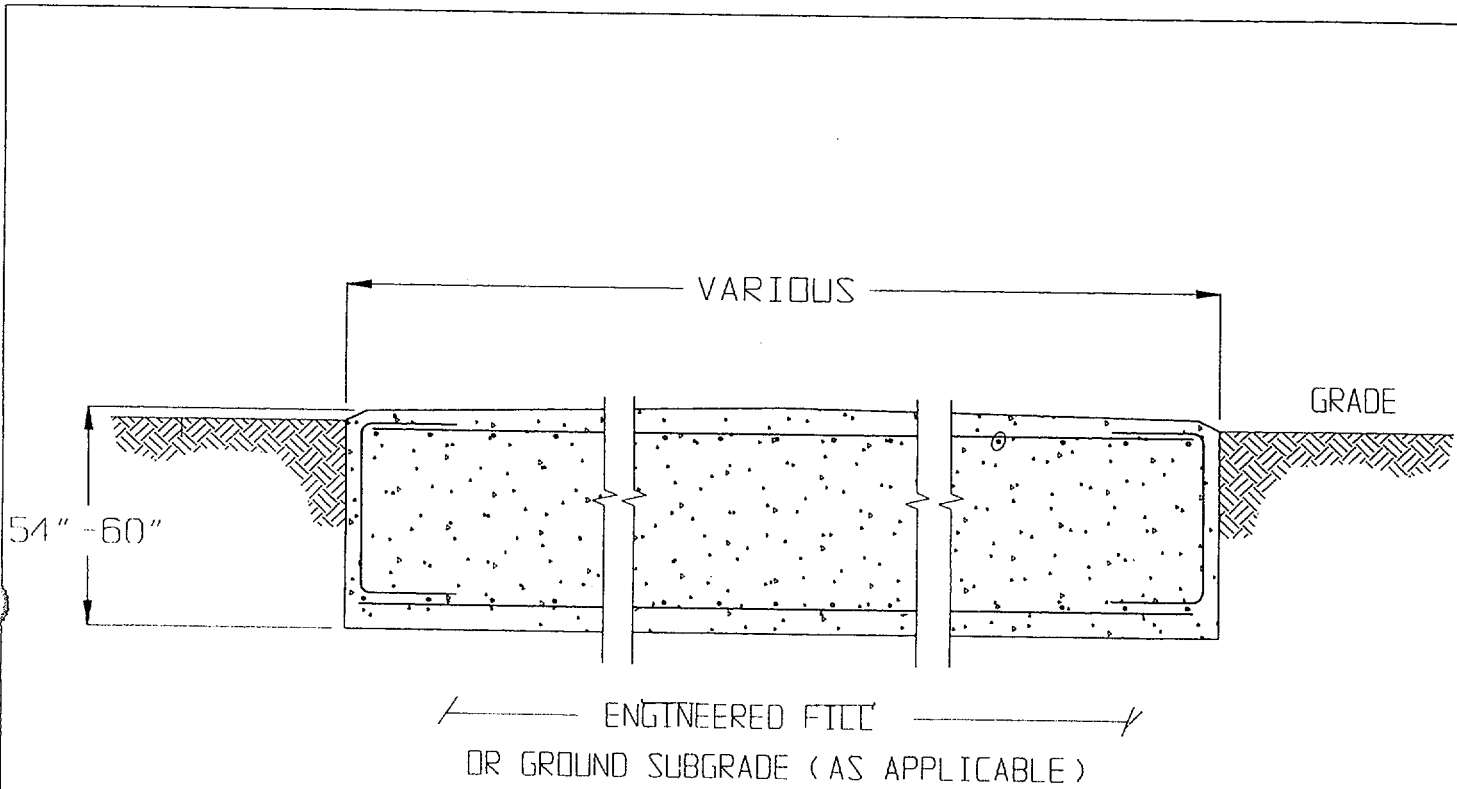


FIGURE 4.1; HI-STAR (HI-STORM) CONCRETE PAD SECTIONAL VIEW

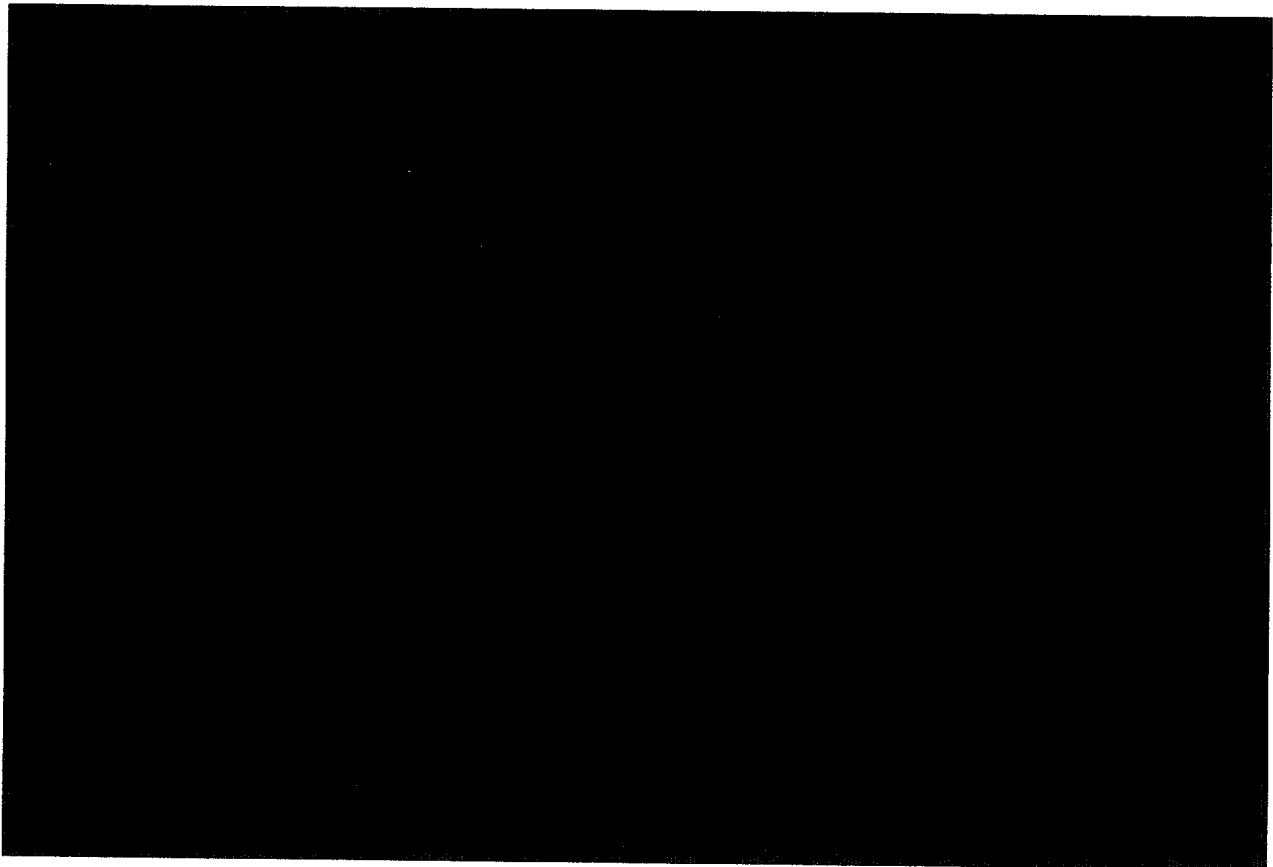
REPORT HI-982004

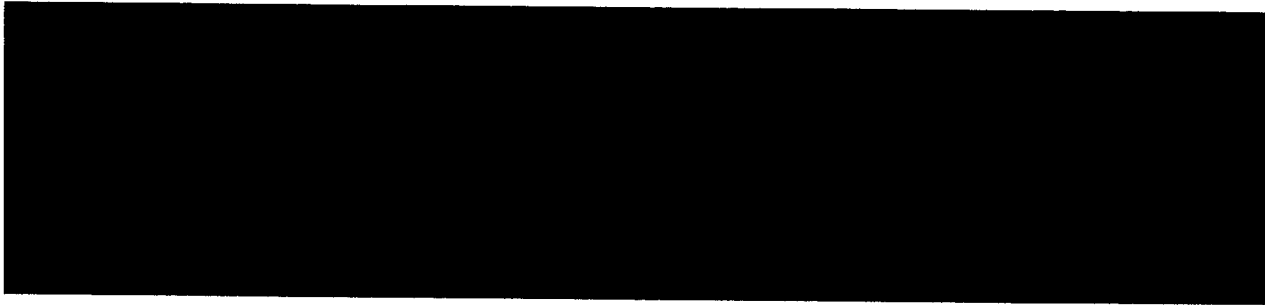
5.0 DESIGN BASIS LOADINGS

Design basis loads for reinforced concrete and steel structures are defined in NUREG-1567 [12, Table 7.1]. Certain of these loads merit additional discussion because of their importance vis-à-vis the interface between the cask and the pad. In particular, seismic loads and other postulated accident loads imparted to the cask warrant further elaboration.

The cask design basis loadings are considered in the appropriate TSAR [3,4]. Seismic, wind, and tornado-borne missiles all impart loads to the pad through the interface structure that provides the attachment of the cask to the pad.

5.1 Seismic Loadings





For structures which can be reasonably simulated as “linear”, the “response spectrum” is considered to be a reliable gage of the severity of the systems’ response to the earthquake. In other words, a response spectrum which uniformly envelops another spectrum can be a priori assumed to produce a more severe seismic response. By selecting a “broad peaked” and high ZPA input spectrum in this topical report, an attempt has been made to bound all pad/cask interface DBE spectra which may be developed for candidate ISFSI sites in the country. Thus, the need for a site-specific evaluation is obviated. However, at ISFSI sites located near multiple capable faults, the ISFSI owner may, within the purview of Part 72.212 provisions, and at his option, perform site-specific structural evaluations using the actual input spectrum to derive input seismic events using the methodologies set forth in this topical report. The site-specific assessment may be particularly warranted in those cases where the postulated seismic inputs may be of long duration, resulting in a large number of cyclic loadings on the attachment structure. Such additional assessments are, however, not mandatory to establish safety, given the large margins of safety and extreme severity of the postulated reference seismic loadings in this topical report.

In order to develop synthetic time histories from the design response spectra, the guidance provided by the Standard Review Plan 3.7.1[16] is used. The synthetic time-history is considered to be adequate if its derivative spectrum generally envelops the target spectrum with the extent of permissible infraction specified in SRP 3.7.1. The SRP further allows that a single artificial time-history (in contrast to multiple time-histories) is sufficient for dynamic evaluation if the power spectral density function of the synthetic acceleration data also bounds its counterpart for

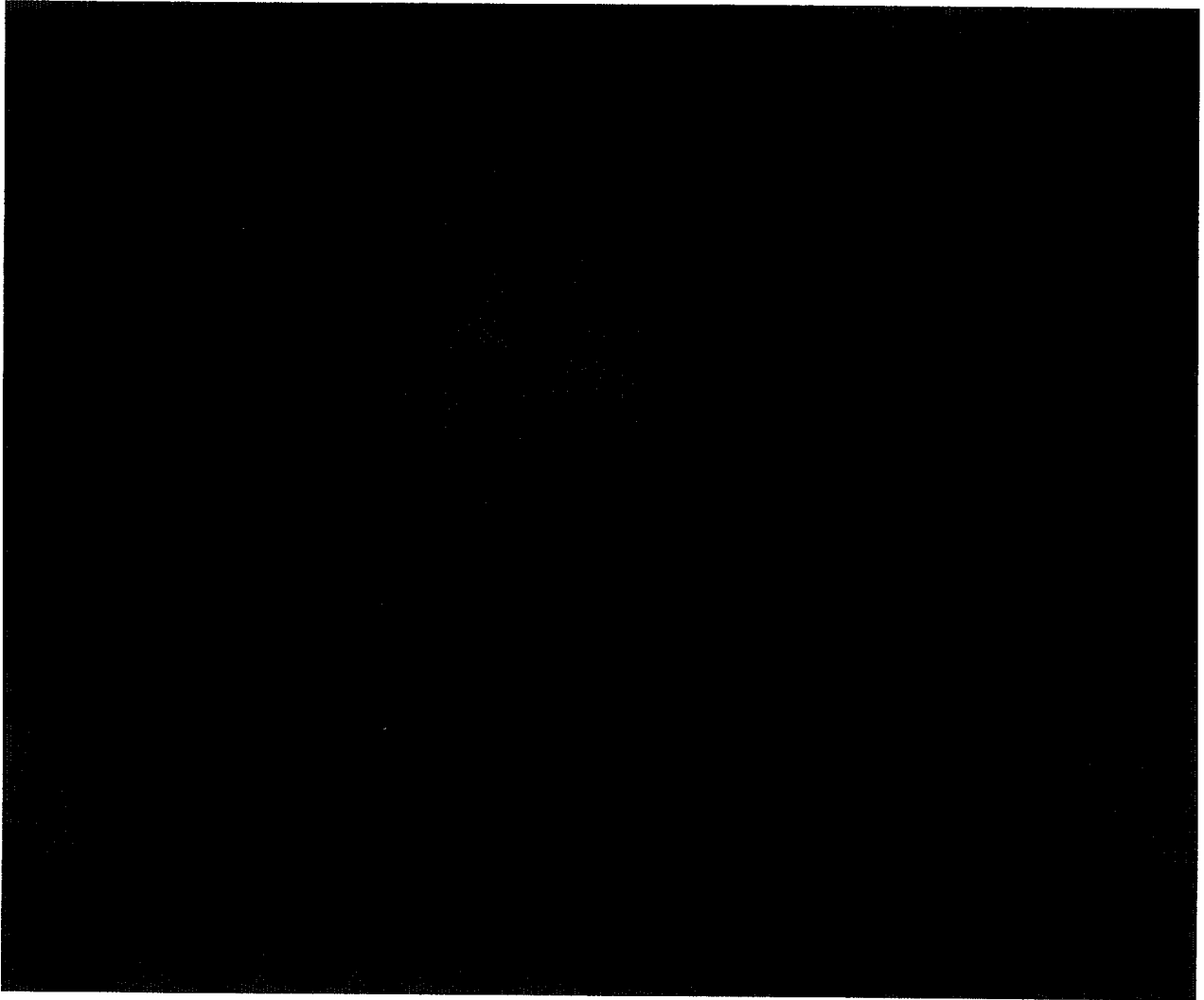
the target spectrum. In this topical report, the single time history option allowed by SRP 3.7.1 is chosen to define the input seismic time histories.

Three time-histories (two horizontal and one vertical), each of twenty-second duration, have been generated from the appropriate response spectrum shown in Figure 5.1. Figures 5.2 through 5.4 show the three accelograms pictorially. The response spectrum comparisons for the three time-histories are illustrated in Figures 5.5 through 5.7 (figures showing Power Spectral Density (PSD) comparisons have been omitted for brevity). As previously discussed, the three time histories are considered to act at the top surface of the ISFSI pad.

Even though the three time-histories are generated from essentially the same spectrum, they are statistically independent. The conventional criterion for statistical independence, namely, $\hat{a}_{ij} \neq 0.15$ (where \hat{a}_{ij} = cross correlation coefficient between accelogram i and j; $i, j = 1, 2, 3$), is found to be satisfied.

Three components of earthquake ground motion satisfying the design response spectrum in Figure 5.1 in the three orthogonal directions act simultaneously on the cask system. The integrity of the cask/pad interface structure and the anchoring attachments to the ISFSI pad are addressed herein once the input seismic loadings are applied in a dynamic simulation to evolve the cask response. Interface forces needed for detailed ISFSI structural design are also provided for subsequent site use and are considered as the DBE seismic load (with the designation "E") in Section 6. In addition to evaluating the effect of these interface loads on the ISFSI, the effect of the interface attachment loads on the cask structure is examined to demonstrate that the cask design bases are not exceeded.

5.2 Bounding Hydraulic, Wind, and Missile Loads



5.3 Other Loadings

NUREG-1567 [12] defines appropriate loads for the reinforced concrete pad and for adjacent steel structures. In addition to those described in Sections 5.1 and 5.2, thermal load T , accident level thermal load T_a , accident load A , wind load W , tornado load W_p , dead load D , lateral soil pressure H , and flood load F , act on the system. In Section 6, we specify the loads and

appropriate factored load combinations that are considered in the design. The loaded cask is considered as a live load in accordance with NUREG-1567.

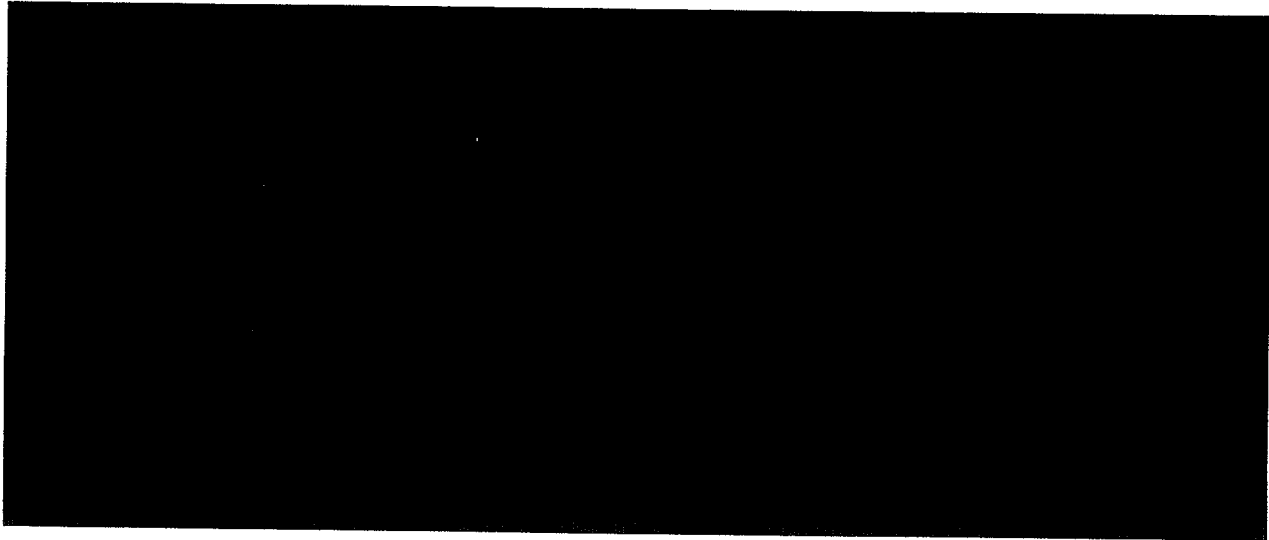
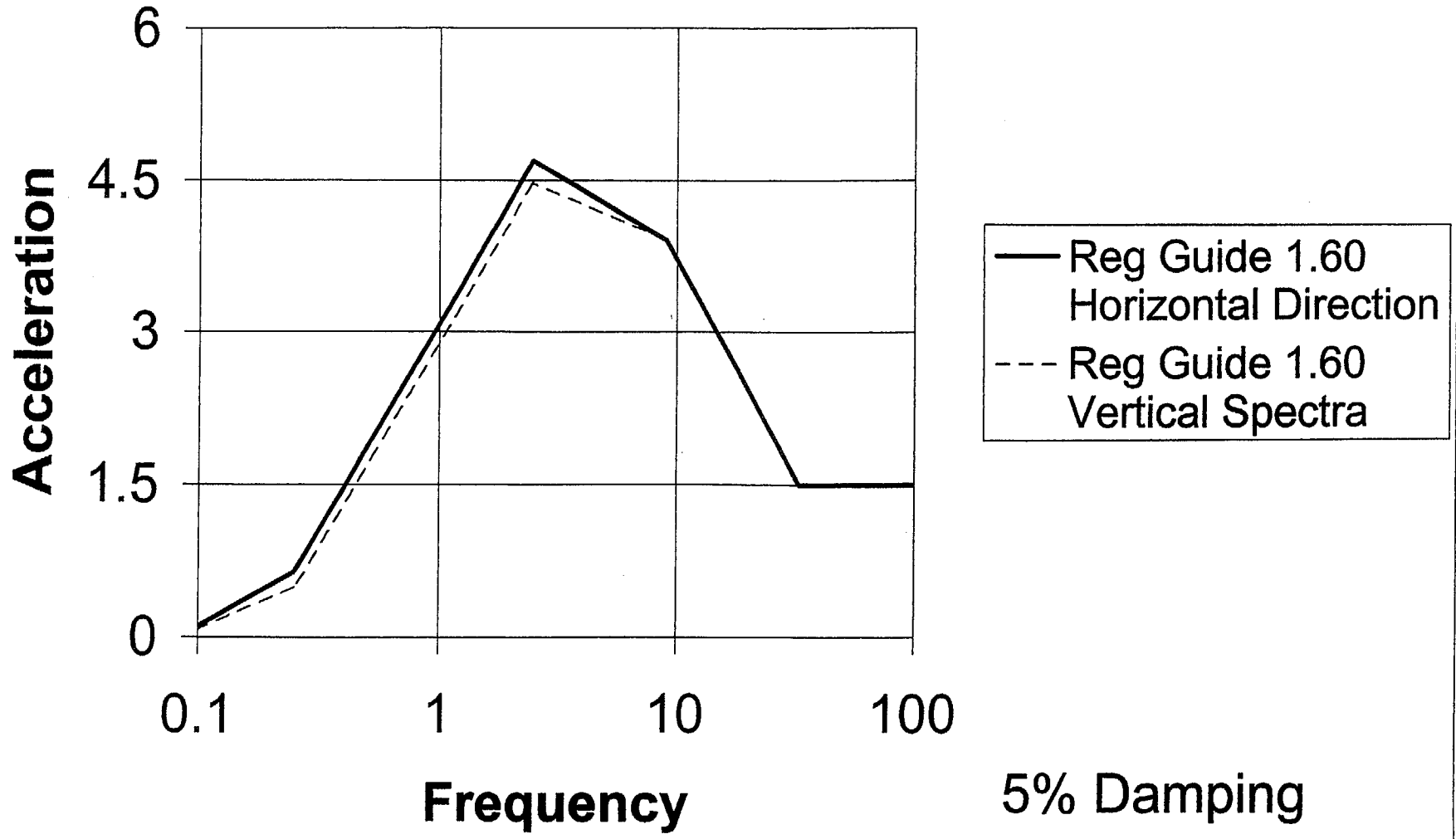


Figure 5.1; Reference Response Spectra



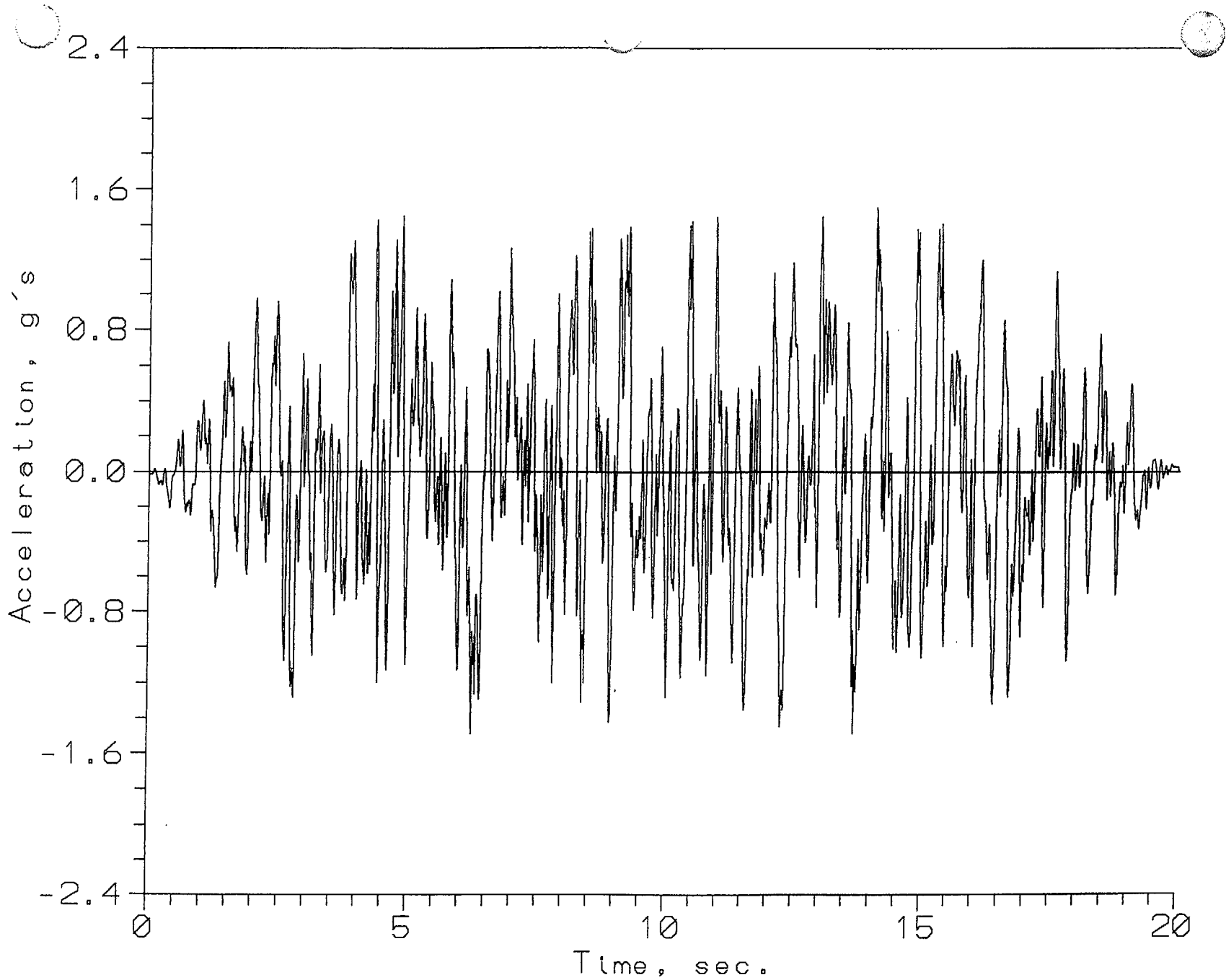


FIGURE 5.2; Synthetic Acceleration Time-History
ACCELT.H1, Synthesized from Reg. Guide 1.60
Horizontal Response Spectra for a Bounding 1.5g ZPA

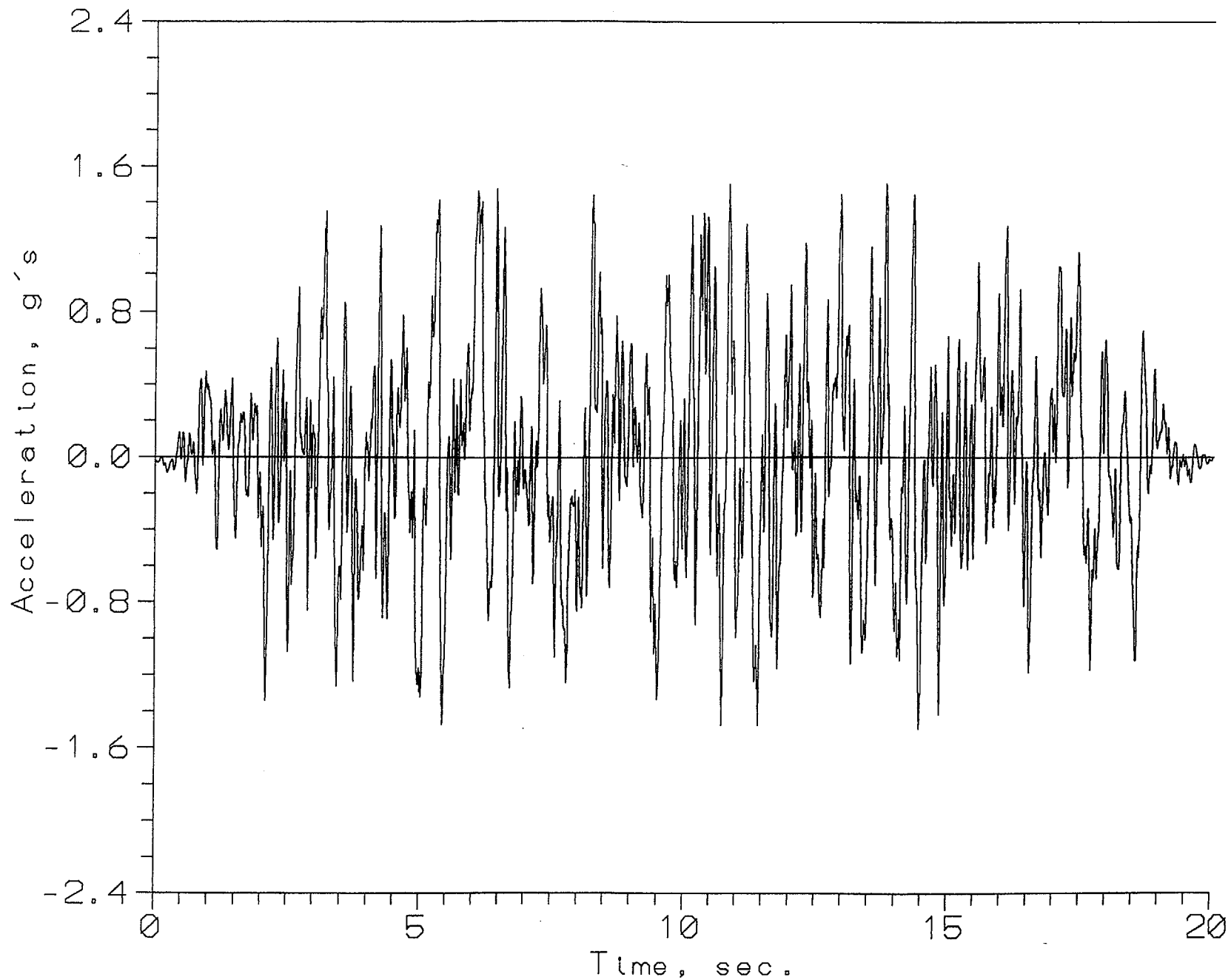


FIGURE 5.3; Synthetic Acceleration Time-History
ACCELT.H2, Synthesized from Reg. Guide 1.60
Horizontal Response Spectra for a Bounding 1.5g ZPA

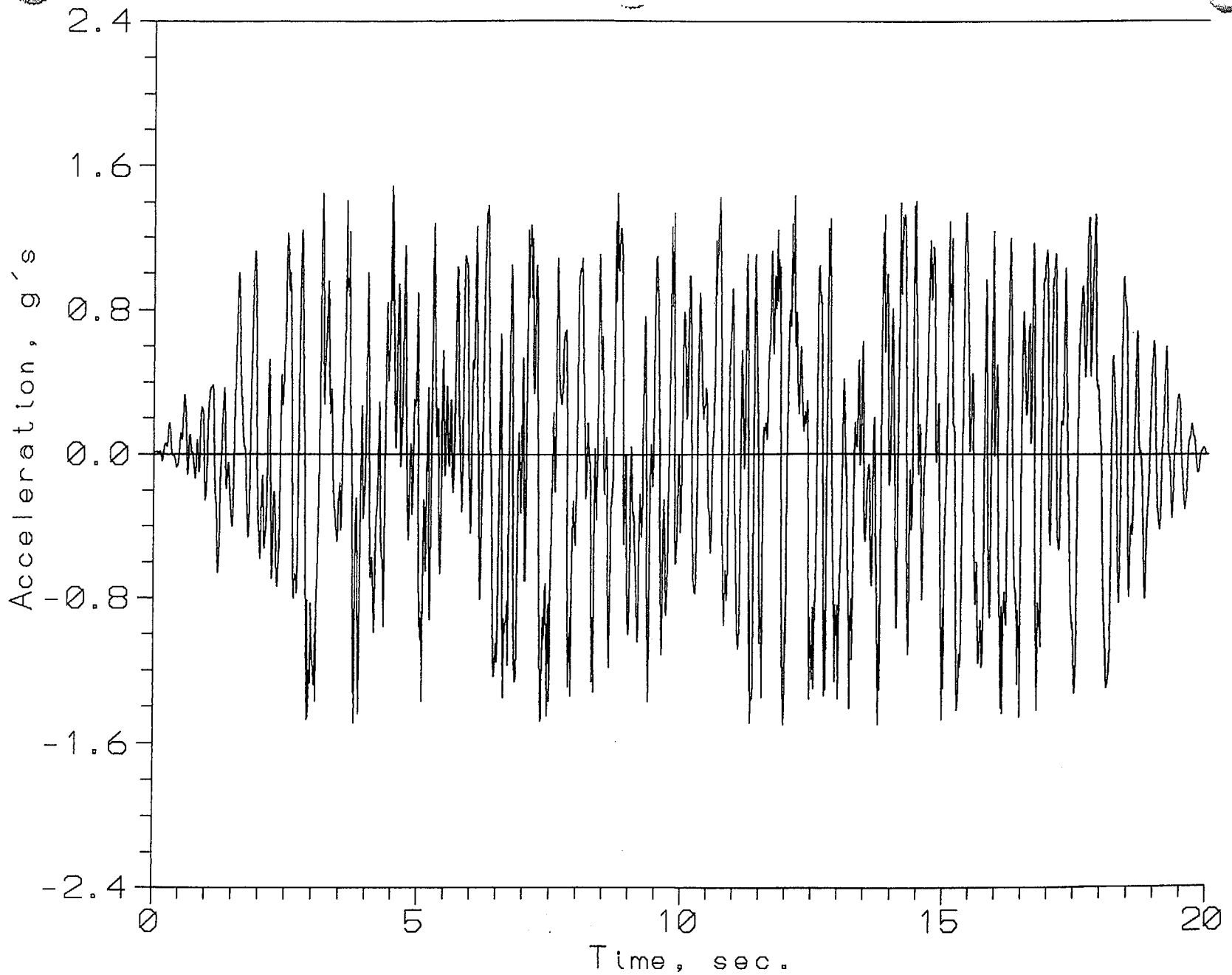


FIGURE 5.4; Synthetic Acceleration Time-History
ACCELT.VT, Synthesized from Reg. Guide 1.60
Vertical Response Spectra for a Bounding 1.5g ZPA

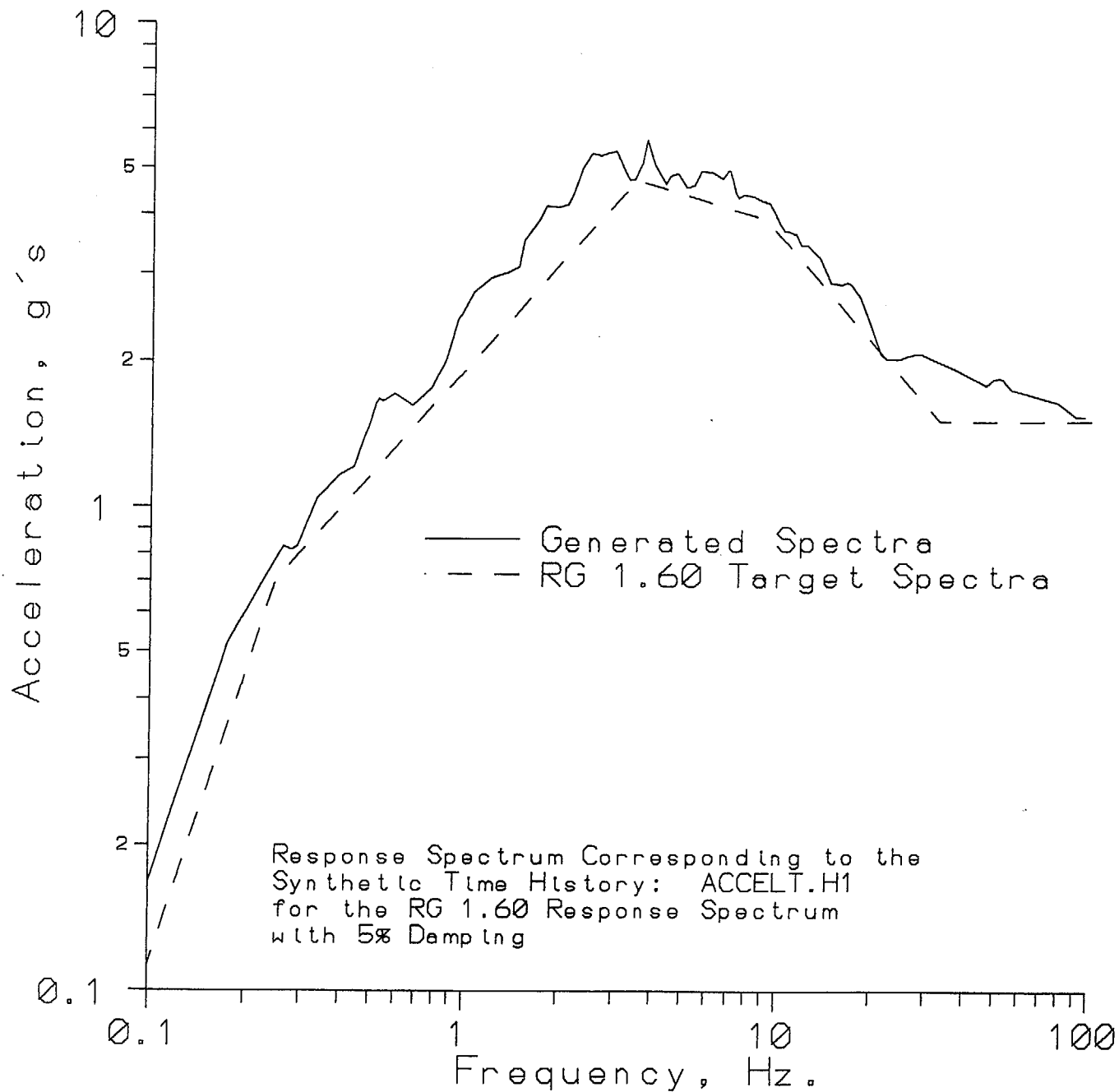


FIGURE 5.5; COMPARISON OF THE TARGET SPECTRUM WITH THE REGENERATED SPECTRUM

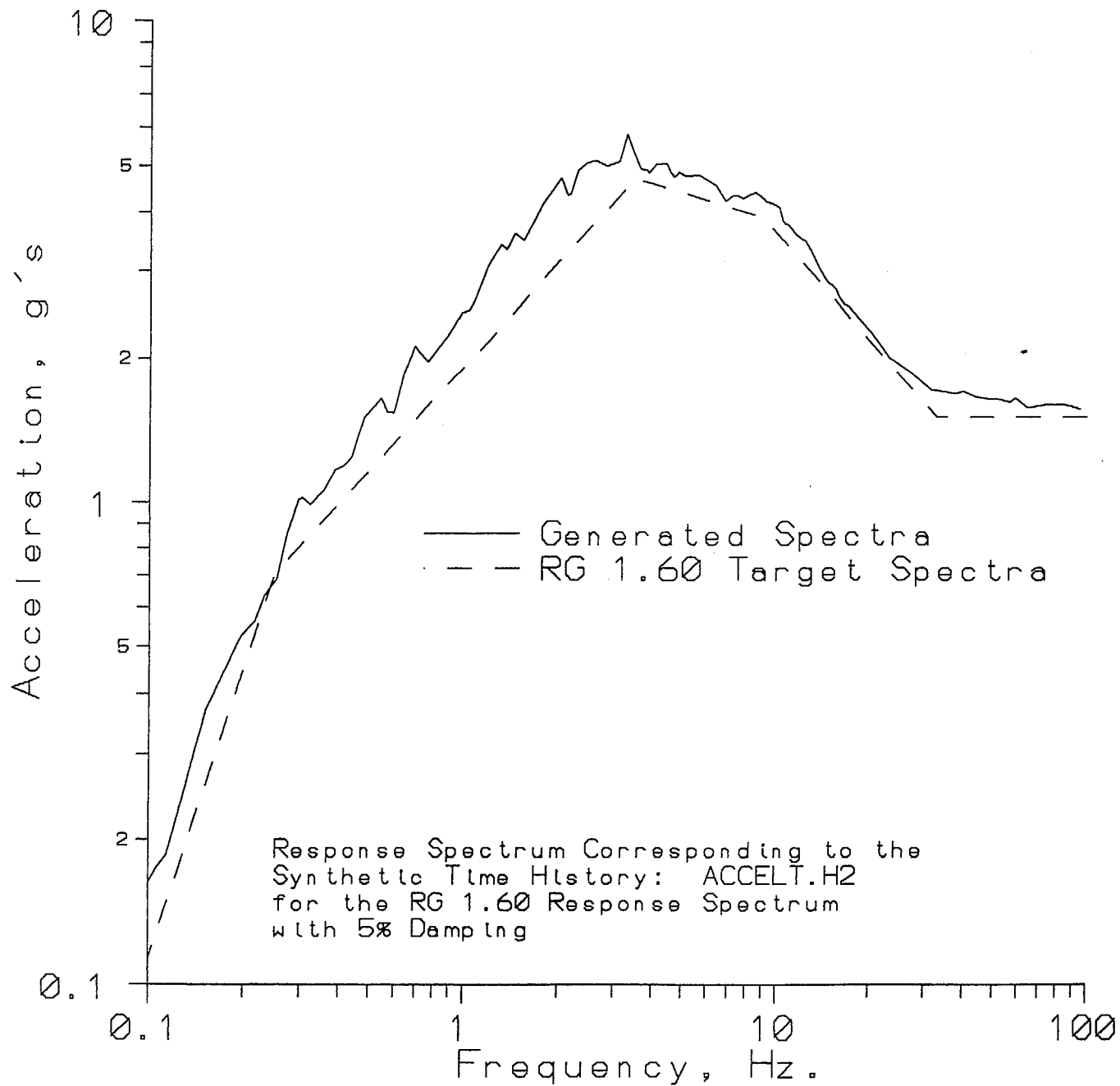


FIGURE 5.6; COMPARISON OF THE TARGET SPECTRUM
 WITH THE REGENERATED SPECTRUM

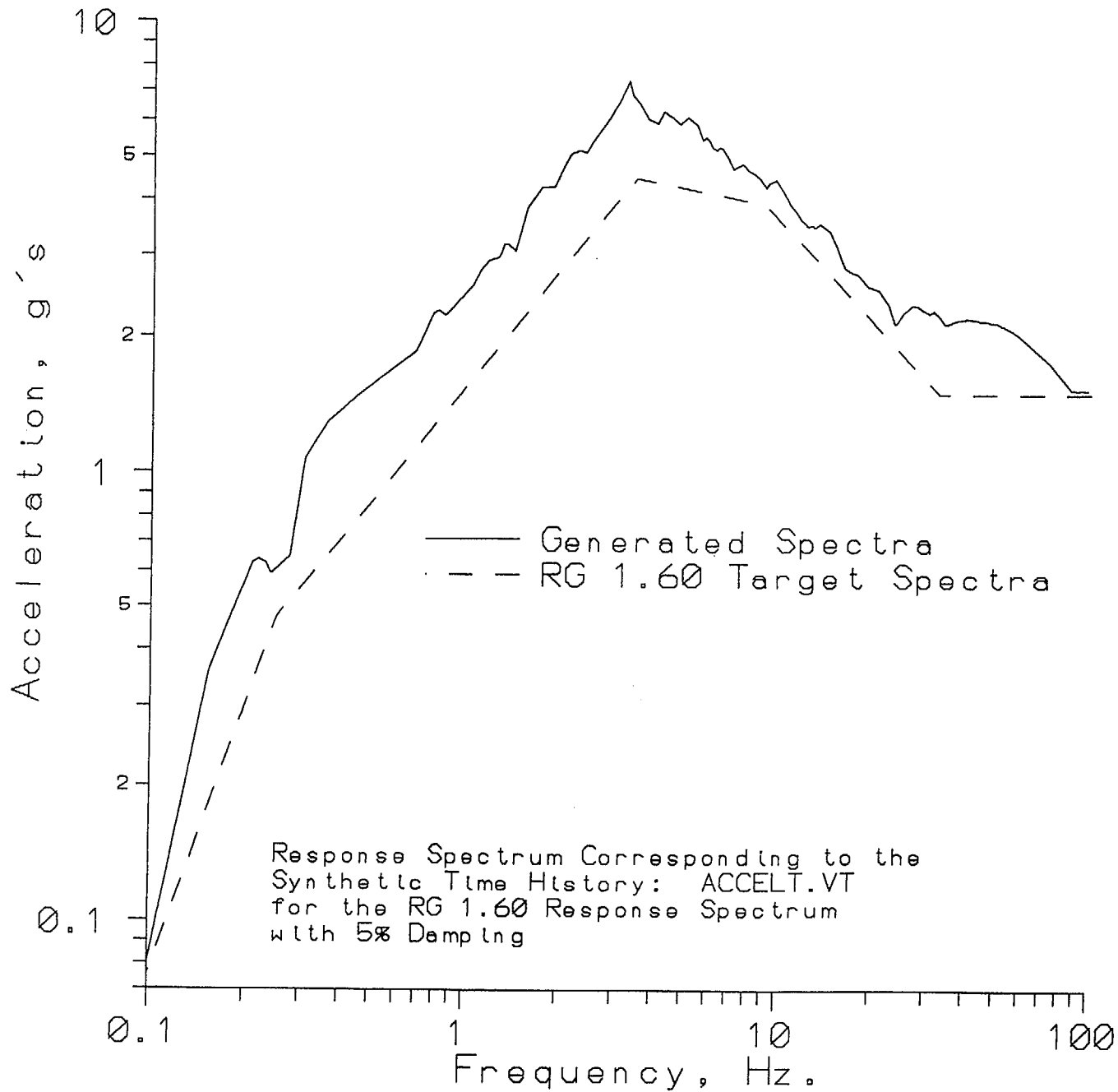
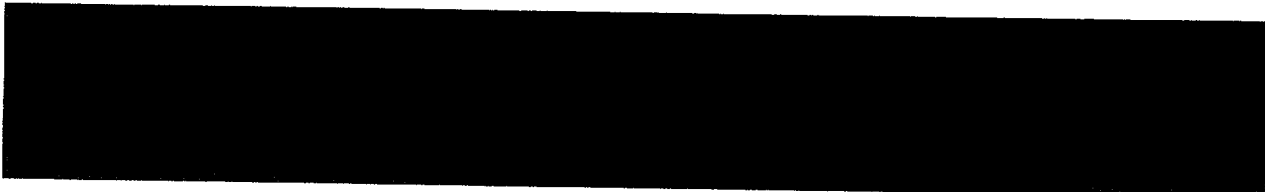


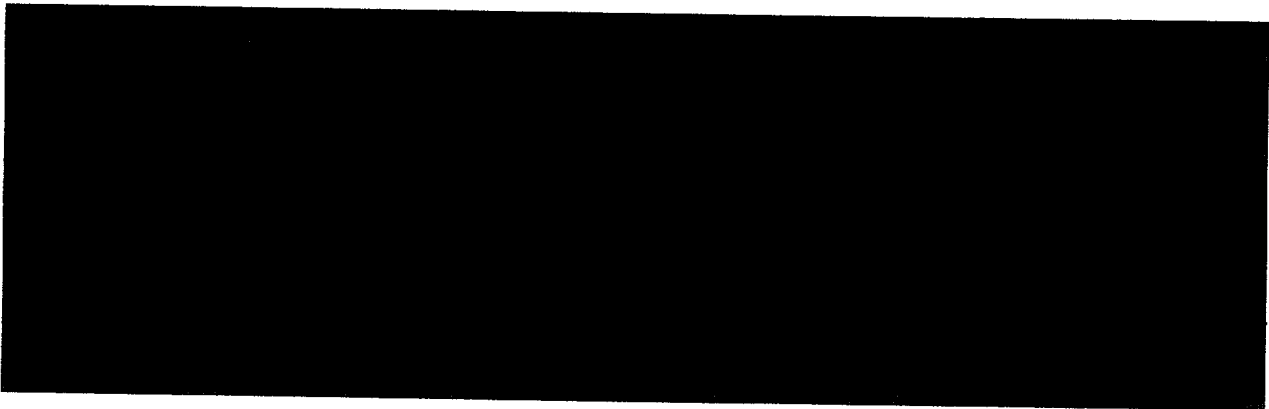
FIGURE 5.7; COMPARISON OF THE TARGET SPECTRUM WITH THE REGENERATED SPECTRUM

6.0 FACTORED LOADS

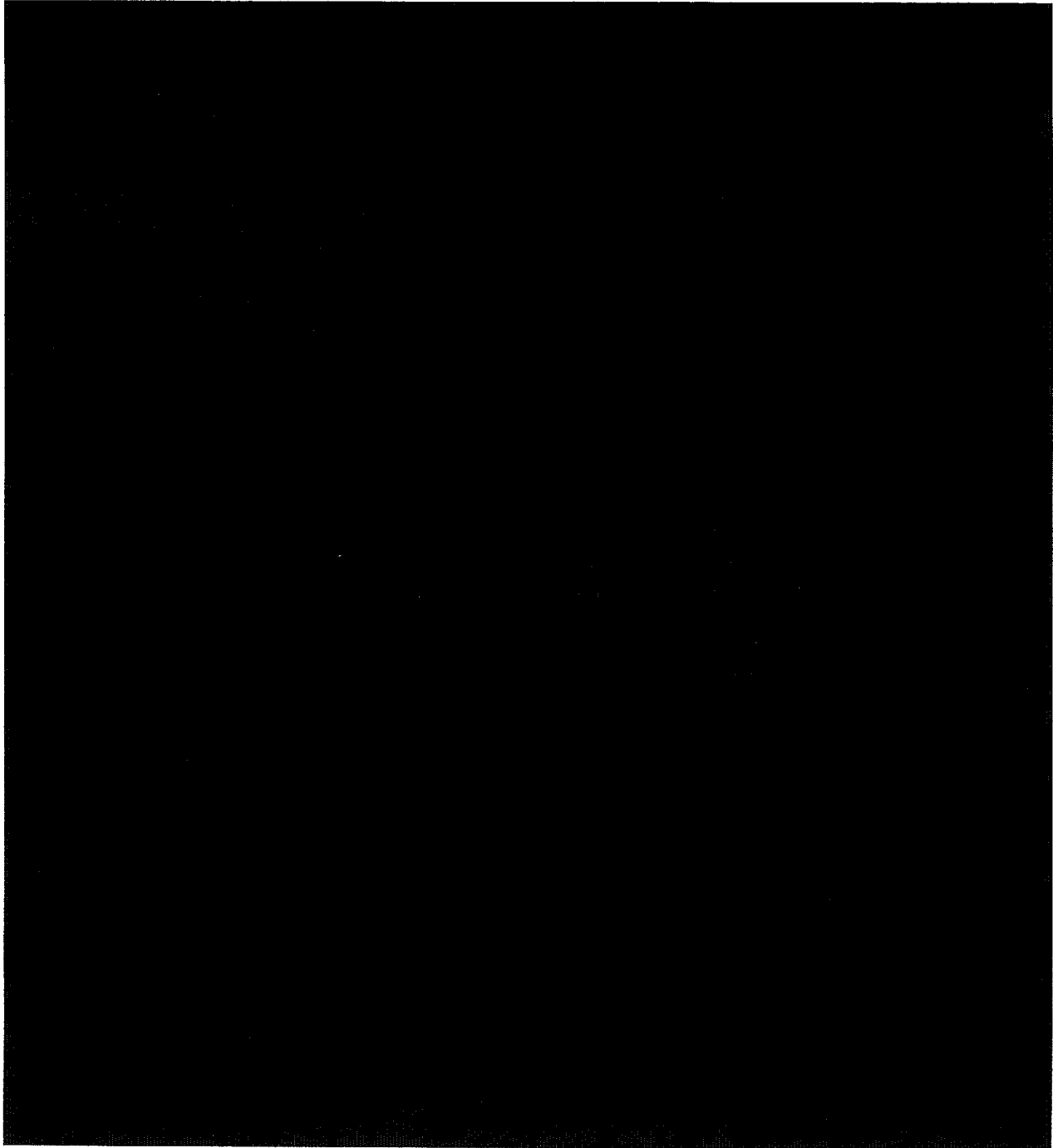
Factored load combinations for ISFSI pad design are provided in the design code ACI-349 [13] and NUREG-1567 [12]. The factored loads applicable to the pad design consist of dead weight of the cask, thermal gradient loads, impact loads arising from handling and accident events, external missiles, and bounding environmental phenomena (such as earthquakes, wind, tornado, and flood).

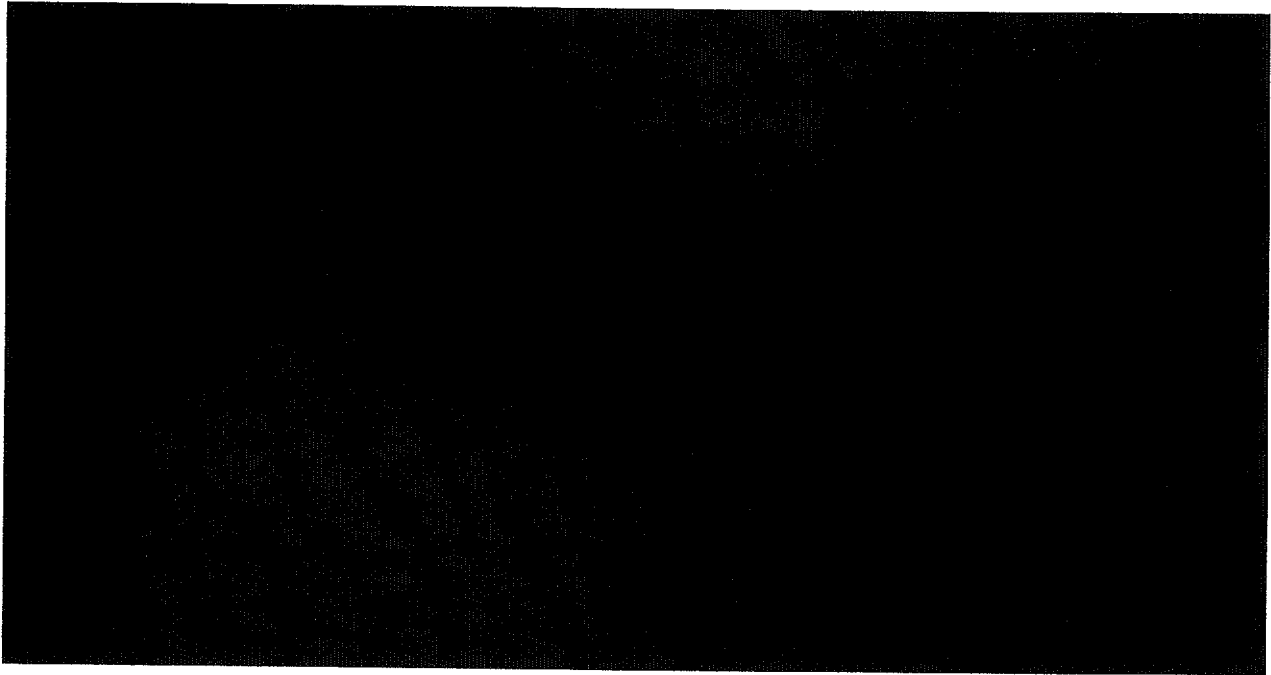


6.1 Definitions

- D = dead load
 - L = live load
 - W = wind load
 - W_t = tornado load
 - T = thermal load
 - F = hydrological load
 - E = DBE seismic load
 - A = accident load
 - H = lateral soil pressure
 - T_a = accident thermal load
 - U_c = reinforced concrete available strength
- 

6.2 Load Combinations for the Concrete Pad

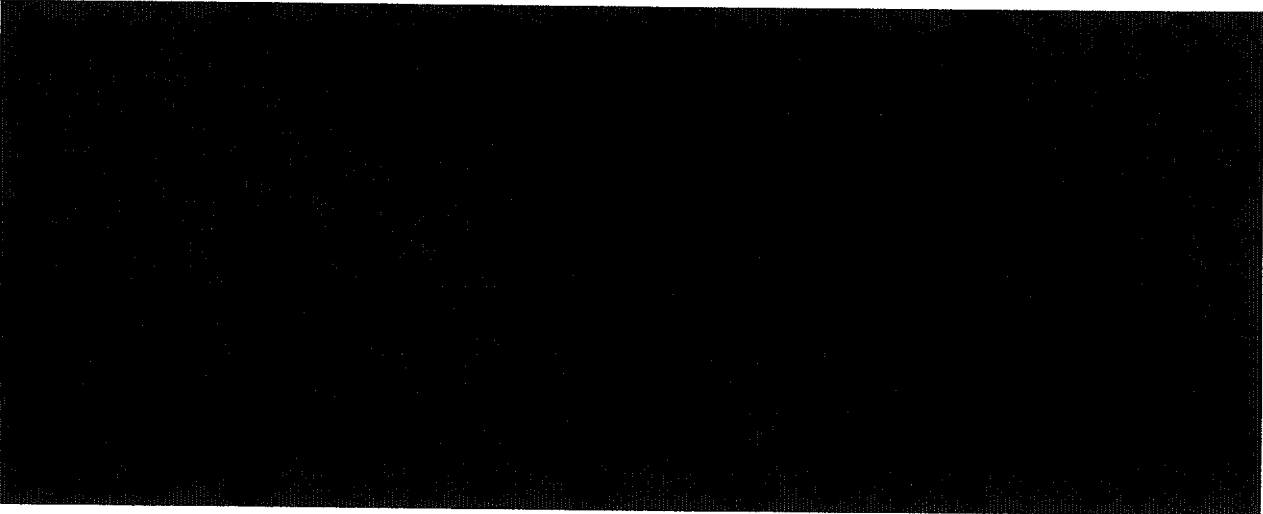




The structural integrity of the slab using the bounding set of load combinations is presented in Section 11.6 of this topical report.

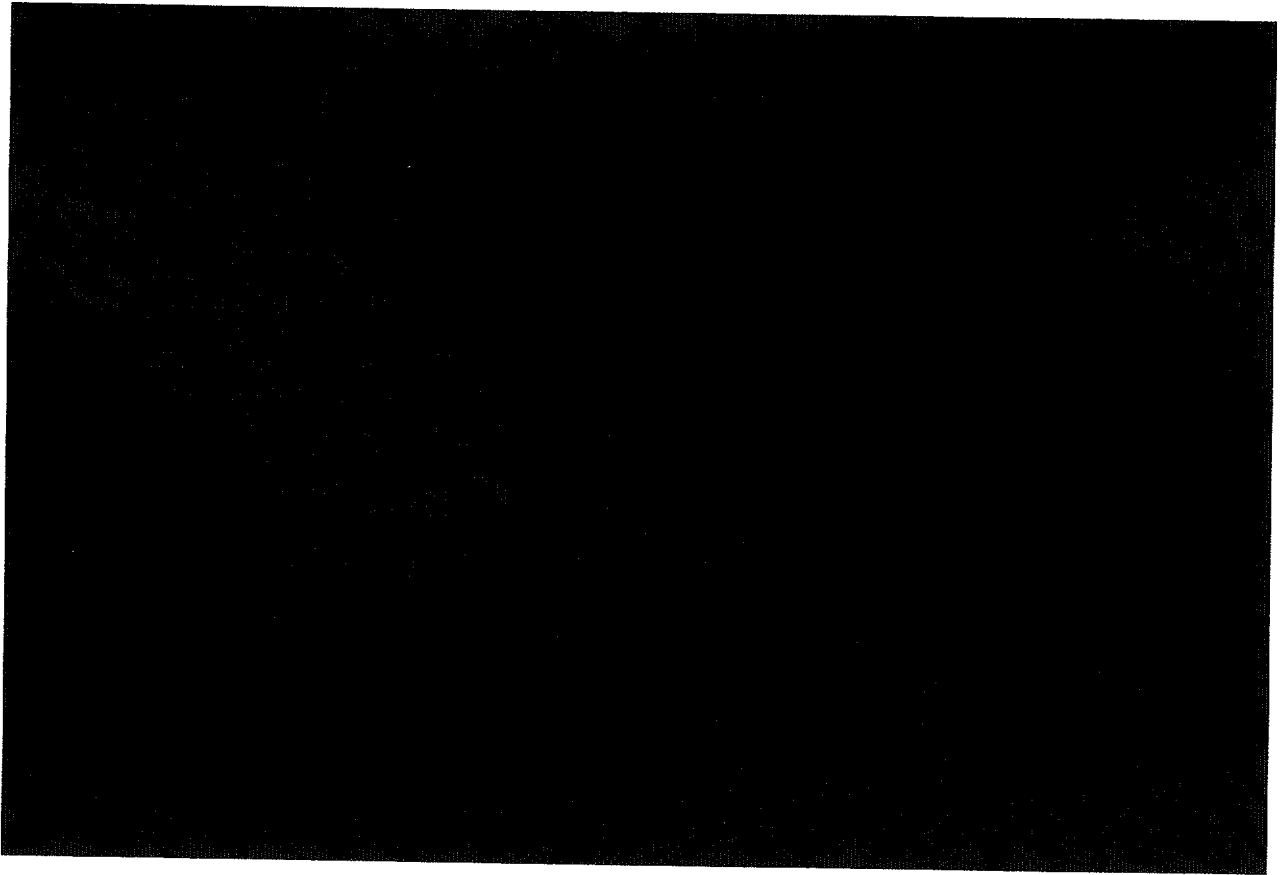
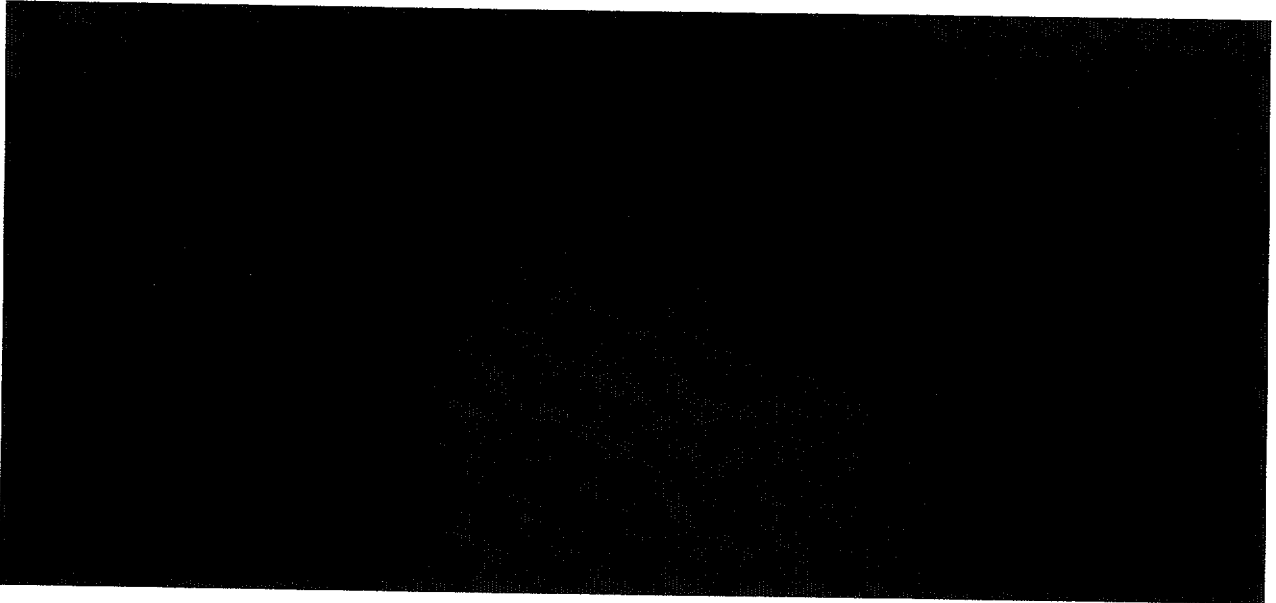
6.3 Load Combinations for the Steel Attachment Structure

The notation and acceptance criteria of NUREG-1567 apply.



† S and S_v are defined in Table 7.1, page 7-48 of Reference 12.

7.0 HI-STAR 100 ANCHOR SYSTEM



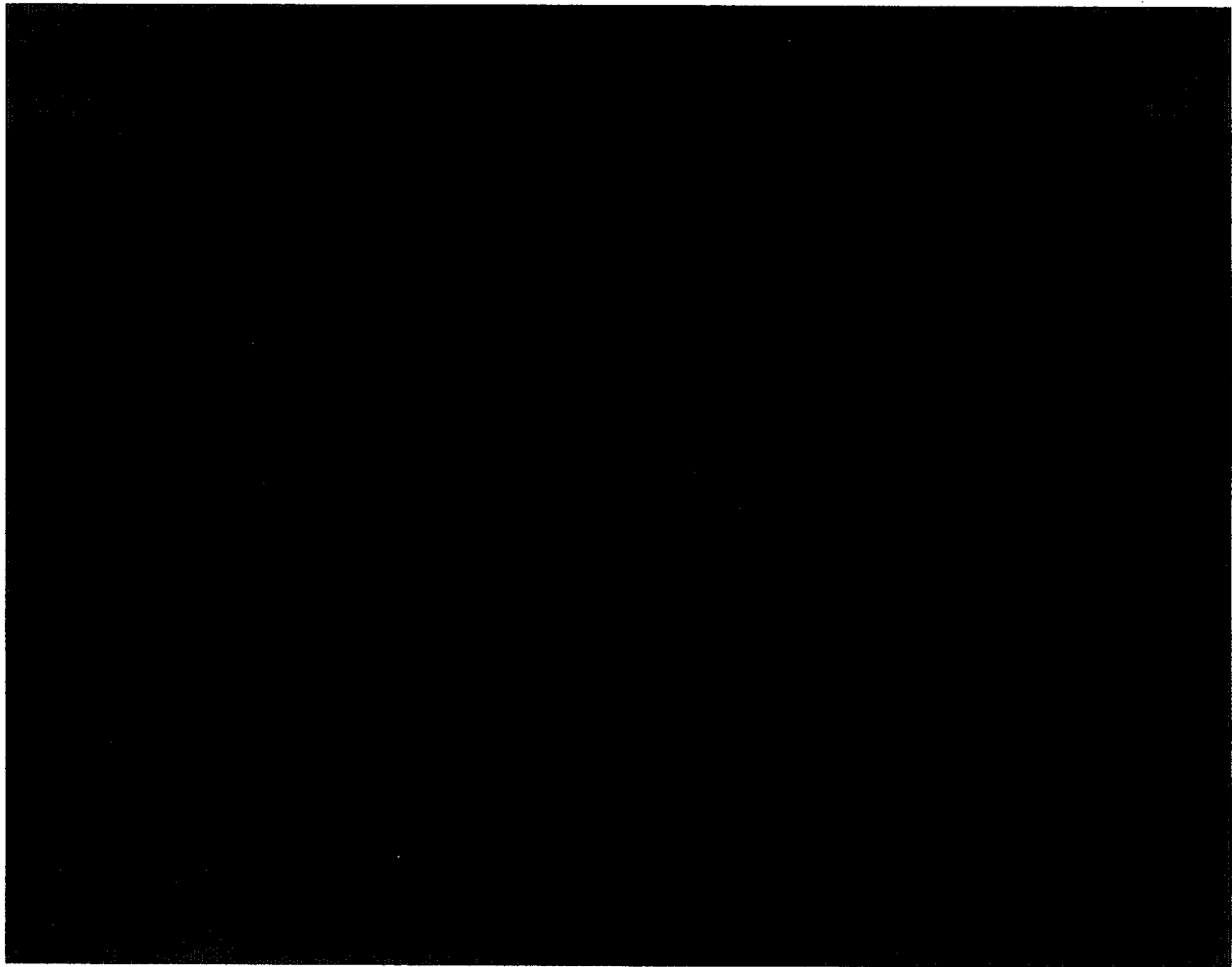


FIGURE 7.1
HOLTEC PROPRIETARY

FIGURE 7.2

HOLTEC PROPRIETARY

FIGURE 7.3
HOLTEC PROPRIETARY

FIGURE 7.4

HOLTEC PROPRIETARY

FIGURE 7.5

HOLTEC PROPRIETARY

FIGURE 7.6
HOLTEC PROPRIETARY

FIGURE 7.7
HOLTEC PROPRIETARY

8.0 HI-STORM 100 ANCHOR SYSTEM

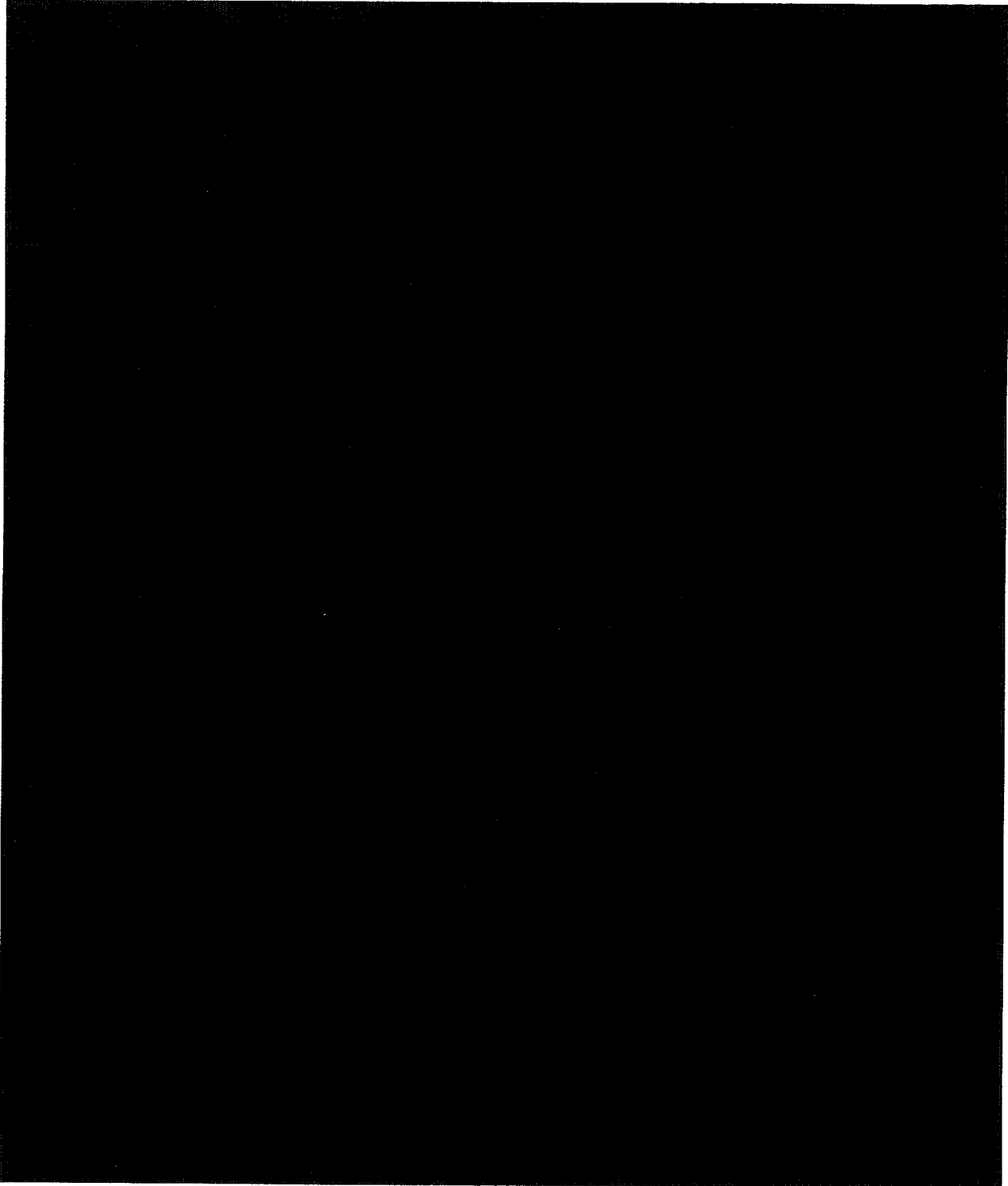




FIGURE 8.1

HOLTEC PROPRIETARY

FIGURE 8.2
HOLTEC PROPRIETARY

FIGURE 8.3

HOLTEC PROPRIETARY

FIGURE 8.4
HOLTEC PROPRIETARY

9.0 STRUCTURAL MATERIALS AND STRESS LIMITS

9.1 HI-STAR 100 Clevis Support Blocks and HI-STORM 100 Sector Lugs

Depending on the "minimum[†] daily average temperature" for a site, the following materials of construction are permissible.

Minimum Daily Average Temperature	Allowable Materials
Greater than 20EF (>20EF)	A36, A515, Gr. 70 or A240-304
Greater than 0EF, but less than 20EF	A515, Gr. 70 or A240-304
Below 0EF	A240-304

9.2 Fasteners

Fastening HI-STAR 100 to the ISFSI involves two sets of bolts. The anchor bolts that connect the clevis assemblage base plate to the concrete pad are made of A-490 anchor bolt material. For the bolts joining the clevis to HI-STAR 100, candidate materials are A193-B7, A564-630 (precipitation hardened), or SB-637-N07718. The final choice for bolt material is based on the structural analysis in Section 11.

Fastening HI-STORM 100 to the ISFSI involves multiple bolts at each sector lug location. A-490 bolting material is designated for these bolts.

Bolting material selection involves the following considerations. A-490 has been selected because of its excellent creep and weather resistance properties demonstrated through decades of use in anchoring applications at chemical, petroleum, and pharmaceutical plants. Likewise,

[†] Should be the 20-year minimum from the National Oceanographic and Atmospheric Administration database.

A193-B7 and A564-630 materials have an excellent performance record in pressure vessel closure applications. Finally, SB-637-N07718 material is currently used for the HI-STAR 100 overpack lid closure bolt.

Table 9.1 provides material strengths for the structural integrity evaluation of the fasteners performed in Section 11 of this report. The design temperature is set at 200 degrees F for all bolting materials used for attachment of HI-STAR 100 to the clevis.

Table 9.1 MATERIAL STRENGTH PROPERTIES		
Material	Yield Stress (ksi) F_Y	Ultimate Strength (ksi) F_u
A-490	104.0 [†]	66.0 [†]
A564-630 (precipitation hardened at 1075EF)	115.6	145
SB637-N07718	144.0	177.6
A193-B7	98.0	116.7

9.3 Allowable Stresses

Reference [20] is adopted to define the allowable stresses for the clevis components. Increases in allowable stresses for certain load combinations are noted in Chapter 6. Reference [13] is adopted for steel embedments in the ISFSI and for the anchor bolts to the reinforced concrete pad. Allowable stresses for the bolt material forming the third component of the clevis and threaded into the lower forging of the HI-STAR 100 are defined in Reference [22] in terms of the material yield and ultimate strengths.

[†] These are allowable stress values for tension and shear in anchor bolts in concrete are based on 80% of the ultimate strength and 55% of the maximum allowable yield strength per Reference 13, B.6.

10.0 DYNAMIC ANALYSIS OF THE CASK

As discussed in Section 5, the governing environmental loading specified for the HI-STAR 100 and HI-STORM 100 systems is a smoothed response spectrum anchored at 1.5g ZPA. The applied earthquake consists of three above-mentioned spectra applied in the three orthogonal directions. A static evaluation of the cask response focuses only on the ZPA of the seismic event and essentially neglects the balance of the spectrum. This approach would be acceptable and accurate if the cask system were a single rigid body rigidly attached to the pad. Unfortunately, the MPC canister, housed inside the cask, is a discrete free-standing body with substantial inertial mass. The lack of a physical connection between the cask and the MPC, and the presence of a "gap" between them, renders the cask system, even when anchored, a non-linear structure. With this configuration, a static solution provides, at best, an independent check on the magnitude of reaction loads. Results from such static evaluations are reported in Section 10.3.

Recognizing the geometric non-linearity of the cask systems (HI-STAR 100 and HI-STORM 100), it is necessary that a non-linear dynamic analysis approach be utilized to determine the structural response of the loaded cask. For this purpose, the response spectrum is converted into equivalent accelerograms in three orthogonal directions in Section 5. In this section, a time-history analysis of the two cask systems is carried out with three orthogonal input acceleration time-histories applied at the cask-pad interface. The time-history analysis provides the key response parameters (viz. the anchor connection load, cask centroid movement, etc.), as a function of time. The peak values of reactions are used in the subsequent stress analysis of the anchor attachments and in the structural adequacy assessment of the pad. Results of the time history analysis are presented in Section 10.1 for the HI-STAR 100 System and in Section 10.2 for the HI-STORM 100 System.

Complementing the time-history analysis (which is truly non-linear), a response spectrum analysis is also used as a confirmatory check on the results obtained from the former. Since the response spectrum analysis pre-supposes a geometrically linear structure, the MPC and its contents is simulated as rigidly attached to the cask in this analysis and the entire system quantified by

appropriate mass and mass moments of inertia. By the nature of the model, the response spectrum analysis cannot yield any information concerning the interaction loads between overpack and MPC; however, the solution provides slab reaction loads that can be compared with the actual loads from the time history simulations. The results from a linear response spectrum analysis of the HI-STAR 100 system (considered as a single rigid mass with appropriate inertia properties supported by linear springs on ground) are presented in Section 10.1.2.

10.1 Dynamic Analysis of HI-STAR 100

Appendix A to this report contains a summary of the dynamic analysis methodology and the modeling of the HI-STAR 100 System simulated as a 23 degrees of freedom structure. The dynamic analysis procedure described in Appendix A provides global forces (i.e., cask-to-attachment system interface load and fuel rattling load), as a function of time. The maximum values of the interface loads are then used as inputs for subsequent structural integrity evaluation of the cask-to-pad connection structure in Section 11.

10.1.1 Time History Analysis of the HI-STAR 100 System

As described in Appendix A, the dynamic model for the 3-D time history analysis of a HI-STAR 100 consist of a twenty-three (23) degree of freedom lumped mass system. The structure connecting the cask to the ISFSI is modeled by a series of discrete compression-only, tension-only springs, and a series of linear springs that describe the behavior of the clevis construction under compressive, tension, and shear loads arising from the interface loads that provide resistance to motion of the HI-STAR 100 System. The details of the model are fully developed in a series of appendices to this topical report. Appendix B provides mathematical details leading to the values used for the “spring constants” that simulate the effect of the eight clevis components that serve to transfer the dynamic reaction to the ISFSI. Appendix C documents the calculation of the mass matrix for the HI-STAR 100 dynamic model. Appendix E provides mathematical details of the conservative estimate of spring constants for the compression-only spring elements that simulate contact between internal components of the HI-STAR 100 system.

The dynamic model is solved using the proprietary time history analysis code DYNAMO[9] and the cask movements and interface forces archived over the duration of the event. The dynamic analysis code DYNAMO has been utilized over the past eighteen years in the design and licensing of spent fuel storage racks and a considerable knowledge base has been amassed concerning appropriate time stems to achieve convergent results. Using an appropriate time step, the dynamic analysis is performed for the dry cask configuration using nominal fuel-to-fuel basket wall gap (within the MPC) and MPC-to-overpack gap, and for two additional configurations where the magnitude of the gaps is altered slightly to encompass tolerances in fabrication and in positioning.

The dynamic simulations of the HI-STAR 100 System attached through the clevis system to the ISFSI pad are summarized in Table 10.1 where run identifiers and gap conditions are defined. Table 10.2 presents key results from each of the analyses for use in structural qualification of the clevis system and the anchor bolts into the pad. Of particular import are the maximum values for the bolt forces and for the compression loads.

Table 10.1 HI-STAR 100 Dynamic Analyses

Run Identifier	MPC-overpack radial clearance (inch)	Fuel-Fuel Basket Wall Nominal Clearance (inch)
250	0.188	0.20
251	0.188	0.11
252	0.150	0.11

Table 10.2 Key Results for HI-STAR 100 Structural Qualification

Output Quantity	Run 250	Run 251	Run 252
Maximum displacement in X direction (Coordinate q_1 in Figure A.1)(inch)	0.150	0.154	0.142
Maximum displacement in Y direction (Coordinate q_2 in Figure A.1)(inch)	0.148	0.151	0.152
Maximum displacement in Z direction (Coordinate q_3 in Figure A.1)(inch)	0.033	0.033	0.033
Max. Tension in Clevis Bolt (kips)	352.3	352.2	356.3
Max X Shear in Clevis Bolt (kips)	94.9	86.6	90.8
Max. Y Shear in Clevis Bolt (kips)	99.0	93.6	89.5
Max. Compression Force at a single location (kips)	294.0	310.5	308.1
Bounding Max. Compression on any Clevis (kips) [†]	508.3	542.4	577.6
Total Bounding MPC-Overpack Horizontal Impact Force (kips)	1157.6	1264.5	1117.2

As a confirmatory check on the size of the time step chosen for the dynamic analyses, two additional simulations, differing only in the magnitude of the time integration step, are performed to confirm convergence. Table 10.3 presents results of the convergence studies where dynamic simulations using the system model are performed using different time steps. Results are presented below for the maximum values (over the entire 20 second event time) of the mass center of the cask displacement, for a typical bolt tensile and shear force maximum value, for a

[†] Sum of results from three compression elements that simulate the compression behavior of any clevis or additional compression block.

typical compression spring force representing a compressive bearing load transfer location to the foundation, and for the compression-only spring elements tracking impact between the MPC and the overpack as a function of time at the top of the MPC.

Table 10.3 - Results From Convergence Study

Response Item	Time step = 0.0000025 sec.	Time step = 0.00000125 sec.	Time step = 0.000000625 sec.
q_1^\dagger displacement (in.)	0.150	0.150	0.150
q_2 displacement (in.)	0.148	0.148	0.148
q_3 displacement (in.)	0.033	0.033	0.033
Clevis Bolt tension (kips)	352.3	352.3	352.3
Clevis Bolt shear (kips)	99.0	99.0	99.0
Typical Clevis Bearing Spring (kips)	294.0	294.0	294.0

The identical results for each time step considered in Table 10.3 confirm that Table 10.2 presents appropriately converged information.

Force results from Table 10.2 are used in Section 11 to demonstrate that the attachment system connecting the HI-STAR 100 cask to the ITS ISFSI pad meets the structural integrity requirements set forth in this document.

The time history results from each of the simulations are archived for subsequent postprocessing analyses. For example, Figures 10.1 and 10.2 show the time histories of the net vertical force on

[†] See Figure A.1 in Appendix A for location and direction of components q_i

the overpack base from the totality of bearing reactions and bolt tensile reactions, and the net horizontal force from the totality of shear forces acting on the bolts, respectively. Results are shown for Case 251. By dividing by the weight of the loaded HI-STAR 100, we can determine the net “g” forces acting on HI-STAR overpack due to the imposed 3-D seismic time histories. For the total cask weight of 250,000 lb., the net ‘g’s” on the overpack are:

Vertical Acceleration = 11.31g’s

Horizontal Acceleration = 3.06g’s.

This maximum “g” force is a compression force on the ISFSI pad. We note that Figure 10.1 demonstrates that there is no global uplift force on the slab at the cask/pad interface. In other words, there is always a net positive compression force on the ISFSI pad. Figure 10.1 shows that at approximately 10.88 seconds, the net compressive force is minimized. Examination of the archive files shows that at this time instant, the maximum tensile forces occur in the clevis pins. The actual load distribution on the compression surfaces and the tension capable clevis’s results in six of the eight tension capable clevis attachments being subject to tension loads, and all of the compression load resisted by four compression bearing surfaces. An instantaneous “neutral axis at the interface is evident and at this instant in time, the interface is subject to the maximum moment tending to overturn the cask.

From Table 10.2, the maximum horizontal impact load applied at the overpack-MPC interface is divided by the total MPC weight to determine the “g” loading on the MPC. Based on the weight used in the dynamic model (90,000 lb.) for the MPC, the effective lateral acceleration imparted to the MPC is 14.1g’s.

The effect of the “rattling” of the MPC during the seismic event is clearly evident.

From these results, it is concluded that the design basis deceleration limit set in the TSAR remains bounded by a large margin when HI-STAR 100 is attached to the ISFSI and subjected to

the bounding seismic loads imposed herein. Therefore, anchoring HI-STAR 100 does not lead to decelerations of the internal components of the system that exceed the design basis limits set in the TSAR for HI-STAR 100.

10.1.2 Confirmatory Response Spectrum Analysis of HI-STAR 100

In addition to the time-history analysis, a response spectrum analysis of the anchored cask system is performed. The purpose of this response spectra analysis is to provide an independent, albeit approximate, check that the results from the rigorous time history analyses are indeed representative and correct. Since the response spectrum analysis presupposes a linear structure, the MPC canister, along with its contents, is assumed to be integrally connected to the overpack. The effect of gaps between various internal components and between the overpack and the MPC is eliminated from the analysis. The elastic compliance of the anchoring system for HI-STAR is explicitly modeled by discrete linear springs and a single spring constant is associated with the support structure at each of eight locations to simulate the tension/compression nature of the attachment. The eight compression-only blocks are not included in the response spectrum simulation.

The simple model used for the confirmatory response spectra analysis of HI-STAR 100 models only the eight clevis type supports that can resist both tension and compression. The model consists of a rigid body representation of the cask and eight sets of three linear springs (1 vertical plus 2 in the horizontal plane) connecting the rigid body to ground. Table 10.4 gives relevant parameters used for the response spectrum model.

Table 10.4 HI-STAR 100 Linear Response Spectrum Model

ITEM	VALUE
Weight (lb.)	250,000
Height (inch)	203
Vertical Spring Constant (lb./inch)	17,500,000
Horizontal Spring Constants (lb./inch)	7,370,000
Contact Diameter for Springs (inch)	83.25

The vertical spring constant is taken as the average value of three compression elements (for each of eight clevis assemblies) and one tension element (representing the tensile resistance at a clevis) as computed from Appendix B and used in the non-linear time history solution. The response spectra analysis is carried out for each direction separately with modal results combined in accordance with Square Root of Sum of Squares (SRSS) methodology. The results from each spectral direction are then combined using SRSS summation. The results of the final combination are presented in Table 10.5. Centroidal displacement and components of the spring force are presented.

Table 10.5 HI-STAR 100 Response Spectra Analysis Results - Comparison With Non-Linear Analysis Results (RunID 251)

Item	SRSS Analysis	Non-Linear Analysis
Vertical Spring Force (lb.)	383,920	542,400
Horizontal Spring Force (lb.)	59,283	93,600
Horizontal Displacement (x or y direction) of Mass Center of the Cask (inch)	0.061	0.154
Vertical Displacement (z) of Mass Center of the Cask (inch)	0.003	0.033

Comparing the results of the simplified linear response spectra analysis with the peak instantaneous results from one of the non-linear analyses demonstrates that the non-linear model

provides conservatively larger results for design analysis. The response spectrum results for vertical forces, for shear forces and for peak displacements are underestimated by the simplified response spectrum analysis.

10.2 Dynamic Analysis of HI-STORM 100

The dynamic analysis procedure described in Appendix A provides global forces (i.e., cask-to-attachment system interface load and fuel rattling load), as a function of time. The dynamic model for HI-STORM consists of 6 degrees of freedom simulating the rigid body motion of the overpack and 5 degrees of freedom modeling the motion of the MPC[†] together with its contents (the fuel and the fuel basket are assumed to move with the MPC). Since the weight of the HI-STORM overpack is approximately 50% larger than that of HI-STAR, good accuracy for global dynamic response of the overpack can be achieved without separately considering the internal (to the MPC) rattling of the smaller fraction of total mass. Figures 10.3 and 10.4 show the dynamic degrees of freedom for the HI-STORM 100 model and the simulation of HI-STORM 100-to-ground contact. Appendix F presents details of the computation of the mass and mass moments of inertia required for the dynamic model of the HI-STORM 100 system. Bounding weights are used for both the overpack and the MPC for conservative results. Appendix G presents details of the evaluation of the spring constants for the analysis. The calculations are based on the figures in Section 8 and the appropriate drawings in [4]. Compression-only elements simulate direct ground contact of the overpack. A total of 108 compression-only elements simulate the compression resistance. That is, three compression-only springs are located along radial lines every 10 degrees around the contact area with the pad. Because of the large expanse of overpack contact with the ISFSI pad surface, friction effects are included at every location of a compression spring. Two friction springs are located orthogonal to each other and normal to each of the compression springs at every compression-only spring location. The instantaneous force in each friction spring is computed using a linear spring model until the spring force exceeds a limit

[†]A bounding weight is used for the MPC plus contents.

value associated with the current magnitude of the local compression force multiplied by a coefficient of friction. If, at any instant in time, there is loss of contact between the cask and the pad, then the force in each of the two orthogonal friction springs is zeroed. Available data indicates that the coefficient of friction between steel and concrete is of the order of 0.7 (e.g., Mark's Handbook of Mechanical Engineering); however, we conservatively assume only 0.2 as a friction coefficient in order to recognize the presence of interface friction yet maximize the shear loads at the sector lugs. The four sector lugs that serve to resist uplift and horizontal movement of the overpack are simulated by tension-only vertically oriented springs and by two orthogonal linear shear springs in the horizontal plane.

The dynamic analysis (time history response of non-linear mass-spring model) provides a complete description of the interface loading over the entire event time. The maximum values of the interface loads are then used as inputs for subsequent structural integrity evaluation of the sector lug structure in Section 11.

As described previously, the dynamic model of the HI-STORM 100 System simulates compression contact with the ground by three (3) compression-only springs along radial lines from the cask bottom center point at thirty six (36) circumferential locations. The tension resistance provided by the five (5) anchor bolts at each of four (4) sector lugs is provided by two (2) tension-only vertical springs and two sets of two (2) orthogonal horizontal springs to resist shear. Therefore, each of these sets of three springs represents the structural effect of 2.5 anchor bolts in the sector lug. Similar to the presentation of the HI-STAR 100 dynamic model, appendices are included as part of this topical report with additional details of the development. Appendix G presents details of the evaluation of the spring constants for the various elements in the dynamic model and Appendix F presents details of the development of appropriate mass and mass moment of inertia properties for the eleven (11) degree of freedom HI-STORM 100 dynamic model. The dynamic model is solved using the time history analysis code DYNAMO[9] and the cask movements and interface forces archived over the duration of the event. Two simulations are carried out, differing only in the magnitude of the overpack-to-MPC lateral gap,

to establish reasonable values of interface loads for subsequent structural integrity evaluation. Based on the earlier HI-STAR 100 convergence study, a time step of 0.00000125 seconds is used for the analyses. Using this time step, the dynamic analysis is performed for the configuration using nominal MPC-to-overpack gap (Run ID 010 assumes 0.28125" radial gap between overpack inner lateral surface and outer surface of MPC canister), and for an additional configuration where the magnitude of the radial gap is reduced (Run ID 020 assumes 0.1875" radial gap) to encompass tolerances in fabrication and in positioning. Table 10.6 presents key results from the two HI-STORM 100 dynamic analyses.

Table 10.6 Key Results for HI-STORM Structural Qualification

Output Force/Deflection	Run 112	Run 113
Max. Cask Center Deflection in X Direction (inch)	0.214	0.215
Max. Cask Center Deflection in Y Direction (inch)	0.225	0.231
Max. Cask Center Deflection in Vertical Direction (inch)	0.032	0.032
Max. Tension in Sector Lug Spring (kips)	355.3	354.4
Max X Shear in Sector Lug Spring (kips)	92.1	88.8
Max. Y Shear in Sector Lug Spring (kips)	87.0	92.0
Max. Compression Force at a single location (kips)	108.2	110.9
Bounding Total MPC-Overpack Lateral Contact Force (kips)	1523.0	1342.3

Force results from Table 10.6 are used in Section 11 to demonstrate that the attachment system connecting the HI-STORM 100 cask to the ITS ISFSI pad meets the structural integrity requirements set forth in this document. We recall that the modeling technique (see Appendix G)

uses two tension springs to represent each sector lug. Each sector lug consists of five anchor bolts. Therefore, the maximum tension force reported above for a single sector lug tension spring represents the peak load resisted by 2.5 anchor bolts. An identical representation of the shear capacity of the sector lug bolts is used in the model. Therefore, the maximum sector lug forces (tension and shear) given above are multiplied by 0.4 (1/2.5) to obtain bounding forces on a single sector lug anchor bolt for design qualification.

The time history results from each of the simulations are archived for subsequent analysis. Figures 10.5 and 10.6 show the time histories of the net vertical upward force on the overpack base (equal to net compressive force on the ISFSI pad) from the totality of bearing reactions minus the sector lug tensile reactions, and the net horizontal force from the totality of shear forces acting on the bolts and friction forces at contact locations around the periphery, respectively. Results are shown for Run ID 112 where the gap clearances are the nominal clearances established from the HI-STORM 100 drawings in Section 1.5 of the TSAR[4]. As with the HI-STAR 100 results, there is no net uplift force on the pad. However, at time instants of minimum compressive force, the overall bending moment at the pad surface is maximized. It is at these time instants, that the tension resisting capacity of the slab is evaluated. By dividing by the weight of the loaded HI-STORM 100, we can determine the net “g” forces acting on HI-STORM due to the imposed 3-D seismic time histories. For the total cask weight of 360,000 lb., the net ‘g’s’ are:

Vertical Acceleration = 6.51g’s

Horizontal Acceleration = 2.58g’s

An estimate of the lateral “g” acceleration applied directly to the MPC, based on the bounding MPC weight, is obtained from the bounding value of MPC-overpack contact force and reflects the rattling of the MPC within the overpack. Using the bounding value from Table 10.6, we obtain lateral acceleration on MPC = 16.92 g’s.

From these results, it is concluded that the design basis deceleration limit set in the TSAR is not exceeded when HI-STORM 100 is attached to the ISFSI..

10.3 Confirmatory Static Analyses for HI-STAR 100 and HI-STORM 100

We consider the cask system to be a rigid body having known mass and center of mass elevation. The rigid body loaded by inertia forces at the mass center that are proportional to the horizontal and vertical ZPA of the response spectra. The cask system is assumed rotating about one point on the outer edge of its contact circle. The resistance to rotation is provided by stretching of all of the tension-resisting elements at the cask/attachment assembly interface. The assumption of a rigid cask permits the tension resisting forces to be expressed in terms of a single unknown parameter. Moment equilibrium about the single point of compression contact determines the unknown tension force parameter and therefore determines the maximum tensile force in terms of cask geometry and applied loading. Appendix D contains details of this static analysis for HI-STAR 100 assuming eight clevis attachments; Appendix I contains results of a similar solution for HI-STORM 100 with four sector lugs. Table 10.7 presents results for maximum static tension force for each case. Also reported in Table 10.7 are results from the values in Tables 10.2 and 10.6 from the true non-linear time history analyses for HI-STAR 100 and HI-STORM 100, respectively

Table 10.7 Maximum Bolt/Anchor Stud Tension Force

ITEM	STATIC ANALYSIS	DYNAMIC ANALYSIS
HI-STAR 100 Tension in Single Connecting Bolt to Overpack Base Plate (lb.)	245,300	356,300
HI-STORM 100 Tension in One Anchor Bolt [†] (lb.)	128,900	142,120

[†] Value for Sector Lug Spring in Table 10.6 is multiplied by 0.4

From Table 10.7 results, we again see that the effects of the non-linear components of the cask and structure play a significant role in the analysis. The static solution underestimates the tensile forces in the respective attachment components.

We conclude that the most conservative evaluation of the structural integrity of the attachment structure for both HI-STAR 100 and HI-STORM 100 is obtained from the results of the non-linear dynamic analysis. Both the static results and the response spectrum results, while confirming the veracity of the non-linear time history analyses, do not provide results that can be used to obtain a conservative evaluation of structural integrity.

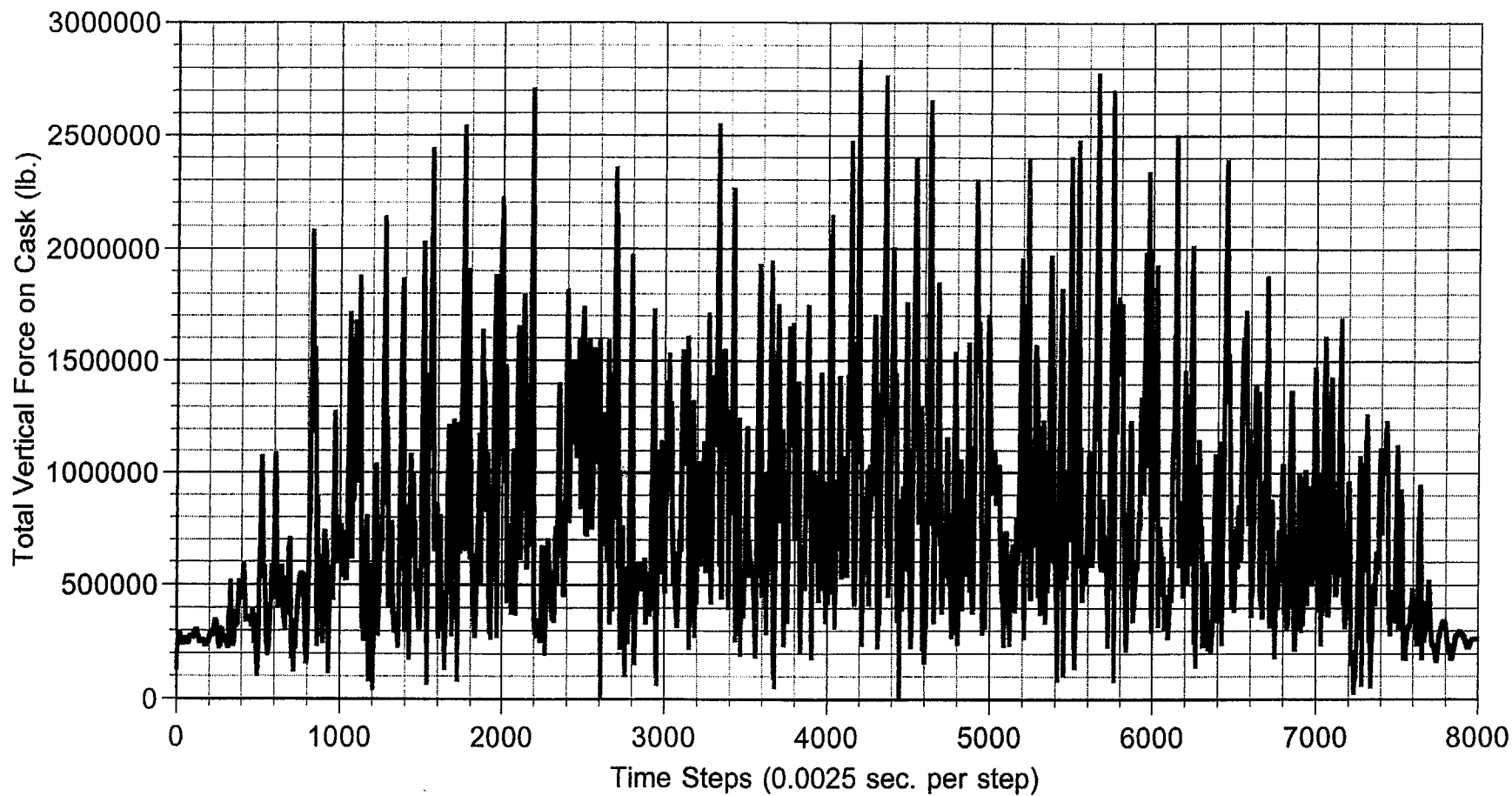


FIGURE 10.1 NET VERTICAL FORCE ON HI-STAR 100 vs. TIME RUNID = 251

HI-982004

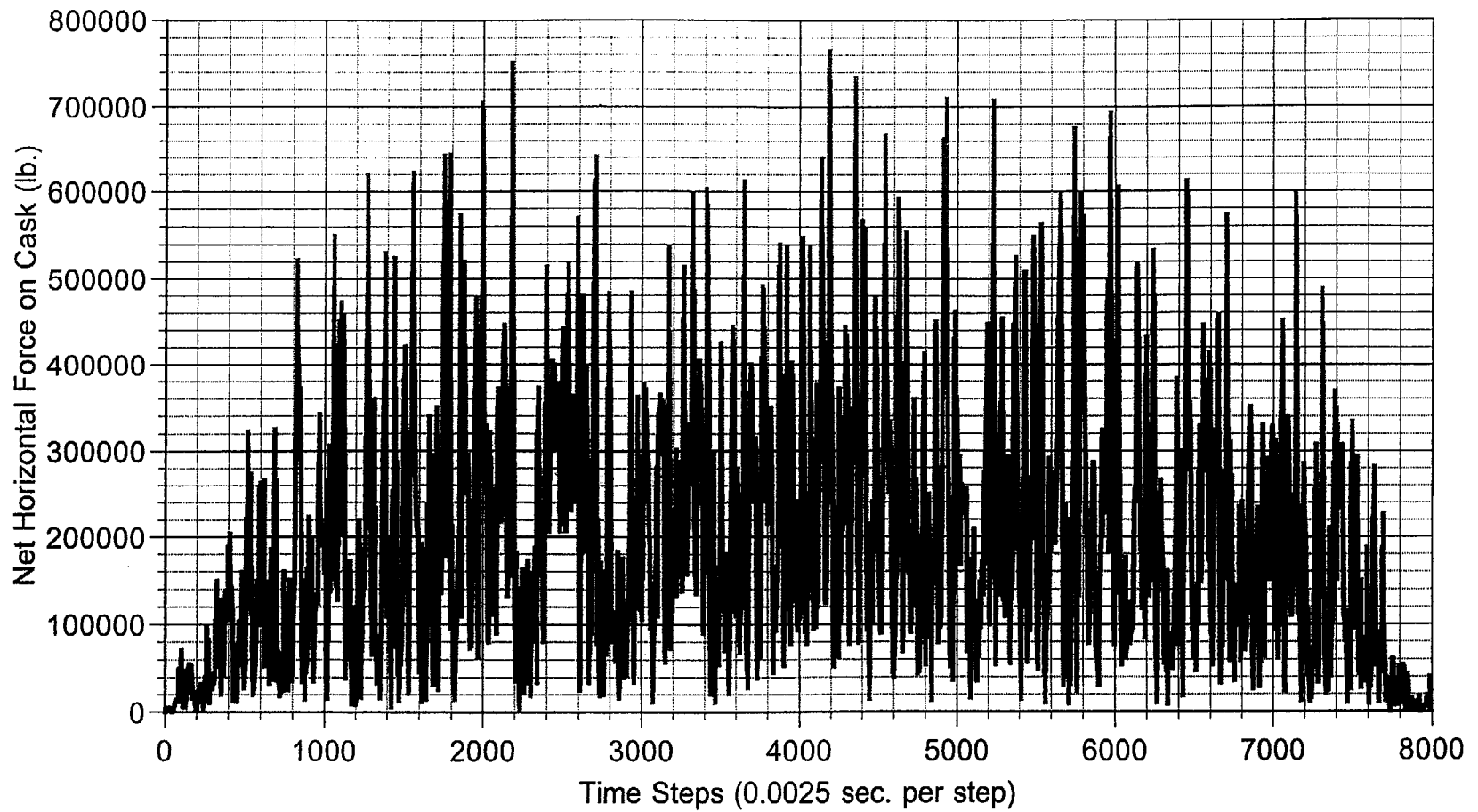


FIGURE 10.2 NET HORIZONTAL FORCE ON HI-STAR 100 vs. TIME RUNID=252

HI-982004

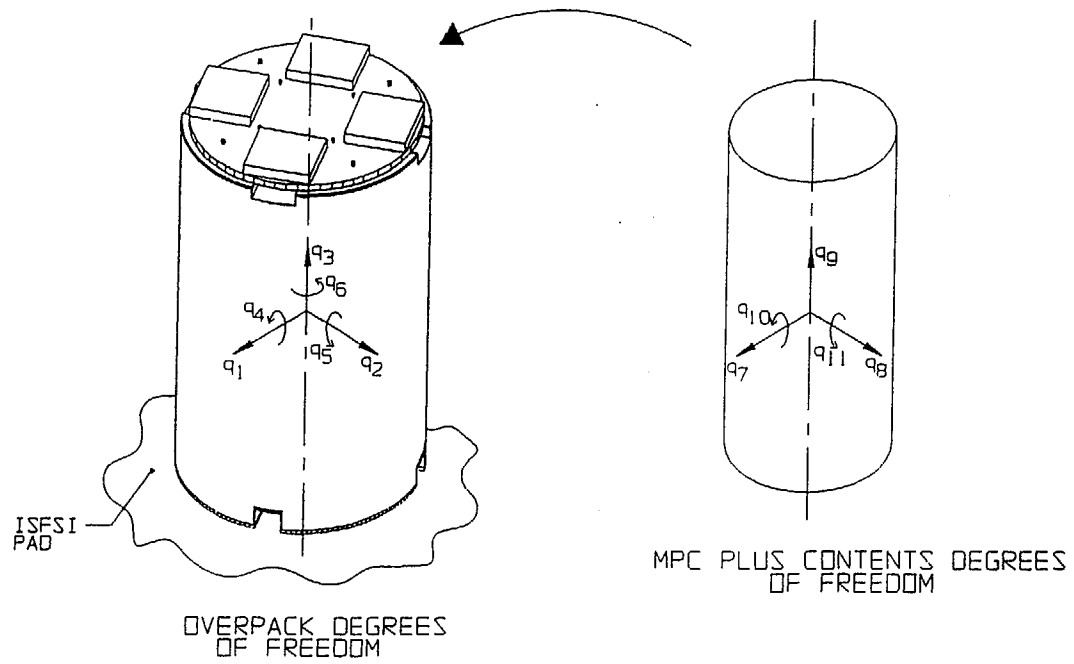


FIGURE 10.3; HI-STORM 100 DYNAMIC MODEL

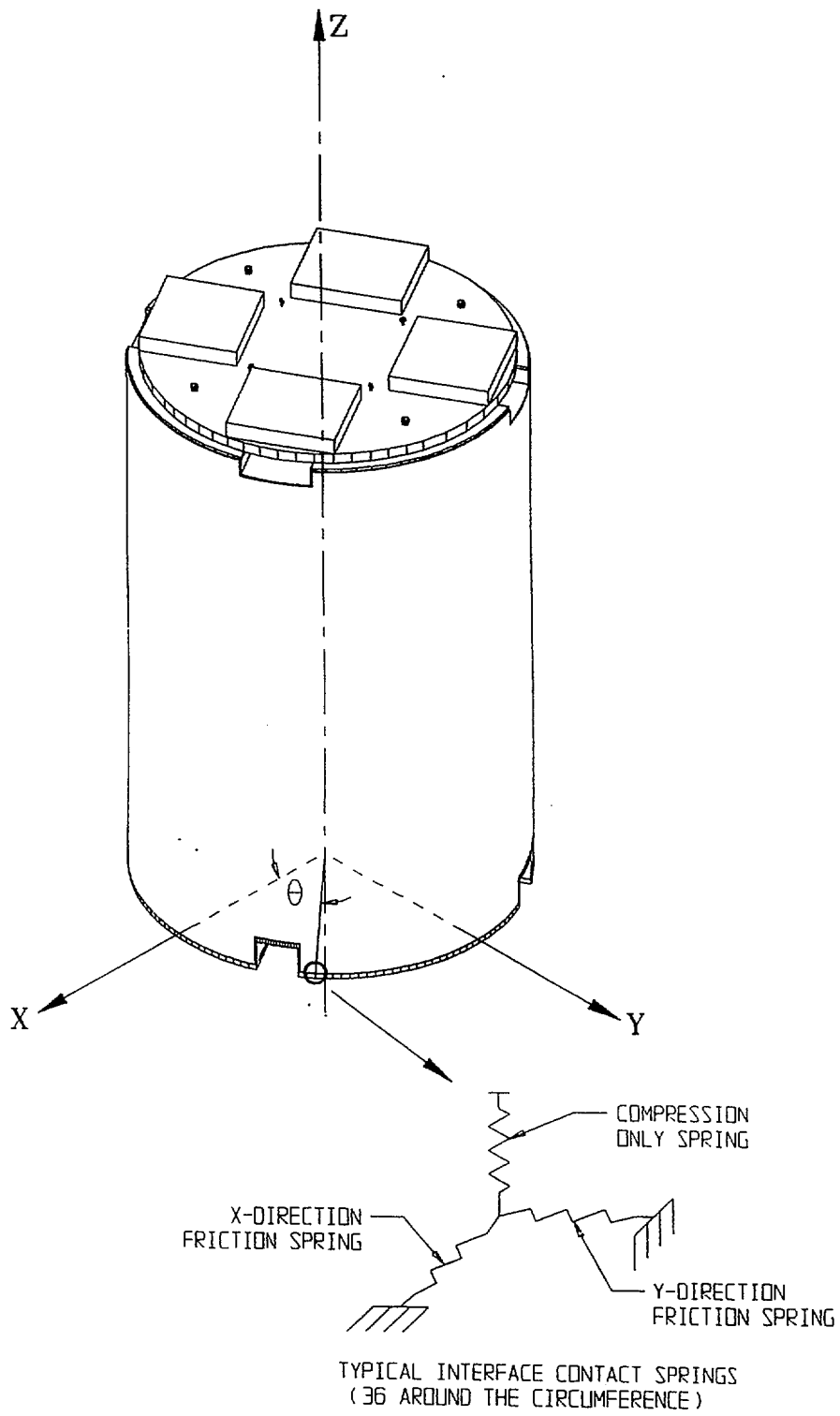


FIGURE 10.4; CASK-ISFSI PAD INTERFACE CONTACT ELEMENTS

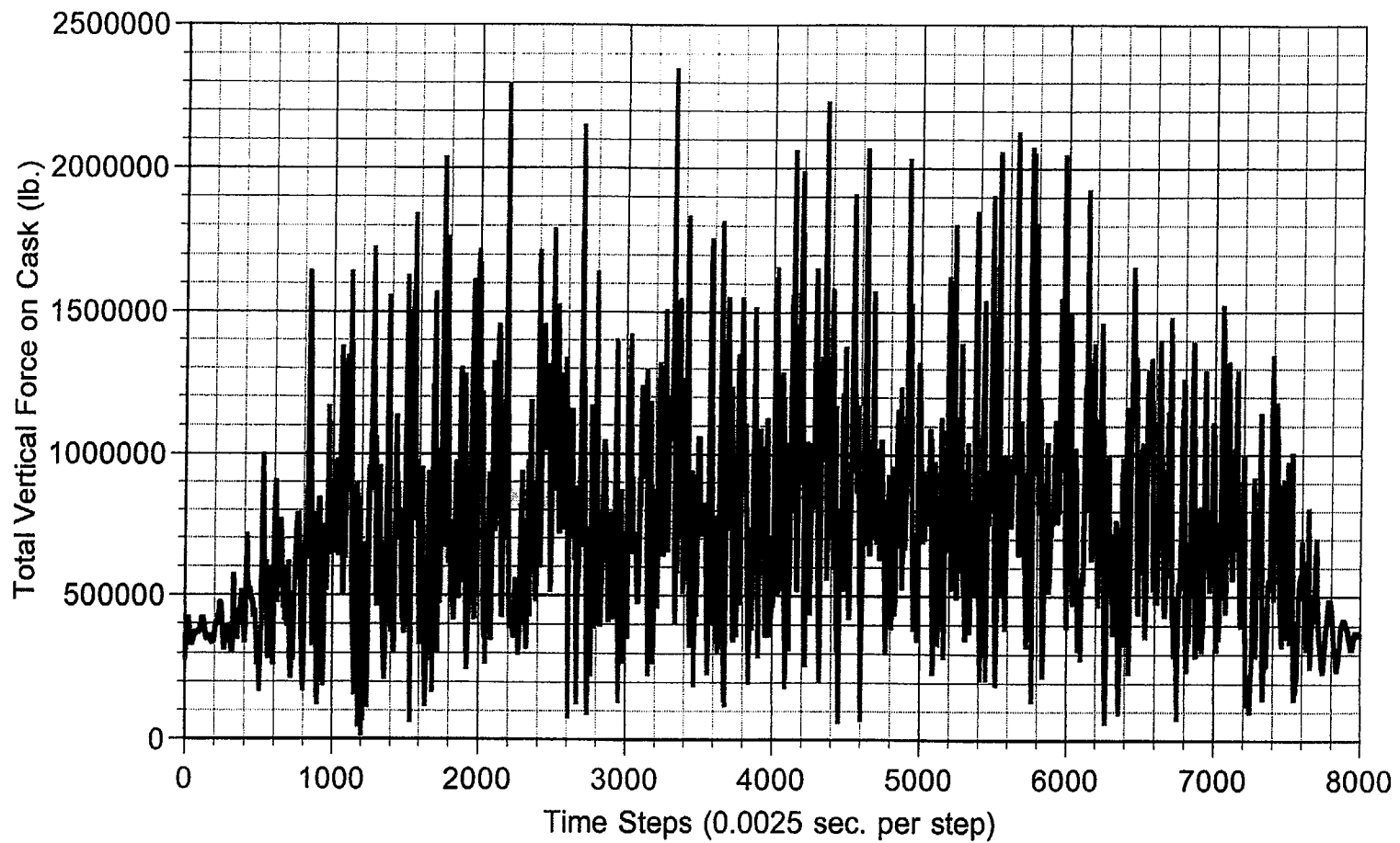
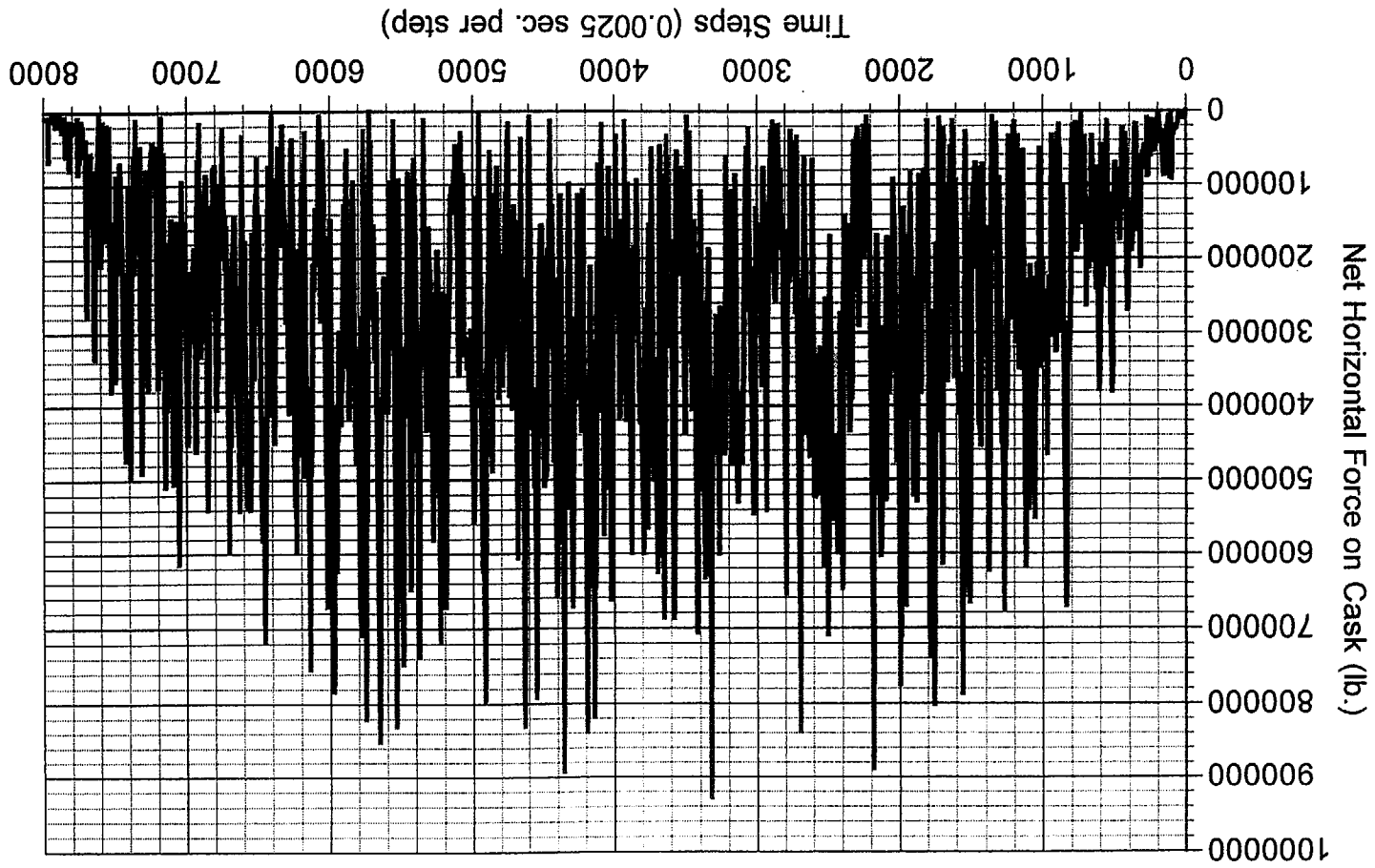


FIGURE 10.5 NET VERTICAL FORCE ON HI-STORM 100 vs. TIME RUNID = 112

HI-982004

HI-982004

FIGURE 10.6 NET HORIZONTAL FORCE ON HI-STORM 100 vs. TIME RUNID=112



11.0 STRUCTURAL ANALYSIS

11.1 Structural Qualification of the HI-STAR 100 Clevis Support

Section 10 provides the time history analysis of the HI-STAR 100 when connected to the ITS ISFSI through the eight (8) clevis assemblies which can resist tension and compression and eight (8) additional compression blocks . The results of the dynamic analysis provide the reaction forces for the clevis assembly structure that are used herein to determine structural integrity. In particular, Table 10.2 provides the necessary bounding reaction loads for the structural evaluation of the clevis assembly. In this section, we use the bounding loads from the set of simulations and demonstrate that the required limits set forth in Section 9.3 are met. The load path from the cask attachment points to the ISFSI bolts and concrete is demonstrated to meet all structural integrity requirements. Simple structural integrity calculations are presented within the text ; however, where a complex calculation is required to demonstrate structural integrity, such calculations are presented in an appendix and their results summarized in a table.

11.1.1 Qualification of the HI-STAR 100 Clevis Stud (Item 4 in Figure 7.4)

From Table 10.2, without regard for the particulars of the simulation or the time instant when the peak loads occur, a conservative analysis of these members is effected by using the following values for tensile and shear loads at the interface with the cask. We note that these results include the dead load of the loaded HI-STAR 100.

Tension = 356.3 kips

Shear Forces in Orthogonal Directions in the Horizontal Plane

Direction 1 Shear Force = 95 kips

Direction 2 Shear Force= 99 kips

Net Shear = $(95^2 + 99^2)^{1/2} = 137.2$ kips

Appendix B considers the clevis stud (also designated as the clevis bolt) capacities only on the basis of either direct tension ([22], Appendix F, F-1335.1) or shear ([22], Appendix F, F-1335.2). Reference [22] also requires that an interaction relationship involving both tension and shear also be satisfied (F-1335.3). Of the three candidate materials for the clevis stud, it is clear from the results in Appendix B, that only SA-564-630 and SB-637-N07718 have the necessary strength limits to meet all required relationships. The following minimum safety factors are obtained based on the bounding loads listed above and the calculations in Appendix B for SA-654-630 and for SB-637-N07718 Safety factors (SF) are defined as calculated load (obtained from the dynamic analysis)/allowable load(from Appendix B). The safety factors are computed with proper accounting of stress area for tensile loads.

SA-564-630

$$\text{SF}(\text{tension}) = 405.8/356.3 = 1.14 > 1.0$$

$$\text{SF}(\text{shear}) = 298.9/137.2 = 2.18 > 1.0$$

Interaction Relation defined in [22], Appendix F, F-1335.3

$$(1/1.14)^2 + (1/2.18)^2 = 0.98 < 1.0 \quad (\text{SF}(\text{interaction}) = 1/0.98 = 1.02)$$

SB-637-N07718

$$\text{SF}(\text{tension}) = 494.3/356.3 = 1.39 > 1.0$$

$$\text{SF}(\text{shear}) = 366.2/137.2 = 2.67 > 1.0$$

Interaction Relation defined in [22], Appendix F, F-1335.3

$$(1/1.39)^2 + (1/2.67)^2 = 0.66 < 1.0 \quad (\text{SF}(\text{interaction}) = 1/0.66 = 1.52)$$

The above results, obtained using conservatively high bounding loads, demonstrate that the eight clevis studs comprising the tension and shear load transfer path from the cask base meet the structural integrity requirements. Either SA-564-630 or SB-637-N07718 materials are acceptable although SB-637-N07718 provides larger safety factors for the bounding seismic event. Most likely, use of SA-564-630 would be considered only for sites with seismic events that do not

approach the bounding seismic event in peak magnitude and ZPA.

Next, we consider the resistance to bearing loads and the propensity for “tear-out” of the minimum section near the hole for the pin drilled in the cubical head of the clevis stud (Item 4 in Figure 7.4). According to [22], F-1334.10, the bearing capacity need not be evaluated for a Level D loading. Nevertheless, we evaluate a safety factor by defining the bearing load to be the resultant of the tensile load and one of the maximum shear loads that is assumed to act normal to the longitudinal axis of the pin (Item 5 in Figure 7.4). Therefore, the resultant load calculated to result in bearing stress is F_b , where

$$F_b = (356.3^2 + 99^2)^{1/2} = 369.8 \text{ kips}$$

The bearing capacity is evaluated as the material yield strength of Item 4 multiplied by the projected area of the pin. Therefore, the bearing capacity is

$$P_{\max} = 144,000 \text{ psi} \times (3.14159/4 \times (2.875")^2) \times 5.875" = 5492.0 \text{ kips}$$

From the preceding computation, it is clear that bearing failure at the hole is not a concern; i.e., the safety factor is $P_{\max} / F_b = 14.85$.

The capacity of the section to resist “tear-out” is measured by the allowable shear stress (42% of ultimate stress per [22], F-1334.2) multiplied by the section area in shear “above the hole” in Figure 7.4. Therefore, the available capacity is “T”, where

$$T = (.42 \times 177,600 \text{ psi}) \times 2 \times (5.875" \times 2.9375") = 2574.6 \text{ kips}$$

Since $T \gg F_b$ (SF = 6.96), tearing failure at the pin hole is not a concern.

Based on the above calculation, the eight stud/block components that resists tensile as well as compressive loads meets the required structural integrity criteria from [22], Appendix F.

11.1.2 Qualification of the Clevis Pin (Item 5 in Figure 7.4)

In Appendix B, the pin spring rate is computed based on a concentrated bending moment being applied to the pin at two locations. From sketch #1 in Appendix B, the bending moment on the pin at either of two points is computed as

$$\text{Moment} = (.5 \times F_b) \times c = .5 \times 369.8 \text{ kips} \times 0.25" = 46,225 \text{ lb.-inch}$$

Note that the pin bending moment is assumed constant over the entire section; the rigidity of the clevis stud head compared to the rigidity of the pin bending as a beam insures that the load is transferred to the pin near the edge of the connecting clevis stud head as assumed in Appendix B.

The pin metal area "A" and metal area moment of inertia "I" are computed as follows:

$$\text{Pin diameter } d = 2.875"$$

$$A = 3.14159/4 \times (2.875")^2 = 6.492 \text{ sq.inch}$$

$$I = 3.14159/64 \times (2.875")^4 = 3.354 \text{ inch}^4$$

Therefore, the pin bending stress and shear stress are computed as

$$\sigma = (\text{Moment} \times d)/(2I) = 19,812 \text{ psi}$$

$$\delta = (.5 \times F_b)/A = 28,481 \text{ psi}$$

Using SA-193-B7 material for the pins, the safety factors for bending and shear are computed

using the methodology described below:

Section 6.4 of this report establishes the ASME Code Section III, Subsection NF as the appropriate design code for the clevis pin. From [22], Subsection NF, NF-3322.1 and Appendix F, F-1334, the allowable Level D bending stress is

$$S_b = 1.4(0.6 \times \text{yield stress}) = 82,320 \text{ psi}$$

The allowable shear stress is 42% of the material ultimate stress, or

$$T_s = 0.42 \times \text{ultimate stress} = 49,000 \text{ psi}$$

Therefore, the safety factors for the clevis pin in bending and shear are

$$SF(\text{bending}) = 82,320/19,812 = 4.16$$

$$SF(\text{shear}) = 49,000/28,481 = 1.72$$

The preceding calculations demonstrate compliance of the clevis pin with the structural limits of [22].

11.1.3 Qualification of the Clevis Blocks (Items 2 and 3 in Figure 7.4)

The clevis blocks (also designated as support blocks) are solid bar stock from SA-36 (or equivalent) material. Different materials are permitted to allow for varied environmental conditions anticipated at the site. For structural qualification, the bounding minimum yield and ultimate strengths are taken from the totality of permitted materials [22, Section II, Part D] (note that the yield and ultimate strengths used represent a hypothetical material with the stated minimum properties):

$$S_y = 30000 \text{ psi}$$

$$S_u = 58000 \text{ psi}$$

The minimum bearing area to support reactions from the pin (Item 5) is on Item 3 and has the value (refer to Figure 7.4 and use the pin diameter and embedded length in the inboard clevis block):

$$\text{Area} = 2.875" \times 5" = 14.375 \text{ sq. in.}$$

From [20, Section F1], the allowable bearing stress is 90% of the material yield stress so that the allowable bearing load is "Lb" where

$$L_b = .9 S_y \times \text{Area} = 388 \text{ kips}$$

Reference [20] does not exclude bearing loads from analysis under accident level events; assuming conservatively that the pin reaction is 50% of the bounding value for "F_b" computed previously, the safety factor against a bearing failure from the pin reaction is

$$SF(\text{bearing}) = L_b / .5F_b = 388 / .5 \times 369.8 = 2.1$$

The area available to resist shear "tear-out" above the hole is conservatively assumed as (per Figure 7.4):

$$A(\text{shear}) = 5" \times 2.75" = 13.75 \text{ sq. inch (On each side of the hole)}$$

Using Reference [20] and Section 6 of this report, the allowable shear stress under normal conditions of storage is 40% of the material yield stress; amplification by 1.4 is permitted for the defined accident event. Therefore, the allowable "tear-out" load "T" for the clevis block is

$$T = 1.4(.4S_y) \times A(\text{shear}) = 16,800 \text{ psi} \times 13.75 \text{ sq.in.} \times 2 = 462 \text{ kips}$$

The safety factor against a "tear-out" is

$$SF(\text{tear}) = T/.5F_b = 462/.5 \times 369.8 = 2.5$$

The above calculations demonstrate the adequacy of the clevis block to support the reactions arising to resist cask uplift.

When clevis block components (Items 2 and 3) are under compression, Table 10.2 gives the maximum compression load on the totality of compression area as (define this load as "CL"):

$$CL = 577.6 \text{ kips}$$

The total bearing area for vertical compression is computed using the detail in Figure 7.4 for the inboard and outboard portions of the clevis support block. Subtracting the area eliminated by the chamfer,

$$\text{Area}(\text{compression}) = 6" \times (6"-0.5") + 6" \times (12.625"-0.5") = 105.75 \text{ sq. inch}$$

The permissible bearing load is based on 90% of the material yield strength with the conservative assumption that no increase is permitted for the accident condition of storage. Therefore, the compression capacity of each two piece clevis assembly is defined as "CC" where

$$CC = .9S_y \times \text{Area}(\text{compression}) = .9 \times 30,000 \text{ psi} \times 105.75 \text{ sq.in.} = 2,855.3 \text{ kips}$$

and the bearing safety factor of this component is computed as

$$SF(\text{bearing}) = CC/CL = 4.94$$

The structural integrity of the clevis blocks is demonstrated by the above calculations. We show later that the bearing pressure developed in the concrete slab due to this load does not exceed the American Concrete Institute (ACI) limits.

11.1.4 Qualification of the Clevis Block Weld (Items 2 and 3 to Item 1 in Figure 7.2)

Each clevis block assembly (Items 2 and 3) is welded to the base plate (Item 1) using fillet welds on four sides of each block. In this subsection, we evaluate the maximum shear stress in the weld to support the bounding three components of clevis stud force developed from the dynamic analysis. .

The allowable fillet weld stress is set by Reference [20, Section J2] as 30% of the ultimate strength of the material for normal conditions of storage. For the analysis including seismic loads, however, following Section 6.3, we amplify the allowable weld shear stress for normal conditions by 1.4. We also allow the weld material to be one grade higher (Grade 70). Therefore, the allowable weld shear stress is “Ta” where

$$T_a = 1.4 \times (.3 \times S_u) = 0.42 \times 70000 \text{ psi} = 29400 \text{ psi}$$

Appendix M contains the details of the weld evaluation and appropriate figures showing the location of the load with respect to the centroid of the weld group. The weld analysis is conservatively performed assuming an all around fillet weld for both portions of the clevis block. It is permissible and conservative to use an equivalent J-groove weld (to minimize installation concerns) along the sides adjacent to the head of the eight clevis studs from the overpack that transmit tensile and shear loads. Both the inboard and outboard sections of the clevis support block are evaluated for weld integrity. We summarize the results from calculations in Appendix M as follows:

The minimum fillet weld thickness is

$$t = 0.75''$$

From Table 10.2, the total load applied to the clevis pin and reacted by the two sections of a clevis support block are bounded by the values:

$$FX = FY = 99,000 \text{ lb.} \quad FZ = 356,300 \text{ lb.}$$

X, Y represent radial and circumferential load orientation, and Z represents a vertically oriented load. The analysis in Appendix M assumes that each section of the clevis support block resists one-half of the above loads transmitted by the clevis pin reactions to the block sections and then through the weld group to the baseplate. The offset of the point of application of the reaction loads from the centroid of the weld group in each section is included in the analysis. The shear stress distribution in the weld group is calculated from force and moment equilibrium equations developed for the weld group. The resultant shear stress, at the most heavily stressed location, is compared to the allowable weld shear stress given above. The results are listed below:

Inboard Clevis Support Block Weld Stress Safety Factor = 1.11

Outboard Clevis Support Block Weld Stress Safety Factor = 2.13

11.1.5 Qualification of the Base Plate (Item 1 in Figure 7.2)

Structural qualification of the local area of the base plate that serves to transfer load to the bolts and then into the concrete pad is consistent with the geometry used in Appendix B. The local bending stress that develops in the vicinity of the anchor bolt is not a primary stress. For structural integrity evaluation consistent with Reference [20], we demonstrate only that the plate

has an appropriate shear capacity to transfer the tensile load of 356.3 kips. There are 4 anchor bolts (studs) associated with each clevis block. Therefore, 25% of the load is transferred in shear to each bolt. The shear capacity of the minimum section is computed using a 6" width of plate multiplied by the 1.25" plate thickness to develop the loaded area and multiplying the result by the allowable shear stress for the accident condition per Section 6.3. The yield strength of the baseplate material is $S_y = 38000$ psi ([22], Section II, Part D). The capacity associated with each section of baseplate is

$$\text{Shear Capacity} = 1.4(.4S_y) \times (1.25" \times 6") = 160 \text{ kips}$$

Therefore, the factor of safety against overstress in shear is

$$\text{SF} = \text{Shear Capacity} / (.25 \times 356.3 \text{ kips}) = 1.8 > 1.0$$

11.1.6 Qualification of the Anchor Bolts (studs) (see Figure 7.6)

The average tensile load in each of the four anchor bolts associated with uplift of a clevis assembly is equal to 25% of the total calculated uplift load on the clevis pin. From Table 10.2, the tensile load "TL" is

$$\text{TL} = \text{FZ}/4 = 89.1 \text{ kips}$$

In addition to the tensile load, two components of horizontal load, assumed conservatively to act at height "h" above the baseplate, also load the anchor bolts. The two components of horizontal load $F_X = F_Y$ that act on a clevis support block load the anchor bolts in direct shear and also impose additional tensile load on the bolts due to the offset height "h". Since the anchor bolts are not pre-loaded, the maximum tensile load in a bolt is developed when the portion of the baseplate connecting the clevis blocks to the anchor bolts is in a condition of "edging" and the

axis of rotation passes through one of the bolts. Figure 11.1 shows the location of the anchor bolts for one of the eight clevis block assemblies and the load components to be resisted. The total moment to be resisted in each of two horizontal directions is:

$$h = 3.25":$$

$$M = FX \times h = 99 \text{ kips} \times 3.25" = 321.75 \text{ kip-inch}$$

Assuming that the plate tends to rotate about an axis through one bolt, then the resisting moment from the remaining three bolts is:

$$F \times (10" \times 1.414) + 2 \times F/2 \times (10" \times 0.7071) = 21.211F \text{ in-lb.}$$

where F is the additional tensile force in the furthest anchor bolt to support the imposed moment M.. Solving for F gives

$$F = 15.2 \text{ kips}$$

The available tensile capacity of the anchor bolt (UNC course threads), using the working stress given in Table 9.1(SA-490), and using the appropriate "stress area" for normal conditions, is given by the equation

$$\text{bolt diameter} = 2.0" \text{ (stress area} = 2.497 \text{ sq. inch)}$$

$$\text{Tensile Capacity} = 104,000 \text{ psi} \times (2.497 \text{ sq. inch}) = 259.7 \text{ kips}$$

Therefore the safety factor for anchor bolt tension under the accident condition is

$$SF(\text{tension}) = 259.7 / (89.1 + 15.2) = 2.49$$

Similarly, the safety factor on net section shear force in the bolt, is computed as

$$\begin{aligned} \text{SF}(\text{shear}) &= \text{Shear Capacity}/\text{Net Shear Force} = (66 \text{ ksi} \times 2.497 \text{ in.}^2)/(.25 \times 1.414 \times 99 \text{ kips}) \\ &= 4.71 \end{aligned}$$

The ACI interaction equation ([13], B.6.3.2) that includes both tension and shear requires that $1/\text{SF}(\text{tension}) + 1/\text{SF}(\text{shear})$ be less than 1.0. Using the safety factors computed above, the interaction equation evaluates to 0.614. Therefore, the anchor bolts meet the requirements of the ACI-349 Code. A safety factor may be defined as $1/0.614 = 1.63$.

The bearing stress at each anchor bolt hole is computed as the 25% of the net horizontal load transmitted to the clevis divided by the projected area of the anchor bolt in contact with the baseplate. Therefore, the calculated bearing stress is:

$$\text{Baseplate bearing stress} = .25 \times 1.414 \times 99 \text{ kips} / (1.25" \times 2") = 14,000 \text{ psi}$$

This is less than the yield strength of the baseplate material so that baseplate anchor bolt hole enlargement due to lateral loading on the clevis block is not credible.

From the sequence of calculations provided above, we have demonstrated that the HI-STAR 100 attachment system from the base of the cask to the bolts into the concrete meets the structural integrity requirements to support the dead loads plus design basis seismic loads.

11.1.7 Qualification of the Anchor Head and Concrete Pullout Capacity

The eight clevis blocks that can resist tension are embedded in the concrete so that the anchor bolt tensile loads from the array of four bolts are resisted by a single anchor head. Each anchor head is considered as a square plate of side length "a" and thickness "t". From the drawings in

Section 7, the pitch between anchor bolts is 10 inches and the nuts on the ends of the anchor bolts meet the requirements of the ACI-349 Code, B.4.5.2 . Therefore, the optional anchor head plate thickness is sufficient and need not be subject to a detailed analysis.

The concrete pullout strength is established by the ACI Code in terms of concrete compressive strength. When the cask is subject to net uplift loads, from [13, B.4.2], the allowable pullout stress in the concrete is (in psi units):

$$P_d = 4\phi(f_c)^{1/2} = 4 \times 0.65 \times 63.246 = 164.44 \text{ psi}$$

The ACI Code establishes a geometric method to establish the effective surface area that can resist tensile pullout. An evaluation of the load distribution at the time instant when tensile loads on the assemblage of clevis attachments is maximized shows that six of the eight clevis attachments are subject to local tensile loading. Based on the geometry and depth of the anchors, the number of clevis attachments under tension, and the minimum pitch between casks, the total effective area available to resist tension is established by a CAD program to be:

$$A_{po} = 13,860.3 \text{ sq. inch}$$

This area is computed in a manner that accounts for any overlap between anchor bolt groups in the manner prescribed by [13, Appendix B]. Multiplying the tensile capacity of the concrete with the total area of concrete able to resist tension gives the total tensile pullout capacity as:

$$\text{Tensile Load Capacity} = P_d \times A_{po} = 2,279,188 \text{ lb.}$$

When the tensile load on a single clevis attachment is maximized, the total tensile load from the six clevis attachments that are under tension and acting to impose maximum bending moment on the ISFSI slab is computed from the computer results to be:

Applied Tensile Load = 1,388,000 lb

Therefore, the safety factor on the actual tensile pullout is:

SF = Tensile Load Capacity/Applied Tensile Load = 1.642

11.1.8 Summary of Safety Factors for the HI-STAR 100 Anchor Support Structure

Table 11.1 summarizes the results obtained from the calculations in Subsections 11.1.1 to 11.1.7. All safety factors exceed 1.0 so that structural integrity requirements under the conservatively developed high seismic event are met or exceeded. The safety factor established for concrete tensile capacity requires some additional comment. Section B.5 of [13] states that the anchorage design shall be controlled by the ultimate strength of the embedment steel (see B.5.1 of [13]). Section B.4.2 of [13] specifies the calculation of tensile capacity of the concrete and the results here follow that section. Section B.4.4 permits using additional reinforcement to insure that the full tensile capacity of the concrete is achieved. The Commentary in [13] associated with Section B.4.4, namely Figure B.4, provides the requirements for additional reinforcement in the form of hairpin anchors that must surround the anchor bolts and intercept potential concrete crack planes. The details of the hairpin reinforcement surrounding the anchor bolts in the ISFSI pad must comply with the foregoing reference.

Table 11.1 Summary of Safety Factors for HI-STAR 100 Clevis Support Structure

ITEM	Safety Factor "SF"
Connecting Bolt - Tensile Stress	1.14(1.39) [†]
Connecting Bolt - Shear Stress	2.18(2.67)
Connecting Bolt - Tension/Shear Interaction	1.02(1.52)
Clevis Bearing Stress in Center Section	14.85
Clevis Tearout Stress in Center Section	6.96
Clevis Pin Bending Stress	4.16
Clevis Pin Shear Stress	1.72
Clevis Local Bearing Stress at Pin Support	2.1
Clevis Local Tearout Stress at Pin Support	2.5
Clevis Compression Stress	4.94
Clevis Weld Shear Stress	1.11
Base Plate Shear Capacity	1.8
Anchor Bolt Tension	2.49
Anchor Bolt Shear	4.71
Anchor Bolt Interaction	1.63
Concrete Tension	1.64

[†] Values in parenthesis are for SB-637-N01178 bolt material

The sector lugs are constructed of welded plate section, which transfer the load to anchor bolts, and appropriate embedment. The analysis for structural integrity of the HI-STORM sector lugs is sufficiently more involved than that for the HI-STAR clevis that for clarity of presentation it is appropriate to devote a separate appendix to the detailed calculations. Appendix H provides the detailed calculations for all components of the sector lug attachment system. Here we summarize the results of the calculations in Appendix H by tabulating results for safety factors. In general, dimensions and property values are employed in the calculations in Appendix H that represent the minimum strengths of the geometry and materials espoused in Sections 4 and 9. Thus additional conservatism exists in the reported safety factors. Safety factors listed are defined as allowable stress (or load) divided by calculated stress (or load). Safety factors must be greater than 1.0 for an acceptable design. Where an interaction relation result is listed, the safety factor represents the inverse of the computed interaction result. The safety factors/interaction relationship is completely defined in the appendix as each calculation is performed. The table below briefly defines the particular item considered. Item numbers listed in the description are shown on Figure 8.3.

Table 11.2 Summary of Safety Factors for HI-STORM Attachment System

Item Description	Safety Factor or Interaction Factor
Weld stress sector lug to cask	1.19
Top plate (item#3) bending stress	1.213
Top plate weld stress (connection to item#1)	1.277
Top plate weld (connection to item#4)	1.601
Anchor bolt (tensile stress)	1.77
Anchor bolt (shear stress)	3.07
Anchor bolt (tension/shear interaction)	1.124
Concrete bearing stress	2.41
Concrete pullout stress - single sector lug	1.5
Concrete pullout stress four sector lugs excluding overlapped areas	1.53
Anchor bolt Threaded Coupling - Tension	2.44
Anchor Bolt Threaded Coupling - Shear	2.92

The above summary demonstrates that the sector lug attachment concept has sufficient ruggedness ascribed to the configuration to insure that the dead plus bounding seismic loads can be accommodated with large margins of safety.

11.3 Structural Integrity Analysis of the Local Cask Region Due to Attachment Loads

In this section we consider the effect on the HI-STAR 100 and HI-STORM 100 Systems of the additional localized loads imparted to the cask by the attachment configuration.

11.3.1 HI-STAR 100

We have demonstrated that the seismic loads impart acceleration levels to the cask that are bounded by the design basis levels in the TSAR [3]. The only additional calculation required is to estimate the stress imparted to the bottom plate of the HI-STAR 100 overpack from the tensile loads in the eight threaded connections. From Table 10.2, the maximum load in any of the attachment bolts to the bottom plate is "P" where:

$$P=356,300 \text{ lb.}$$

For a simple, yet conservative analysis of the bottom plate, we assume that all eight of the bolts experience this maximum load at the same instant in time. Further, we assume that this loading is conservatively simulated by a uniform pressure acting on the plate surface; this will tend to overestimate the plate stress.

The equivalent plate pressure is based on the cavity diameter of the overpack.

$$p = 8 \times 356,300 \text{ lb.} / (3.14159 \times 68.75^2 \text{ sq.in.} / 4) = 767.8 \text{ psi}$$

For additional conservatism, we assume the loaded MPC also exerts a additive pressure to the bottom plate. Using the loaded bounding weight of 90,000 lb., we also compute the pressure

$$q = (90,000 / (8 \times 356,300)) \times 767.8 = 24.2 \text{ psi}$$

Assuming a clamped plate, the maximum bending stress is

$$\sigma = .75 \times (p+q) \times (R/h)^2$$

For $R = (68.75/2)$ inch and $h = 6$ " (see drawings in Section 1.5 of [3])

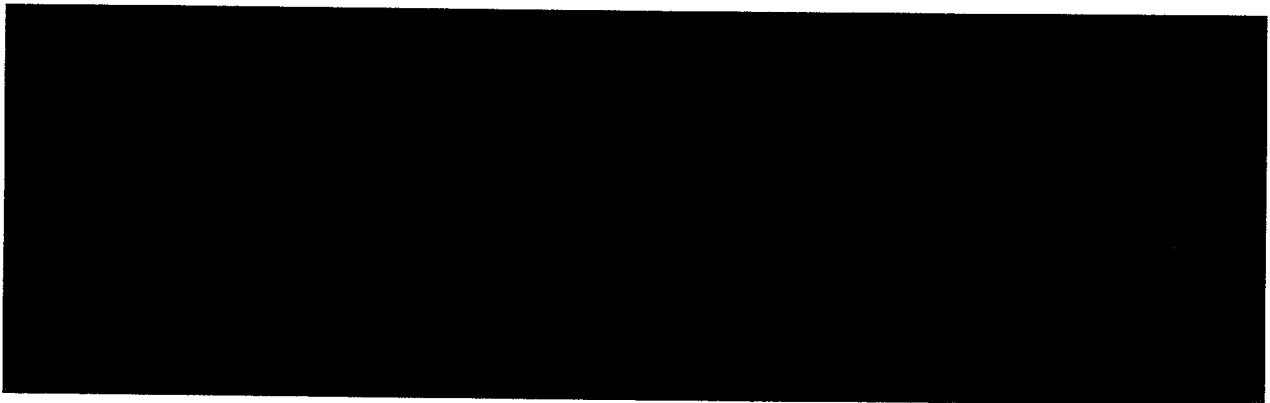
$$\sigma = 19,497 \text{ psi}$$

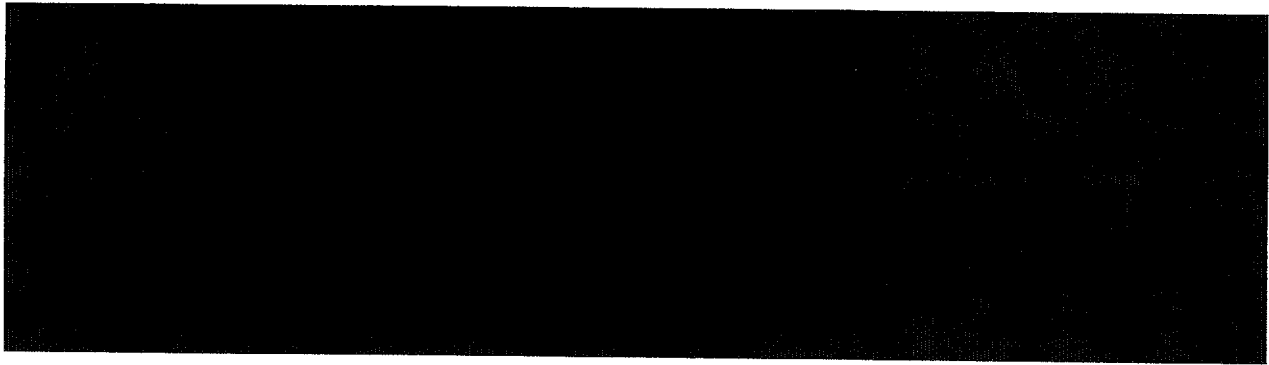
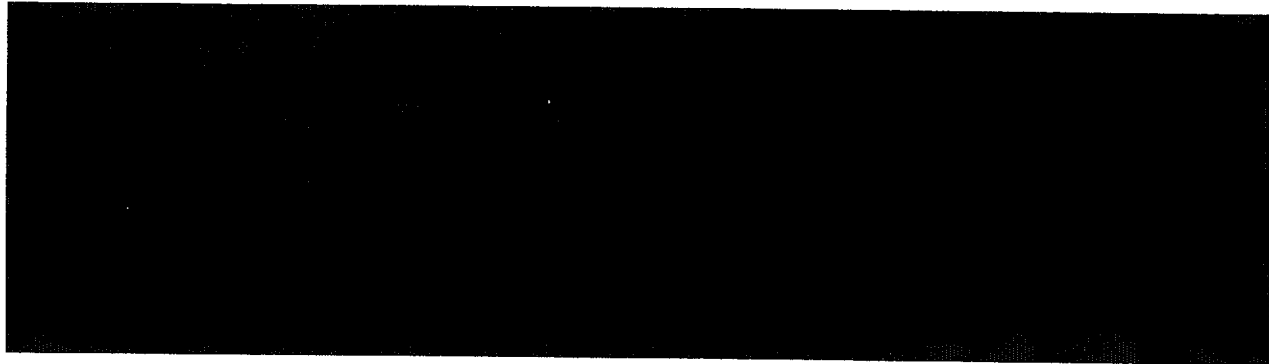
The maximum stress intensity is $19,497 \text{ psi} + 768.7 \text{ psi} + 24.2 \text{ psi} = 20,290 \text{ psi}$.

This is well below the ASME Section III, Subsection NB allowable stress intensity value for Level D conditions presented in [3]. Therefore, the loads from the connecting bolts during a seismic event do not exceed the design basis allowable stress intensity for the HI-STAR 100 overpack bottom plate.

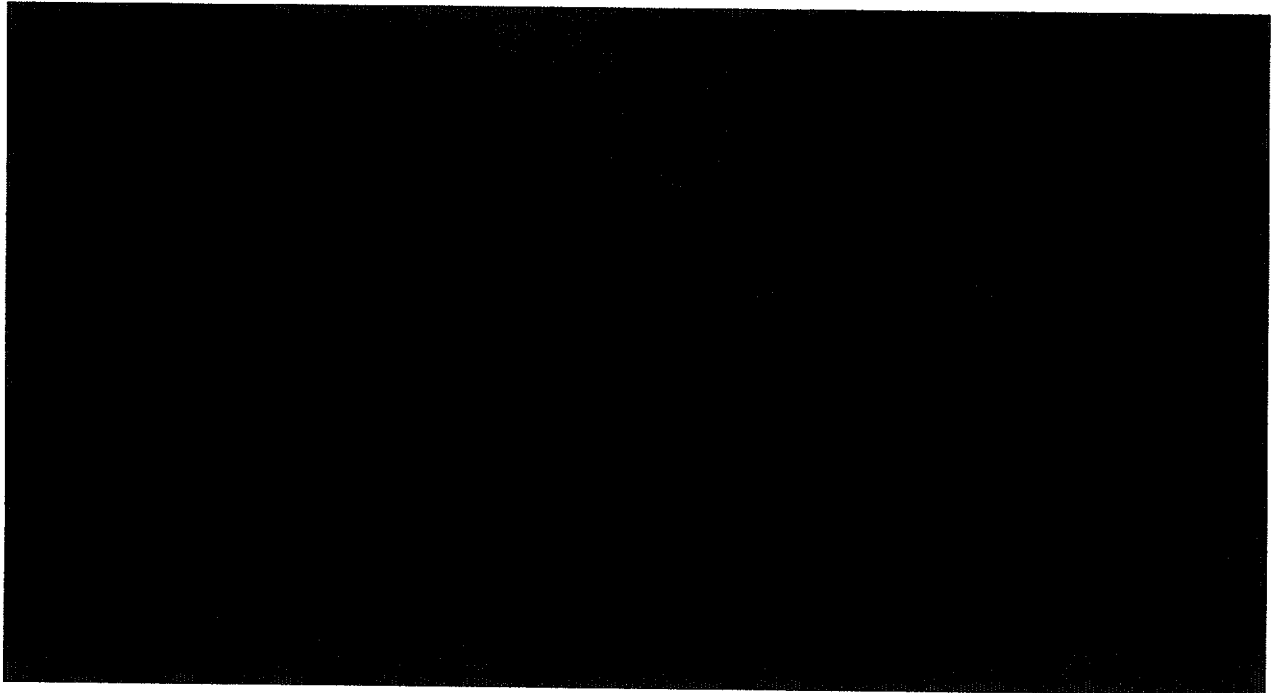
11.3.2 HI-STORM 100

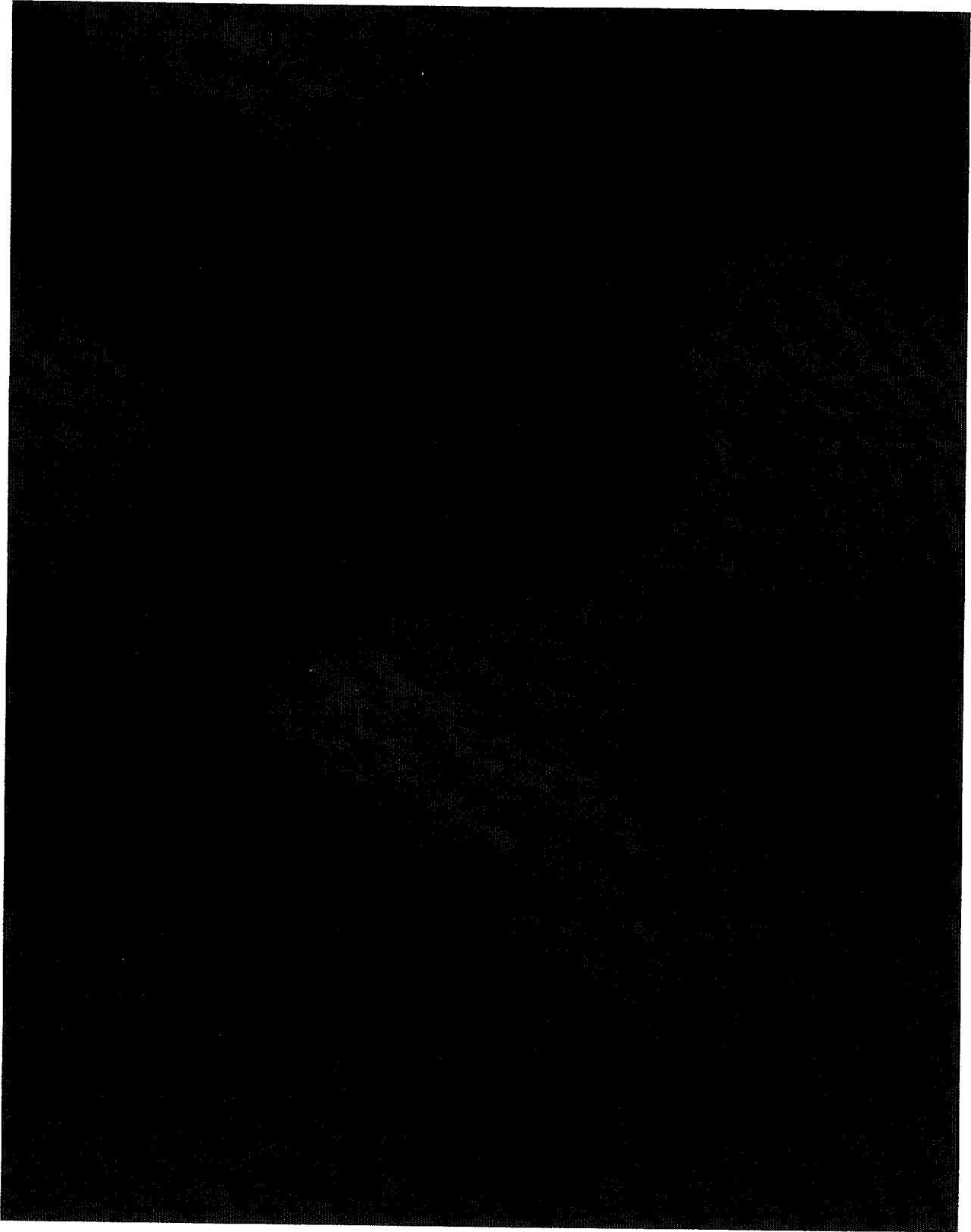
Appendix H calculations have demonstrated that the interface connection to HI-STORM 100 (the J-Groove weld connecting Item 1 in Figure 8.3 to the cask) meets structural integrity requirements. To insure that there are no local distortions to the cask outer shell at the locations of the sector lugs, four ½" thick gussets are provided to act as stiffeners (see Figure 8.1). These stiffeners insure that the overpack outer shell and the overpack baseplate resist any tendency for local deformations. Appropriate drawing in the TSAR [4] will reflect this additional requirement for casks destined for a high seismic environment site.

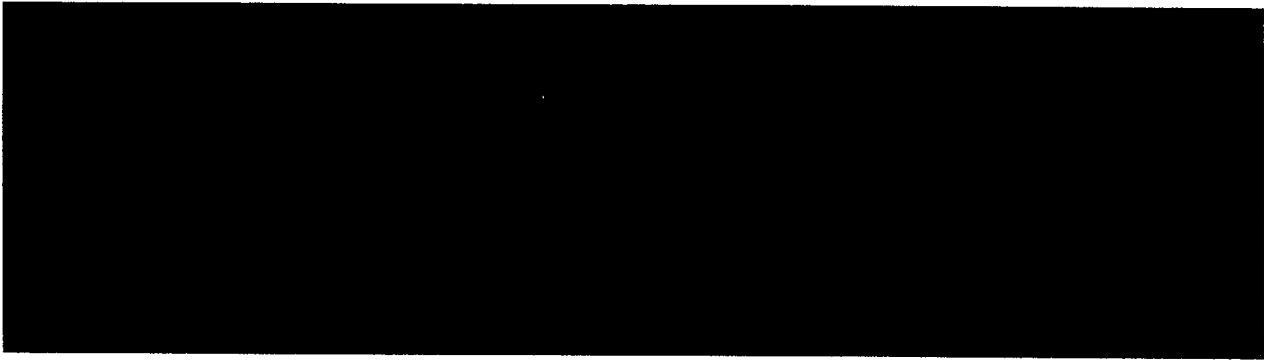




11.4 Structural Considerations Setting Upper Bounds on the Hydrological Loads







11.5 ISFSI Concrete Slab Evaluation

In this section, we demonstrate that the ISFSI slab is sufficiently robust to meet the slab load combinations in Section 6.2. All results are based on the minimum thickness slab and the minimum subgrade modulus per Table 4.1. This renders the results for safety factors conservatively low. The ISFSI slab analysis inputs are the dynamic analysis results of Table 10.2 (HI-STAR 100) and Table 10.6 (HI-STORM 100). The load combinations are those in Section 6.2. The qualification methodology uses “ultimate strength” design formulas and considers slab bending capacity, slab shear capacity, and concrete bearing capacity. Both a global analysis (where the load is assumed applied over the surface contact patch shadowed by the cask contact diameter) and a local analysis (where the peak load applied on a single clevis assembly or on a single sector lug) are performed. The capacity of the slab to resist bending moments, punching shear forces, and direct bearing loads is evaluated. Appendix K contains complete details of the myriad analyses leading to the final minimum safety factors in the bounding slab supporting the HI-STAR 100. The results are summarized in Table 11.3. Similarly, Appendix L contains the calculations for the ISFSI slab supporting the HI-STORM 100; the results for the HI-STORM 100 slab are summarized in Table 11.4. A minimum pitch between casks is used in Appendices K and L to maximize the computed steady-state soil bearing pressure.

HI-STAR 100 minimum pitch (between cask centers) = 12'

HI-STORM 100 minimum pitch (between cask centers) = 13'

Table 11.3 ISFSI Slab Safety Factors Under HI-STAR 100 Loading

ITEM	CALCULATED VALUE
NORMAL CONDITIONS OF STORAGE	
Global Slab Bending Moment From Total Cask Load	6.96
Global Slab Punching Shear From Total Cask Load	11.36
Local Slab Bending Moment From Clevis Load	31.2
Local Slab Punching Shear From Clevis Assembly Load	49
Average Concrete Bearing Pressure Under Cask	60.97
ACCIDENT CONDITIONS OF STORAGE	
Global Slab Bending From Total Cask Load	1.05
Global Slab Punching Shear From Total Cask Load	1.85
Local Slab Bending From Clevis Assembly Load	1.12
Local Slab Punching Shear From Clevis Assembly Load	4.51
Average Concrete Bearing Pressure Under Cask	2.86
Local Concrete Bearing Pressure Under Clevis	1.75

Table 11.4 ISFSI Slab Safety Factors Under HI-STORM 100 Loading

ITEM	CALCULATED VALUE
NORMAL CONDITIONS OF STORAGE	
Global Slab Bending Moment From Total Cask Load	6.17
Global Slab Punching Shear From Total Cask Load	10.22
Local Slab Bending Moment Under Sector Lug	10.86
Local Slab Punching Shear Around Sector Lug	17.1
Average Concrete Bearing Pressure Under Cask	107.3
ACCIDENT CONDITIONS OF STORAGE	
Global Slab Bending Moment From Total Cask Load	1.69
Global Slab Punching Shear From Total Cask Load	3.06
Local Slab Bending Moment Under Sector Lug	1.8
Local Slab Punching Shear Around Sector Lug	3.67
Average Concrete Bearing Pressure Under Cask	28.0
Local Concrete Bearing Pressure Under Sector Lug	9.28

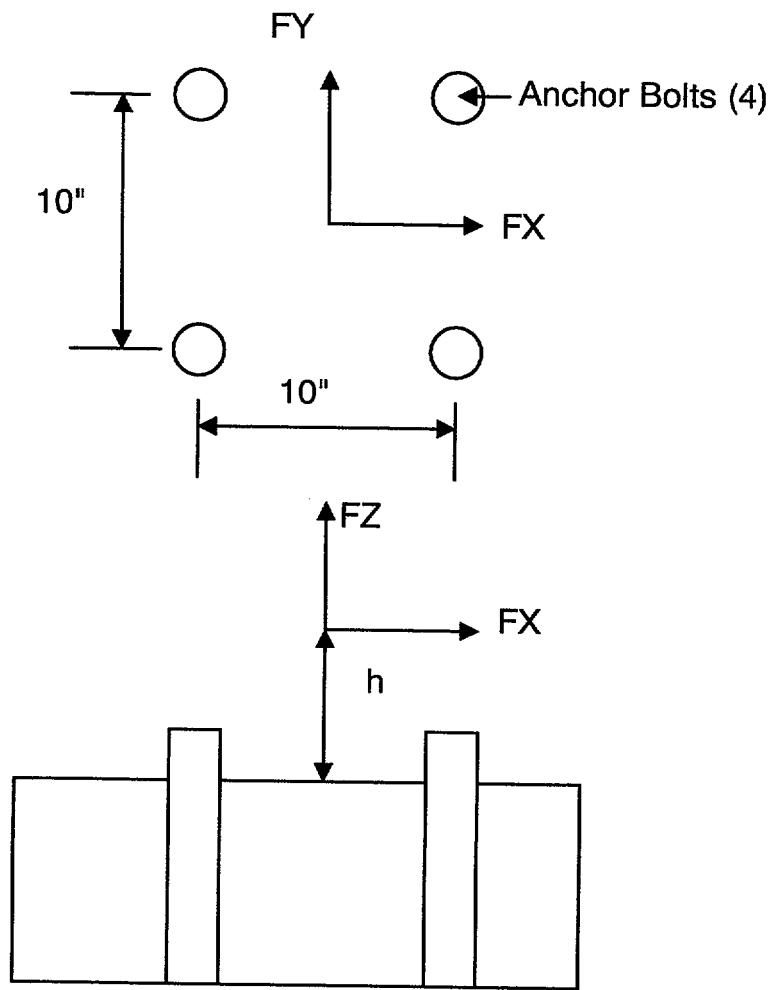


FIGURE 11.1 - ANCHOR BOLT LOADING

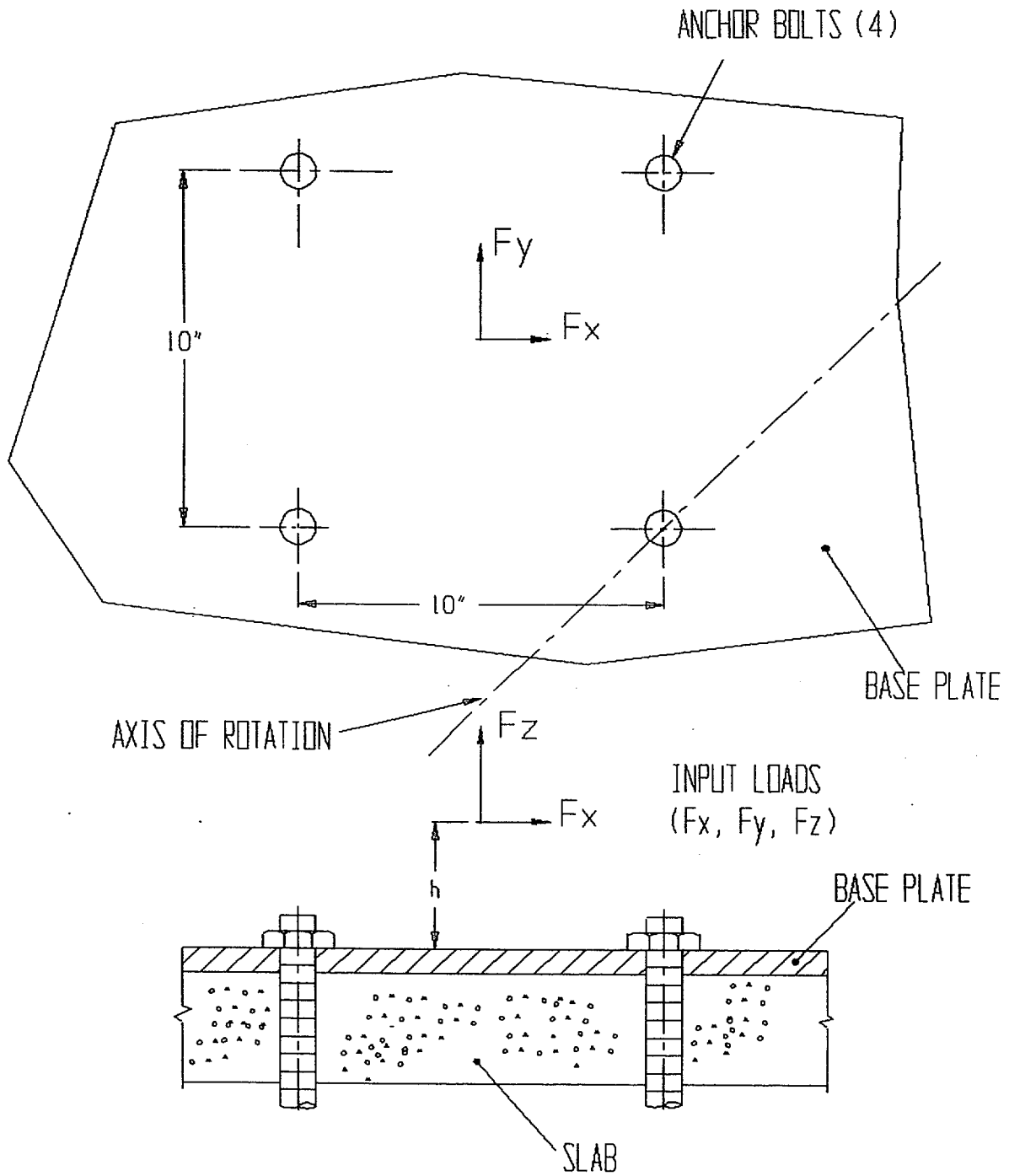


FIGURE 11.1; HI-STAR 100 ANCHOR BOLT LOAD ANALYSIS

12.0 ACCEPTABLE CARRY HEIGHTS FOR HI-STAR AND HI-STORM

The procedure that is used to determine the deceleration levels experienced by a cask due to an accidental drop on to the ISFSI pad is outlined in a recently published NUREG [21]. The NRC-compliant computer model, implemented on the public domain code LS-DYNA3D [17] by Holtec International, was presented to the NRC in 1997 and have been accepted by the Commission [24]. In this section, we provide results of dynamic impact simulation of loaded HI-STAR and HI-STORM on a bounding (stiff) ISFSI pad (defined in this document) using the benchmarked model. Details of the models used for both HI-STAR 100 and for HI-STORM 100 are available in Appendix 3.A of the respective TSARs. The only modifications to those models are in the ISFSI properties used which reflect the bounding maximum properties and geometry of the ISFSI defined in this topical report.

Since the casks are fastened to the pad for long-term storage, the non-mechanistic tipover scenario need not be considered. The only relevant handling event that is considered within this report is vertical handling. For specific sites planning to utilize the technology presented in this topical report, a site specific analysis may be performed to establish a minimum vertical handling height for the loaded cask. In this report, we consider the thickest reference pad with the stiffest soil subgrade modulus permitted in Table 4.1. The purpose of the analyses performed herein is to demonstrate that a loaded HI-STAR or HI-STORM can be carried at a sufficient height over the pad to permit fastening to the pad. For the analysis, we consider the following limiting pad configuration:

Pad thickness $h=60$ "

Aged concrete compressive strength = 6000 psi

Subgrade depth = assumed to be sufficiently deep so that the sub-grade modulus can be computed from the analytical solution for a loaded semi-infinite elastic foundation [23].

Subgrade Modulus = 3000 pci.

From Reference [23], the spring constant “K” associated with a semi-infinite elastic foundation loaded by a circular rigid plate is given by

$$K = E\sqrt{A} / 0.96(1 - \nu^2)$$

where “E” is the Young’s Modulus associated with the elastic foundation, “A” is the area of the circular contact patch at the top surface of the foundation, and $\nu = 0.4$ is assumed as the Poisson’s Ratio for the foundation material. The units of K are lb./in if E is given in “psi” and A is given in “in²”. The Standard Subgrade Modulus “k”, that is used to characterize the foundation under the pad, is defined with units of pounds per cubic inch “pci”, and is obtained by dividing the spring constant by the contact area. Therefore, the Subgrade Modulus is expressed in the form

$$k_{sg} = E / 0.96(1 - \nu^2)\sqrt{A}$$

As we are assuming a bounding value for the subgrade modulus in the analysis, the above relationship can be used to define a bounding value for the Young’s Modulus E to be entered into the benchmarked dynamic analysis model of the vertical handling accident. The area A, entered into the above formulation, is the area at the top surface of the foundation (i.e., the bottom surface of the assumed ISFSI pad) based on a diameter of 30" (the standard size test piece used to develop tabular data characterizing subgrade modulus with a qualitative description of foundation type). Finally, solving for the Young’s Modulus of the foundation in terms of the subgrade modulus gives the relationship:

$$E = k_{sg} \sqrt{A} 0.96(1 - \nu^2)$$

Using the bounding values for subgrade modulus and pad thickness gives the appropriate values for foundation Young's Modulus as $E = 64319$ psi. In the subsequent dynamic drop analysis, a value of 65,000 psi is used.

Table 12.1 Upper Bound Values for Foundation Young's Modulus

CASK	Young's Modulus (psi)
HI-STAR 100 or HI-STORM 100	65,000

The LS-DYNA model benchmarked in Reference [17] and utilized in the HI-STAR 100 and HI-STORM 100 TSARs [3,4] is applied to the bounding stiff ISFSI pad/foundation to establish that the casks may be carried over the pad without exceeding the design basis decelerations established for drop accidents in the respective TSAR's. The extent of the pad/foundation finite element model, the boundary conditions, and the materials used to model the concrete pad and the underlying foundation are identical to the same items used in the HI-STAR and HI-STORM TSAR's [3,4]. Figures 12.1-2 show the finite element model and the resulting cask deceleration time history for the HI-STAR 100 System analysis and Figures 12.3-12.4 present similar results for the HI-STORM 100 System. For both analyses, the overpack nodes are constrained to move vertically as a rigid body. Table 12.2 gives results for cask carry heights (elevation of bottom surface of cask baseplate above top surface of ISFSI pad) that are established for the bounding pad/foundations defined:

Table 12.2 Cask Elevation/Decelerations for Bounding Configurations

CASK	Elevation Above Pad (inch)	Initial Impact Velocity (inch/sec.)	Filtered Vertical Deceleration (g's)
HI-STAR	12	96.3	45.9
HI-STORM	10	87.9	45.0

In accordance with the bench marking of DYNA3D, the cask vertical deceleration time histories are filtered at 350 Hz. The deceleration for HI-STAR 100 is measured at the top surface of the overpack baseplate, while the deceleration for HI-STORM is measured at the top surface of the internal concrete shielding block supporting the MPC.

The results of the drop analyses show that both the HI-STAR 100 and HI-STORM 100 can be safely carried over the attachment structure constructed on the strongest ISFSI pad without exceeding the design basis deceleration in the TSAR that is set to insure retrievability of the stored fuel by normal means.

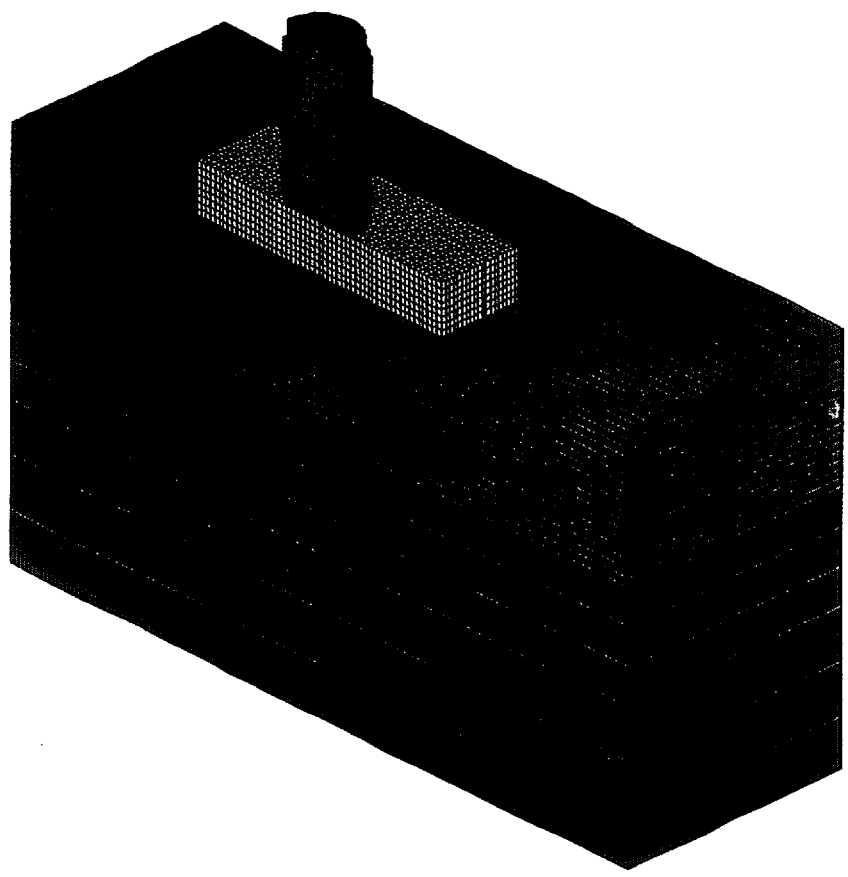
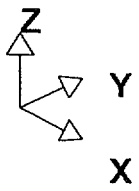


FIGURE 12.1: FINITE ELEMENT GRID FOR HI-STAR 100 12" DROP

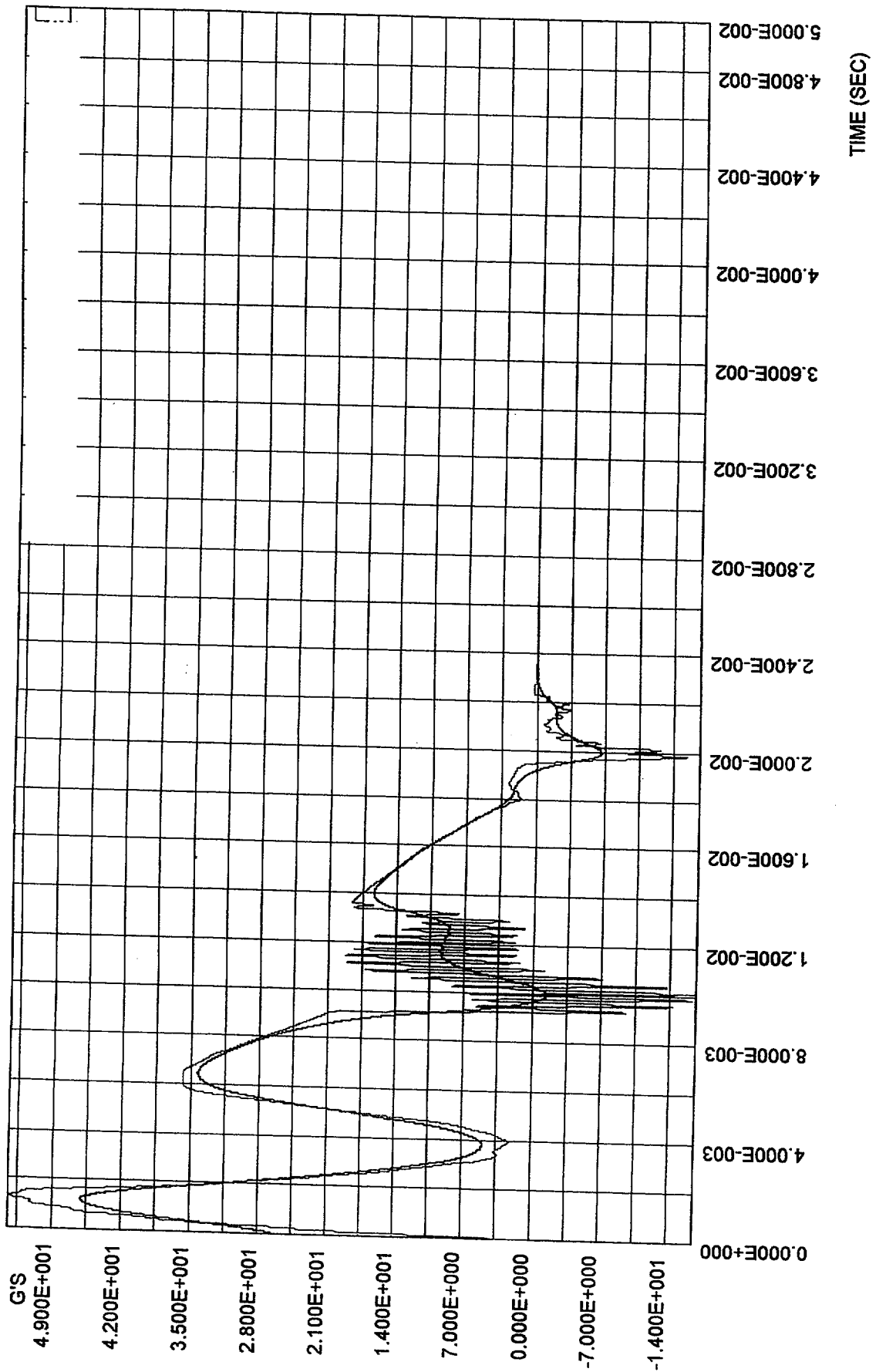


FIGURE 12.2: HI-STAR UNFILTERED AND FILTERED DECELERATION

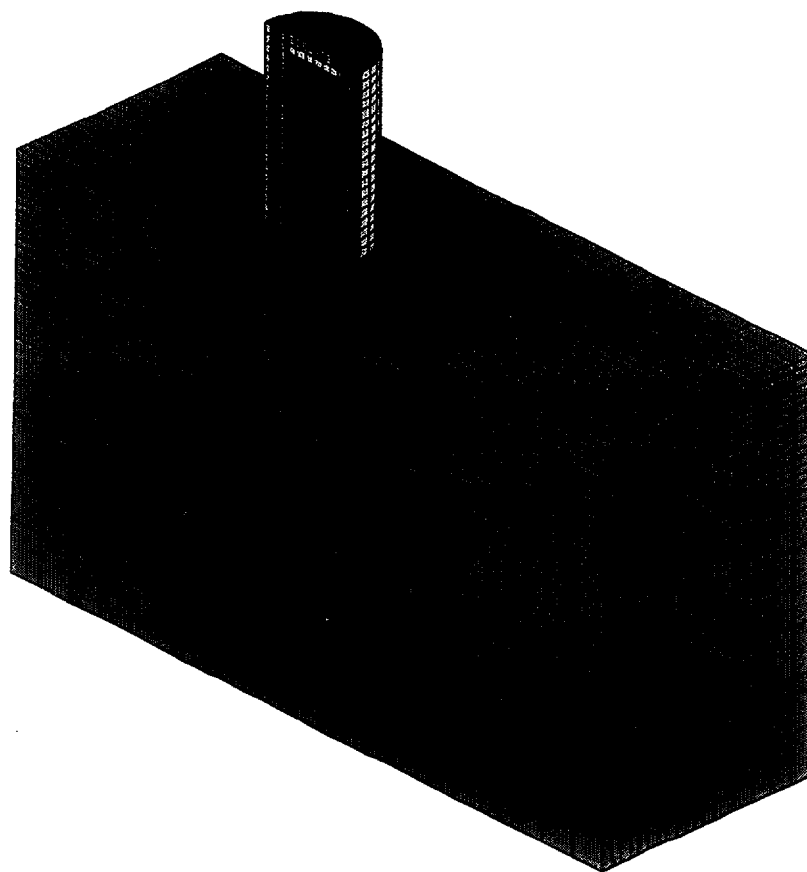


FIGURE 12.3: FINITE ELEMENT GRID FOR HI-STORM 100

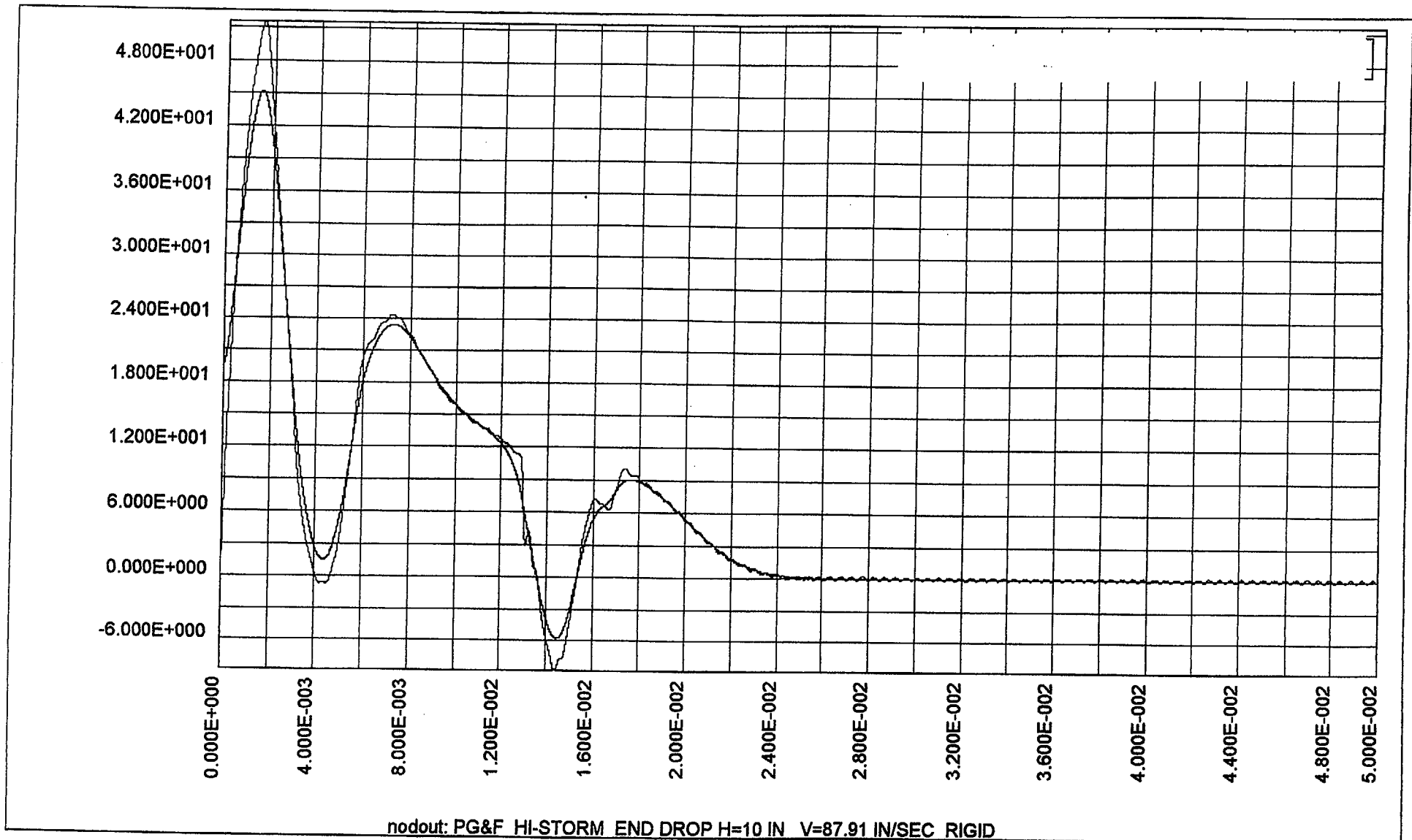


FIGURE 12.4: UNFILTERED AND FILTERED DECELERATION AT BASE OF MPC

13.0 TECHNICAL SPECIFICATION

13.1 Scope

This Specification provides the requirements for deploying HI-STAR 100 or HI-STORM 100 systems in an anchored configuration at an ISFSI.

13.2 Pad

The structural design of the pad will comply with the requirements specified in Section 4 herein. The construction of the pad shall meet the requirements in Section 3.2 and the codes/standards referenced therein.

Quality procedures suitable for Category C Important to Safety classification shall apply to all aspects of pad design, material acquisition, and construction activities.

13.3 Anchorage System

The design of the anchorage system for HI-STAR 100 shall be in compliance with the provisions of Section 7 of this topical report. The anchoring system for HI-STORM 100 shall be designed, fabricated, and installed in accordance with the provisions of Section 8 of this topical report.

13.4 Maintenance and Design Life

The installed system shall be subjected to periodic inspection and preventive maintenance to prevent corrosion damage. The initial design life of the installed system shall be 20 years.

14.0 INSTALLATION PROCEDURES

14.1 INTRODUCTION

This chapter provides the installation procedures for installation of the HI-STAR 100 System and HI-STORM 100 System Anchor Systems for storage operations in high seismic environments. The procedures are prescriptive to the extent that it provides the basis and guidance for plant personnel to prepare detailed site-specific written procedures.

14.2 DISCUSSION

These procedures are prescriptive to the extent that they provide the basis and general guidance for plant personnel in preparing detailed written site-specific installation procedures. Licensees (Users) will utilize this procedure, the Technical Specifications, the conditions of the HI-STAR 100 and/or HI-STORM 100 Certificate(s) of Compliance, equipment-specific operating instructions, and plant working procedures and apply them to develop the site-specific installation procedures. The steps contained herein describe acceptable methods for performing HI-STAR 100 and HI-STORM 100 operations. Users may alter the steps in this chapter to allow operations to be performed in parallel or out of sequence as long as the general intent of the procedure is met. Users may also use adapt these procedures to use alternate alignment and handling methods. Users may select alternate configurations to accommodate their specific needs and available equipment. Any deviations to the rigging should be approved by the user's load handling authority.

Users are required to implement controls in order to assure that requirements of the HI-STAR 100 System and/or HI-STORM 100 System TSAR(s) are met. These include, but are not limited to: controls to ensure that lifted weights do not exceed the trunnion design limits and limits to maintain the overpacks within the allowable lift heights.

The HI-STAR 100 and HI-STORM 100 overpacks may be transferred between the ISFSI and the fuel loading facility using a specially designed transporter, heavy haul transfer trailer, or any other load handling equipment designed for such applications as long as the lifting requirements described in the applicable Technical Specifications are met. Users shall develop detailed

written procedures to control on-site transport operations.

14.3 RESPONSIBILITIES

14.3.1 Responsibilities vary according to specific organization within the site. Users are responsible to assign duties and responsibilities in accordance with their specific organizational requirements. The procedure refers to organizations by general function. Users shall interpret the general names to specific names within the organization.

14.4 PROCEDURE

14.4.1 Initial Conditions/Requirements:

- 14.4.1.1 All personnel assigned to specific tasks are trained and qualified in accordance with site procedures for their respective assigned tasks.
- 14.4.1.2 All personnel have been briefed on the precautions and limitations necessary for cask placement operations.
- 14.4.1.3 The HI-STAR 100 or HI-STORM 100 (as applicable) has been loaded in accordance with approved site procedures and is ready for placement at the ISFSI.
- 14.4.1.4 The corresponding anchor chair (storage location) has been identified and inspected and is ready to accept the loaded HI-STAR 100 or HI-STORM 100 System.
- 14.4.1.5 All tools are ready and available for use.
- 14.4.1.6 The hardware has been inspected and are available for use.
- 14.4.1.7 The transport vehicle and equipment is ready and available for use.
- 14.4.1.8 All lifting equipment has been inspected and displays valid load handling certification tags.
- 14.4.1.9 The RWP/SWP has been issued for the work to be performed.

14.4.2 Precautions/Limitations:

- 14.4.2.1 Users shall ensure that all requirements identified in the applicable TSAR are met. The procedure contains specific steps and requirements that must be observed to ensure compliance with the requirements. These include lift heights and trunnion load limits (as applicable).

- 14.4.2.2 Radiation dose rates are higher on the underside of the HI-STAR 100 and around the air inlet ducts of the HI-STORM 100. Workers shall utilize appropriate ALARA precautions and utilize remote observation and handling tools as necessary.
- 14.4.2.3 All Notes/ Warnings and Cautions shall be read, understood and followed by all workers involved in the relevant steps of the procedure.

14.4.3 HI-STAR 100 System Preparation for Placement on the Anchor Chairs:

Note:

The HI-STAR 100 overpack may be handled in several different configurations and may be transported on-site in a horizontal or vertical orientation. This section provides general guidance for installation of the HI-STAR 100 clevis blocks to the underside of the HI-STAR 100 Overpack and installation of the HI-STAR 100 Overpack in the anchor chair. Refer to the TSAR for lifting requirements. Refer to Figure 14.4.1.

- 14.4.3.1 Installation of the clevis blocks with the HI-STAR 100 Overpack in the vertical orientation:

Note:

The location and orientation of the clevis blocks are crucial. All clevis studs must be located in their respective locations and oriented to their correct rotational alignment for the clevis studs and the clevis blocks to align.

Warning:

Radiation dose rates are higher on the underside of the HI-STAR 100. Workers shall utilize appropriate ALARA precautions and utilize remote observation and handling tools as necessary.

- 14.4.3.1.1 RAISE the HI-STAR 100 and position cribbing under the HI-STAR 100 Overpack. The cribbing must allow access to the clevis stud locations.

Note:

A rolling garage-type car jack with a rotating saddle may be helpful in positioning the clevis stud for installation.

- 14.4.3.1.2 INSTALL eight (8) clevis studs in the bottom of the HI-STAR 100 Overpack.
- 14.4.3.1.3 TIGHTEN the clevis studs to hand tight.
- 14.4.3.1.4 IF necessary, BACK OUT the clevis studs until the holes are in alignment. The hole in each clevis stud must be aligned with the hole in the opposite clevis stud.

14.4.3.1.5 **INSTALL** a length of pipe through the holes in the opposite pair of clevis studs to check the alignment of the clevis studs.
REPEAT for the remaining three pairs of clevis studs.

14.4.3.1.6 **CAREFULLY** remove the pipe while maintaining the clevis studs in their respective alignment.

14.4.3.1.7 **RAISE** the HI-STAR 100 Overpack and remove the cribbing.

14.4.3.2 Installation of the clevis blocks with the HI-STAR 100 Overpack in the horizontal orientation:

Note:

The orientation of the clevis blocks is crucial. All clevis studs must be oriented to their correct rotational alignment for the clevis studs and the clevis blocks to align.

Warning:

Radiation dose rates are higher on the underside of the HI-STAR 100. Workers shall utilize appropriate ALARA precautions and utilize remote observation and handling tools as necessary.

14.4.3.2.1 **INSTALL** eight (8) clevis studs in the bottom of the HI-STAR 100 Overpack.

14.4.3.2.2 **TIGHTEN** the clevis studs to hand tight.

14.4.3.2.3 **IF** necessary, **BACK OUT** the clevis studs until the holes are in alignment. The hole in each clevis stud must be aligned with the hole in the opposite clevis stud.

14.4.3.2.4 **INSTALL** a length of pipe through the holes in the opposite pair of clevis studs to check the alignment of the clevis studs.
REPEAT for the remaining three pairs of clevis studs.

14.4.3.2.5 **CAREFULLY** remove the pipe while maintaining the clevis studs in their respective alignment.

14.4.3.2.6 RAISE the HI-STAR 100 Overpack and remove the cribbing.

14.4.3.3 TRANSPORT the HI-STAR 100 Overpack to the ISFSI in accordance with approved site handling procedures.

14.4.3.4 Installation of the HI-STAR 100 Overpack on the anchor chairs.

Note:

The HI-STAR 100 Overpack may be raised and positioned at the ISFSI using a crane system or special transporter system designed for such application.

14.4.3.4.1 IF necessary, align the transporter to the anchor chair using the alignment marks.

14.4.3.4.2 RAISE the HI-STAR 100 Overpack to a height necessary to clear the height of the clevis blocks with the clevis studs.

14.4.3.4.3 POSITION the HI-STAR 100 Overpack over the anchor chair using the alignment approach guide marks and guidance from the spotters.

Note:

The clevis studs and top plate are tapered to assist in alignment and installation of the clevis studs. Once these clevis studs have commenced engagement, all clevis studs will automatically align. A length of pipe installed in the holes of an opposite pair of clevis studs may be used to help rotate the cask.

14.4.3.4.4 SLOWLY lower the HI-STAR 100 Overpack until the clevis studs begin to engage the anchor chair holes.

14.4.3.4.5 REMOVE the pipe and/or alignment devices and perform a visual inspection to look for interference. ADJUST the position of HI-STAR 100 accordingly.

14.4.3.4.6 SLOWLY lower the HI-STAR 100 Overpack until the bottom end is fully seated in the anchor chair.

- 14.4.3.4.7 DISCONNECT the transporter or crane from the HI-STAR 100 Overpack and remove it from the operations area.

Note:

The threaded hole of the clevis pins faces the outside.

- 14.4.3.4.8 INSTALL the clevis pins into the clevis blocks until fully seated.
- 14.4.3.4.9 INSTALL the clevis pin cap and install the plug.
- 14.4.3.4.10 FILL the clevis pin reservoir with grease and install the sealing cap.
- 14.4.3.4.11 IF necessary, INSTALL the HI-STAR 100 bottom shield ring around the HI-STAR 100 base.

14.4.4 HI-STORM 100 System Preparation for Placement on the Anchor Chairs:

Note:

The HI-STORM 100 overpack may be handled in several different configurations in the vertical orientation. This section provides general guidance for installation of the HI-STORM 100 Overpack in the anchor chair. Refer to the HI-STORM 100 TSAR for lifting requirements.

Note:

The location and orientation of the HI-STORM 100 is crucial to assure alignment of all HI-STORM 100 Systems.

Warning:

Radiation dose rates are higher around the air inlet ducts of the HI-STORM 100. Workers shall utilize appropriate ALARA precautions and utilize remote observation and handling tools as necessary.

- 14.4.4.1.1 IDENTIFY the storage destination and orientation of the HI-STORM 100 System.
- 14.4.4.1.2 CLEAN out any debris from the threaded anchor holes at the storage location.
- 14.4.4.1.3 APPLY a light layer of site-approved thread lubricant to the tie-down bolt threads.
- 14.4.4.1.4 RUN the tie-down bolts by hand into each threaded anchor hole to assure that the holes are free and clear of debris.
- 14.4.4.1.5 CLEAR any debris from the storage location to assure that debris does not fall into the anchor holes.
- 14.4.4.1.6 REMOVE the tie-down bolts.
- 14.4.4.2 TRANSPORT the HI-STORM 100 Overpack to the ISFSI in accordance with approved site handling procedures.
- 14.4.4.3 Installation of the HI-STORM 100 Overpack on the anchor chairs.

Note:

The HI-STORM 100 Overpack may be raised and positioned at the ISFSI using a crane system, air pad system or special transporter system designed for such application.

- 14.4.4.3.1 POSITION the HI-STORM 100 Overpack over the anchor chair using alignment approach guide marks and/or guidance from the spotters.

Note:

A pair of alignment pins may be used to help position the HI-STORM 100 at its correct location and orientation.

- 14.4.4.3.2 ALIGN the HI-STORM 100 over its storage position. If necessary, install alignment pins. If necessary, two opposite holes. (See Figure 14.4.2)
- 14.4.4.3.3 SLOWLY lower the HI-STORM 100 Overpack using the alignment pins to adjust the position.
- 14.4.4.3.4 REMOVE the alignment pins and/or any other alignment devices.
- 14.4.4.3.5 DISCONNECT the transporter or crane from the HI-STORM 100 Overpack and remove it from the operations area.
- 14.4.4.3.6 INSTALL the tie-down bolts into the anchor holes. (See Figure 14.4.3).
- 14.4.4.3.7 TIGHTEN the anchor bolts to 80 + 20/-0 ft-lbs.

FIGURE 14.4.1
HOLTEC PROPRIETARY

FIGURE 14.4.2
HOLTEC PROPRIETARY

FIGURE 14.4.3

HOLTEC PROPRIETARY

15.0 REFERENCES

- [1] J.W. McConnell, A.L. Ayers, and M.J. Tyacke,, "Classification of Transportation Packaging and Dry Spent fuel Storage System Component According to Important to Safety," Idaho National Engineering Laboratory, NUREG/CF-6407, INEL-95-0551.
- [2] NRC Regulatory Guide 7.10, "Establishing Quality Assurance Programs for Packaging Used in the Transport of Radioactive Material," USNRC, Washington, D.C., Rev. 1 (1986).
- [3] Topical Safety Analysis Report for HI-STAR 100 Cask System, Holtec Report No. HI-941184, Rev. 8.
- [4] Topical Safety Analysis Report for HI-STORM 100 Cask System, Holtec Report No. HI-951312, Rev. 4.
- [5] NRC Information Notice 95-28, "Emplacement of Support Pads for Spent Fuel Dry Storage Installations at Reactor Sites," USNRC, Washington, D.C. (1995).
- [6] K. P. Singh, A. I. Soler, and M. G. Smith,, "Seismic Response Characteristics of HI-STAR 100 Cask System on Storage Pads," INMM, Washington, D.C., January 14, 1998.
- [7] S. Levy and J. Wilkenson, The Component Element Method in Dynamics, McGraw-Hill, 1976.
- [8] R. W. Clough and J. Penzien, Dynamics of Structures, p. 273, McGraw Hill (1975).
- [9] Holtec Proprietary Computer Code DYNAMO, QA Validation Manual, HI-91700.
- [10] Code of Federal Regulations, Energy, 10, Chapter 1, Part 72, U.S. Government Printing Office, Washington, D.C. (1997).
- [11] K. P. Singh and A. I. Soler, "Mechanical Design of Heat Exchangers and Pressure Vessel Components," Chapter 21, Arcturus Publishers, Cherry Hill, NJ, 1984.
- [12] NUREG-1567, Standard Review Plan for Spent Fuel Dry Storage Facilities (Draft Report for Comment), October 1996.
- [13] ACI 349, "Code Requirements for Nuclear Safety Related Concrete Structures."

- [14] ANSI/AWS D1.1-98, "Structural Welding Code-Steel."
- [15] NRC Regulatory Guide 1.60, "Design Response Spectra for Seismic Design of Nuclear Power Plants."
- [16] United States Nuclear Regulatory Commission, NUREG-0800, "Standard Review Plan for the Review of Safety Analysis Reports for Nuclear Power Plants," 3.7.1, "Seismic Design Parameters," Washington, D.C. (1981).
- [17] "Benchmarking of the Holtec LS-DYNA3D Model for Cask Drop Events," Holtec Report HI-971779.
- [18] United States Nuclear Regulatory Commission Regulatory Guide 1.59, "Design Basis Floods for Nuclear Power Plants", August 1973 and Rev. 1, April 1976.
- [19] "Estimate of Tsunami Effect at Diablo Canyon Nuclear Generating Station, California." B.W. Wilson, PG&E (September 1985, Revision 1).
- [20] "Manual of Steel Construction," 9th Edition, American Institute of Steel Construction, Chicago, Illinois 60601.
- [21] NUREG/CR-6608, UCRL-ID-129211, Summary and Evaluation of Low-Velocity Impact Tests of Solid Steel Billet Onto Concrete Pads, February 1998.
- [22] ASME Code, Section III, Subsection NF and Appendix F, and Code Section II, Part D, Materials, 1998.
- [23] Timoshenko and Goodier, Theory of Elasticity, 3rd Edition, McGraw-Hill, 1970, p.407.
- [24] "Safety Evaluation Report for the HI-STAR 100 System", Docket Number 72-1008, USNRC (September 30, 1998).

APPENDIX A

DYNAMIC ANALYSIS PROCEDURE

In nonlinear dynamic analysis, the response of the structure from individual loadings cannot be summed linearly or by the traditional square-root-of-the-sum-of-square method common in linear simulations. The three orthogonal ground accelerations must be applied *simultaneously* to obtain a meaningful solution for the seismic response. Accordingly, in the dynamic analysis methodology presented herein, seismic accelerations in the three orthogonal directions are applied simultaneously to the slab supporting the cask.

The DBE seismic excitation for a site is a complex function of a wide array of geophysical variables. Each specific ISFSI site has its own signature earthquake developed by the geotechnical engineers. The strength of an earthquake, however, is definitively portrayed by its response spectrum [11, Chapter 22]. It is commonly recognized that the response of a structure to two seismic inputs can be reliably compared by examining their response spectra. If one spectrum uniformly envelopes another, then the response of the structure to the "enveloping" earthquake will bound that to the "enveloped" one. With this axiom in mind, a Regulatory Guide 1.60 [15] response spectrum grounded at 1.5g ZPA is selected as the reference spectrum. A twenty-second synthetic time-history that envelopes the reference spectrum and the related power spectrum density function is developed in compliance with the provisions of NUREG-0800 [16]. Figures 5.2-5.4 show three artificial acceleration time-histories with ZPA = 1.5 (5% damping), all of which meet Reference 16 enveloping requirements. Furthermore, these time-histories are statistically independent of each other (defined as the cross correlation coefficient $\rho_{ij} \neq 0.15$; $i,j = 1,2,3$). As shown in Figures 5.5-5.7, the response spectra corresponding to the synthetic time-histories bound the design spectra uniformly within the prescriptions of Reference 16.

A.1 Dynamic Model

The cask dynamic model seeks to define a relatively rigid overpack containing an autonomous structure (MPC) supported on a foundation (ISFSI) with a defined coefficient of friction, Φ . The first step in the dynamic analysis is to represent the structure to be analyzed with sufficient degrees of freedom to capture its dynamic response accurately in the mathematical model. Accordingly, six degrees of freedom (6 DOF) describe the translation and rotation of the cask overpack as a rigid body; three translational (DOF 1-3) and three rotational (DOF 4-6) degrees of freedom are defined at the cask center of gravity location. The MPC is fully confined in the overpack; however, the small lateral and vertical gaps permit independent MPC canister (the shell, lid, and baseplate) motion relative to the overpack. Contained within the MPC shell and top and bottom closures is a multi-cell fuel basket which is a free-standing structure capable of vertical movement within the canister. Five degrees of freedom describe translation (DOF 7-9) and rotation (DOF 10-11) about two orthogonal horizontal axes of the MPC. Degrees of freedom 7, 8, 10, and 11 include the mass and inertia of both the MPC canister and the fuel basket. Degree of freedom 9 includes only the mass of the MPC canister as a separate degree of freedom used to describe the vertical motion of the fuel basket. The fuel assemblies contained within the MPC are considered very flexible components compared to the various structural components of the cask system; ten degrees of freedom describe the translation in the horizontal plane of each of five fuel assembly lumped masses located along the centerline of the system. The lumped masses represent all fuel assemblies stored in the cask system; the independent masses are located at the MPC top (DOF 12-13), the MPC three-quarter height (DOF 14-15), the MPC half-height (DOF 16-17), the MPC quarter-height (DOF 18-19), and the MPC bottom (DOF 20-21). The vertical motion of the totality of fuel assemblies is described by a single degree of freedom (DOF 22). Finally, the vertical movement of the fuel basket, within the MPC canister, is described by one translational degree of freedom (DOF 23). Figure A.1 shows a disassembled view of the HI-STAR 100 cask system model with the degrees of freedom shown. For HI-STORM 100, a simpler model is used in that the fuel and the fuel basket masses are “lumped with the MPC mass; only eleven degrees of freedom are used to simulate the dynamic system with relative motion between the MPC plus contents and the HI-STORM 100 overpack explicitly

included in the analysis. In the HI-STORM 100 dynamic model, only DOF's 1-11 are included and the mass and inertia properties of the MPC include the mass of the contained fuel basket and spent nuclear fuel.

The attachment system is represented in the dynamic model by appropriate spring elements. For HI-STAR 100, there are discrete clevis assemblies each represented by compression-only springs for bearing, and tension-only springs where bolts are located. Linear shear springs provide a model of the horizontal shear resistance of the bolts. The spring rates are determined from the characteristics of the anchoring system and a detailed development of suitable values is documented in a separate appendix. For the dynamic model of HI-STORM 100, there are discrete locations where sector lugs provide both compression, tensile, and shear connection with the concrete slab. Compression-only spring elements and tension-only spring elements simulate the compression resistance of the sector lugs and tensile resistance of the anchor bolts, respectively. Linear springs provide shear resistance at these locations. Compression resistance is also provided by a series of peripheral springs simulating the local resistance of the slab around the periphery of the HI-STORM 100 interface. The compression only springs are located every 10 degrees around the periphery of the base of the overpack. Frictional resistance at these compression locations is simulated by two orthogonal springs in the horizontal plane of the slab that are active only when the compression-only spring is active. These friction springs have the characteristic of linear springs up until a limit force is achieved. Subsequent to achievement of the limiting force, the resistance is constant until the spring unloads. Unloading is governed by the same relation as initial loading. The limiting force in the friction springs at each location is a function of the interface coefficient of friction multiplied by the instantaneous value of the force in the local compression-only spring. Details concerning the calculation of spring rates for both HI-STAR 100 and HI-STORM 100 are provided in separate appendices. For both cask simulations, a bounding set of forces for detailed stress analysis of the anchoring system is obtained by choosing spring rates at conservatively large values to maximize the interface reactions. Also included in the model are compression-only elements to simulate the opening and closing of the small gaps between various cask components and between the fuel and the fuel basket. Representative gaps between the components are used in the simulation and the

contact stiffness between components are set at conservatively high values to maximize the impact loads.

The governing equations of motion for either cask simulation are derived using the classical Lagrangian method [7,8] wherein the kinetic energy of the system is written in terms of the generalized coordinates of the problem. Performing certain partial differentiation operations on the kinetic energy and equating the results of the operations to the appropriate generalized forces associated with each degree of freedom yields the appropriate system equations of motion. In general terms, if K is defined as the system kinetic energy, then the equations of motion for the cask system can be written by differentiating the system kinetic energy and calculation and subsequent inspection of the extensions of the spring elements in the problem expressed in terms of generalized coordinates, as described below using the HI-STAR 100 model for illustrative purposes.

Referring to the nomenclature, the constituent components of the system kinetic energy are written for the HI-STAR simulation as follows:

a. Overpack

$$K_1 \ni \frac{1}{2} M_1 (\phi_1^2 \% \phi_2^2 \% \phi_3^2) \% \frac{1}{2} I_1 (\phi_4^2 \% \phi_5^2) \% \frac{1}{2} I_3 \phi_6^2$$

b. MPC plus the Fuel Basket (except for the kinetic energy of fuel basket due to vertical motion)

$$K_2 \ni \frac{1}{2} M_2 (\phi_7^2 \% \phi_8^2) \% \frac{1}{2} M_3 \phi_9^2 \% \frac{1}{2} I_4 (\phi_{10}^2 \% \phi_{11}^2)$$

c. MPC Fuel Basket - Vertical Motion

$$K_3 \ni \frac{1}{2} M_4 \phi_{23}^2$$

d. Fuel Assembly Mass

$$K_4 \ni \frac{1}{2} M_f (\phi_{12}^2 \% \phi_{13}^2 \% \phi_{14}^2 \% \phi_{15}^2 \% \phi_{16}^2 \% \phi_{17}^2 \% \phi_{18}^2 \% \phi_{19}^2 \% \phi_{20}^2 \% \phi_{21}^2) \% \frac{5}{2} M_f \phi_{22}^2$$

(Note that the total mass of the SNF is given by $5M_f$).

Lagrange's Equations of Motion have the general form

$$\frac{d}{dt} \left(\frac{\partial K}{\partial \dot{\phi}_i} \right) \% \frac{\partial K}{\partial \phi_i} \ni Q_i \quad i \ni 1, 2, \dots, 23$$

where K = the total kinetic energy of the system.

Since the component mass and inertia do not change with position during the seismic event, we have

$$\frac{\partial K}{\partial \phi_i} \ni 0 \quad i \ni 1, 2, \dots, 23$$

Using the above expressions for kinetic energy, we can carry out the differentiations

$$\frac{d}{dt} \left(\frac{\partial K}{\partial \dot{\phi}_i} \right) \quad \text{where } K \ni K_1 \% K_2 \% K_3 \% K_4$$

and set the result to Q_i , for $i = 1, 2, \dots, 23$ to obtain the 23 equations of motion for the system. In this application, the system is inertially decoupled (i.e., the final generalized mass matrix is diagonal); coupling is only through the various terms in the generalized force expressions. Nonlinear compression-only elements simulate contact and piecewise linear elements simulate friction between surfaces rendering the generalized forces nonlinear.

The final set of equations can be written in matrix form as

$$[M] \{\ddot{q}_i\} \ni \{Q_i(t)\}$$

where, the non-zero elements of the diagonal [M] are m_{ij} and

$$m_{11} \ni M_1 ; m_{22} \ni M_1 ; m_{33} \ni M_1$$

$$m_{44} \ni I_1 ; m_{55} \ni I_1 ; m_{66} \ni I_3$$

$$m_{77} \ni M_2 ; m_{88} \ni M_2 ; m_{99} \ni M_3$$

$$m_{10,10} \ni I_4 ; m_{11,11} \ni I_4$$

$$m_{12,12} \ni m_{13,13} \ni m_{14,14} \ni m_{15,15} \ni m_{16,16} \ni M_f$$

$$m_{17,17} \ni m_{18,18} \ni m_{19,19} \ni m_{20,20} \ni m_{21,21} \ni M_f$$

$$m_{22,22} \ni 5M_f \quad m_{23,23} \ni M_4$$

The contributions to generalized force Q_i have spring-like behavior involving the difference between displacement components. Therefore, if all of the translational degrees of freedom are redefined to represent displacements relative to ground in the appropriate directions, then the generalized forces are unaltered. Therefore, the equations can be rewritten in terms of relative coordinates $p_i(t)$, where

$$p_i(t) \ni q_i(t) \& U_1(t) \quad i \ni 1,7,12,14,16,18,20$$

$$p_i(t) \ni q_i(t) \& U_2(t) \quad i \ni 2,8,13,15,17,19,21$$

$$p_i(t) \ni q_i(t) \& U_3(t) \quad i \ni 3,9,22,23$$

$p_i(t) \ni q_i(t)$ all remaining (rotational) degrees of freedom

The final system equations of motion are, in terms of $p_i(t)$, given as

$$[M] \{\ddot{p}_i\} \ni \{Q_i(p,t)\} \& [M] \{U\} \ddot{U}_1(t) \& [M] \{V\} \ddot{U}_2(t) \& [M] \{W\} (\ddot{U}_3(t) \% g)$$

with $U(t)$ being the input ground acceleration time-histories, and where the column matrices $\{U\}$, $\{V\}$, $\{W\}$, consist of zero except as noted below.

$$\{U\}^T = [1,0,0,0,0,0,1,0,0,0,0,1,0,1,0,1,0,1,0,1,0,0,0]$$

$$\{V\}^T = [0,1,0,0,0,0,0,1,0,0,0,0,1,0,1,0,1,0,1,0,1,0,0]$$

$$\{W\}^T = [0,0,1,0,0,0,0,0,1,0,0,0,0,0,0,0,0,0,0,0,0,0,1,1]$$

Finally, the generalized forces can be developed in terms of the spring constants and the deformation of the springs associated with the simulation of contact, friction, or tension-only behavior. In the Lagrangian formulation, the generalized forces for spring-like components can be written in the form

$$Q_i \ni \& \sum_{j=1}^{NF} F_j(\ddot{A}_j) \frac{M\ddot{A}_j}{Mq_i} \quad i \ni 1,2,\dots,23$$

where $F_j(\ddot{A}_j)$ is a spring force associated with a kinematic extension \ddot{A}_j that arises due to contact. The representation above allows for any $F_j(\ddot{A}_j)$ to be zero during some time period due, for example, to loss of contact. For a given spring force representation identified by an extension \ddot{A} , the components

$$\frac{\ddot{M}_j}{\ddot{M}_i}$$

can be identified by inspection of the particular \ddot{A} . The coefficients

$$\frac{\ddot{M}_j}{\ddot{M}_i}$$

are labeled as the "coupling coefficients" associating a degree of freedom q_i to a particular spring force.

For example, for the cask with contact patch diameter d , then the "extension" of a vertical contact element at ground at the perimeter of the patch is given as

$$\ddot{A} \ni q_3 \text{ \% } \frac{d}{2} \sin \epsilon \text{ } q_4 \text{ \& } \frac{d}{2} \cos \epsilon \text{ } q_5$$

where ϵ is measured in the horizontal plane from the x axis and locates the particular contact element around the edge. Therefore, for this particular contact spring, the coupling coefficients are, by inspection of \ddot{A}

$$\frac{\ddot{M}_j}{\ddot{M}_3} \ni 1 ; \frac{\ddot{M}_j}{\ddot{M}_4} \ni \frac{d}{2} \sin \epsilon ; \frac{\ddot{M}_j}{\ddot{M}_5} \ni \text{ \& } \frac{d}{2} \cos \epsilon$$

The process of internally forming the generalized force matrix is built into Holtec International's QA-validated simulation code DYNAMO [9]; the user needs only identify the various coupling coefficients for each spring.

For the application at hand, all spring forces can be written in the generic form

$$F_j \ni \&K_j \ddot{A}_j$$

where K_j is zero or non-zero based on the current state (tension or compression, restrained or sliding, etc.). The algorithm for establishing the current state of a spring force is also built into DYNAMO.

A similar set of coupled differential equations can be developed for the HI-STORM 100 simulation. Since the contents of the MPC (fuel plus fuel basket) are “lumped” with the MPC for this simulation, the final system of equations represents an eleven degree of freedom system with six degrees representing the rigid body motion of the overpack and the remaining five degrees of freedom describing the relevant motion of the MPC plus contents.

A.2 Sensitivity Studies

The DYNAMO numerical analyses is validated for accuracy using the following approaches:

- a. Rerunning of the DYNAMO model using a smaller integration time-step (check for numerical convergence).
- b. Running cases where the gap data is varied. An anchored system, which is inherently stable, should not exhibit abrupt changes in response due to minor changes in input data.

Detailed numerical results are presented in the main body of this report.

A.3 Nomenclature

I_1	mass moment of inertia of overpack about x or y axis through the centroid
I_3	mass moment of inertia of overpack about z axis through the centroid
I_4	mass moment of inertia of MPC (canister plus fuel basket) about x or y axis through the centroid
K_i	kinetic energy of i^{th} component ($i = 1$ overpack, $i = 2$ MPC, $i = 3$ fuel basket vertical motion, $i = 4$ fuel assembly)

M_1	mass of overpack
M_2	mass of MPC (canister plus fuel basket)
M_3	mass of MPC enclosure vessel
M_4	mass of fuel basket
Q_i	generalized force for i^{th} degree of freedom
$q_1 - q_6$	overpack translational and rotational degrees of freedom
$q_7 - q_{11}$	MPC translational and rotational degrees of freedom
$q_{12} - q_{21}$	fuel translational (horizontal) degrees of freedom (HI-STAR only)
q_{22}	vertical degree of freedom of stored SNF (HI-STAR only)
q_{23}	fuel basket vertical degree of freedom (HI-STAR only)
$S_1:$	overpack-to-ISFSI pad contact stiffness
$S_2:$	fuel basket-to-fuel assembly contact stiffness
$S_3:$	MPC-to-overpack bottom plate contact stiffness
$S_4:$	fuel basket-to-MPC contact stiffness
U_j ($j=1,2,3$)	ground displacement (functions of time)
Φ	overpack/slab interface friction coefficient (not applicable to HI-STAR)

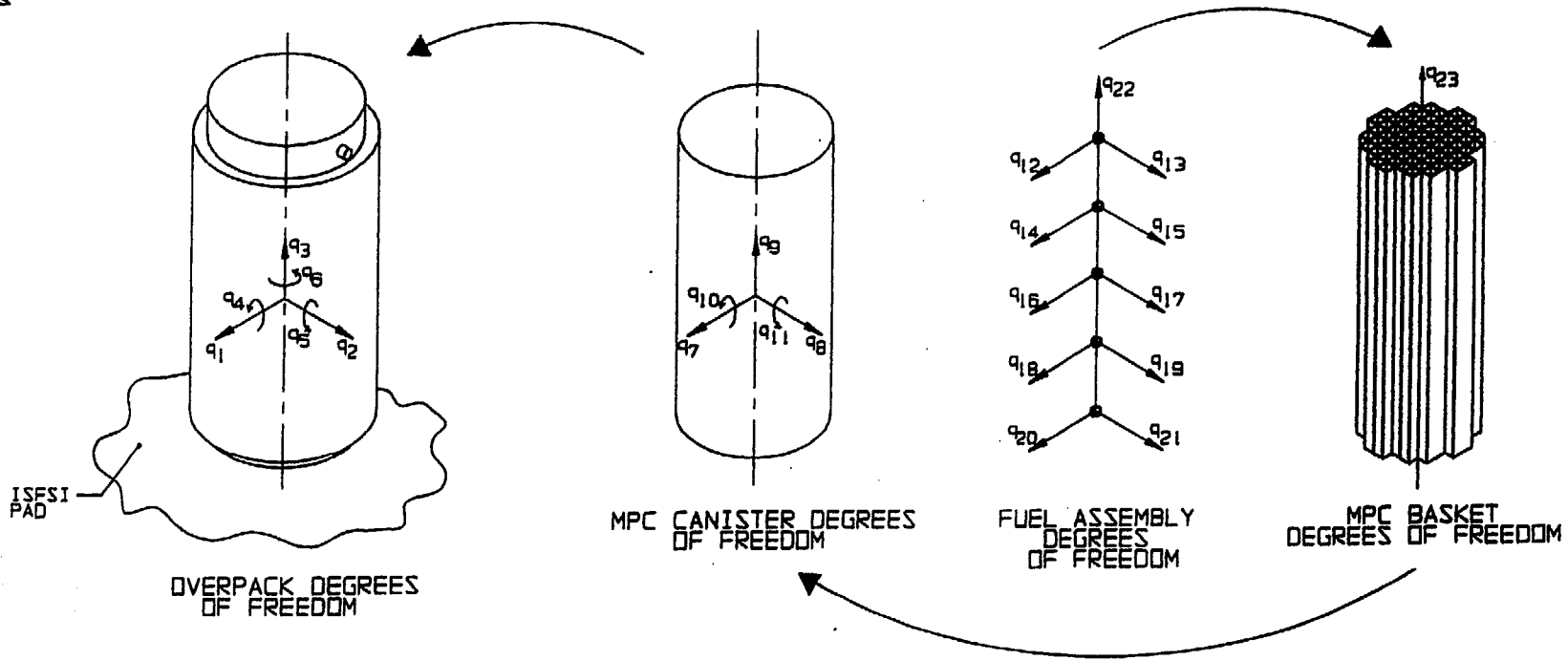


FIGURE A.1; CASK DYNAMIC MODEL

APPENDIX B - HI-STAR 100 HIGH SEISMIC ATTACHMENT

B.1 Scope of Appendix

This appendix consists of two separate analyses. First, the bolts on the HI-STAR 100 overpack baseplate that are used to secure a fully loaded HI-STAR 100 to an ISFSI are analyzed for load capacity based on bolt diameter and thread engagement length. Next, the appropriate spring constants are developed to simulate the effect of the attachment between the HI-STAR 100 and the ISFSI for modeling in a dynamic analysis. Included in the spring rate analysis are contributions from the attachment bolts, portions of the connecting structure, the ISFSI studs, and the underlying ISFSI.

This document is prepared using the MATHCAD electronic spread sheet program and the notation used is specific to that program. In particular, the notation ":= " is an assignment operation, while "=" denotes the calculation of a numerical result. The appearance of a small solid rectangle after an equation means that the equation is used as text in that location and is not associated with any calculation. This notation appears first in this appendix but is used elsewhere.

B.2 Configuration

B.2.1 - Attachment Bolt Engagement Length

The required data for analysis is 1) the number of bolts NB; 2) the bolt diameter db; 3) the total load; and 4), the details of the individual bolts.

B.2.2 - Spring Constant Calculation

The configuration of the entire attachment structure is shown in a series of figures presented in the main body of the report. These figures are supplemented by sketches as necessary within this appendix to aid in the spring constant calculation.

B.3 Acceptance Criteria

B.3.1 Bolts

ASME Code Section III, Appendix F stress limits for bolts apply. The allowable strengths in shear are set at 42 percent of the ultimate strength in tension. The allowable average tensile strength is 70% of the ultimate strength.

B.3.2 Spring Rates

Since this appendix defines the magnitudes of the spring rates, there is no acceptance criteria defined for this portion of the calculational results.

B.4 Composition of Appendix

This appendix is created using the Mathcad (version 7) software package. Mathcad uses the symbol ':=' as an assignment operator, and the equals symbol '=' retrieves values for constants or variables.

B.5 References

[B.1] E. Oberg and F.D. Jones, *Machinery's Handbook*, Fifteenth Edition, Industrial Press, 1957, pp987-990.

[B.2] FED-STD-H28/2A, *Federal Standard Screw-Thread Standards for Federal Services*, United States Government Printing Office, April, 1984.

[B.3] ASME Code, Section II, Part D, 1998.

[B.4] S.P. Timoshenko and J. Goodier, *Theory of Elasticity*, Third Edition, 1956, McGraw Hill, p. 407.

[B.5] ACI-349-95, Code for Reinforced Concrete Design in Nuclear Plants, American Concrete Institute.

[B.6] S.P. Timoshenko, *Strength of Materials*, Third Edition, Van Nostrand, 1955.

[B.7] HI-951184, HI-STAR 100 Topical Safety Analysis Report (TSAR), Revision 8.

B.6 Calculation of Limiting Bolt Capacity

B.6.1 Input Data

Bolt diameter $db := 2.5 \cdot \text{in}$ [B.7, Section 1.5]

Number of Bolts $NB := 8$ [B.7, Section 1.5]

$A_d := \pi \cdot \frac{db^2}{4}$ $A_d = 4.909 \cdot \text{in}^2$ is the area of the unthreaded portion of the bolt

$A_{\text{stress}} := 3.9976 \cdot \text{in}^2$ is the stress area of the bolt [B.1]

$d_{\text{pitch}} := 2.3376 \cdot \text{in}$ is the pitch diameter of the bolt [B.1]

$dm_{\text{ext}} := 2.1933 \cdot \text{in}$ is the minor diameter of the bolt [B.1]

$dm_{int} := 2.2294 \cdot \text{in}$ is the minor diameter of the hole [B.1]

The design temperature of the material is set at 200 deg. F based on thermal evaluation of the MPC during normal storage.

The yield and ultimate strengths of the lid and potential bolt materials are .

SA-350 LF3

$S_{ulid} := 68500 \cdot \text{psi}$ $S_{ylid} := 34200 \cdot \text{psi}$ [B.7]

SA-564-630

SA-193-B7

SB-637 N07718

$S_{ubolt} := 145000 \cdot \text{psi}$

$S_{uboltA} := 116667 \cdot \text{psi}$

$S_{uboltB} := 177600 \cdot \text{psi}$

$S_{ybolt} := 115600 \cdot \text{psi}$

$S_{yboltA} := 98000 \cdot \text{psi}$

$S_{yboltB} := 144000 \cdot \text{psi}$

[B.7]

[B.3] Note: Ultimate stress at temperature for SA-193-B7 obtained by reducing room temperature ultimate strength by the ratio of yield strength at temperature to yield strength at room temperature.

[B.7]

B.6.2 Calculations for SA-564-630 Material

In this section, load capacities are determined. The method and terminology of Reference B.2 is followed.

$N := 4 \cdot \frac{1}{\text{in}}$ is the number of threads per inch (UNC)

$p := \frac{1}{N}$ is the thread pitch

$H := 4 \cdot 0.21651 \cdot p$ $H = 0.217 \cdot \text{in}$

$\text{Depth}_{ext} := \frac{17}{24} \cdot H$ $\text{Depth}_{ext} = 0.153 \cdot \text{in}$

$\text{Depth}_{int} := \frac{5}{8} \cdot H$ $\text{Depth}_{int} = 0.135 \cdot \text{in}$

$dmaj_{ext} := dm_{ext} + 2 \cdot \text{Depth}_{ext}$ $dmaj_{ext} = 2.5 \cdot \text{in}$

$L_{eng} := 2.5 \cdot \text{in}$ is the length of engagement

Using page 103 of reference B.2,

$$\text{Bolt_thrd_shr_A} := \pi \cdot N \cdot L_{eng} \cdot dm_{int} \left[\frac{1}{2 \cdot N} + .57735 \cdot (d_{pitch} - dm_{int}) \right]$$

$$\text{Bolt_thrd_shr_A} = 13.13 \cdot \text{in}^2$$

$$\text{Ext_thrd_shr_A} := \pi \cdot N \cdot L_{eng} \cdot dmaj_{ext} \left[\frac{1}{2 \cdot N} + 0.57735 \cdot (dmaj_{ext} - d_{pitch}) \right]$$

$$\text{Ext_thrd_shr_A} = 17.183 \cdot \text{in}^2$$

The load capacities of the bolt and the lid material based on ultimate strength are:

$$\text{Load_Capacity}_{bolt} := .7 \cdot S_{ubolt} \cdot A_{stress} \quad \text{Load_Capacity}_{bolt} = 4.058 \cdot 10^5 \cdot \text{lbf}$$

$$\text{Load_Capacity}_{boltthrd} := (0.42 \cdot S_{ubolt}) \cdot \text{Bolt_thrd_shr_A}$$

$$\text{Load_Capacity}_{boltthrd} = 7.996 \cdot 10^5 \cdot \text{lbf}$$

$$\text{Load_Capacity}_{boltshear} := .42 \cdot S_{ubolt} \cdot A_d$$

$$\text{Load_Capacity}_{boltshear} = 2.989 \cdot 10^5 \cdot \text{lbf}$$

$$\text{Load_Capacity}_{lid} := (0.42 \cdot S_{ulid}) \cdot \text{Ext_thrd_shr_A}$$

$$\text{Load_Capacity}_{lid} = 4.943 \cdot 10^5 \cdot \text{lbf}$$

The above results show that the maximum tensile load in the bolt is governed by the bolt tensile capacity.

$$\text{Max_Tension_Load} := \text{Load_Capacity}_{bolt}$$

$$\text{Max_Tension_Load} = 4.058 \cdot 10^5 \cdot \text{lbf}$$

The maximum shear load on a bolt is

$$\text{Max_Shear_Load} := \text{Load_Capacity}_{boltshear}$$

$$\text{Max_Shear_Load} = 2.989 \cdot 10^5 \cdot \text{lbf}$$

B.6.3 Calculations for SA-193-B7 Material

The load capacities of the bolt and the lid material based on ultimate strength are:

$$\text{Load_Capacity}_{\text{bolt}} := .7 \cdot S_{\text{uboltA}} \cdot A_{\text{stress}} \qquad \text{Load_Capacity}_{\text{bolt}} = 3.265 \cdot 10^5 \cdot \text{lbf}$$

$$\text{Load_Capacity}_{\text{boltthrd}} := (0.42 \cdot S_{\text{uboltA}}) \cdot \text{Bolt_thrd_shr_A}$$

$$\text{Load_Capacity}_{\text{boltthrd}} = 6.434 \cdot 10^5 \cdot \text{lbf}$$

$$\text{Load_Capacity}_{\text{boltshear}} := .42 \cdot S_{\text{uboltA}} \cdot A_{\text{d}}$$

$$\text{Load_Capacity}_{\text{boltshear}} = 2.405 \cdot 10^5 \cdot \text{lbf}$$

$$\text{Load_Capacity}_{\text{lid}} := (0.42 \cdot S_{\text{ulid}}) \cdot \text{Ext_thrd_shr_A}$$

$$\text{Load_Capacity}_{\text{lid}} = 4.943 \cdot 10^5 \cdot \text{lbf}$$

The above results show that the maximum tensile load in the bolt is governed by the bolt tensile capacity.

$$\text{Max_Tension_Load} := \text{Load_Capacity}_{\text{bolt}} \qquad \text{Max_Tension_Load} = 3.265 \cdot 10^5 \cdot \text{lbf}$$

The maximum shear load on a bolt is

$$\text{Max_Shear_Load} := \text{Load_Capacity}_{\text{boltshear}} \qquad \text{Max_Shear_Load} = 2.405 \cdot 10^5 \cdot \text{lbf}$$

B.6.4 Calculations for SB-637-N07718 Material

The load capacities of the bolt and the lid material based on ultimate strength are:

$$\text{Load_Capacity}_{\text{bolt}} := .7 \cdot S_{\text{uboltB}} \cdot A_{\text{stress}} \qquad \text{Load_Capacity}_{\text{bolt}} = 4.97 \cdot 10^5 \cdot \text{lbf}$$

$$\text{Load_Capacity}_{\text{boltthrd}} := (0.42 \cdot S_{\text{uboltB}}) \cdot \text{Bolt_thrd_shr_A}$$

$$\text{Load_Capacity}_{\text{boltthrd}} = 9.794 \cdot 10^5 \cdot \text{lbf}$$

$$\text{Load_Capacity}_{\text{boltshear}} := .42 \cdot S_{\text{uboltB}} \cdot A_{\text{d}}$$

$$\text{Load_Capacity}_{\text{boltshear}} = 3.662 \cdot 10^5 \cdot \text{lbf}$$

$$\text{Load_Capacity}_{\text{lid}} := (0.42 \cdot S_{\text{ulid}}) \cdot \text{Ext_thrd_shr_A}$$

$$\text{Load_Capacity}_{\text{lid}} = 4.943 \cdot 10^5 \cdot \text{lbf}$$

The above results show that the maximum tensile load in the bolt is governed by the lid external thread capacity.

$$\text{Max_Tension_Load} := \text{Load_Capacity}_{\text{lid}}$$

$$\text{Max_Tension_Load} = 4.943 \cdot 10^5 \cdot \text{lbf}$$

The maximum shear load on a bolt is

$$\text{Max_Shear_Load} := \text{Load_Capacity}_{\text{boltshear}}$$

$$\text{Max_Shear_Load} = 3.662 \cdot 10^5 \cdot \text{lbf}$$

B.7 Calculation of Spring Constants for Dynamic Analysis

B.7.1 - Compression Spring Constant - Cask Bearing Down on Support

Use the formula from Reference [B.4]. We use the Young's Modulus of the maximum strength concrete to conservatively compute the largest value for the spring constant.

$$f_c := 6000 \cdot \text{psi} \quad \text{Aged compression strength of concrete}$$

$$E_c := 57000 \cdot \sqrt{f_c \cdot \text{psi}} \quad \text{ACI-349 equation for Young's Modulus of Concrete}$$

$$E_c = 4.415 \cdot 10^6 \cdot \text{psi}$$

Based on the geometry of the support block carrying compression, we compute the spring rate on the bases of the following dimensions:

$$L_b := 4 \cdot \text{in} + 12.625 \cdot \text{in} \quad \text{Total assumed active length of compression block (two pieces)}$$

$$W_b := 6 \cdot \text{in} \quad \text{Width of Support Block}$$

$$T_p := 1.25 \cdot \text{in} \quad \text{Thickness of Baseplate}$$

$$A := (L_b) \cdot (W_b) \quad \text{Compression Area for bearing}$$

$$A = 99.75 \cdot \text{in}^2$$

$$\frac{(L_b)}{(W_b)} = 2.771$$

Concrete Poisson's Ratio

$$\nu_c := 0.16$$

$$K := \frac{E_c \cdot \sqrt{A}}{.89 \cdot (1 - \nu_c^2)} \quad K = 5.085 \cdot 10^7 \frac{\text{lbf}}{\text{in}}$$

We simulate each compression support block with three springs oriented radially at each of the support blocks. Therefore, the spring rate for each compression only spring attributed to the concrete subgrade is

$$k := \frac{K}{3} \quad k = 1.695 \cdot 10^7 \frac{\text{lbf}}{\text{in}}$$

Acting in series with the foundation springs are springs reflecting the flexibility of the overpack in axial compression, and the local compression stiffness of the clevis blocks. The overpack axial stiffness is taken as the stiffness of a bar of area "Ao" and length equal to 50% of the overpack length.

Young's Modulus of overpack $E_o := 29000000 \cdot \text{psi}$

$$D_o := 83.25 \cdot \text{in} \quad D_i := 68.75 \cdot \text{in} \quad L_o := 102 \cdot \text{in}$$

$$A_o := \frac{\pi}{4} \cdot (D_o^2 - D_i^2) \quad A_o = 1.731 \cdot 10^3 \cdot \text{in}^2$$

Therefore the spring constant associated with overpack compression stiffness is

$$k_1 := E_o \cdot \frac{A_o}{L_o} \quad k_1 = 4.922 \cdot 10^8 \frac{\text{lbf}}{\text{in}}$$

1/8 th of this value is associated with each clevis, and 1/3 of the result is in series with with each of the three springs representing the concrete compression under the clevis. Neglecting the local compression stiffness of the clevis block itself (a solid compact metal block), we find the effective spring constant at each location for compression resistance to be as computed below:

$$k_2 := \frac{k_1}{8 \cdot 3} \quad k_2 = 2.051 \cdot 10^7 \frac{\text{lbf}}{\text{in}} \quad \text{This is the value from the overpack in series with } k$$

Combining the two springs gives the result

$$X := \frac{1}{k} + \frac{1}{k_2}$$

$$k_{\text{eff}} := \frac{1}{X}$$

$$k_{\text{eff}} = 9.28 \cdot 10^6 \frac{\text{lbf}}{\text{in}}$$

Three of these compression springs act at each of the clevis locations.

In the dynamic analysis, we use the value

$$k_{\text{eff}} := 1.0 \cdot 10^7 \frac{\text{lbf}}{\text{in}}$$

B.7.2 Tension Spring Constant

The tension spring rate is evolved by noting the following flexible components that act in series

1. The bolt connecting the overpack to the support block pin
 2. The pin through the bolt head
 3. The structural connection between the pin and the studs imbedded into the concrete pad.
 4. The studs embedded into the concrete pad
 5. The base of the stud that transfers the tensile load to the overbearing concrete
 6. The concrete that finally supports the tensile load
- These contributions are computed below and then added in series to the appropriate tensile spring representing the overpack stiffness associated with the local region.:

B.7.2.1 Bolt spring constant

$$L_{\text{bolt}} := 5.5625 \cdot \text{in}$$

Elastic Length of Bolt

$$E_{\text{bolt}} := 29000000 \cdot \text{psi}$$

Young's Modulus of bolt

$$A_d = 4.909 \cdot \text{in}^2$$

Bolt area for spring rate computation

$$k_{\text{bolt}} := \frac{E_{\text{bolt}} \cdot A_d}{L_{\text{bolt}}}$$

$$k_{\text{bolt}} = 2.559 \cdot 10^7 \frac{\text{lbf}}{\text{in}}$$

B.7.3.2 Spring rate of pin

The pin connects the two portions of the support block with the bolt block from the overpack through a clearance hole. The clearance between the bolt block and each of the support blocks is set at "c"

$$c := 0.25 \cdot \text{in}$$

The spring constant is based on the deflection of the pin by a combination of shear and rotation due to a moment load as shown in sketch 1 at the end of this appendix:

Referring to that sketch, let the maximum value of P be

$$P := 250000 \cdot \text{lbf} \quad \begin{array}{l} \text{50\% of maximum load that could be supported by} \\ \text{SB-637 bolt material} \end{array}$$

$$\text{The bending moment is computed as } M := P \cdot c$$

$$\text{The pin diameter is } d := 2.875 \cdot \text{in} \quad \begin{array}{l} \text{(a 1/8" diametral} \\ \text{clearance hole)} \end{array}$$

We compute first the central deflection of the pin under the action of the maximum moment and demonstrate that no contact with the bolt head occurs. This will allow us to utilize simple beam solutions to compute the spring rates without considering the effects of contacts due to gap closure.

$$L_p := 5.75 \cdot \text{in} \quad \text{Unsupported length between moments}$$

$$E_{\text{pin}} := 29000000 \cdot \text{psi} \quad \text{Young's Modulus of pin}$$

$$I_{\text{pin}} := \frac{\pi}{64} \cdot d^4 \quad I_{\text{pin}} = 3.354 \cdot \text{in}^4$$

From [B.6], the central deflection of the beam end loaded by bending moments is

$$\delta := \frac{M \cdot L_p^2}{8 \cdot E_{\text{pin}} \cdot I_{\text{pin}}} \quad \delta = 2.656 \cdot 10^{-3} \cdot \text{in} \quad < \text{ than the diametral clearance}$$

The rotation under the point of application of the moment can be computed using formulas in [B.6] as

$$\theta := \frac{M \cdot L_p}{2 \cdot E_{\text{pin}} \cdot I_{\text{pin}}} \quad \theta = 1.848 \cdot 10^{-3}$$

The relative deflection between the support block and the bolt block, due to pin deflection caused by bending, is

$$\Delta_b := \frac{P \cdot L_p \cdot c^2}{2 \cdot E_{pin} \cdot I_{pin}} \quad \text{where} \quad \Delta_b := \theta \cdot c$$

In a similar manner, [B.6] gives an expression for the rotation due to shear effects as

$$\theta_s := \frac{4}{3} \cdot \frac{P}{A \cdot G} \quad \text{where } G \text{ is the Shear Modulus, and } A \text{ is the pin cross section area}$$

The corresponding relative deflection due to shear effects is

$$\Delta_s := \theta_s \cdot c$$

Computing the total deflection in terms of P (50% of the applied load on the pin) gives

$$\Delta_{total} := \frac{P L_p c^2}{2 \cdot E_{pin} \cdot I_{pin}} + \left[\frac{4}{3} \cdot \frac{(P \cdot c)}{A \cdot G} \right]$$

and defines the relation between total deflection and total applied load as

$$k_{pin} := \frac{(2 \cdot P)}{\Delta_{total}}$$

$$k_{pin} := \frac{4 \cdot E_{pin} \cdot I_{pin}}{L_p \cdot c^2} \cdot \left[\frac{1}{\left(1 + \frac{1.3}{3} \cdot \frac{d^2}{L_p \cdot c} \right)} \right]$$

$$k_{pin} = 3.1 \cdot 10^8 \frac{\text{lb}}{\text{in}}$$

B.7.3.3 Spring Rate of Connection between pin and stud

We estimate this spring rate from the solution to a guided cantilever beam that represents the flexibility of the thick plate that connects the pin block to the studs. From the figures, the length of the plate that is free to bend is equal to the span between bolt centers less the span of the support block. 50% of the free span acts between the centerline of each ISFSI stud and the edge of the support block. The width of each of the elastic sections is taken as the span between studs

$$L_{\text{plate}} := \frac{(10 - 6)}{2} \cdot \text{in} \quad t_{\text{plate}} := T_p \quad \text{width} := (10) \cdot \text{in}$$

$$I_{\text{plate}} := \frac{\text{width} \cdot t_{\text{plate}}^3}{12} \quad I_{\text{plate}} = 1.628 \cdot \text{in}^4 \quad E_{\text{plate}} := 28000000 \cdot \text{psi}$$

$$k_{\text{plate}} := 4 \cdot \left(\frac{12 \cdot E_{\text{plate}} \cdot I_{\text{plate}}}{L_{\text{plate}}^3} \right) \quad k_{\text{plate}} = 2.734 \cdot 10^8 \cdot \frac{\text{lbf}}{\text{in}}$$

B.7.3.4 Spring Rate of Studs (4 total)

$$L_{\text{stud}} := 38 \cdot \text{in} \quad d_{\text{stud}} := 1.875 \cdot \text{in} \quad A_{\text{stud}} := \frac{\pi}{4} \cdot d_{\text{stud}}^2 \quad A_{\text{stud}} = 2.761 \cdot \text{in}^2$$

$$k_{\text{stud}} := \frac{E_{\text{plate}} \cdot A_{\text{stud}}}{L_{\text{stud}}} \cdot 4 \quad k_{\text{stud}} = 8.138 \cdot 10^6 \cdot \frac{\text{lbf}}{\text{in}}$$

B.7.3.5 Spring Rate of Stud Base

We set the allowable bearing strength of the concrete to be that given by the ACI Code for unconfined concrete.

$$f_{\text{bearing}} := 0.8 \cdot 0.7 \cdot f_c \quad f_{\text{bearing}} = 3.36 \cdot 10^3 \cdot \text{psi}$$

The plate area to support the largest maximum tension load in each bolt is

$$\text{Max_Tension_Load} = 4.943 \cdot 10^5 \cdot \text{lbf}$$

$$A_{\text{bearing}} := \frac{\text{Max_Tension_Load}}{4 \cdot f_{\text{bearing}}} \quad A_{\text{bearing}} = 36.782 \cdot \text{in}^2$$

There are 4 studs per connection assumed. The radius of a circular plate under each stud is

$$R_{\text{head}} := \sqrt{\frac{1}{\pi} \cdot A_{\text{bearing}} \cdot \frac{1}{4}} + 0.5 \cdot d_{\text{stud}} \quad R_{\text{head}} = 2.648 \cdot \text{in}$$

For a stiffness calculation, we assume a minimum stud base of

$$R_{\text{head}} := 3 \cdot \text{in} \quad t_{\text{head}} := 0.75 \cdot \text{in} \quad \frac{R_{\text{head}}}{.5 \cdot d_{\text{stud}}} = 3.2$$

The spring constant may be estimated from [B.6], Volume 2, Case 5 of Table 5 in Section 23:

$$k_{\text{head}} := \pi \frac{\left[1 - \left(.5 \cdot \frac{d_{\text{stud}}}{R_{\text{head}}} \right)^2 \right] \cdot E_{\text{plate}} \cdot t_{\text{plate}}^3}{0.179 \cdot R_{\text{head}}^2} \quad k_{\text{head}} = 9.623 \cdot 10^7 \cdot \frac{\text{lbf}}{\text{in}}$$

B.7.3.6 Concrete Spring Rate

$$A := \pi \cdot R_{\text{head}}^2 \quad k_{\text{concrete}} := \frac{4 \cdot E_c \cdot \sqrt{A}}{.95 \cdot (1 - \nu_c^2)} \quad k_{\text{concrete}} = 1.014 \cdot 10^8 \cdot \frac{\text{lbf}}{\text{in}}$$

B.7.3.7 Effective Spring Rate for Tension

$$X := \frac{1}{k_{\text{bolt}}} + \frac{1}{k_{\text{pin}}} + \frac{1}{k_{\text{plate}}} + \frac{1}{k_{\text{stud}}} + \frac{1}{k_{\text{head}}} + \frac{1}{k_{\text{concrete}}}$$

$$k_{\text{eff}} := \frac{1}{X} \quad k_{\text{eff}} = 5.289 \cdot 10^6 \cdot \frac{\text{lbf}}{\text{in}}$$

This spring acts in series with 1/8th of the axial spring constant computed for the overpack

$$K_{\text{eff}} := \frac{1}{\frac{1}{k_{\text{eff}}} + \frac{1}{k_1}} \quad K_{\text{eff}} = 4.87 \cdot 10^6 \cdot \frac{\text{lbf}}{\text{in}}$$

B.7.3 Spring Constant of ISFSI Studs in Shear

The ISFSI Studs fit through clearance holes in the baseplate. To provide sufficient shear flexibility, a washer is inserted sufficient to insure a free length totaling 3 and 3/32 inch. We estimate that a 3/8" washer is sufficient with the remaining "free length" obtained by local deformation of the concrete near the top surface.

$$L_s := 3.09375 \cdot \text{in}$$

There are 4 studs per support block and conservatively computing the spring constant based on bending as a guided cantilever including shear deformation, we have the spring constant in the horizontal plane given for a single stud (see sketch 2, below) as:

$$\Delta_{\text{total}} := \frac{(F_s \cdot L_s^3)}{12 \cdot (E_s \cdot I_s)} + \frac{4}{3} \cdot F_s \cdot \frac{L_s}{G \cdot A_s}$$

Therefore the spring rate for dynamics analysis is computed, for a group of four studs, by the following:

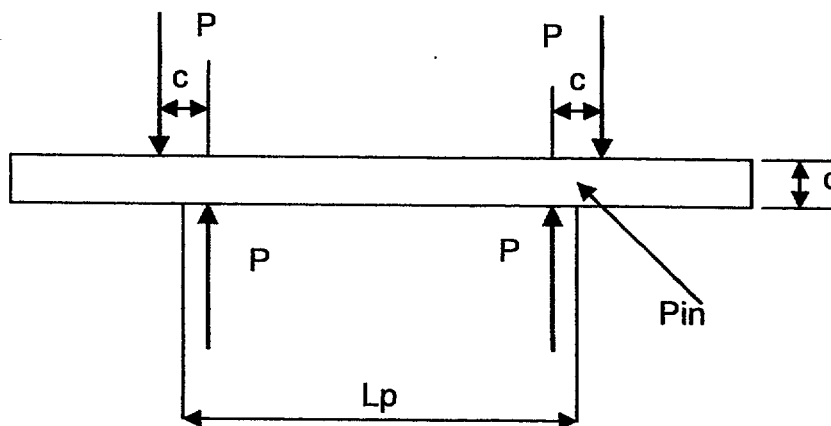
$$E_s := 29000000 \cdot \text{psi}$$

$$I_s := \frac{\pi}{64} \cdot d_{\text{stud}}^4$$

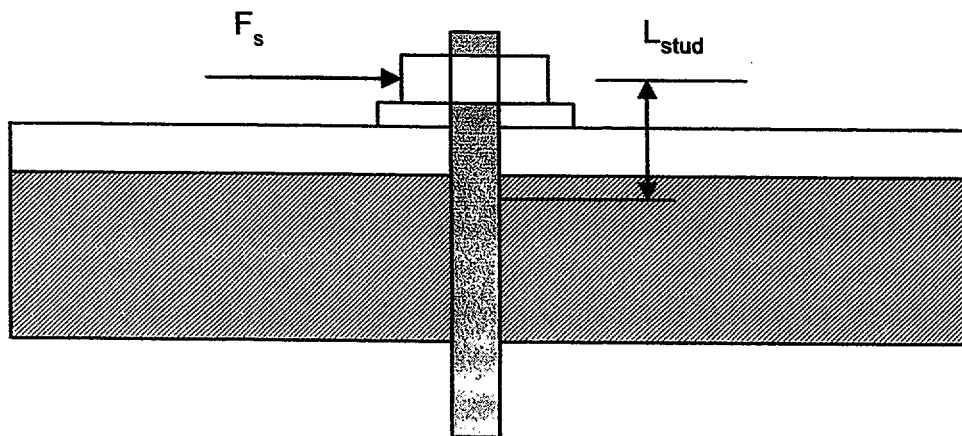
$$k_{\text{shear}} := \frac{4}{\left[\frac{L_s^3}{12 \cdot E_s \cdot I_s} + 4 \cdot \frac{L_s}{\left(\frac{E_s}{2.6} \right) \cdot \pi \cdot \frac{d_{\text{stud}}^2}{4}} \right]}$$

$$k_{\text{shear}} = 7.379 \cdot 10^6 \cdot \frac{\text{lbf}}{\text{in}}$$

B.8 Supplementary Sketches



Sketch #1- Pin Loading



SKETCH #2 - Stud into ISFSI Pad

APPENDIX C - CALCULATION OF CASK MASS AND INERTIA PROPERTIES FOR HIGH SEISMIC DYNAMIC ANALYSIS

C.1.0 Assumptions

For calculating masses and inertias, use bounding weights from Table 3.2.4 of the TSAR (HI-941184).

Assume centroids of cylinders are at half length when computing property values. This is consistent with approximations of modeling and is conservative.

Assume centroid of composite structure (lids plus cylinder) is at center of cylinder when obtaining total inertia properties. Any numerical differences due to this assumption are within the accuracy of the basic model.

C.2.0 Analysis

C.2.1 Overpack

Consider as hollow cylinder plus upper and lower lids

Input Data

$$a_o := .5 \cdot 83.25 \cdot \text{in}$$

$$a_i := .5 \cdot 68.75 \cdot \text{in}$$

$$L := 192 \cdot \text{in}$$

$$t_{\text{lid}} := 6 \cdot \text{in}$$

$$\text{Weight}_{\text{lid}} := \frac{18000}{2} \cdot \text{lbf}$$

$$W := 155000 \cdot \text{lbf} - 2 \cdot \text{Weight}_{\text{lid}}$$

$$W = 1.37 \cdot 10^5 \cdot \text{lbf}$$

$$\text{Area} := \pi \cdot (a_o^2 - a_i^2)$$

$$\text{Area} = 1.731 \cdot 10^3 \cdot \text{in}^2$$

$$\rho_{\text{eff}} := \frac{W}{g \cdot \text{Area} \cdot L}$$

$$\rho_{\text{eff}} = 1.068 \cdot 10^{-3} \cdot \text{lbf} \cdot \frac{\text{sec}^2}{\text{in}^4}$$

$$\text{mass}_{\text{ovp}} := \frac{W}{g}$$

$$\text{mass}_{\text{ovp}} = 354.841 \cdot \text{lbf} \cdot \frac{\text{sec}^2}{\text{in}}$$

Therefore, the inertia property of the hollow cylinder is

$$I_{ovp} := \frac{1}{12} \cdot (\rho_{eff}) \cdot (\pi \cdot a_o^2 \cdot L) \cdot (3 \cdot a_o^2 + L^2) \dots \\ + \left(-\frac{1}{12} \cdot \rho_{eff} \right) \cdot (\pi \cdot a_i^2 \cdot L) \cdot (3 \cdot a_i^2 + L^2)$$

$$I_{ovp} = 1.349 \cdot 10^6 \cdot \text{lbf} \cdot \text{sec}^2 \cdot \text{in}$$

Next compute the contribution of the upper and lower lids.

$$\text{mass lid} := \frac{\text{Weight lid}}{g} \quad \text{mass lid} = 23.311 \cdot \text{lbf} \cdot \frac{\text{sec}^2}{\text{in}}$$

$$\text{Weight lid} := \text{mass lid} \cdot g \quad \text{Weight lid} = 9 \cdot 10^3 \cdot \text{lbf}$$

OK

$$I_{lid} := \frac{1}{12} \cdot \text{mass lid} \cdot (3 \cdot a_o^2 + t_{lid}^2) \quad I_{lid} = 1.017 \cdot 10^4 \cdot \text{lbf} \cdot \text{sec}^2 \cdot \text{in}$$

Compute total inertia about a lateral axis through the overpack centroid

$$I_{total} := I_{ovp} + 2 \cdot I_{lid} + 2 \cdot \text{mass lid} \cdot \left(\frac{L + t_{lid}}{2} \right)^2$$

$$I_{total} = 1.826 \cdot 10^6 \cdot \text{lbf} \cdot \text{sec}^2 \cdot \text{in}$$

The moment of inertia about a longitudinal axis through the center of the overpack is

$$I_{longovp} := \frac{1}{2} \cdot (\rho_{eff} \cdot \pi \cdot a_o^2 \cdot L) \cdot a_o^2 - \frac{1}{2} \cdot (\rho_{eff} \cdot \pi \cdot a_i^2 \cdot L) \cdot a_i^2$$

plus the contribution from the lids

$$I_{long} := I_{longovp} + \text{mass lid} \cdot \frac{a_o^2}{2} \quad I_{long} = 5.372 \cdot 10^5 \cdot \text{lbf} \cdot \text{sec}^2 \cdot \text{in}$$

The total mass of the overpack plus lid and baseplate is

$$\text{Mass}_{\text{ovp}} := \text{mass}_{\text{ovp}} + 2 \cdot \text{mass}_{\text{lid}}$$

$$\text{Mass}_{\text{ovp}} = 401.463 \cdot \text{lbf} \cdot \frac{\text{sec}^2}{\text{in}}$$

C.2.2 MPC

C.2.2.1 Input data

$$a_o := .5 \cdot 68.375 \cdot \text{in} \quad a_i := a_o - .5 \cdot \text{in} \quad a_i = 33.687 \cdot \text{in}$$

$$L := 178.5 \cdot \text{in} \quad t_{\text{lid}} := 9.5 \cdot \text{in} \quad t_{\text{b lid}} := 2.5 \cdot \text{in}$$

The following weight data is obtained from TSAR Table 3.2.4

$$\text{Weight}_{\text{lidb}} := 3000 \cdot \text{lbf} \quad \text{Weight}_{\text{lidt}} := (10400 \cdot \text{lbf})$$

$$\text{Weight}_{\text{basket}} := 13000 \cdot \text{lbf} \quad (\text{bounding estimate from table 3.2.4})$$

$$\text{Weight}_{\text{fuel}} := 1680 \cdot 32 \cdot \text{lbf} \quad \text{Weight}_{\text{fuel}} = 5.376 \cdot 10^4 \cdot \text{lbf}$$

The weight of the MPC canister (including bracing, etc.) is (include basket for lateral effects).

$$W := 36000 \cdot \text{lbf} - 1 \cdot \text{Weight}_{\text{lidb}} - \text{Weight}_{\text{lidt}}$$

$$W = 2.26 \cdot 10^4 \cdot \text{lbf} \quad \text{MPC-32}$$

$$\text{Area} := \pi \cdot (a_o^2 - a_i^2) \quad \text{Area} = 106.618 \cdot \text{in}^2$$

$$\rho_{\text{eff}} := \frac{W}{g \cdot \text{Area} \cdot L} \quad \rho_{\text{eff}} = 3.076 \cdot 10^{-3} \cdot \text{lbf} \cdot \frac{\text{sec}^2}{\text{in}^4}$$

$$\text{mass}_{\text{can}} := \frac{W}{g} \quad \text{mass}_{\text{can}} = 58.536 \cdot \text{lbf} \cdot \frac{\text{sec}^2}{\text{in}}$$

$$I_{\text{can}} := \frac{1}{12} \cdot (\rho_{\text{eff}}) \cdot (\pi \cdot a_o^2 \cdot L) \cdot (3 \cdot a_o^2 + L^2) \dots$$

$$+ \left(-\frac{1}{12} \cdot \rho_{\text{eff}} \right) \cdot (\pi \cdot a_i^2 \cdot L) \cdot (3 \cdot a_i^2 + L^2)$$

$$I_{\text{can}} = 1.891 \cdot 10^5 \cdot \text{lbf} \cdot \text{sec}^2 \cdot \text{in}$$

Next compute the contribution of the upper and lower lids to the inertia

Top Lid

$$\text{mass lidt} := \frac{\text{Weight lidt}}{g} \quad \text{mass lidt} = 26.937 \cdot \text{lbf} \cdot \frac{\text{sec}^2}{\text{in}}$$

$$\text{Weight lidt} := \text{mass lidt} \cdot g \quad \text{Weight lidt} = 1.04 \cdot 10^4 \cdot \text{lbf} \quad \text{OK}$$

$$I_{\text{lidt}} := \frac{1}{12} \cdot \text{mass lidt} \cdot (3 \cdot a_o^2 + t_{\text{lidt}}^2) \quad I_{\text{lidt}} = 8.073 \cdot 10^3 \cdot \text{lbf} \cdot \text{sec}^2 \cdot \text{in}$$

Bottom Lid

$$\text{mass lidb} := \frac{\text{Weight lidb}}{g} \quad \text{mass lidb} = 7.77 \cdot \text{lbf} \cdot \frac{\text{sec}^2}{\text{in}}$$

$$\text{Weight lidb} := \text{mass lidb} \cdot g \quad \text{Weight lidb} = 3 \cdot 10^3 \cdot \text{lbf} \quad \text{OK}$$

$$I_{\text{lidb}} := \frac{1}{12} \cdot \text{mass lidb} \cdot (3 \cdot a_o^2 + t_{\text{lidb}}^2)$$

$$I_{\text{lidb}} = 2.274 \cdot 10^3 \cdot \text{lbf} \cdot \text{sec}^2 \cdot \text{in}$$

Compute total inertia about a lateral axis through the MPC shell centroid

$$I_{\text{mpc}} := I_{\text{can}} + 1 \cdot I_{\text{lidt}} + I_{\text{lidb}} + 1 \cdot \text{mass}_{\text{lidt}} \cdot \left(\frac{L + \text{tt}_{\text{lid}}}{2} \right)^2 \dots$$

$$+ \text{mass}_{\text{lidb}} \cdot \left(\frac{L + \text{tb}_{\text{lid}}}{2} \right)^2$$

$$I_{\text{mpc}} = 5.011 \cdot 10^5 \cdot \text{lbf} \cdot \text{sec}^2 \cdot \text{in}$$

The moment of inertia of the proposed MPC-32 basket is obtained from the mathcad calculation basket.mcd

$$I_{32} := 7.461 \cdot 10^4 \cdot \text{lbf} \cdot \text{sec}^2 \cdot \text{in}$$

Therefore, the lateral inertia of the MPC is

$$I_{\text{lat}} := I_{\text{mpc}} + I_{32}$$

$$I_{\text{lat}} = 5.757 \cdot 10^5 \cdot \text{lbf} \cdot \text{sec}^2 \cdot \text{in}$$

The vertical mass of the MPC is computed as

$$\text{Mass}_{\text{mpcvrt}} := \text{mass}_{\text{can}} + \text{mass}_{\text{lidt}} + \text{mass}_{\text{lidb}}$$

$$\text{Mass}_{\text{mpcvrt}} = 93.243 \cdot \text{lbf} \cdot \frac{\text{sec}^2}{\text{in}}$$

The lateral MPC mass is

$$\text{Mass}_{\text{mpclat}} := \text{Mass}_{\text{mpcvrt}} + \frac{\text{Weight}_{\text{basket}}}{g}$$

$$\text{Mass}_{\text{mpclat}} = 126.914 \cdot \text{lbf} \cdot \frac{\text{sec}^2}{\text{in}}$$

The mass associated with vertical motion of the basket is

$$\text{Mass}_{\text{bask}} := \frac{\text{Weight}_{\text{basket}}}{g}$$

$$\text{Mass}_{\text{bask}} = 33.671 \cdot \text{lbf} \cdot \frac{\text{sec}^2}{\text{in}}$$

Finally, the fuel mass is distributed over five masses; therefore, for horizontal degrees of freedom at any location

$$\text{Mass}_{\text{fuelh}} := \frac{\text{Weight}_{\text{fuel}}}{5 \cdot g}$$

$$\text{Mass}_{\text{fuelh}} = 27.849 \cdot \text{lbf} \cdot \frac{\text{sec}^2}{\text{in}}$$

$$\text{Mass}_{\text{fuelvrt}} := 5 \cdot \text{Mass}_{\text{fuelh}}$$

$$\text{Mass}_{\text{fuelvrt}} = 139.243 \cdot \text{lbf} \cdot \frac{\text{sec}^2}{\text{in}}$$

APPENDIX D STATIC ANALYSIS FOR MAXIMUM CASK ATTACHMENT BOLT FORCES IN HI-STAR 100

1.0 Purpose

The calculation aims to estimate by static analysis the maximum cask bolt forces in the attachment of the HI-STAR 100 to the clevis assemblies during a severe seismic event (2.12g horizontal acceleration and 0.5g net vertical upward acceleration). The purpose is to provide scoping results that can be compared with the true non-linear dynamic analysis results.

2.0 Assumptions

- 2.1 The calculation is carried out using the force and moment balance formulas.
- 2.2 The cask is treated as a rigid body, and linearly distributed bolt forces are assumed.
- 2.3 The vertical seismic event is assumed upward to maximize the bolt tension.
- 2.4 The cask is assumed to be rotating about a point on the edge of the contact periphery so that all bolts are in tension.

3.0 References

All geometry data comes from text and drawings in the main sections of this report, or from applicable tables in Reference [3], Section 14.

4.0 Input Data (refer to Reference [3], to figures in Section 7, and to the sketch given below)

Loads:

$$W_{\text{cask}} := 250000 \cdot \text{lbf} \quad (\text{HI-STAR cask weight})$$

$$F_v := 0.5 \cdot W_{\text{cask}} \quad F_v = 1.25 \cdot 10^5 \cdot \text{lbf} \quad F_h := 2.12 \cdot W_{\text{cask}} \quad F_h = 5.3 \cdot 10^5 \cdot \text{lbf}$$

Dimensions:

$$d_0 := 52 \cdot \text{in} \quad W_{\text{cb}} := 5.5 \cdot \text{in} \quad L_{\text{block2}} := 12.625 \cdot \text{in} \quad h := \frac{203.125}{2} \cdot \text{in}$$

$$\text{clr} := 0.25 \cdot \text{in} \quad (\text{Clearance between the blocks})$$

Distances between the center point and the tip-over points (refer to the sketch given below):

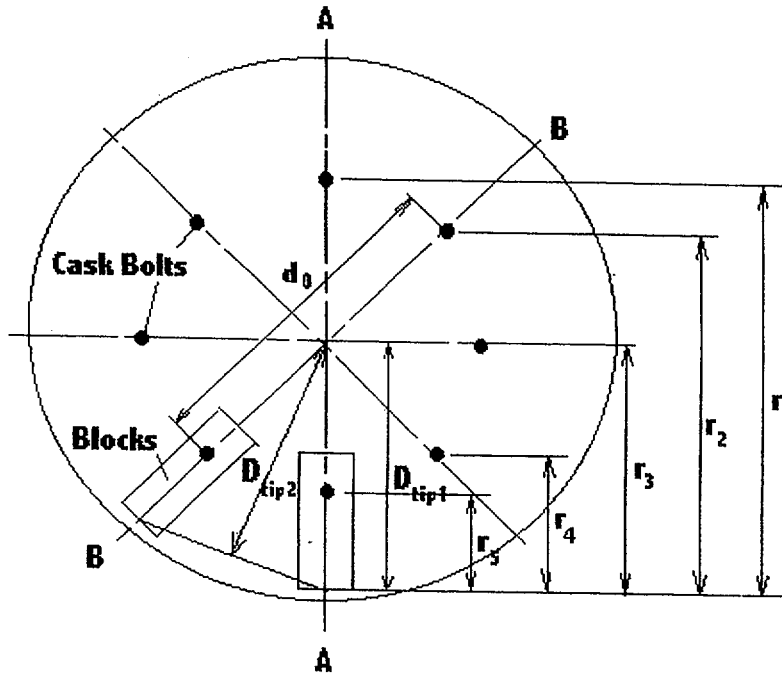
$$D_{\text{tip1}} := \frac{d_0 + W_{\text{cb}}}{2} + 2 \cdot \text{clr} + L_{\text{block2}} \quad D_{\text{tip1}} = 41.875 \cdot \text{in}$$

$$D_{tip2} := D_{tip1} \cdot \cos\left(\frac{\pi}{8}\right)$$

$$D_{tip2} = 38.687 \text{ in}$$

5.0 Calculations

First assume that the horizontal seismic load is applied along the direction of two opposite anchor "elements" (A-A direction) as shown in the following sketch. Dimensions (r1 through r5) shown in the sketch are the distances between the cask bolts and the edge point.



$$r1 := D_{tip1} + \frac{d0}{2}$$

$$r2 := D_{tip1} + \frac{d0}{2} \cdot \sin\left(\frac{\pi}{4}\right)$$

$$r3 := D_{tip1}$$

$$r4 := D_{tip1} - \frac{d0}{2} \cdot \sin\left(\frac{\pi}{4}\right)$$

$$r5 := D_{tip1} - \frac{d0}{2}$$

$$r1 = 67.875 \text{ in}$$

$$r2 = 60.26 \text{ in}$$

$$r3 = 41.875 \text{ in}$$

$$r4 = 23.49 \text{ in}$$

$$r5 = 15.875 \text{ in}$$

$$e2 := \frac{r2}{r1}$$

$$e3 := \frac{r3}{r1}$$

$$e4 := \frac{r4}{r1}$$

$$e5 := \frac{r5}{r1}$$

$$e2 = 0.888$$

$$e3 = 0.617$$

$$e4 = 0.346$$

$$e5 = 0.234$$

$$c1 := 1 + e5 + 2 \cdot (e2 + e3 + e4)$$

$$c1 = 4.936$$

$$c2 := r1 + 2 \cdot (e2 \cdot r2 + e3 \cdot r3 + e4 \cdot r4) + e5 \cdot r5$$

$$c2 = 246.514 \text{ in}$$

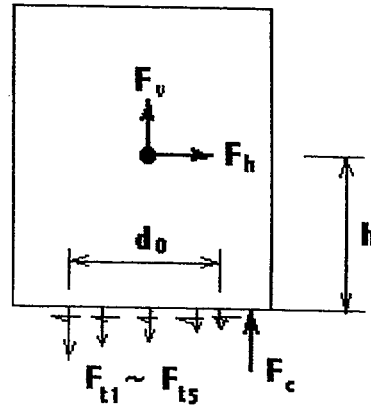
A free body diagram for the cask is shown in the right figure. With that we can obtain the cask bolt forces by solving the force and moment balance equations.

$$Ft1 := \frac{Fh \cdot h + Fv \cdot r3}{c2}$$

$$Fc := Ft1 \cdot c1 - Fv$$

$$Ft1 = 2.396 \cdot 10^5 \text{ lbf}$$

$$Fc = 1.058 \cdot 10^6 \text{ lbf}$$



$$Ft2 := e2 \cdot Ft1$$

$$Ft3 := e3 \cdot Ft1$$

$$Ft4 := e4 \cdot Ft1$$

$$Ft5 := e5 \cdot Ft1$$

$$Ft2 = 2.127 \cdot 10^5 \text{ lbf}$$

$$Ft3 = 1.478 \cdot 10^5 \text{ lbf}$$

$$Ft4 = 8.292 \cdot 10^4 \text{ lbf}$$

$$Ft5 = 5.604 \cdot 10^4 \text{ lbf}$$

The maximum pullout force at the connecting bolt is:

$$T_{\max A} := Ft1$$

$$T_{\max A} = 2.396 \cdot 10^5 \text{ lbf}$$

Now calculate the maximum bolt force when the horizontal seismic load is applied along the direction that is between the anchor elements (B-B direction). The following dimensions of r1 through r4 are not shown in the above sketch.

$$r1 := D_{\text{tip}2} + \frac{d0}{2} \cdot \cos\left(\frac{\pi}{8}\right)$$

$$r2 := D_{\text{tip}2} + \frac{d0}{2} \cdot \sin\left(\frac{\pi}{8}\right)$$

$$r3 := D_{\text{tip}2} - \frac{d0}{2} \cdot \sin\left(\frac{\pi}{8}\right)$$

$$r4 := D_{\text{tip}2} - \frac{d0}{2} \cdot \cos\left(\frac{\pi}{8}\right)$$

$$r1 = 62.708 \text{ in}$$

$$r2 = 48.637 \text{ in}$$

$$r3 = 28.738 \text{ in}$$

$$r4 = 14.667 \text{ in}$$

$$e2 := \frac{r2}{r1}$$

$$e3 := \frac{r3}{r1}$$

$$e4 := \frac{r4}{r1}$$

$$e2 = 0.776$$

$$e3 = 0.458$$

$$e4 = 0.234$$

$$c1 := 2 \cdot (1 + e2 + e3 + e4)$$

$$c1 = 4.936$$

$$c2 := 2 \cdot (r1 + e2 \cdot r2 + e3 \cdot r3 + e4 \cdot r4) \quad c2 = 234.064 \text{ in}$$

$$Ft1 := \frac{Fh \cdot h + Fv \cdot r3}{c2} \quad Fc := Ft1 \cdot c1 - Fv$$

$$Ft1 = 2.453 \cdot 10^5 \text{ lbf} \quad Fc = 1.086 \cdot 10^6 \text{ lbf}$$

$$Ft2 := e2 \cdot Ft1 \quad Ft3 := e3 \cdot Ft1 \quad Ft4 := e4 \cdot Ft1 \quad Ft5 := e5 \cdot Ft1$$

$$Ft2 = 1.903 \cdot 10^5 \text{ lbf} \quad Ft3 = 1.124 \cdot 10^5 \text{ lbf} \quad Ft4 = 5.738 \cdot 10^4 \text{ lbf} \quad Ft5 = 5.738 \cdot 10^4 \text{ lbf}$$

The maximum pullout force at the connecting bolt is:

$$T_{\max B} := Ft1 \quad T_{\max B} = 2.453 \cdot 10^5 \text{ lbf}$$

Comparing between the maximum tension forces obtained in the above two cases, the real maximum tension force is:

$$T_{\max} := \text{if}(T_{\max A} > T_{\max B}, T_{\max A}, T_{\max B}) \quad T_{\max} = 2.453 \cdot 10^5 \text{ lbf}$$

Assuming uniform shear forces in the cask bolts, the shear force in each bolt is:

$$F_s := \frac{Fh}{8} \quad F_s = 6.625 \cdot 10^4 \text{ lbf}$$

6.0 Conclusion

The maximum tension and shear force in the cask bolts are found to be 2.453×10^5 lbf and 6.625×10^4 lbf, respectively. The result is based on a static analysis and assumes a 2-D seismic configuration. This maximum tensile force is compared to results of the dynamic analyses in Section 10.

APPENDIX E - DOCUMENTATION OF DYNAMIC ANALYSIS COMPRESSION ONLY SPRING CONSTANTS - HI-STAR 100

This appendix contains archival calculations documenting the calculation of spring rates for the dynamic model of HI-STAR. MPC-to-overpack, MPC-to-fuel basket, and fuel-to-fuel basket are considered here. The geometric and material data are taken from appropriate tables and drawings in the Holtec TSAR for HI-STAR 100. Calculated spring constants are denoted by "S" within this appendix. All calculations are performed using property values that overestimate the internal stiffness so as to maximize the contact forces from the dynamic simulation.

Fuel Basket-to-Fuel Assembly Contact Spring

This stiffness is calculated by computing the deflection \ddot{a} of a long plate of width b , thickness subject to lateral pressure p . The stiffness is based on the MPC dimensions and assumes that the boundary conditions are between pinned and clamped so that the displacement is twice that of a fully clamped edge. Applying this spring constant formula to a plate length equal to the width so that the total applied load causing the deflection is based on a square area, we can develop the spring constant as follows:

From classical plate theory, for a clamped section,

$$\ddot{a} \ni \frac{p b^4}{384D}$$

where

$$D \ni \frac{E t^3}{12 (1 + \nu^2)}$$

E: Young's Modulus of plate material = 28.14E+06 psi @ room temperature.

b: 9.218" (cell pitch)

t: 0.28125"

ν : Poisson's ratio = 0.3

The stiffness is given by (assume 50% of the stiffness using clamped boundary conditions)

$$\begin{aligned} \frac{pb^2}{\ddot{a}} &\ni \frac{384D}{2b^2} \\ &\ni \frac{(384) (28.14E+06) (0.2815)^3}{2(12) (0.91) (9.218)^2} \\ &\ni 259,082/2 \text{ lb/inch} \end{aligned}$$

For 32 fuel assemblies moving in-phase (a conservative high stiffness results from this assumption), we have

$$S_2 \ni (129,541) (32) \ni 4,145,312 \text{ lb/inch}$$

In the analysis, we use

$$S_2 \ni 4.25E+06 \text{ lb/inch}$$

MPC-to-Overpack Vertical Contact Spring

The contact stiffness relating relative axial movement between the MPC centroid and the overpack centroid (that is, coordinates 3 and 9 in Appendix A) is primarily influenced by the compression resistance of the lower half of the MPC shell for contact at the bottom plate and at the top forging. Appendix G contains the details of this calculation where it is determined that the value for this spring constant is calculated as

$$S_3 = 3.293 \times 10^7 \text{ lb./inch}$$

We set $S_3 = 33.0E+06 \text{ lb./inch}$ in the dynamic simulations.

Fuel Basket-to-MPC Vertical Contact Spring Constant for Bottom and Top of MPC

The fuel basket is a honeycomb structure. Its axial stiffness is estimated by considering the Bousinesq solution for an elastic half-space and reducing the half-space stiffness by the solidity ratio (ratio of metal area to the cross sectional area). MPC-68 has the highest solidity, 0.25 inch thick plates at 6 inch pitch.

The solidity, therefore, is $\frac{4t}{C}$

where $t = 0.25"$, $C = \text{cell pitch} = 6"$

$$\hat{a} \ni \frac{(4)(0.25)}{(6)} \ni 0.167$$

The appropriate half-space stiffness is taken from Timoshenko and Woinowsky-Kreiger, Theory of Plates and Shells, McGraw-Hill, 1970, p.408.

$$K \ni \frac{2E a}{1 + i^2}$$

where

- a: honeycomb planar radius = 33.6875 (I.D. of MPC used so as to obtain a conservative value of K).
- E: Young's Modulus of the honeycomb material (Alloy X) at room temperature = 28.14E+06 psi.

Therefore

$$K \ni \frac{(2)(28.14E+06)(33.6875)}{(0.91)} \\ \ni 20.83E+08 \text{ lb/inch}$$

$$S_4 \ni \hat{a}K \ni (0.167)(20.83E+08) \\ \ni 3.48E+08 \text{ lb/inch}$$

We set S_4 conservatively at 3.5E+08 lb./inch.

$$S_4 \ni 3.50E+08 \text{ lb/inch}$$

The spring constant associated with the resistance to lateral deflection of the MPC baseplate together with the spring constant associated with the resistance to axial displacement of the MPC shell wall act in series with the spring constant computed above. These latter two spring constants are calculated in detail in Appendix G. The values obtained from the calculations in Appendix G are

$$k_{mpc} = 3.293 \times 10^7 \text{ lb./inch}$$

$$k_{plate} = 7.542 \times 10^5 \text{ lb./inch}$$

Therefore, the relative resistance acting in compression between the vertical degree of freedom of the fuel basket and the vertical degree of freedom of the MPC centroid, is

$$K_{vrt} = \frac{1}{\left(\frac{1}{S_4} + \frac{1}{k_{mpc}} + \frac{1}{k_{plate}}\right)}$$

or

$$K_{vrt} = 7.358 \times 10^5 \text{ lb./inch}$$

The fuel basket may make contact with the MPC closure plate. The spring constant that simulates this resistance is computed by combining three springs in series; the only difference from the previous calculation is that instead of the plate thickness being the MPC baseplate thickness, the plate thickness for contact at the top of the MPC is the closure plate thickness. Since the thickness is five times larger, the spring constant increases by 125. Therefore, the vertical spring constant for contact between the MPC fuel basket and the MPC canister is

$$K_{t,vrt} = 2.35 \times 10^8 \text{ lbf/inch}$$

MPC-to-Overpack Lateral Contact

We set this stiffness, S_6 , conservatively equal to S_2 :

$$S_6 \ni 4.250E+06 \text{ lb./inch}$$

Fuel-Assembly-to-MPC

We set fuel assembly-to-MPC lid or baseplate stiffness, S_7 equal to the stiffness associated with the deflection of the MPC baseplate; i.e.,

$$S_7 \ni 7.542E+05 \text{ lb/inch}$$

We have conservatively neglected any flexibility of the fuel assembly or the MPC shell in setting this value. For the corresponding spring constant acting at the location of the top fuel spacers, we increase the above value by a factor of 10.

APPENDIX F - HI-STORM CASK MASS AND INERTIA PROPERTIES

F-1.0 Assumptions

For calculating masses and inertia, use bounding weights of MPC.

Assume centroids of cylinders are at half length when computing property values. This is consistent with approximations of modeling and is conservative.

Assume centroid of composite structure is at center of cylinder when obtaining total inertia properties. Any numerical differences due to this assumption are within the accuracy of the basic model.

Assume that mass and inertia properties of MPC are based on total weight including contents. That is, fuel is not separately modeled in this analysis.

F-2.0 Analysis

F-2.1 Overpack

Consider as hollow cylinder with specified weight

Input Data from Reference [4] in main text of this report.

$$a_o := .5 \cdot 132.5 \cdot \text{in} \quad a_i := .5 \cdot 73.5 \cdot \text{in} \quad L := 231.25 \cdot \text{in}$$

Overpack weight is the total weight on the pad - weight of bounding MPC

$$W_{\text{ovp}} := 270000 \cdot \text{lbf} \quad W_{\text{mpc}} := 90000 \cdot \text{lbf} \quad [3 \text{ (in main text), table 3.2.4}]$$

$$W_{\text{total}} := W_{\text{ovp}} + W_{\text{mpc}} \quad W_{\text{total}} = 3.6 \cdot 10^5 \cdot \text{lbf}$$

Compute the cross-section area so that an equivalent mass density may be defined

$$\text{Area} := \pi \cdot (a_o^2 - a_i^2) \quad \text{Area} = 9.546 \cdot 10^3 \cdot \text{in}^2$$

$$\rho_{\text{eff}} := \frac{W_{\text{ovp}}}{g \cdot \text{Area} \cdot L} \quad \rho_{\text{eff}} = 3.168 \cdot 10^{-4} \cdot \text{lbf} \cdot \frac{\text{sec}^2}{\text{in}^4}$$

$$\text{mass}_{\text{ovp}} := \frac{W_{\text{ovp}}}{g} \quad \text{mass}_{\text{ovp}} = 699.322 \cdot \text{lbf} \cdot \frac{\text{sec}^2}{\text{in}}$$

Therefore, the inertia property of the hollow cylinder about a lateral axis is

$$I_{\text{ovp}} := \frac{1}{12} \cdot (\rho_{\text{eff}}) \cdot (\pi \cdot a_o^2 \cdot L) \cdot (3 \cdot a_o^2 + L^2) \dots$$

$$+ \left(-\frac{1}{12} \cdot \rho_{\text{eff}} \right) \cdot (\pi \cdot a_i^2 \cdot L) \cdot (3 \cdot a_i^2 + L^2)$$

$$I_{\text{ovp}} = 4.12 \cdot 10^6 \cdot \text{lbf} \cdot \text{sec}^2 \cdot \text{in}$$

The moment of inertia about a longitudinal axis through the center of the overpack is

$$I_{\text{longovp}} := \frac{1}{2} \cdot (\rho_{\text{eff}} \cdot \pi \cdot a_o^2 \cdot L) \cdot a_o^2 - \frac{1}{2} \cdot (\rho_{\text{eff}} \cdot \pi \cdot a_i^2 \cdot L) \cdot a_i^2$$

$$I_{\text{longovp}} = 2.007 \cdot 10^6 \cdot \text{lbf} \cdot \text{sec}^2 \cdot \text{in}$$

F-2.2 MPC

Input data

$$a_o := .5 \cdot 68.375 \cdot \text{in}$$

$$L := 190.5 \cdot \text{in}$$

Properties are computed assuming MPC is a solid cylinder

$$\text{Area} := \pi \cdot a_o^2$$

$$\text{Area} = 3.672 \cdot 10^3 \cdot \text{in}^2$$

$$\text{mass}_{\text{mpc}} := \frac{W_{\text{mpc}}}{g}$$

$$\text{mass}_{\text{mpc}} = 233.107 \cdot \text{lbf} \cdot \frac{\text{sec}^2}{\text{in}}$$

$$I_{\text{mpc}} := \left(\frac{1}{12} \cdot \text{mass}_{\text{mpc}} \right) \cdot (3 \cdot a_o^2 + L^2)$$

$$I_{\text{mpc}} = 7.731 \cdot 10^5 \cdot \text{lbf} \cdot \text{sec}^2 \cdot \text{in}$$

APPENDIX G - CALCULATION OF SPRING CONSTANTS FOR HI-STORM 100 DYNAMIC ANALYSIS

G.1 SCOPE

This appendix computes values for the different spring rates used in the HI-STORM 100 dynamic analysis under high seismic loads.

G.2 METHODOLOGY

The effective tensile spring constant for each of the sector lugs is computed by first determining the deflection under a uniform loaded square plate clamped on three sides and free on the fourth side. This can be used to define a spring constant for the plate. This spring acts in series with the spring constant of an anchor bolt. The two contributions add in series to determine an effective tensile spring rate. The spring constant for shear resistance is computed from a guided cantilever beam solution.

For the compression spring rate, we use the solution for an elastic half-space and set a series of compression only springs at 10 degree intervals around the periphery.

Spring rates simulating contact between the MPC and the overpack at various locations are based on the local geometry at the contact point and on strength of materials and elasticity solutions relevant to the deformation at that location.

G.3 REFERENCES

[G.1] Timoshenko and Woinowsky-Krieger, Theory of Plates and Shells, McGraw-Hill, 1959, 2nd Edition, Section 47.

[G.2] Timoshenko and Goodier, Theory of Elasticity, McGraw-Hill, 3rd Edition, 1970, p. 407.

G.4 Tension Spring Constant at Anchor Bolt Locations

G.4.1 Input Data

The figure below provides the necessary geometry. Specific data is taken from Figure 8.3 in Section 8 of the main body of the report.

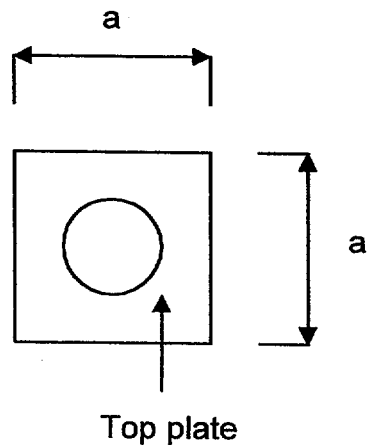
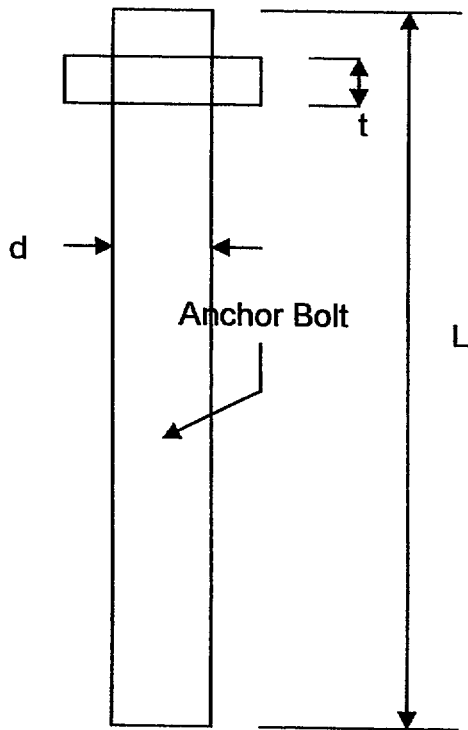


Figure G.1 - Sketch of a single plate and anchor bolt in an sector lug



The following geometry is used based on the figures in Section 8

$$a := 6 \cdot \text{in} \quad t := 1.75 \cdot \text{in} \quad d := 2 \cdot \text{in} \quad L := 38 \cdot \text{in} + 9.5 \cdot \text{in}$$

Estimated elastic length

The Young's Modulus and Poisson's Ratio of the plate and anchor bolt material is set at

$$E := 29000000 \cdot \text{psi} \quad \nu := 0.3$$

G.4.2 Calculations

From Table 44 of [G.1], for a square plate clamped on three sides and free on the fourth side,

$$\alpha := .0023 \quad \beta := 0.0853 \quad \gamma := 0.628$$

The total load applied to the plate surface is

$$P := qa$$

and the spring constant can be written as

$$k_1 := E \cdot \frac{t^3}{\alpha \cdot a^2 \cdot 12 \cdot (1 - \nu^2)} \quad k_1 = 1.719 \cdot 10^8 \cdot \frac{\text{lbf}}{\text{in}}$$

For a single anchor bolt,

$$k_2 := \frac{E \cdot \left(\frac{\pi}{4} \cdot d^2 \right)}{L} \quad k_2 = 1.918 \cdot 10^6 \cdot \frac{\text{lbf}}{\text{in}}$$

The two springs (simulating the plate and the bolts) act in series; therefore, the effective spring constant for a single bolt/plate section is

$$K_{\text{eff}} := \frac{k_1 \cdot k_2}{k_1 + k_2} \quad K_{\text{eff}} = 1.897 \cdot 10^6 \cdot \frac{\text{lbf}}{\text{in}}$$

Each sector lug subtends a 22.5 degree angle. Therefore, we represent the tensile resistance of the lug by two springs 10 degrees apart. Since there are 5 springs per sector lug (see Figures in Section 8), each spring has constant

$$K_{\text{tension}} := \frac{5 \cdot K_{\text{eff}}}{2} \quad K_{\text{tension}} = 4.742 \cdot 10^6 \frac{\text{lbf}}{\text{in}}$$

This tension spring is further modified by the effect of the stiffness of the overpack acting as a bar in tension or compression. The appropriate stiffness contribution that acts in series with the local stiffness at the anchors is computed as EA/L with a fraction of the final value ascribed to each location. The contribution to this stiffness is provided by assuming the steel shells act as tension members. Since the outer From drawing 1495 of [4], we see that we can define an "I" beam steel section adjacent to each sector lug running vertically the full length of the overpack.

The area "A" of the steel section is computed as follows:

From the bill of materials for the HI-STORM 100 overpack [4], the thickness of the outer shell, the inner shell, and the radial plates are, respectively

$$t_o := 0.75 \cdot \text{in} \quad t_i := 1.25 \cdot \text{in} \quad t_p := 0.75 \cdot \text{in}$$

The shell mean diameters and the plate width are, respectively

$$D_o := 132.5 \cdot \text{in} - t_o \quad D_i := 73.5 \cdot \text{in} + t_i \quad w_p := 27.5 \cdot \text{in}$$

The angle subtended associated with each sector lug is approximately 30 degrees for area calculation purposes. Then the total tensile area used in the spring constant calculation of the overpack is

$$\theta := 30 \cdot \text{deg}$$

$$A := \pi \cdot (D_o \cdot t_o + D_i \cdot t_i) \cdot \frac{\theta}{180 \cdot \text{deg}} + t_p \cdot w_p \quad A = 121.287 \cdot \text{in}^2$$

$$E = 2.9 \cdot 10^7 \cdot \text{psi}$$

The length associated with the spring constant is taken as 50% of the overpack height or

$$L := 115.5 \cdot \text{in}$$

Then the spring constant contribution, per sector lug, is

$$K_{ovp} := E \frac{A}{L} \quad K_{ovp} = 3.045 \cdot 10^7 \frac{\text{lbf}}{\text{in}}$$

The final effective tensile spring constant per spring (two per lug) is computed as

$$X_T := \frac{1}{K_{tension}} + \frac{2}{K_{ovp}}$$

$$K_{lug \text{ tension}} := \frac{1}{X_T} \quad K_{lug \text{ tension}} = 3.616 \cdot 10^6 \frac{\text{lbf}}{\text{in}}$$

The shear resistance of the sector lug is obtained from the solution of a guided cantilever beam with free length "Lf"

$$L_f := 10.5 \cdot \text{in} \quad \text{Assumed based on 9" free length above the surface and an additional 1.5" to represent the effect of local flexibility below the surface.}$$

The moment of inertia of a single anchor bolt is

$$I := \frac{\pi}{64} \cdot d^4 \quad I = 0.785 \cdot \text{in}^4$$

$$K := \frac{12 \cdot E \cdot I}{L_f^3} \quad K = 2.361 \cdot 10^5 \frac{\text{lbf}}{\text{in}}$$

There are 5 bolts per sector lug and we represent each set of 5 by 2 discrete linear spring elements. Therefore, for each of the two elements, we have the following shear springs in the horizontal plane (in x,y directions).

$$K_{shear} := 5 \cdot \frac{K}{2} \quad K_{shear} = 5.903 \cdot 10^5 \frac{\text{lbf}}{\text{in}}$$

The bolt circle radius is $R := 70.75 \cdot \text{in}$

The coordinates of the eight sets of springs representing the tension and shear stiffness of the four sector lugs is given below:

$$\theta := 10 \cdot \text{deg} \quad \sin(\theta) = 0.174 \quad \cos(\theta) = 0.985$$

$$\begin{aligned} x_0 &:= R & y_0 &:= 0 & x_{10} &:= R \cdot \cos(\theta) & x_{10} &= 69.675 \cdot \text{in} \\ & & & & y_{10} &:= R \cdot \sin(\theta) & y_{10} &= 12.286 \cdot \text{in} \end{aligned}$$

G.5 Cask-to-Pad Spring Constants

Conservatively use elastic spring rate based on classical solution for rigid punch on a semi-infinite half space. For the purpose of establishing a local spring rate for the pad resistance, the solution for a circular contact patch on a concrete half space is used. There will be 36 locations around the periphery and 3 springs per radial location to simulate the foundation effect. All of these springs are assumed to provide support within the outer annulus of the overpack. This is consistent with physical results since it is known that the resistance to a rigid cylinder resting on an elastic half space has larger reactions around the periphery.

To compute the area associated with a contact patch having three radial springs, we define the radius of the inner and outer shells of the HI-STORM overpack. Note that all geometry is taken from the latest revision of the HI-STORM TSAR (Reference [4] in Section 15 of this report).

$$a_0 := .5 \cdot 132.5 \cdot \text{in} \quad a_i := .5 \cdot 73.5 \cdot \text{in}$$

Then the radial span of the area to be supported (per segment) is

$$\text{span} := a_0 - a_i \quad \text{span} = 29.5 \cdot \text{in}$$

There are to be 36 segments around the periphery of the cask. Therefore, the mean circumferential length of each segment is

$$c := \pi \cdot \frac{(a_0 + a_i)}{2} \cdot \frac{10}{180} \quad c = 8.988 \cdot \text{in}$$

The segment area is

$$\text{Area}_t := c \cdot \text{span} \quad \text{Area}_t = 265.159 \cdot \text{in}^2$$

Properties

$$\text{Concrete compressive strength} \quad f_c := 6000 \cdot \text{psi}$$

We use maximum strength from Table 4.1 to maximize the stiffness. This is conservative for the prediction of peak compressive forces.

Concrete Young's Modulus

$$E_c := 57000 \cdot \sqrt{f_c} \cdot \text{psi} \quad (\text{ACI Code, 349, or similar})$$

$$E_c = 4.415 \cdot 10^6 \cdot \text{psi}$$

$$\text{Poisson's Ratio of Concrete} \quad \nu_c := .16$$

Contact Patch Radius of Each Cask

The spring rate for the contact between cask and concrete pad is set as (per [G.2])

$$K = (E_c (\text{Area}_t)^{1/2}) / (m(1 - \nu_c^2)) \quad m := .88$$

This value is based on the segment contact length and width

$$K := \frac{E_c \cdot \sqrt{\text{Area}_t}}{m \cdot (1 - \nu_c^2)} \quad K = 8.385 \cdot 10^7 \frac{\text{lbf}}{\text{in}}$$

The resistance to the cask motion is concentrated around the periphery; therefore, if NS is the number of individual springs situated at a segment, the value for K for each spring is the calculated spring constant for the segment divided by the number of springs used to simulate a segment resistance.

$$NS := 3 \quad k := \frac{K}{NS} \quad k = 2.795 \cdot 10^7 \frac{\text{lbf}}{\text{in}}$$

Each of these springs acts in series with a compression spring calculated from the action of the metal shells plus the radial plates acting as compression members over the length L, plus the concrete.

$$D_o = 131.75 \cdot \text{in} \quad D_i = 74.75 \cdot \text{in}$$

$$t_o = 0.75 \cdot \text{in} \quad t_i = 1.25 \cdot \text{in} \quad t_{ii} := 0.75 \cdot \text{in} \quad t_{in} := t_i + t_{ii}$$

$$\text{Area}_s := \pi \cdot (D_o \cdot t_o + D_i \cdot t_{in}) + 4 \cdot w_p \cdot t_p \quad \text{Area}_s = 862.597 \cdot \text{in}^2$$

$$\text{Area}_c := \frac{\pi}{4} \cdot (D_o^2 - D_i^2) \quad \text{Area}_c = 9.245 \cdot 10^3 \cdot \text{in}^2$$

$$E = 2.9 \cdot 10^7 \cdot \text{psi}$$

$$L = 115.5 \cdot \text{in}$$

$$E_{\text{concrete}} := 57000 \cdot \sqrt{4000 \cdot \text{psi}^2}$$

$$E_{\text{concrete}} = 3.605 \cdot 10^6 \cdot \text{psi}$$

Here we use the overpack concrete compressive strength listed in the TSAR [4].

Therefore the compression stiffness of the lower portion of the overpack

$$Kc_{\text{ovp}} := \frac{(E \cdot \text{Area}_s + E_{\text{concrete}} \cdot \text{Area}_c)}{L} \quad Kc_{\text{ovp}} = 5.051 \cdot 10^8 \frac{\text{lbf}}{\text{in}}$$

Dividing this value by 108 (3 springs x 36 locations) give the appropriate value to combine in series with "k"

$$k = 2.795 \cdot 10^7 \frac{\text{lbf}}{\text{in}}$$

$$XC := \frac{1}{k} + \frac{108}{Kc_{\text{ovp}}}$$

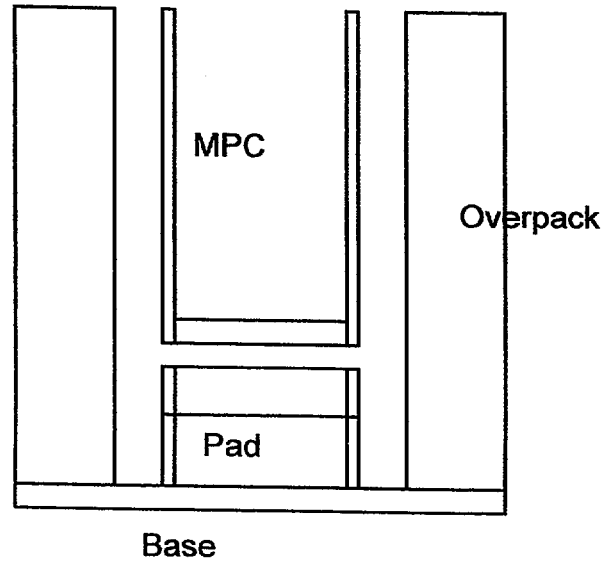
$$Kc_{\text{eff}} := \frac{1}{XC}$$

$$Kc_{\text{eff}} = 4.007 \cdot 10^6 \frac{\text{lbf}}{\text{in}}$$

G-6 MPC/Overpack Contact

G-6.1 MPC-to Overpack at base of cask

The following sketch shows the lower half of the MPC, the concrete/steel pad supporting the MPC, the overpack baseplate, and the lower half of the overpack.



This spring constant relates the resistance to vertical relative deformation under a compressive load that is available between the centroid of the overpack and the centroid of the MPC. The major contributors to the calculation of this resistance are:

1. The stiffness of the lower half of the MPC shell in axial compression
2. The stiffness of the cylindrical portion of the ring surrounding the lower concrete shielding block in axial compression.
3. The stiffness of the overpack base plate considered as a plate section bending under a uniform load.
4. The axial stiffness of the lower half of the overpack shells in axial tension.

The contribution of the overpack in the load path is ignored as it is significantly stiffer than the components mentioned and therefore, has no measurable effect on the total stiffness obtained by combining the other three springs in series.

Axial stiffness from MPC shell - the mean radius of the shell "b", and the shell thickness "t1" are

$$t1 := 0.5 \cdot \text{in} \quad b := \frac{68.375}{2} \cdot \text{in} - t1$$

Note that all geometry values come from appropriate drawings in Section 1.5 of the TSAR's [3,4 in the main body of the report]. We use a representative value for Young's Modulus for the stiffness calculations

$$E := 28000000 \cdot \text{psi}$$

The MPC shell length "Ls" that compresses is approximately equal to 50% of the MPC shell length.

$$Ls := 90 \cdot \text{in}$$

Therefore, the compression spring rate due to axial compression of the canister is

$$k_{\text{mpc}} := E \cdot \frac{(2 \cdot \pi \cdot b \cdot t1)}{Ls} \quad k_{\text{mpc}} = 3.293 \cdot 10^7 \frac{\text{lbf}}{\text{in}}$$

Axial stiffness from pedestal shell (item 5 of Drawing 1495 in Section 1.5 of [4]) - the mean radius of the shell "b2", and the shell thickness "t2" are

$$t2 := 0.25 \cdot \text{in} \quad b2 := \frac{68.375}{2} \cdot \text{in} - t2$$

$$\text{The Young's Modulus is} \quad E := 28000000 \cdot \text{psi}$$

The pedestal shell length "Lp" that compresses is

$$Ls := 21.875 \cdot \text{in}$$

Therefore, the compression spring rate due to axial compression is

$$k_{\text{ped}} := E \cdot \frac{(2 \cdot \pi \cdot b2 \cdot t2)}{Ls} \quad k_{\text{ped}} = 6.824 \cdot 10^7 \frac{\text{lbf}}{\text{in}}$$

The contribution from the baseplate of the MPC is approximated by the deflection of a shell under uniform pressure that is assumed simply supported at the connection to the inner shell of the overpack.

From [G.1], this spring constant can be written in terms of the plate geometry, the Young's Modulus, and the Poisson's Ratio.

Let b3 = the diameter of the base plate	b3 := 73.25·in
t3 = the plate thickness	t3 := 2·in
Poisson's Ratio	v := 0.3

The spring constant defined as total load divided by central deflection of the simply supported plate is

$$k_{\text{plate}} := \frac{64 \cdot (1 + \nu) \cdot \pi}{(5 + \nu) \cdot 12 \cdot (1 - \nu^2)} \cdot \frac{E \cdot t^3}{(.5 \cdot b3)^2} \quad k_{\text{plate}} = 7.542 \cdot 10^5 \frac{\text{lbf}}{\text{in}}$$

Therefore the combined spring constant, recognizing that the three springs given above act in series is

$$K_{\text{eff}} := \frac{1}{\left(\frac{1}{k_{\text{mpc}}} + \frac{1}{k_{\text{ped}}} + \frac{1}{k_{\text{plate}}} \right)} \quad K_{\text{eff}} = 7.294 \cdot 10^5 \frac{\text{lbf}}{\text{in}}$$

For the spring that simulates contact between the top of the MPC and the overpack lid (Item 10 in Drawing 1495 in section 1.5 of [4]), we account for the elasticity of the upper half of the MPC shell and the elasticity of the overpack top lid. All other contributions are assumed to be so large as to render their effect on the overall spring constant negligibly small.

The spring constant of the top lid of the overpack is computed based on the solution for a uniformly loaded circular plate assumed simply supported at diameter "d" and having thickness "t". From [4, Drg. 1495],

d := 103·in	t := 4·in
-------------	-----------

$$k_{\text{lid}} := \frac{64 \cdot (1 + \nu) \cdot \pi}{(5 + \nu) \cdot 12 \cdot (1 - \nu^2)} \cdot \frac{E \cdot t^3}{(.5 \cdot d)^2} \quad k_{\text{lid}} = 3.051 \cdot 10^6 \frac{\text{lbf}}{\text{in}}$$

Therefore the effective spring constant is

$$K_{\text{efft}} := \frac{1}{\left(\frac{1}{k_{\text{mpc}}} + \frac{1}{k_{\text{lid}}} \right)} \quad K_{\text{efft}} = 2.793 \cdot 10^6 \frac{\text{lbf}}{\text{in}}$$

G-6 MPC Cannister to Overpack Containment Shell

First assume the impact is of a steel structure (the MPC) radially against a concrete structure (the overpack), use the solution from [G.2] for a circular contact patch on a semi-infinite foundation with 4000 psi concrete assuming a 6" diameter contact patch.

$$b_2 := 3 \cdot \text{in} \quad f_{c2} := 4000 \cdot \text{psi} \quad \text{Area}_t := \pi \cdot b_2^2$$

$$E_{c2} := 57000 \cdot \sqrt{f_{c2} \cdot \text{psi}} \quad E_{c2} = 3.605 \cdot 10^6 \cdot \text{psi}$$

$$K := \frac{E_{c2} \cdot \sqrt{\text{Area}_t}}{m \cdot (1 - \nu_c^2)} \quad K = 2.236 \cdot 10^7 \frac{\text{lbf}}{\text{in}}$$

This spring acts in series with the spring constant from a channel. The finite element results give a spring constant per channel (6" length)

$$k_{\text{chan}} := 1788990 \cdot \frac{\text{lbf}}{\text{in}}$$

We conservatively assume 1 channel acts in concert with 1 circular patch, but that two sets are in contact for any impact. Therefore, the calculated spring rate for the combination is doubled for input into the dynamic analysis program.

$$K_{\text{combo}} := \frac{2 \cdot k_{\text{chan}} \cdot K}{K + k_{\text{chan}}} \quad K_{\text{combo}} = 3.313 \cdot 10^6 \frac{\text{lbf}}{\text{in}}$$

APPENDIX H - HI-STORM ANCHOR SYSTEM STRESS ANALYSIS

1.0 Purpose

This appendix contains calculations to assess whether the anchor system devised for HI-STORM is adequate for a severe seismic event and provides details for the remarks in Section 11.2 of this report. The anchor system contains a total of four "sector lugs" attached to the outer shell of the HI-STORM overpack by fillet welding, as shown in Figs 8.1 and 8.2 in Section 8 of the main text. These lugs contain a dual-plate system that lends length to the anchor bolts. In addition to the analysis for sector lugs, dimensions of the embedment are determined based on the corresponding calculations.

2.0 Methodology and Acceptance Criteria

2.1 The analysis is carried out using strength of materials formulations.

2.2 The allowable stresses for the steel members and the concrete are obtained in accordance with the materials specified in Section 9 of the report.

2.3 The maximum load applied to the anchor bolts due to the seismic accelerations is determined from the dynamic analyses in Section 10. Bounding loads in space and time are used for conservatism.

3.0 References

- 3.1 Timoshenko and Woinowsky-Kreiger, Theory of Plates and Shells, McGraw-Hill, 2nd Edition, 1959.
- 3.2 Manual of Steel Construction, Eighth Edition, AISC, Inc., 1980.
- 3.3 Roark's Formulas for Stress & Strain, Sixth Edition, 1989.
- 3.4 Code Requirements for Nuclear Safety Related Concrete Structures (ACI 349-97), 1997.

4.0 Input Data

Material properties:

Plate stocks: We base the analysis on allowable strengths that reasonably represent the materials listed in Section 9.1. For the seismic event, permit a 1.6 increase in allowable strength in tension and a 1.4 increase in shear. The ultimate and yield strengths of the plate stock, F_{pu} and F_{py} are taken as

$$F_{pu} := 58000 \cdot \text{psi}$$

$$F_{py} := 30000 \cdot \text{psi}$$

Note that the values for ultimate strength and for yield strength bound from below the possible values for any of the materials proposed in Section 9.1; therefore, although the two values, taken together, do not reflect any of the real materials, the results of the structural analysis will conservatively bound all of the proposed materials.

The allowable stresses in tension and shear are therefore given as

$$F_{pb} := 0.6 \cdot F_{py} \cdot (1.6) \quad F_{pa} := 0.4 \cdot F_{py} \cdot (1.4) \quad [3.2, \text{ and Section 6.3 of the main text of this report}]$$

$$F_{pb} = 2.88 \cdot 10^4 \cdot \text{psi} \quad F_{pa} = 1.68 \cdot 10^4 \cdot \text{psi}$$

These values are used for the sector lugs. For embedment steel in concrete, the allowable strengths are taken from the ACI-349 Code, Appendix B

$$F_{pbc} := .9 \cdot F_{py} \quad F_{pbc} = 2.7 \cdot 10^4 \cdot \text{psi}$$

$$F_{pac} := .55 \cdot F_{py} \quad F_{pac} = 1.65 \cdot 10^4 \cdot \text{psi}$$

Anchor bolts: A490

$$F_{bu} := 130000 \cdot \text{psi} \quad F_{by} := 120000 \cdot \text{psi} \quad \text{Maximum value permitted by ACI for embedment steel per ACI-349, B.6.}$$

The working stresses for the bolts are

$$F_{ba} := .8 \cdot F_{bu} \quad F_{bs} := .55 \cdot F_{by}$$

Therefore, the tensile and shear allowables are

$$F_{ba} = 1.04 \cdot 10^5 \cdot \text{psi} \quad F_{bs} = 6.6 \cdot 10^4 \cdot \text{psi}$$

Concrete:

We use the minimum concrete strength per Table 4.1 for conservatism and note that anchor head is not in the compression zone of the slab.

$$\text{Compressive strength:} \quad f_{cp} := 4000 \cdot \text{psi} \quad \phi := 0.65$$

$$\text{Allowable pullout stress:} \quad F_{Pd} := 4 \cdot \phi \cdot \sqrt{f_{cp}} \cdot \text{psi} \quad F_{Pd} = 164.438 \cdot \text{psi}$$

Allowable weld stress for sector lugs (require one grade higher weld wire):

$$\sigma_{wld} := 0.3 \cdot (F_{pu} + 10000 \cdot \text{psi}) \quad (\text{For a normal condition})$$

Allowing a 40% increase for the accident condition

$$\sigma_{weld} := 1.4 \cdot \sigma_{wld} \quad \sigma_{weld} = 2.856 \cdot 10^4 \cdot \text{psi}$$

Dead + Seismic Loads:

From the dynamic analyses in Section 10, the following peak reaction loads are extracted. We neglect any time phasing or specific location and conservatively use peak tensile and shear loads without regard to the particular simulation.

From Table 10.6, we have the maximum vertical load in each lug spring (two springs per sector lug) as

$$P_z := 355300 \cdot \text{lbf}$$

The peak shear forces in the horizontal plane in each spring (2 sets of springs per sector lug) are

$$P_x := 92100 \cdot \text{lbf}$$

Use Ph for either direction

$$P_h := 92100 \cdot \text{lbf}$$

$$P_y := 92000 \cdot \text{lbf}$$

We note that in the dynamic model, each of the four sector lugs is modeled by two sets of linear springs (each set consists of a vertical spring plus two springs in the horizontal plane that are orthogonal). Therefore, the maximum loads listed above from the dynamic analysis represent loads on 1/2 of the lug structure. Since each sector lug consists of 5 anchor bolt and plate sections, to obtain loads for qualification of a single bolt, we need to divide all of the loads by 2.5. Therefore, for analysis purposes, the following loads, **per bolt** are also defined:

$$F_v := P_z \cdot \frac{1}{2.5} \quad F_v = 1.421 \cdot 10^5 \cdot \text{lbf}$$

$$F_h := \frac{1}{2.5} \cdot \left(P_x^2 + P_y^2 \right)^{\frac{1}{2}} \quad F_h = 5.207 \cdot 10^4 \cdot \text{lbf}$$

Net shear load on a single sector lug bolt from both components of shear force.

$$F_{sh} := \frac{1}{2.5} \cdot Ph$$

$$F_{sh} = 3.684 \cdot 10^4 \cdot \text{lbf}$$

Shear in either direction on a single sector lug bolt.

5.0 Design Calculations

5.1 Welding Check:

First check the welds of plate #1 which attaches to the cask. Assume the welding is along the four sides of plate #1 (Figure 8.3). The sector lug supports 5 bolts. We compute the effect of various loads on the fillet weld attaching the plate to the cask. We neglect the curvature of the plate and consider the plate as flat. The following sketch shows the total resultant load (from 5 bolts) on the plate. A J-groove weld is assumed.

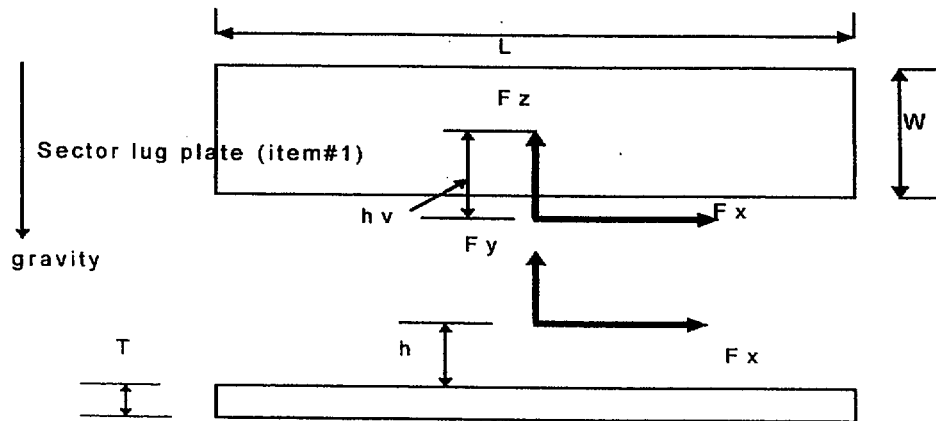
$$t_{\text{weld}} := 0.75 \cdot \text{in} \quad T := 1 \cdot \text{in} \quad h := 70.75 \cdot \text{in} - 66.25 \cdot \text{in} - \frac{T}{2}$$

$$L := \left(66.25 \cdot \text{in} + \frac{T}{2} \right) \cdot \pi \cdot \frac{27}{180} \quad L = 31.455 \cdot \text{in}$$

$$W := 11 \cdot \text{in}$$

$$h = 4 \cdot \text{in}$$

$$h_v := 7.5 \cdot \text{in}$$



SKETCH SHOWING
LOADS ACTING ON
ITEM#1 AND DEFINED
GEOMETRY

Note that Fz is the global vertical load (from both sets of lug springs simulating a single sector lug) and Fx, Fy are global horizontal loads (from both sets of lug springs). Since the plate is attached to the side of the overpack, Fy is a lateral load on the plate. Note also that we have conservatively assumed that there is no moment arising in the bolts so that the moment developed due to the entire offset "hv" is assumed to be reacted by the plate weld group to create a bending and torsional moment in the weld group.

We now compute the weld properties assuming a J-groove weld all 4 sides

$$A_{\text{weld}} := 2 \cdot (L + W) \cdot t_{\text{weld}} \quad A_{\text{weld}} = 63.683 \cdot \text{in}^2$$

$$I_x := t_{\text{weld}} \cdot L \cdot \left(\frac{W}{2}\right)^2 \cdot 2 + 2 \cdot t_{\text{weld}} \cdot \frac{W^3}{12} \quad I_x = 1.594 \cdot 10^3 \cdot \text{in}^4$$

$$I_z := t_{\text{weld}} \cdot W \cdot \left(\frac{L}{2}\right)^2 \cdot 2 + 2 \cdot t_{\text{weld}} \cdot \frac{L^3}{12} \quad I_z = 7.972 \cdot 10^3 \cdot \text{in}^4$$

$$A_{\text{included}} := L \cdot W \quad A_{\text{included}} = 346.007 \cdot \text{in}^2 \quad (\text{used in torsion stress calculation})$$

The contributions to the weld stress from each load (assume worst case direction for each load so that all contributions add) are as follows:

Fx Load

$$F_x := 2 \cdot Ph \quad F_x = 1.842 \cdot 10^5 \cdot \text{lbf}$$

$$\text{Direct Shear Stress} \quad \tau_x := \frac{F_x}{A_{\text{weld}}} \quad \tau_x = 2.892 \cdot 10^3 \cdot \text{psi}$$

$$\text{Bending Stress} \quad \sigma_x := \frac{F_x \cdot h \cdot L}{2 \cdot I_z} \quad \sigma_x = 1.454 \cdot 10^3 \cdot \text{psi}$$

$$\text{Torsion Stress} \quad \tau_t := \frac{F_x \cdot hv}{2 \cdot A_{\text{included}} \cdot t_{\text{weld}}} \quad \tau_t = 2.662 \cdot 10^3 \cdot \text{psi}$$

Fy Load

$$F_y := 2 \cdot Ph \quad F_y = 1.842 \cdot 10^5 \cdot \text{lbf}$$

$$\text{Direct stress} \quad \sigma_d := \frac{F_y}{A_{\text{weld}}} \quad \sigma_d = 2.892 \cdot 10^3 \text{ psi}$$

$$\text{Bending Stress} \quad \sigma_y := \frac{F_y \cdot h_v \cdot W}{2 \cdot I_x} \quad \sigma_y = 4.768 \cdot 10^3 \text{ psi}$$

Fz Load

$$F_z := 2 \cdot P_z \quad F_z = 7.106 \cdot 10^5 \text{ lbf}$$

$$\text{Shear Stress} \quad \tau_z := \frac{F_z}{A_{\text{weld}}} \quad \tau_z = 1.116 \cdot 10^4 \text{ psi}$$

$$\text{Bending Stress} \quad \sigma_z := \frac{F_z \cdot h \cdot W}{2 \cdot I_x} \quad \sigma_z = 9.81 \cdot 10^3 \text{ psi}$$

Net shear stress in weld at the most limiting corner location

$$\tau_{\text{weld}} := \sqrt{(\tau_x + \tau_t)^2 + (\tau_z + \tau_t)^2 + (\sigma_d + \sigma_x + \sigma_y + \sigma_z)^2}$$

$$\tau_{\text{weld}} = 2.408 \cdot 10^4 \text{ psi}$$

The safety factor on the weld stress is

$$SF_{\text{weld}} := \frac{\sigma_{\text{weld}}}{\tau_{\text{weld}}} \quad SF_{\text{weld}} = 1.186 \quad > 1.0$$

5.2 Maximum bending and Shear stresses in plate #3 (Item 3 in Figure 8.3)

This plate section was considered in Appendix G for the purpose of estimating its flexibility. It was considered as a plate welded on three sides and subject to a uniform load. We first consider the capacity of the two sided weld connecting item#3 to item#1 (see figure 8.3).

$$t_{\text{weldf}} := 0.5 \text{ in} \quad t_{3p} := 1.75 \text{ in} \quad (\text{weld size and plate thickness, respectively})$$

The weld moment capacity is

$$M_{\text{weld}} := \sigma_{\text{weld}} \cdot 0.7071 \cdot t_{\text{weldf}} (t_{3p} + 0.667 \cdot t_{\text{weldf}}) \quad M_{\text{weld}} = 2.104 \cdot 10^4 \cdot \text{lbf} \cdot \frac{\text{in}}{\text{in}}$$

The elastic moment capacity of the plate section itself is

$$M_{\text{plate}} := F_{\text{pb}} \frac{t_{3p}^2}{6} \quad M_{\text{plate}} = 1.47 \cdot 10^4 \cdot \text{lbf} \cdot \frac{\text{in}}{\text{in}}$$

Therefore, the calculation based on the plate section considering three sides clamped and the fourth side free is appropriate. From Table 44 in [3.1], we compute the maximum bending stress in the plate section as

$$P := F_v \quad P = 1.421 \cdot 10^5 \cdot \text{lbf}$$

$$\sigma_{\text{bend}} := 6 \cdot \frac{0.0853 \cdot P}{t_{3p}^2} \quad \sigma_{\text{bend}} = 2.375 \cdot 10^4 \cdot \text{psi}$$

The safety factor on the plate bending stress is

$$SF_{\text{bend}} := \frac{F_{\text{pb}}}{\sigma_{\text{bend}}} \quad SF_{\text{bend}} = 1.213$$

The safety factor on shear is computed by determining the total capacity with the load to be transmitted. We assume a 6" square plate for this calculation.

$$c := 6 \cdot \text{in} \quad \text{Length of each side used for computing capacity}$$

There are two fillet welds connecting item#3 to item#1 and two fillet welds connecting item#3 to items#4 (see Figure 8.3). There are two horizontal loads and a vertical load. Each horizontal load and the vertical load that is supported by shear has the magnitude F_s and F_v , respectively

$$F_s := F_{\text{sh}} \quad F_s = 3.684 \cdot 10^4 \cdot \text{lbf} \quad \text{in either horizontal direction}$$

$$F_v = 1.421 \cdot 10^5 \cdot \text{lbf}$$

The weld shear stress due to the vertical load is

$$\tau_1 := \frac{F_v}{4 \cdot 7071 \cdot t_{\text{weld}} \cdot c} \quad \tau_1 = 1.675 \cdot 10^4 \cdot \text{psi}$$

This stress acts at all three locations in the direction parallel to the cask longitudinal axis.

The weld stress due to F_s is

$$\tau_2 := \frac{F_s}{4 \cdot 7071 \cdot t_{\text{weld}} \cdot c} \quad \tau_2 = 4.342 \cdot 10^3 \cdot \text{psi}$$

This stress has both a radial component and a tangential component since F_s acts in both horizontal direction simultaneously.

Finally, there is a weld stress acting on the connection to item#1 due to the bending developed in the plate. From Table 44 in [3.1], the maximum bending moment developed along this wall is

$$M := 0.051 \cdot F_v \quad M = 7.248 \cdot 10^3 \cdot \text{in} \cdot \frac{\text{lbf}}{\text{in}}$$

Therefore, the actual weld shear stress developed due to this bending of the plate is

$$\tau_3 := \frac{M}{M_{\text{weld}}} \cdot \sigma_{\text{weld}} \quad \tau_3 = 9.84 \cdot 10^3 \cdot \text{psi}$$

This weld stress acts only at the connection to item#1 and is radially directed.

The combined weld stress at the most limiting location is determined in the following:

Connection to item#1

$$\tau_{w1} := \sqrt{\tau_1^2 + \tau_2^2 + (\tau_2 + \tau_3)^2} \quad \tau_{w1} = 2.237 \cdot 10^4 \cdot \text{psi}$$

$$SF := \frac{\sigma_{\text{weld}}}{\tau_{w1}} \quad SF = 1.277$$

Connection to item#4

$$\tau_{w4} := \sqrt{\tau_1^2 + \tau_2^2 + (\tau_2)^2} \quad \tau_{w4} = 1.784 \cdot 10^4 \text{ psi}$$

$$SF := \frac{\sigma_{weld}}{\tau_{w4}} \quad SF = 1.601$$

5.3 Anchor Bolts

The anchor bolt diameter is defined as the variable d6 and the anchor bolt stress metal area as A6. A6 is defined by a formula in the ACI-349 Code, Appendix B.

$$d6 := 2.0 \cdot \text{in} \quad A6 := \pi \cdot \frac{\left(d6 - \frac{.9743 \cdot \text{in}}{4}\right)^2}{4} \quad A6 = 2.423 \cdot \text{in}^2$$

The tensile and net shear loads on a single anchor bolt are:

$$F_v = 1.421 \cdot 10^5 \cdot \text{lbf} \quad F_h = 5.207 \cdot 10^4 \cdot \text{lbf}$$

The maximum tensile stress in each anchor bolt in a sector lug is:

$$\sigma_{bolt} := \frac{F_v}{A6} \quad \sigma_{bolt} = 5.866 \cdot 10^4 \text{ psi} \quad SF_{bolt} := \frac{F_{ba}}{\sigma_{bolt}} \quad SF_{bolt} = 1.773$$

The shear stress in each bolt is:

(conservatively neglect any friction at the interface with the concrete)

$$\tau_{bolt} := \frac{F_h}{A6} \quad \tau_{bolt} = 2.149 \cdot 10^4 \text{ psi} \quad SF_{bolts} := \frac{F_{bs}}{\tau_{bolt}} \quad SF_{bolts} = 3.071$$

Check to insure that the requirements of ACI-349, B.6.3.2 are satisfied for combined tension and shear

$$\frac{1}{SF_{bolt}} + \frac{1}{SF_{bolts}} = 0.89$$

$$SF_{\text{combined}} := \frac{1}{\left(\frac{1}{SF_{\text{bolt}}} + \frac{1}{SF_{\text{bolts}}} \right)} \quad SF_{\text{combined}} = 1.124$$

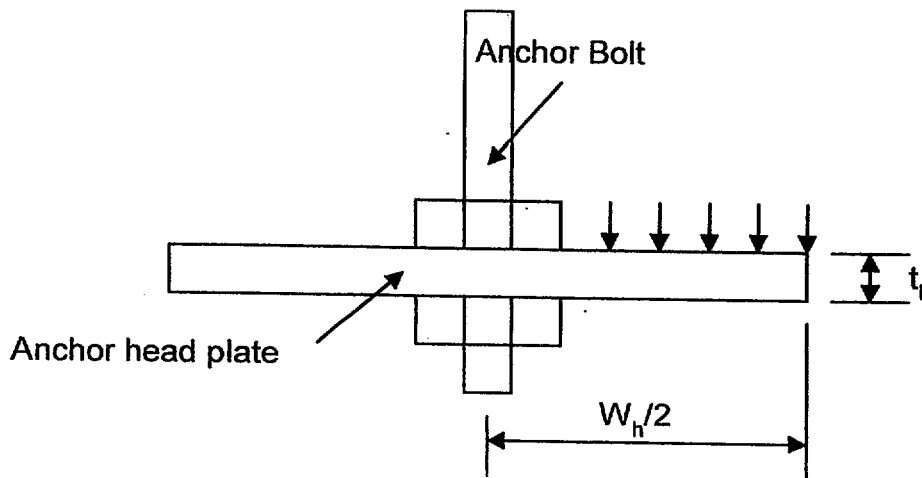
Anchor Head Design

Each anchor bolt passes through a plate that serves as the anchor head for the five sector lug bolts. This plate is embedded in the concrete and must transfer the tensile load from the five anchor bolts to the concrete. The dimensions and load applied to the anchor head are:

$$L_h := 36 \cdot \text{in} \quad W_h := 20 \cdot \text{in} \quad t_h := 0.75 \cdot \text{in}$$

$$F_z = 7.106 \cdot 10^5 \cdot \text{lbf}$$

$$\text{The pitch between individual studs is} \quad \text{pitch} := 5.5 \cdot \text{in}$$



The anchor head plate is shown to meet the requirements of the ACI code, B.4.5.2 For the purpose of this calculation assume the effective anchor head plate for each anchor bolt is equal to a square plate having side length equal to the 50% of the pitch of the anchor bolts.

$$\frac{(.5 \cdot \text{pitch})^2}{A_6} = 3.121 \quad \text{This is greater than 2.5 so condition (a) of B.4.5.2 is satisfied.}$$

$$\frac{(.5 \cdot \text{pitch} - d_6)}{2} = 0.375 \cdot \text{in}$$

This value is exceeded by the plate thickness itself and neglects any effect from the anchor bolt nut. Therefore, condition (b) of B.4.5.2 is satisfied. Condition (c) of B.4.5.2 is automatically satisfied by the actual extent of the material in place.

5.4 Concrete Calculations

5.4.1 Bearing

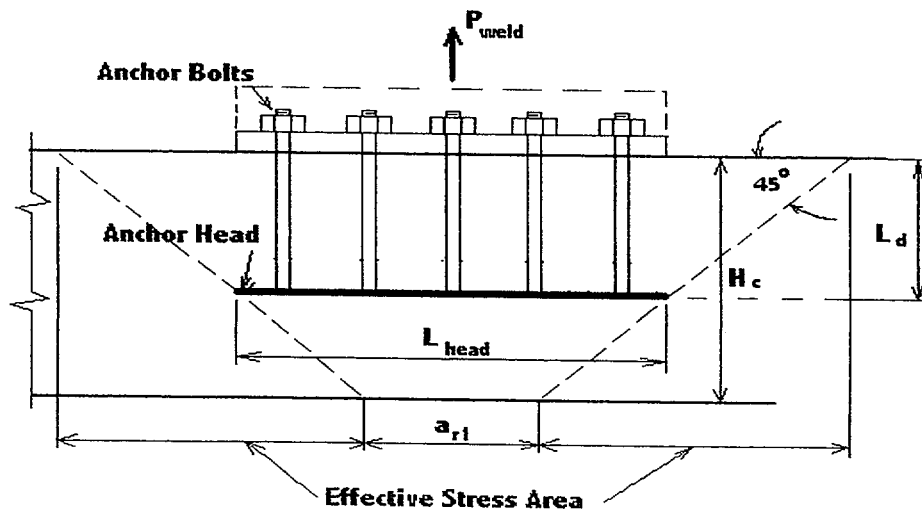
Assuming a group of five bolts are connected to the same anchor head plate embedded into the concrete, the minimum bearing area for such an anchor head subject to the total tension load is calculated based on section 10.15. of Ref. 3.4:

$$\phi_b := 0.7 \quad A_{bv} := \frac{5 \cdot F_v}{\phi_b \cdot (0.85 \cdot f_{cp})} \quad A_{bv} = 298.571 \cdot \text{in}^2$$

A anchor plate of $L_{\text{head}} \times W_{\text{head}}$ is used to meet the above requirement.

The total vertical load is $P_{\text{weld}} = 5P_v$

$$L_{\text{head}} := L_h \quad W_{\text{head}} := W_h \quad SF_{56a} := \frac{L_{\text{head}} \cdot W_{\text{head}}}{A_{bv}} \quad SF_{56a} = 2.411$$



To resist the shear loads, a certain minimum embedment length is required. On a per bolt basis,

$$\phi_b = 0.7$$

$$A_{bh} := \frac{F_h}{\phi_b \cdot (0.85 \cdot f_{cp})} \quad A_{bh} = 21.879 \cdot \text{in}^2$$

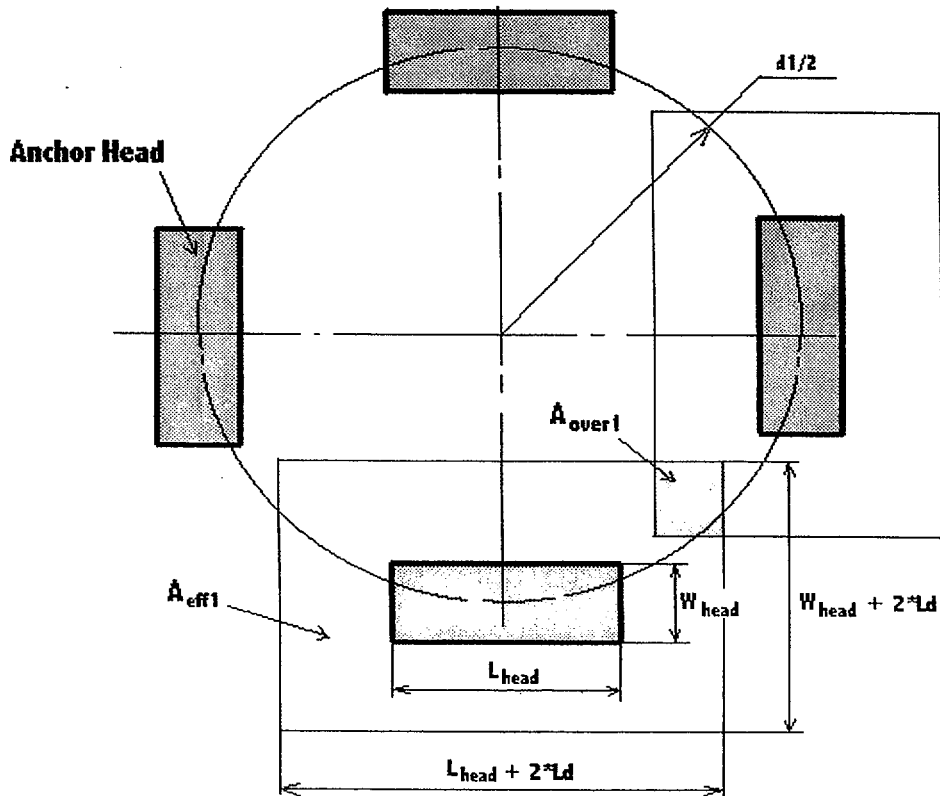
The minimum embedment depth is $L_{dmin} := \frac{A_{bh}}{d_6} \quad L_{dmin} = 10.939 \cdot \text{in}$

Choose the following concrete depth and the embedment depth of the anchor head.

$H_c := 54 \cdot \text{in}$ $L_d := 38 \cdot \text{in}$ Minimum thickness pad per Table 4.1 and depth of anchors per Appendix G.

5.4.2 Concrete pullout strength

For a given concrete thickness (H_c) and an embedment depth of the anchor head (L_d), the effective stress area (A_{eff1}) for a group of anchor bolts is determined by subtracting the area reduction for limited depth (A_{r1}) from the projected area of stress cone of the anchor head. The methodology is given in [3.4].



Compute the following quantities

$$a_{r1} := L_{\text{head}} + 2 \cdot L_d - 2 \cdot H_c \quad a_{r1} = 4 \cdot \text{in} \quad a_{\text{red1}} := \text{if}(a_{r1} > 0 \cdot \text{in}, a_{r1}, 0 \cdot \text{in})$$

$$b_{r1} := W_{\text{head}} + 2 \cdot L_d - 2 \cdot H_c$$

$$b_{r1} = -12 \cdot \text{in} \quad b_{\text{red1}} := \text{if}(b_{r1} > 0 \cdot \text{in}, b_{r1}, 0 \cdot \text{in})$$

Therefore

$$a_{\text{red1}} = 4 \cdot \text{in}$$

$$b_{\text{red1}} = 0 \cdot \text{in}$$

Area reduction due to limited concrete depth:

$$A_{r1} := a_{\text{red1}} \cdot b_{\text{red1}} \quad A_{r1} = 0 \cdot \text{in}^2$$

$$A_{\text{eff1}} := (L_{\text{head}} + 2 \cdot L_d) \cdot (W_{\text{head}} + 2 \cdot L_d) - A_{r1} \quad A_{\text{eff1}} = 1.075 \cdot 10^4 \cdot \text{in}^2$$

Area reduction due to proximity of adjacent cask

Because of the minimum spacing between casks, a further adjustment shall be made to eliminate overlapping areas. The effective width is reduced to

$$W_{\text{eff}} := W_{\text{head}} + L_d \quad \text{so that}$$

$$A_{\text{eff2}} := (L_{\text{head}} + 2 \cdot L_d) \cdot W_{\text{eff}} \quad A_{\text{eff2}} = 6.496 \cdot 10^3 \cdot \text{in}^2$$

The safety factor on the individual sector lug anchoring is

$$\sigma_{\text{ct1}} := \frac{5 \cdot F_v}{A_{\text{eff2}}} \quad \sigma_{\text{ct1}} = 109.39 \cdot \text{psi} \quad SF_{56b} := \frac{F_{\text{Pd}}}{\sigma_{\text{ct1}}} \quad SF_{56b} = 1.503$$

The total effective stress area for all four groups of anchor heads shall exclude the overlapped stress areas.

$$d1 := 2 \cdot 71.75 \cdot \text{in}$$

$$L_{\text{over1}} := \left(\frac{L_{\text{head}}}{2} + L_d \right) - \left(\frac{d1}{2} - L_d - \frac{W_{\text{head}}}{2} \right) \quad L_{\text{over1}} = 32.25 \cdot \text{in}$$

The overlapped stress area of two neighboring anchor heads is:

$$A_{\text{over1}} := L_{\text{over1}}^2 \quad A_{\text{over1}} = 1.04 \cdot 10^3 \cdot \text{in}^2$$

$$L_{\text{over2}} := \text{if} \left[(W_{\text{head}} + 2 \cdot L_d - d1) < 0.0 \cdot \text{in}, 0 \cdot \text{in}, (W_{\text{head}} + 2 \cdot L_d - d1) \right]$$

$$L_{\text{over2}} = 0 \cdot \text{in}$$

The overlapped stress area of two opposite anchor heads is:

$$A_{\text{over2}} := (L_{\text{head}} + 2 \cdot L_d) \cdot L_{\text{over2}} \quad A_{\text{over2}} = 0 \cdot \text{in}^2$$

The total effective stress area, excluding the overlapped stress areas and correcting for the proximity of adjacent casks, is:

$$A_{\text{eff}} := 4 \cdot A_{\text{eff2}} - 4 \cdot A_{\text{over1}} - 2 \cdot A_{\text{over2}} \quad A_{\text{eff}} = 2.182 \cdot 10^4 \cdot \text{in}^2$$

Considering the total tension load applied on the entire anchoring system, we note that the dynamic analysis results for HI-STORM 100 predict a maximum total compressive vertical load on the surface of the ISFSI pad (see Section 11)

$$F_{\text{total}} := 6.51 \cdot 360000 \cdot \text{lbf} \quad F_{\text{total}} = 2.344 \cdot 10^6 \cdot \text{lbf}$$

The load is computed based on the instantaneous peak vertical acceleration on the loaded cask. Conservatively, assuming a tensile load of the same magnitude,

$$\sigma_{\text{ct}} := \frac{F_{\text{total}}}{A_{\text{eff}}} \quad \sigma_{\text{ct}} = 107.387 \cdot \text{psi} \quad \text{SF}_{56\text{c}} := \frac{F_{\text{Pd}}}{\sigma_{\text{ct}}} \quad \text{SF}_{56\text{c}} = 1.531$$

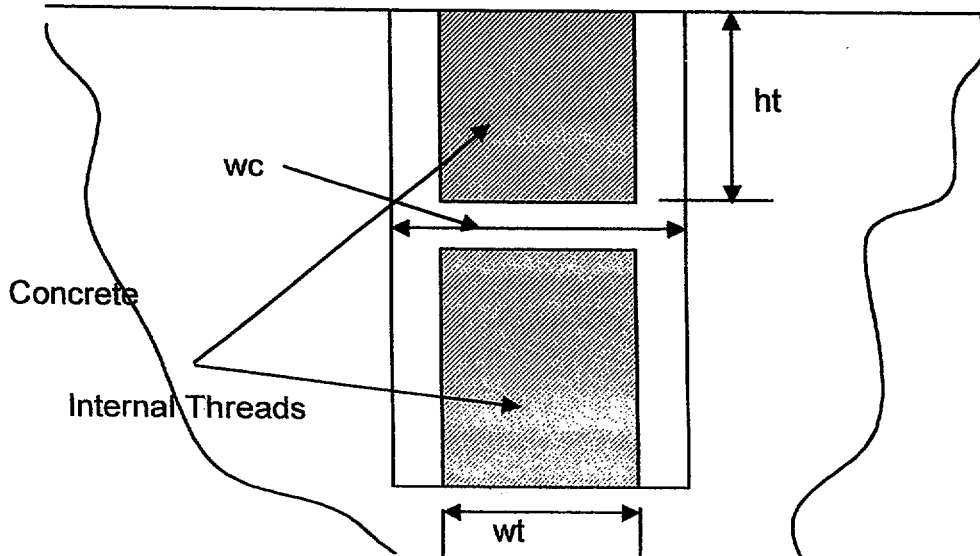
Appropriate additional hairpin reinforcement should be provided as required by Figure B.4 of the Commentary in Reference [13] cited in the main text to insure that tensile cracking is inhibited.

5.4.3 Shearing

Since the concrete pad is so designed that the shearing force is parallel to the free surface of the concrete, local shearing is not a concern for this specific design.

6.0 Anchor Bolt Upper Connector

In order to install the HI-STORM 100 on the pad, the anchor bolts must be removable during HI-STORM 100 movement over the location of the anchor bolts. To this end, anchor bolt connectors, flush with the surface are embedded as shown below:



The depth of the internal threads must be sufficient to resist the tensile load on a single anchor stud, while the connector cross section area must be such as to enable the load transfer to be carried out between upper and lower anchor components. We assume that the connector bar is made from embedment material having the minimum yield and ultimate strengths from all candidate materials.

The load to be resisted is

$$F_v = 1.421 \cdot 10^5 \cdot \text{lbf}$$

Diameter of internal thread $wt := d_6$ $wt = 2 \cdot \text{in}$

Square connector side length $wc := 4.0 \cdot \text{in}$

Depth of internal thread $ht := 4 \cdot \text{in}$

$$A_{\text{metal}} := wc^2 - \pi \frac{d_6^2}{4} \quad A_{\text{metal}} = 12.858 \cdot \text{in}^2$$

Compute the average tensile stress in the connector

$$\sigma_{\text{connect}} := \frac{F_v}{A_{\text{metal}}} \quad \sigma_{\text{connect}} = 1.105 \cdot 10^4 \text{ psi}$$

The safety factor against tension failure is

$$SF_{\text{connect}} := \frac{F_{\text{pac}}}{\sigma_{\text{connect}}} \quad SF_{\text{connect}} = 2.443$$

The shear stress in the threaded region is

$$\tau_{\text{thread}} := \frac{F_v}{\pi \cdot wt \cdot ht} \quad \tau_{\text{thread}} = 5.655 \cdot 10^3 \text{ psi}$$

The safety factor on the thread shear stress is

$$SF_{\text{connect_shear}} := \frac{F_{\text{pac}}}{\tau_{\text{thread}}} \quad SF_{\text{connect_shear}} = 2.918$$

Although we have provided a design calculation for this member, standard connectors (couplings) are available for anchor bolts to perform this function. Should a standard coupling be used, the same safety factors should be maintained.

7.0 Conclusions

6.1 Analysis indicates that all the structure members can satisfy the strength requirements under a severe seismic event. All calculated safety factors are above 1.0 based on the allowable stresses for the component.

APPENDIX I - STATIC CALCULATION OF ANCHOR BOLT FORCES IN HI-STORM 100

1.0 Purpose

The calculation estimates the maximum anchor bolt forces in the HI-STORM anchor system during a severe seismic event (2.12g horizontal acceleration and 0.5g net vertical upward acceleration). The purpose of the analysis is to provide a comparison scoping calculation that can be compared with the results of the non-linear analysis. The anchor system contains a total of four "sector lugs" attached to the outer shell of the HI-STORM overpack by welds as shown in Figs 8.1 and 8.2 in Ref. 3.1.

2.0 Assumptions

- 2.1 The analysis is carried out using static force and moment balance formulas.
 2.2 The cask is treated as a rigid body, and linearly distributed bolt forces are assumed.

3.0 References

- 3.1 Text and Figures in Section 8 and appropriate drawings and data from Reference [4] in Section 15.

4.0 Input Data

Seismic Loads:

$$W_{\text{cask}} := 360000 \cdot \text{lbf} \quad (\text{weight of the cask})$$

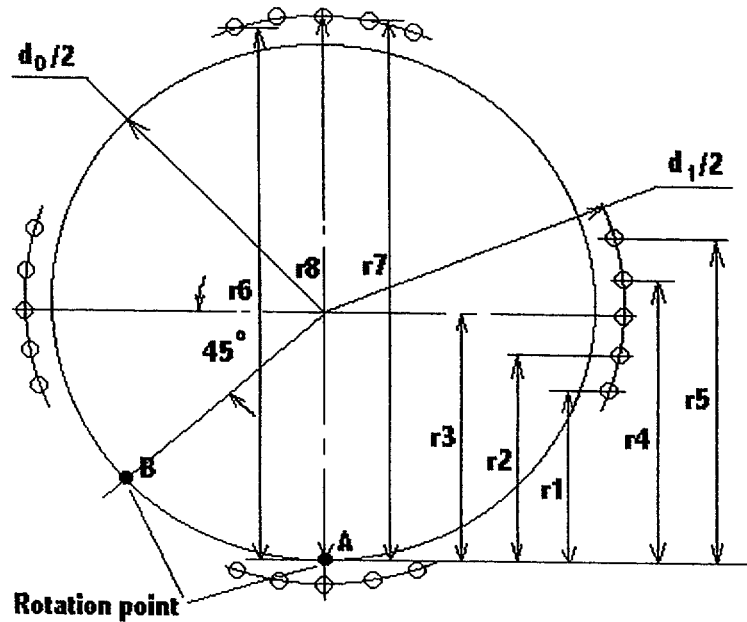
$$F_v := 0.5 \cdot W_{\text{cask}} \quad F_v = 1.8 \cdot 10^5 \cdot \text{lbf} \quad F_h := 2 \cdot 1.414 \cdot W_{\text{cask}} \quad F_h = 1.018 \cdot 10^6 \cdot \text{lbf}$$

Dimensions (see sketch below):

$$d_0 := 132.5 \cdot \text{in} \quad d_1 := 141.5 \cdot \text{in} \quad d_2 := 146.5 \cdot \text{in} \quad h := \frac{231.25 \cdot \text{in}}{2} \quad h = 115.625 \cdot \text{in} \quad \alpha := \frac{4.5 \cdot \pi}{180}$$

5.0 Calculations

The maximum tension force in anchor bolts occurs when the horizontal seismic load forces the cask to rotate about the tangent line through either point A or point B as shown in the sketch below. In the first case, dimensions r1 through r8 shown in the sketch are the distances between the anchor bolts and point A.



$$d0 := 132.5\text{-in} \quad d1 := 141.5\text{-in} \quad d2 := 146.5\text{-in} \quad h := \frac{231.25\text{-in}}{2} \quad h = 115.625\text{-in} \quad \alpha := \frac{4.5 \cdot \pi}{180}$$

$$r1 := \frac{d0}{2} - \frac{d1}{2} \cdot \sin(2 \cdot \alpha) \quad r2 := \frac{d0}{2} - \frac{d1}{2} \cdot \sin(\alpha) \quad r3 := \frac{d0}{2} \quad r4 := \frac{d0}{2} + \frac{d1}{2} \cdot \sin(\alpha)$$

$$r5 := \frac{d0}{2} + \frac{d1}{2} \cdot \sin(2 \cdot \alpha) \quad r6 := \frac{d0}{2} + \frac{d1}{2} \cdot \cos(2 \cdot \alpha) \quad r7 := \frac{d0}{2} + \frac{d1}{2} \cdot \cos(\alpha) \quad r8 := \frac{d0 + d1}{2}$$

$$r1 = 55.182\text{-in} \quad r2 = 60.699\text{-in} \quad r3 = 66.25\text{-in} \quad r4 = 71.801\text{-in}$$

$$r5 = 77.318\text{-in} \quad r6 = 136.129\text{-in} \quad r7 = 136.782\text{-in} \quad r8 = 137\text{-in}$$

$$e1 := \frac{r1}{r8} \quad e2 := \frac{r2}{r8} \quad e3 := \frac{r3}{r8} \quad e4 := \frac{r4}{r8}$$

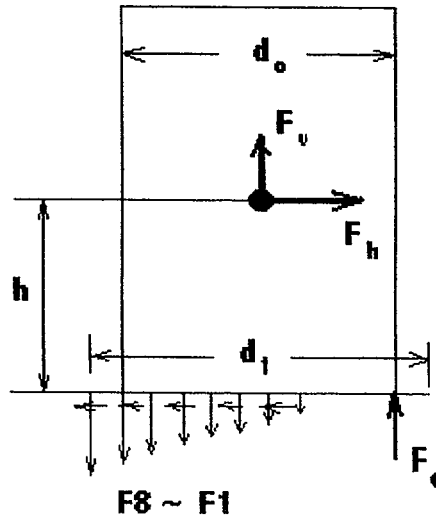
$$e5 := \frac{r5}{r8} \quad e6 := \frac{r6}{r8} \quad e7 := \frac{r7}{r8}$$

$$e1 = 0.403 \quad e2 = 0.443 \quad e3 = 0.484 \quad e4 = 0.524 \quad e5 = 0.564 \quad e6 = 0.994 \quad e7 = 0.998$$

$$c1 := 1 + 2 \cdot (e1 + e2 + e3 + e4 + e5 + e6 + e7) \quad c1 = 9.82$$

$$c2 := r8 + 2 \cdot (e1 \cdot r1 + e2 \cdot r2 + e3 \cdot r3 + e4 \cdot r4 + e5 \cdot r5 + e6 \cdot r6 + e7 \cdot r7) \quad c2 = 1.006 \cdot 10^3\text{-in}$$

The horizontal seismic load is balanced by the assumed uniform shear forces generated in the anchor bolts. The vertical seismic load is balanced by the tension forces (F1 to F8) in the anchor bolts and the vertical reaction force (F_c) at the cask edge. The moments of the tension forces and the reaction force also balance that generated by the seismic loads.



$$F_8 := \frac{F_h \cdot h + \frac{F_v \cdot d_0}{2}}{c_2}$$

$$F_c := F_8 \cdot c_1 - F_v$$

$$F_8 = 1.289 \cdot 10^5 \text{ lbf}$$

$$F_c = 1.086 \cdot 10^6 \text{ lbf}$$

$$F_1 := e_1 \cdot F_8$$

$$F_2 := e_2 \cdot F_8$$

$$F_3 := e_3 \cdot F_8$$

$$F_4 := e_4 \cdot F_8$$

$$F_5 := e_5 \cdot F_8$$

$$F_6 := e_6 \cdot F_8$$

$$F_7 := e_7 \cdot F_8$$

$$F_1 = 5.193 \cdot 10^4 \text{ lbf}$$

$$F_2 = 5.712 \cdot 10^4 \text{ lbf}$$

$$F_3 = 6.235 \cdot 10^4 \text{ lbf}$$

$$F_4 = 6.757 \cdot 10^4 \text{ lbf}$$

$$F_5 = 7.276 \cdot 10^4 \text{ lbf}$$

$$F_6 = 1.281 \cdot 10^5 \text{ lbf}$$

$$F_7 = 1.287 \cdot 10^5 \text{ lbf}$$

$$F_8 = 1.289 \cdot 10^5 \text{ lbf}$$

The maximum pullout force applied at the sector lug is:

$$F_A := F_8 + 2 \cdot (F_6 + F_7)$$

$$F_A = 6.426 \cdot 10^5 \text{ lbf}$$

The maximum tension force in the anchor bolt is:

$$T_{\max A} := F_8 \quad T_{\max A} = 1.289 \cdot 10^5 \text{ lbf}$$

In the second case when the cask tips over at point B, r1 through r10 are the distances between the bolts and point B which are not shown in the sketch.

$$r_1 := \frac{d_0}{2} - \frac{d_1}{2} \cdot \cos\left(\frac{\pi}{4} - 2 \cdot \alpha\right) \quad r_2 := \frac{d_0}{2} - \frac{d_1}{2} \cdot \cos\left(\frac{\pi}{4} - \alpha\right) \quad r_3 := \frac{d_0}{2} - \frac{d_1}{2} \cdot \cos\left(\frac{\pi}{4}\right)$$

$$r4 := \frac{d0}{2} - \frac{d1}{2} \cdot \cos\left(\frac{\pi}{4} + \alpha\right) \quad r5 := \frac{d0}{2} - \frac{d1}{2} \cdot \cos\left(\frac{\pi}{4} + 2 \cdot \alpha\right) \quad r6 := \frac{d0}{2} + \frac{d1}{2} \cdot \sin\left(\frac{\pi}{4} - 2 \cdot \alpha\right)$$

$$r7 := \frac{d0}{2} + \frac{d1}{2} \cdot \sin\left(\frac{\pi}{4} - \alpha\right) \quad r8 := \frac{d0}{2} + \frac{d1}{2} \cdot \sin\left(\frac{\pi}{4}\right) \quad r9 := \frac{d0}{2} + \frac{d1}{2} \cdot \sin\left(\frac{\pi}{4} + \alpha\right)$$

$$r10 := \frac{d0}{2} + \frac{d1}{2} \cdot \sin\left(\frac{\pi}{4} + 2 \cdot \alpha\right)$$

$$r1 = 9.012 \text{ in} \quad r2 = 12.451 \text{ in} \quad r3 = 16.222 \text{ in} \quad r4 = 20.302 \text{ in} \quad r5 = 24.664 \text{ in}$$

$$r6 = 107.836 \text{ in} \quad r7 = 112.198 \text{ in} \quad r8 = 116.278 \text{ in} \quad r9 = 120.049 \text{ in} \quad r10 = 123.488 \text{ in}$$

$$e1 := \frac{r1}{r10} \quad e2 := \frac{r2}{r10} \quad e3 := \frac{r3}{r10} \quad e4 := \frac{r4}{r10} \quad e5 := \frac{r5}{r10}$$

$$e6 := \frac{r6}{r10} \quad e7 := \frac{r7}{r10} \quad e8 := \frac{r8}{r10} \quad e9 := \frac{r9}{r10}$$

$$e1 = 0.073 \quad e2 = 0.101 \quad e3 = 0.131 \quad e4 = 0.164 \quad e5 = 0.2 \quad e6 = 0.873 \quad e7 = 0.909$$

$$e8 = 0.942 \quad e9 = 0.972$$

$$c1 := 2 \cdot (e1 + e2 + e3 + e4 + e5 + e6 + e7 + e8 + e9 + 1) \quad c1 = 10.73$$

$$c2 := 2 \cdot (e1 \cdot r1 + e2 \cdot r2 + e3 \cdot r3 + e4 \cdot r4 + e5 \cdot r5 + e6 \cdot r6 + e7 \cdot r7 + e8 \cdot r8 + e9 \cdot r9 + r10) \quad c2 = 93.016 \text{ ft}$$

$$F10 := \frac{Fh \cdot h + \frac{Fv \cdot d0}{2}}{c2} \quad Fc := F10 \cdot c1 - Fv$$

$$F10 = 1.161 \cdot 10^5 \text{ lbf} \quad Fc = 1.066 \cdot 10^6 \text{ lbf}$$

$$F1 := e1 \cdot F10 \quad F2 := e2 \cdot F10 \quad F3 := e3 \cdot F10 \quad F4 := e4 \cdot F10 \quad F5 := e5 \cdot F10$$

$$F6 := e6 \cdot F10 \quad F7 := e7 \cdot F10 \quad F8 := e8 \cdot F10 \quad F9 := e9 \cdot F10$$

$$F1 = 8.476 \cdot 10^3 \text{ lbf} \quad F2 = 1.171 \cdot 10^4 \text{ lbf} \quad F3 = 1.526 \cdot 10^4 \text{ lbf} \quad F4 = 1.909 \cdot 10^4 \text{ lbf}$$

$$F5 = 2.32 \cdot 10^4 \text{ lbf} \quad F6 = 1.014 \cdot 10^5 \text{ lbf} \quad F7 = 1.055 \cdot 10^5 \text{ lbf} \quad F8 = 1.094 \cdot 10^5 \text{ lbf}$$

$$F_9 = 1.129 \cdot 10^5 \text{ lbf} \quad F_{10} = 1.161 \cdot 10^5 \text{ lbf}$$

The maximum pullout force applied at the sector lug is: $F_B := F_6 + F_7 + F_8 + F_9 + F_{10}$ $F_B = 5.454 \cdot 10^5 \text{ lbf}$

In this case, the maximum tension force in the anchor bolts is:

$$T_{\max B} := F_{10} \quad T_{\max B} = 1.161 \cdot 10^5 \text{ lbf}$$

Comparing between the maximum tension forces obtained in the above two cases, the real maximum tension force is:

$$T_{\max} := \text{if}(T_{\max A} > T_{\max B}, T_{\max A}, T_{\max B}) \quad T_{\max} = 1.289 \cdot 10^5 \text{ lbf}$$

Assuming uniform shear forces in the bolts, the shear force in each bolt is:

$$F_s := \frac{F_h}{20} \quad F_s = 5.09 \cdot 10^4 \text{ lbf}$$

6.0 Conclusion

The maximum tension and shear force in the anchor bolts are found to be 1.289×10^5 lbf and 5.09×10^4 lbf, respectively. This result is compared with the non-linear time history result in Section 10 of the report.

APPENDIX J
HYDROLOGICAL LOAD CONSIDERATIONS
HOLTEC PROPRIETARY

APPENDIX K - STRUCTURAL EVALUATION OF ISFSI SLAB SUPPORTING HI-STAR 100 CASK

K.1 INTRODUCTION

The ISFSI concrete pad structural design is considered herein. The objective of the analysis is to demonstrate that the specified minimum pad thickness, reinforcement, and slab subgrade modulus in Table 4.1 of Section 4 of this report are sufficient to structurally qualify the pad under appropriate load combinations from Section 6.2. The cask seismic loading on the ISFSI is taken from Table 10.2 of this report.

K.2 METHODOLOGY AND LOAD COMBINATIONS

K.2.1 Methodology

The design approach is to assume a concrete pad thickness with appropriate reinforcement and minimal support from the engineered fill, and demonstrate that the appropriate safety factors or safety margins are maintained for all static and dynamic loadings. Calculation methodologies used are based on charts, formulas, empirical results from various documents on the subject matter, and analytical or numerical solutions.

K.2.2 Load Combinations

Bounding Load Combinations are taken from Section 6.2 of this report.

Normal Events

$$U_c > 1.4D + 1.7(L)$$

Off-Normal Events

$$U_c > 1.05D + 1.275(L+F)$$

Accident-Level Events

$$U_c > D+L+E$$

From Section 11.4, we need not consider the Off-Normal event since the hydrological pressure and debris loads are appropriately limited (see Appendix J) to insure that if the slab is structurally adequate to support the Accident Level loads, then it is automatically adequate to support the Off-Normal level loads.

K.3 ACCEPTANCE REQUIREMENTS

The slab must meet the requirements of ACI-349-97 [11.1.1,] for adequate resistance to bending, shear, and bearing loads.

K.4 ASSUMPTIONS

K.4.1 Concrete slab structural design is based on the Ultimate Strength Method. Cracked sections are conservatively assumed in the computation of section ultimate moment capacity.

K.4.2 For structural integrity calculations, the minimum subgrade modulus is used for the calculation of slab resultants.

K.4.3 The dead load from the concrete directly under the cask contact patch is assumed to provide a pressure to the pad surface that adds to the bending moment directly under the load patch. This is conservative.

K.5.0 INPUT DATA

K.5.1 Pad Geometry, Concrete and Reinforcement Properties

Thickness of reinforced concrete $h := 54 \cdot \text{in}$ Table 4.1 in Section 4

Reinforced concrete properties $f_c := 4000 \cdot \text{psi}$ Table 4.1 $v_c := .16$

Reinforcement #11 bars, 2 way, top and bottom, with 3" cover
(for calculation purposes), spaced at 8"

The reinforcement bar diameter, the cover depth, the width of the concrete section used for property calculations, and the bar spacing, respectively, are

$d_{\text{bar}} := 1.41 \cdot \text{in}$ $d_c := 3 \cdot \text{in}$ $b := 12 \cdot \text{in}$ $sp := 8 \cdot \text{in}$

Note: b is defined as 1', sp is spacing.

Yield strength and Young's Modulus of Reinforcement

$\sigma_y := 60000 \cdot \text{psi}$ $E_s := 29 \cdot 10^6 \cdot \text{psi}$

reinforcement
area in width b

$$A_r := \pi \cdot \frac{d_{\text{bar}}^2}{4} \cdot \frac{b}{sp} \quad A_r = 2.342 \cdot \text{in}^2$$

K.5.2 Engineered Subgrade Properties

The following minimum foundation subgrade modulus k_{sr} , at the slab/subgrade interface, is defined in Table 4.1.

$$k_{sr} := 200 \cdot \frac{\text{lbf}}{\text{in}^3}$$

K.5.3 Cask Weight and Contact Circle Diameter (with the pad) from [11.2.3]

$$Wt_{star} := 250000 \cdot \text{lbf}$$

$$D_{star} := 83.25 \cdot \text{in}$$

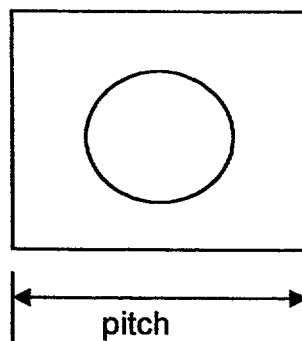
K.5.5 Seismic Loading

Dynamic analysis results from Section 10 are used for this load combination. Appropriate values are input as needed throughout the calculations.

K.5.6 Pad Layout and Cask Spacing

A schematic of the layout is shown below for one cask and its surrounding pad (one pitch in each direction) The pitch between casks is assumed:

Pad Concrete (per cask)



$$\text{pitch} := 12 \cdot \text{ft}$$

The weight of the concrete underneath the cask is computed based on a concrete weight density

$$\gamma_c := 150 \cdot \frac{\text{lbf}}{\text{ft}^3} \quad h = 4.5 \text{ ft}$$

$$\text{Wt}_{\text{conc}} := \gamma_c \cdot \frac{\pi}{4} \cdot D_{\text{star}}^2 \cdot h \quad \text{Wt}_{\text{conc}} = 2.552 \cdot 10^4 \cdot \text{lbf}$$

K.6 COMPUTER CODES

Computer Codes used are listed in the References (Section K.11)

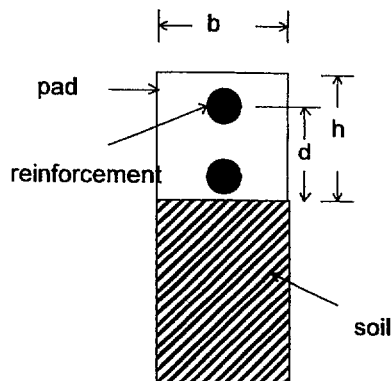
K.7 CALCULATIONS

K.7.1 Calculated Concrete Properties

K.7.1.1 Young's Modulus of Reinforced Concrete

Use the formulation from the ACI Code which gives concrete Young's Modulus in terms of specified concrete compressive strength.

$$E_c := 57000 \cdot \sqrt{f_c \cdot \text{psi}} \quad E_c = 3.605 \cdot 10^6 \cdot \text{psi} \quad [11.1.1]$$



The notation "soil" is generic and applies also to engineered fill. In the figure, h is the total pad depth, and d is the distance from the center of the reinforcement group to the opposite pad edge.

K.7.1.2 Ultimate Moment Capacity of Slab - Cracked Sections

The ultimate moment capacity is computed per the ACI Code; concrete is assumed to carry only compression with the reinforcing steel carrying only tension.

Consider the view of the slab with subgrade. with the cover depth and bar size specified, then:

$$d := h - d_c - d_{\text{bar}} \cdot 5 \quad d = 50.295 \cdot \text{in} \quad h - d = 3.705 \cdot \text{in}$$

Compute the quantity "a" defined below:

$$a := \sigma_y \cdot \frac{A_r}{.85 \cdot f_c \cdot b} \quad a = 3.444 \cdot \text{in}$$

$$a := \text{if}(a > h - d, a, h - d) \quad a = 3.705 \cdot \text{in}$$

The notation if(a>h.....) if the Mathcad built-in "If/Then/Else" function.

Compute the section ultimate moment capacity as defined in the ACI Concrete Code.

$$M_u := .9 \cdot \sigma_y \cdot (d - .5 \cdot a) \cdot A_r \quad M_u = 6.127 \cdot 10^6 \cdot \text{lbf} \cdot \text{in}$$

K.7.2 Slab Analysis Under Vertical Mechanical load

Two features are critical: (1) the reinforced slab must be thick enough to meet the requirements of punching shear. To check this, standard ACI Code formulas are used. (2) the reinforced slab must support the maximum bending moment created by the applied loading without exceeding the Code allowable bending moment for the section. The allowable bending moment is computed from a Code formula, while the actual moment due to the load on a circular load patch is computed from a formulation which includes the effect of the subgrade modulus. Two cases are considered which differ only in the size of the contact load patch and reflect the potential concentration of vertical reaction load near an edge of the cask due to the peak local loads from the clevis.

1. The load patch is that of the HI-STAR contact diameter

To check punching shear, follow ACI for 2-way slabs; define d_s , b_0 , and the allowable shear force V_{c1} , as

$$d_s := h - d_c - d_{\text{bar}}$$

$$b_0 := \pi \cdot (d_s + D_{\text{star}}) \quad V_{c1} := 4 \cdot \sqrt{\frac{f_c}{\text{psi}}} \cdot b_0 \cdot \frac{d_s}{\text{in}^2} \cdot \text{lbf}$$

$$V_{c1} = 5.236 \cdot 10^6 \cdot \text{lbf}$$

To evaluate the section bending moment under load, an analytical calculation, which uses direct stress formulas evolved from the theory of plates on elastic foundations, can also be used to determine the maximum section bending moment under mechanical loads. The solution is taken from [11.2.3]. The plate constant D , a parameter β , and the developed bending moment M_{c1} due to the uniform pressure load representing the cask contact region, are given

$$D := E_c \cdot \frac{h^3}{12 \cdot (1 - \nu_c^2)} \quad \beta := \left(\frac{1 \cdot k_{sr}}{D} \right)^{.25} \quad \beta = 8.012 \cdot 10^{-3} \cdot \text{in}^{-1}$$

$$\frac{1}{\beta} = 10.402 \text{ ft}$$

Then the pad bending moment under the load patch is

$$M_{c1} := (1 + \nu_c) \cdot \frac{Wt_{star} \cdot b}{4 \cdot \pi} \cdot \left(\ln \left(\frac{1}{\beta \cdot .5 \cdot D_{star}} \right) + .616 \right) \quad \text{Eq. 5.111 of [11.2.3]}$$

$$M_{c1} = 4.747 \cdot 10^5 \cdot \text{in} \cdot \text{lbf}$$

We now add a correction for larger contact patch per eq. 6.5 of [11.2.3]

$$M_{c1} := M_{c1} + \frac{.046}{6} \cdot Wt_{star} \cdot b \cdot (\beta \cdot .5 \cdot D_{star})^2 \cdot \frac{(1 + \nu_c)^{.5}}{(1 - \nu_c)^{.5}}$$

$$M_{c1} = 4.777 \cdot 10^5 \cdot \text{in} \cdot \text{lbf}$$

2. A reduced area is used as the bearing patch to reflect local loads applied at a clevis assembly or impact event. The loaded area is a reduced contact patch defined by a circular region of diameter D_{eff} where D_{eff} is a fraction of D_{star} . The reduced contact patch area is defined as the equivalent circular area at the top surface of the pad that has the same contact area as the rectangular clevis assembly after accounting for the spreading of the load through the clevis assembly baseplate (See Figures in Section 7). The contact patch area is computed as follows:

From Figure 7.4 in Section 7 of this report, the length and width of the two compression supporting elements of the clevis are

$$L_1 := 6 \cdot \text{in}$$

$$L_2 := 12.625 \cdot \text{in}$$

$$W := 6.5 \cdot \text{in}$$

The baseplate thickness is $T_{bp} := 1.25 \cdot \text{in}$

We assume that the load spreads out by a 45 degree angle through the baseplate so that the total effective compression contact patch area at the top surface of the slab is

$$\text{Area}_c := (W + 2 \cdot T_{bp}) \cdot [(L_1 + 2 \cdot T_{bp}) + (L_2 + 2 \cdot T_{bp})]$$

$$\text{Area}_c = 212.625 \cdot \text{in}^2$$

The effective circular contact patch diameter at this local location is

$$D_{\text{eff}} := \sqrt{\frac{4}{\pi} \cdot \text{Area}_c} \quad D_{\text{eff}} = 16.454 \cdot \text{in}$$

To check punching shear, follow ACI for 2-way slabs; define d_s , b_0 , and the allowable shear force V_{c1} , as

$$d_s := h - d_c - d_{\text{bar}}$$

$$b_0 := \pi \cdot (d_s + D_{\text{eff}}) \quad V_{c2} := 4 \cdot \sqrt{\frac{f_c}{\text{psi}}} \cdot b_0 \cdot \frac{d_s}{\text{in}^2} \cdot \text{lbf} \quad V_{c2} = 2.603 \cdot 10^6 \cdot \text{lbf}$$

Continuing, the analytical calculation, which uses direct stress formulas evolved from the theory of plates on elastic foundations, is again used to determine the maximum section bending moment in this case. The result is altered since the contact patch is smaller.

The pad bending moment under the load patch is

$$M_{c2} := (1 + \nu_c) \cdot \frac{Wt_{\text{star}} \cdot b}{4 \cdot \pi} \cdot \left(\ln \left(\frac{1}{\beta \cdot 5 \cdot D_{\text{eff}}} \right) + .616 \right)$$

$$M_{c2} := M_{c2} + \frac{.046}{6} \cdot Wt_{\text{star}} \cdot b \cdot (\beta \cdot 5 \cdot D_{\text{eff}})^2 \cdot \frac{(1 + \nu_c)^5}{(1 - \nu_c)^5}$$

$$M_{c2} = 9.238 \cdot 10^5 \cdot \text{in} \cdot \text{lbf}$$

Note that because of the reduced contact area, this result is greater than M_{c1} .

K.7.3 Evaluation of Load Combinations

K.7.3.1 Normal

K.7.3.1.1 Global Calculation

The formulas for moments have been derived in terms of the total weight of the loaded cask. Therefore, to form the load combinations, we define

$$AMP1 := \frac{Wt_{conc}}{Wt_{star}} \quad AMP1 = 0.102$$

$$M_{LC1} := AMP1 \cdot M_{c1} \cdot 1.4 + 1.7 \cdot M_{c1} \quad M_{LC1} = 8.804 \cdot 10^5 \cdot \text{in} \cdot \text{lbf}$$

$$r_{LC1} := \frac{M_u}{M_{LC1}} \quad r_{LC1} = 6.959 \quad > 1 \text{ OK}$$

The factored shear load for this load case is

$$FShear := Wt_{star} \cdot (1.7 + AMP1 \cdot 1.4) \quad FShear = 4.607 \cdot 10^5 \cdot \text{lbf}$$

$$r_{sLC1} := \frac{V_{c1}}{FShear} \quad r_{sLC1} = 11.364 \quad > 1$$

K.7.3.1.2 Local Calculation

We neglect the dead load of the concrete under the clevis for this calculation. We conservatively assume that the local load is computed based only on 8 of the available clevis assemblies.

$$AMP2 := 0.125$$

$$M_{LC2} := AMP2 \cdot M_{c2} \cdot 1.7 \quad M_{LC2} = 1.963 \cdot 10^5 \cdot \text{lbf} \cdot \text{in}$$

$$r_{LC2} := \frac{M_u}{M_{LC2}} \quad r_{LC2} = 31.21 \quad > 1 \text{ OK}$$

The calculated shear force for this load case is

$$FShear := Wt_{star} \cdot (AMP2 \cdot 1.7) \quad FShear = 5.312 \cdot 10^4 \cdot \text{lbf}$$

$$r_{s LC2} := \frac{V_{c2}}{F_{Shear}} \quad r_{s LC2} = 48.997 > 1$$

K.7.3.2 Accident

K.7.3.2.1 Global Calculation

The formulas for moments have been derived in terms of the total weight of the loaded cask. Therefore, to form the load combinations, we define amplifications based on the results from Section 10.1.1. The amplifier is defined as the peak vertical g reaction load from the dynamic analysis.

$$AMP1 := \frac{11.31 \cdot Wt_{star}}{Wt_{star}} \quad AMP1 = 11.31$$

$$M_{LC1} := AMP1 \cdot M_{c1} \quad M_{LC1} = 5.403 \cdot 10^6 \cdot \text{in} \cdot \text{lbf}$$

$$r_{LC1} := \frac{M_u}{M_{LC1}} \quad r_{LC1} = 1.134 > 1 \text{ OK}$$

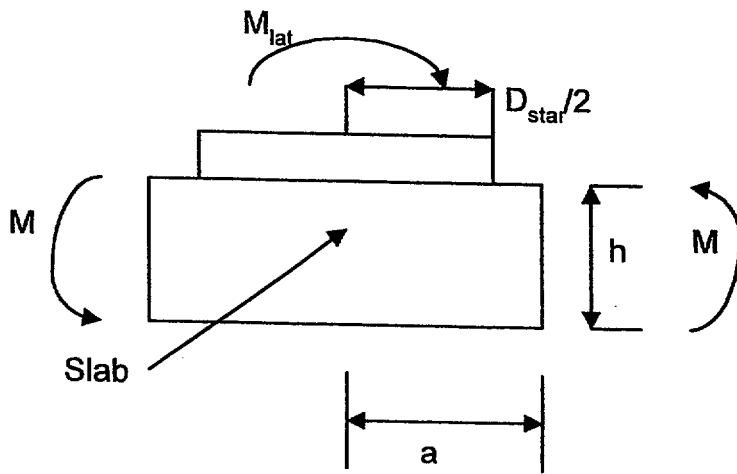
The calculation above does not consider the additional bending moment induced by the shear load acting at the surface of the slab. The computation of this bending moment is site dependent in that it depends on the frictional characteristics of the underlying foundation. Here, we provide a bounding computation that assumes the underlying foundation can support a shear load equal to the net horizontal surface load provided. Therefore, the surface shear load multiplied by the slab thickness is an additional moment that is resisted by slab bending

$$H := 3.06 \cdot 250000 \cdot \text{lbf} \quad h = 54 \cdot \text{in}$$

H is the net horizontal load computed as the peak horizontal acceleration computed from the dynamic analysis multiplied by the cask weight. Then the additional moment to be resisted by slab bending as a plate is

$$M_{lat} := H \cdot h \quad M_{lat} = 4.131 \cdot 10^7 \cdot \text{in} \cdot \text{lbf}$$

To estimate the additional moment in the slab, we consider the plate solution from [11.2.4] to apply. The figure below shows the configuration analyzed:



The figure represents a circular plate (thickness h and radius a) that is clamped at its outer extremity and subject to a specified moment over a radius equal to the contact diameter of the cask. For calculation purposes, we assume that a is 25% larger than the radius over which the moment is applied. Table 64 in the cited reference provides the maximum radial stress in the slab as a function of the geometry and loading.

From the table cited, the maximum radial stress in the slab is

$$a := .5 \cdot D_{star} \cdot 1.25 \quad a = 52.031 \cdot \text{in}$$

$$s_r := 82.26 \cdot \frac{h}{a} \cdot \frac{M_{lat}}{314 \cdot h^3} \quad s_r = 71.328 \cdot \text{psi}$$

The bending moment corresponding to this stress, over a circumferential length "b" is:

$$M := s_r \cdot \frac{b \cdot h^2}{6} \quad M = 4.16 \cdot 10^5 \cdot \text{in} \cdot \text{lbf}$$

The safety factor, adjusted to account for this additional moment is:

$$r_{LC1} := \frac{M_u}{M_{LC1} + M} \quad r_{LC1} = 1.053 > 1 \text{ OK}$$

The factored vertical shear load for this load case is

$$F_{\text{Shear}} := W_{t_{\text{star}}} \cdot (\text{AMP1}) \quad F_{\text{Shear}} = 2.828 \cdot 10^6 \cdot \text{lbf}$$

$$r_{\text{LC1}} := \frac{V_{c1}}{F_{\text{Shear}}} \quad r_{\text{LC1}} = 1.852 > 1$$

K.7.3.2.2 Local Calculation

We neglect the dead load of the concrete under the clevis for this calculation. We conservatively assume that the local load is computed based only on the peak clevis compression load from the dynamic analyses.

$$\text{AMP2} := \frac{577600 \cdot \text{lbf}}{W_{t_{\text{star}}}} \quad \text{AMP2} = 2.31 \quad \text{Table 10.2}$$

$$M_{\text{LC2}} := \text{AMP2} \cdot M_{c2} \quad M_{\text{LC2}} = 2.134 \cdot 10^6 \cdot \text{lbf} \cdot \text{in}$$

$$r_{\text{LC2}} := \frac{M_u}{M_{\text{LC2}}} \quad r_{\text{LC2}} = 2.871 > 1 \text{ OK}$$

This safety factor is also corrected for the effect of local surface shear in the same manner as performed for the global calculation.

Using the maximum local shear force on a clevis as reported in Section 11.1.1

$$H := 137200 \cdot \text{lbf}$$

H is the net horizontal load computed as the peak horizontal acceleration computed from the dynamic analysis multiplied by the cask weight. Then the additional moment to be resisted by slab bending as a plate is

$$M_{\text{lat}} := H \cdot h \quad M_{\text{lat}} = 7.409 \cdot 10^6 \cdot \text{in} \cdot \text{lbf}$$

From the table cited, the maximum radial stress in the slab is

$$a := .5 \cdot D_{\text{star}} \cdot 1.25 \quad a = 52.031 \cdot \text{in}$$

$$s_r := 82.26 \cdot \frac{h}{a} \cdot \frac{M_{\text{lat}}}{314 \cdot h^3} \quad s_r = 12.792 \cdot \text{psi}$$

The bending moment corresponding to this stress, averaged over a circumferential length "b" is:

$$M := s_r \cdot \frac{b \cdot h^2}{6} \quad M = 7.461 \cdot 10^4 \cdot \text{in} \cdot \text{lbf}$$

The safety factor, adjusted to account for this additional moment is:

$$r_{LC1} := \frac{M_u}{M_{LC1} + M} \quad r_{LC1} = 1.119 \quad > 1 \text{ OK}$$

The calculated shear force for this local load case is

$$F_{\text{Shear}} := W_{t_{\text{star}}} \cdot (\text{AMP2}) \quad F_{\text{Shear}} = 5.776 \cdot 10^5 \cdot \text{lbf}$$

$$r_{s_{LC2}} := \frac{V_{c2}}{F_{\text{Shear}}} \quad r_{s_{LC2}} = 4.506 \quad > 1$$

K.7.4 Slab and Soil Bearing Loads

K.7.4.1 Average Bearing Pressure at Subgrade Under Dead Load

First compute load due to pad weight, W_{conc} . The weight density of concrete is

$$W_{\text{conc}} := \gamma_c \cdot h \cdot \text{pitch}^2 \quad W_{\text{conc}} = 9.72 \cdot 10^4 \cdot \text{lbf}$$

Next compute the total average pressure due to the pad plus the cask

$$P_{\text{average}} := \frac{W_{t_{\text{star}}} + W_{\text{conc}}}{\text{pitch}^2} \quad P_{\text{average}} = 16.744 \cdot \text{psi}$$

The soil bearing strength must exceed the average bearing pressure in order to avoid long term creep under the pad.

K.7.4.2 Average Global Bearing Pressure Under Normal Conditions Under the Cask Using Factored Global Load and Constrained Concrete

$$P_{\text{if}} := \frac{1.7 \cdot W_{t_{\text{star}}}}{2 \cdot \left(\pi \cdot \frac{D_{\text{star}}^2}{4} \right)} \quad P_{\text{if}} = 39.039 \cdot \text{psi}$$

Note that we have computed the bearing pressure based on 2 times the pad area to reflect the constraint afforded by the adjacent concrete.

$$P_{allowc} := .7 \cdot .85 \cdot f_c \quad P_{allowc} = 2.38 \cdot 10^3 \cdot \text{psi} \quad [11.1.1, \text{Sec. 10.15}]$$

$$\frac{P_{allowc}}{P_{if}} = 60.965 \quad > 1 \text{ OK}$$

K.7.4.3 Average Global Bearing Pressure Under Accident Conditions Under the Cask Using Accident Load and Constrained Concrete

$$P_{if} := \frac{11.31 \cdot Wt_{star}}{16 \cdot \left(\pi \cdot \frac{D_{eff}^2}{4} \right)} \quad P_{if} = 831.127 \cdot \text{psi}$$

Note that we have computed the bearing pressure based on 2 times the pad area to reflect the constraint afforded by the adjacent concrete. We have conservatively considered only 8 clevis assemblies even though there are 16 compression blocks.

$$\frac{P_{allowc}}{P_{if}} = 2.864 \quad > 1 \text{ OK}$$

K.7.4.5 Average Local Concrete Bearing Pressure Under Accident Conditions Under One Clevis Assembly Using Accident Load and Constrained Concrete

$$AMP2 := \frac{577600 \cdot \text{lbf}}{Wt_{star}} \quad AMP2 = 2.31 \quad \text{Table 10.2}$$

$$P_{if} := \frac{AMP2 \cdot Wt_{star}}{2 \cdot \left(\pi \cdot \frac{D_{eff}^2}{4} \right)} \quad P_{if} = 1.358 \cdot 10^3 \cdot \text{psi}$$

$$\frac{P_{allowc}}{P_{if}} = 1.752 \quad > 1 \text{ OK}$$

Note that we have computed the bearing pressure based on 2 times the pad area to reflect the constraint afforded by the adjacent concrete.

K.7.4.5 Average Soil Bearing Pressure Under Accident Conditions at the Bottom Surface of the ISFSI Pad

Here we estimate the soil pressure at the interface with the concrete under accident conditions. For this calculation, we assume that the average compressive load includes the amplified load from the cask (which includes the cask dead load) plus twice the dead load of the pad associated with the cask.

$$P_{if} := \frac{(11.31 \cdot W_{t \text{ star}} + 2 \cdot W_{\text{conc}})}{1 \cdot (\text{pitch}^2)} \quad P_{if} = 2.099 \cdot 10^4 \cdot \frac{\text{lbf}}{\text{ft}^2}$$

K.8 COMPUTER FILES

This Mathcad created document is archived on server directory \projects\971178\ais\hi982004. No other files are used for this document.

K.9 RESULTS

All results obtained during the course of the analyses are contained within Section 7.0. No additional evaluations are required to demonstrate that the acceptance requirements are satisfied.

K.10 CONCLUSIONS

K.10.1 An acceptable slab thickness and reinforcement pattern is:

Slab thickness = $h = 4.5 \text{ ft}$

Reinforcement #11 bars top and bottom @ 8"; 3" cover for bottom reinforcement, 2" cover for top reinforcement.

K.10.2 All load combination limits are met as required by the ACI Reinforced Concrete design codes.

K.10.3 Concrete Bearing pressure limits are satisfied.

K.10.4 The minimum subgrade modulus of 200 pci is acceptable.

K.11 REFERENCES

K.11.1 Governing Documents

11.1.1 ACI-349-97, Code for Nuclear Safety Related Concrete Structures, American Concrete Institute, 1997.

K.11.2 Other Documents

11.2.1 Designing Floor Slabs on Grade, B.C. Ringo and R.B. Anderson, The Aberdeen Group, Addison Ill., 1992.

11.2.2 HI-941184, HI-STAR 100 TSAR, Rev. 7, submitted to USNRC, Nov., 1997.

11.2.3 Foundation Analysis, R.F. Scott, Prentice Hall, 1981, p.157.

11.2.4 Theory of Plates and Shells, Timoshenko and Woinowsky-Krieger, McGraw-Hill, 2nd Edition, 1959, Section 63.

K.11.3 Applicable Computer Codes

11.3.1 MATHCAD 7.0, Mathsoft, Inc., 1997.

The computer environment where these codes are applied is Windows 95 using a Pentium Processor

APPENDIX L - STRUCTURAL EVALUATION OF ISFSI SLAB SUPPORTING HI-STORM 100 CASK

L.1 INTRODUCTION

The ISFSI concrete pad structural design is considered herein. The objective of the analysis is to demonstrate that the specified minimum pad thickness, reinforcement, and slab subgrade modulus in Table 4.1 of Section 4 of this report are sufficient to structurally qualify the pad under appropriate load combinations from Section 6.2. The cask seismic loading on the ISFSI is taken from Table 10.6 of this report.

L.2 METHODOLOGY AND LOAD COMBINATIONS

L.2.1 Methodology

The design approach is to assume a concrete pad thickness with appropriate reinforcement and minimal support from the engineered fill, and demonstrate that the appropriate safety factors or safety margins are maintained for all static and dynamic loadings. Calculation methodologies used are based on charts, formulas, empirical results from various documents on the subject matter, and analytical or numerical solutions.

L.2.2 Load Combinations

Bounding Load Combinations are taken from Section 6.2 of this report.

Normal Events

$$U_c > 1.4D + 1.7(L)$$

Off-Normal Events

$$U_c > 1.05D + 1.275(L+F)$$

Accident-Level Events

$$U_c > D+L+E$$

From Section 11.4, we need not consider the Off-Normal event since the hydrological pressure and debris loads are appropriately limited (see Appendix J) to insure that if the slab is structurally adequate to support the Accident Level loads, then it is automatically adequate to support the Off-Normal level loads.

L.3 ACCEPTANCE REQUIREMENTS

The slab must meet the requirements of ACI-349-97 [11.1.1,] for adequate resistance to bending, shear, and bearing loads.

L.4 ASSUMPTIONS

L.4.1 Concrete slab structural design is based on the Ultimate Strength Method. Cracked sections are conservatively assumed in the computation of section ultimate moment capacity.

L.4.2 For structural integrity calculations, the minimum subgrade modulus is used for the calculation of slab resultants.

L.4.3 The dead load from the concrete directly under the cask contact patch is assumed to provide a pressure to the pad surface that adds to the bending moment directly under the load patch. This is conservative.

L.5.0 INPUT DATA

L.5.1 Pad Geometry, Concrete and Reinforcement Properties

Thickness of reinforced concrete $h := 54 \cdot \text{in}$ Table 4.1 in Section 4

Reinforced concrete properties $f_c := 4000 \cdot \text{psi}$ Table 4.1

$$v_c := .16$$

Reinforcement #11 bars, 2 way, top and bottom, with 3" cover (for calculation purposes), spaced at 8".

The reinforcement bar diameter, the cover depth, the width of the concrete section used for property calculations, and the bar spacing, respectively, are

$$d_{\text{bar}} := 1.41 \cdot \text{in} \quad d_c := 3 \cdot \text{in} \quad b := 12 \cdot \text{in} \quad \text{sp} := 8 \cdot \text{in}$$

Note: b is defined as 1', sp is spacing.

Yield strength and Young's Modulus of Reinforcement

$$\sigma_y := 60000 \cdot \text{psi} \quad E_s := 29 \cdot 10^6 \cdot \text{psi}$$

reinforcement
area in width b

$$A_r := \pi \cdot \frac{d_{\text{bar}}^2}{4} \cdot \frac{b}{\text{sp}} \quad A_r = 2.342 \cdot \text{in}^2$$

L.5.2 Engineered Subgrade Properties

The following minimum foundation subgrade modulus k_{sr} , at the slab/subgrade interface, is defined in Table 4.1.

$$k_{sr} := 200 \cdot \frac{\text{lb}}{\text{in}^3}$$

L.5.3 Cask Weight and Contact Circle Diameter (with the pad) from [11.2.3]

$$Wt_{\text{storm}} := 360000 \cdot \text{lb} \quad D_{\text{storm}} := 132.5 \cdot \text{in}$$

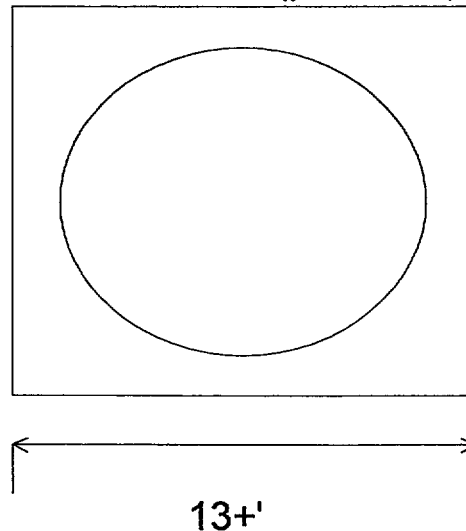
L.5.5 Seismic Loading

Dynamic analysis results from Section 10 are used for this load combination. Appropriate values are input as needed throughout the calculations.

L.5.6 Pad Layout and Cask Spacing

A schematic of the layout is shown below for one cask and its surrounding pad (one pitch in each direction) The pitch between casks is assumed:

Pad Concrete (per cask)



$$\text{pitch} := 2 \cdot \text{ft} + D_{\text{storm}}$$

$$\text{pitch} = 13.042 \text{ ft}$$

$$d := h - d_c - d_{\text{bar}} \cdot 5 \quad d = 50.295 \cdot \text{in} \quad h - d = 3.705 \cdot \text{in}$$

Compute the quantity "a" defined below:

$$a := \sigma_y \cdot \frac{A_r}{.85 \cdot f_c \cdot b} \quad a = 3.444 \cdot \text{in}$$

$$a := \text{if}(a > h - d, a, h - d) \quad a = 3.705 \cdot \text{in}$$

The notation $\text{if}(a > h \dots)$ is the Mathcad built-in "If/Then/Else" function.

Compute the section ultimate moment capacity as defined in the ACI Concrete Code.

$$M_u := .9 \cdot \sigma_y \cdot (d - .5 \cdot a) \cdot A_r \quad M_u = 6.127 \cdot 10^6 \cdot \text{lbf} \cdot \text{in}$$

L.7.2 Slab Analysis Under Vertical Mechanical load

Two features are critical: (1) the reinforced slab must be thick enough to meet the requirements of punching shear. To check this, standard ACI Code formulas are used. (2) the reinforced slab must support the maximum bending moment created by the applied loading without exceeding the Code allowable bending moment for the section. The allowable bending moment is computed from a Code formula, while the actual moment due to the load on a circular load patch is computed from a formulation which includes the effect of the subgrade modulus. Two cases are considered which differ only in the size of the contact load patch and reflect the potential concentration of vertical reaction load near an edge of the cask due to the peak local loads from the clevis.

1. The load patch is that of the HI-STORM contact diameter

To check punching shear, follow ACI for 2-way slabs; define d_s , b_0 , and the allowable shear force V_{c1} , as

$$d_s := h - d_c - d_{\text{bar}}$$

$$b_0 := \pi \cdot (d_s + D_{\text{storm}}) \quad V_{c1} := 4 \cdot \sqrt{\frac{f_c}{\text{psi}}} \cdot b_0 \cdot \frac{d_s}{\text{in}^2} \cdot \text{lbf}$$

$$V_{c1} = 7.177 \cdot 10^6 \cdot \text{lbf}$$

To evaluate the section bending moment under load, an analytical calculation, which uses direct stress formulas evolved from the theory of plates on elastic foundations, can also be used to determine the maximum section bending moment under mechanical loads. The solution is taken from [11.2.3]. The plate constant D , a parameter β , and the developed bending moment M_{c1} due to the uniform pressure load representing the cask contact region, are given

$$D := E_c \cdot \frac{h^3}{12 \cdot (1 - \nu_c^2)} \quad \beta := \left(\frac{1 \cdot k_{sr}}{D} \right)^{.25} \quad \beta = 8.012 \cdot 10^{-3} \cdot \text{in}^{-1}$$

$$\frac{1}{\beta} = 10.402 \text{ ft}$$

Then the pad bending moment under the load patch is

$$M_{c1} := (1 + \nu_c) \cdot \frac{Wt_{\text{storm}} \cdot b}{4 \cdot \pi} \cdot \left(\ln \left(\frac{1}{\beta \cdot 5 \cdot D_{\text{storm}}} \right) + .616 \right) \quad \text{Eq. 5.111 of [11.2.3]}$$

$$M_{c1} = 4.982 \cdot 10^5 \cdot \text{in} \cdot \text{lbf}$$

We now add a correction for larger contact patch per eq. 6.5 of [11.2.3]

$$M_{c1} := M_{c1} + \frac{.046}{6} \cdot Wt_{\text{storm}} \cdot b \cdot (\beta \cdot 5 \cdot D_{\text{storm}})^2 \cdot \frac{(1 + \nu_c)^{.5}}{(1 - \nu_c)^{.5}}$$

$$M_{c1} = 5.092 \cdot 10^5 \cdot \text{in} \cdot \text{lbf}$$

2. A reduced area is used as the bearing patch to reflect local loads applied at a sector lug. The loaded area is a reduced contact patch defined by a circular region of diameter D_{eff} where D_{eff} is a fraction of D_{storm} . The reduced contact patch area is defined as the equivalent circular area at the top surface of the pad that has the same contact area as the rectangular sector lug after accounting for the spreading of the load through the clevis assembly baseplate (See Figures in Section 8). The contact patch area is computed as follows:

From Figure 8.3 in Section 8 of this report, the length and width of a sector lug is

$$L_1 := 70.75 \cdot \text{in} \cdot \pi \cdot \frac{25}{180}$$

$$L_1 = 30.871 \cdot \text{in}$$

$$W := 7 \cdot \text{in}$$

The baseplate thickness is $T_{bp} := 1.25 \cdot \text{in}$

$$\text{Area}_c := (W) \cdot (L_1)$$

$$\text{Area}_c = 216.094 \cdot \text{in}^2$$

The effective circular contact patch diameter at this local location is

$$D_{\text{eff}} := \sqrt{\frac{4}{\pi} \cdot \text{Area}_c} \quad D_{\text{eff}} = 16.587 \cdot \text{in}$$

To check punching shear, follow ACI for 2-way slabs; define d_s , b_0 , and the allowable shear force V_{c1} , as

$$d_s := h - d_c - d_{\text{bar}}$$

$$b_0 := \pi \cdot (d_s + D_{\text{eff}}) \quad V_{c2} := 4 \cdot \sqrt{\frac{f_c}{\text{psi}}} \cdot b_0 \cdot \frac{d_s}{\text{in}^2} \cdot \text{lbf}$$

$$V_{c2} = 2.608 \cdot 10^6 \cdot \text{lbf}$$

Continuing, the analytical calculation, which uses direct stress formulas evolved from the theory of plates on elastic foundations, is again used to determine the maximum section bending moment in this case. The result is altered since the contact patch is smaller.

The pad bending moment under the load patch is

$$M_{c2} := (1 + \nu_c) \cdot \frac{Wt_{\text{storm}} \cdot b}{4 \cdot \pi} \cdot \left(\ln \left(\frac{1}{\beta \cdot 5 \cdot D_{\text{eff}}} \right) + .616 \right)$$

$$M_{c2} := M_{c2} + \frac{.046}{6} \cdot Wt_{\text{storm}} \cdot b \cdot (\beta \cdot 5 \cdot D_{\text{eff}})^2 \cdot \frac{(1 + \nu_c)^{.5}}{(1 - \nu_c)^{.5}}$$

$$M_{c2} = 1.327 \cdot 10^6 \cdot \text{in} \cdot \text{lbf}$$

Note that because of the reduced contact area, this result is greater than M_{c1} .

L.7.3 Evaluation of Load Combinations

L.7.3.1 Normal

L.7.3.1.1 Global Calculation

The formulas for moments have been derived in terms of the total weight of the loaded cask. Therefore, to form the load combinations, we define

$$AMP1 := \frac{Wt_{conc}}{Wt_{storm}} \quad AMP1 = 0.18$$

$$M_{LC1} := AMP1 \cdot M_{c1} \cdot 1.4 + 1.7 \cdot M_{c1} \quad M_{LC1} = 9.937 \cdot 10^5 \cdot \text{in} \cdot \text{lbf}$$

$$r_{LC1} := \frac{M_u}{M_{LC1}} \quad r_{LC1} = 6.166 > 1 \text{ OK}$$

The factored shear load for this load case is

$$F_{Shear} := Wt_{storm} \cdot (1.7 + AMP1 \cdot 1.4) \quad F_{Shear} = 7.025 \cdot 10^5 \cdot \text{lbf}$$

$$r_{sLC1} := \frac{V_{c1}}{F_{Shear}} \quad r_{sLC1} = 10.216 > 1$$

L.7.3.1.2 Local Calculation

We neglect the dead load of the concrete under the clevis for this calculation. We conservatively assume that the local load is computed based only on 4 of the sector lugs.

$$AMP2 := 0.25 \quad M_{LC2} := AMP2 \cdot M_{c2} \cdot 1.7 \quad M_{LC2} = 5.64 \cdot 10^5 \cdot \text{lbf} \cdot \text{in}$$

$$r_{LC2} := \frac{M_u}{M_{LC2}} \quad r_{LC2} = 10.863 > 1 \text{ OK}$$

The calculated shear force for this load case is

$$F_{Shear} := Wt_{storm} \cdot (AMP2 \cdot 1.7) \quad F_{Shear} = 1.53 \cdot 10^5 \cdot \text{lbf}$$

$$r_{s\ LC2} := \frac{V_{c2}}{F_{Shear}} \quad r_{s\ LC2} = 17.047 > 1$$

Note that even if we assume compression only through the sector lugs, the safety factors are much greater than 1.0.

L.7.3.2 Accident

L.7.3.2.1 Global Calculation

The formulas for moments have been derived in terms of the total weight of the loaded cask. Therefore, to form the load combinations, we define amplifications based on the results from Section 10.1.1. The amplifier is defined as the peak vertical g reaction load from the dynamic analysis.

$$AMP1 := \frac{6.51 \cdot Wt_{storm}}{Wt_{storm}} \quad AMP1 = 6.51$$

$$M_{LC1} := AMP1 \cdot M_{c1} \quad M_{LC1} = 3.315 \cdot 10^6 \cdot \text{in} \cdot \text{lbf}$$

$$r_{LC1} := \frac{M_u}{M_{LC1}} \quad r_{LC1} = 1.848 > 1 \text{ OK}$$

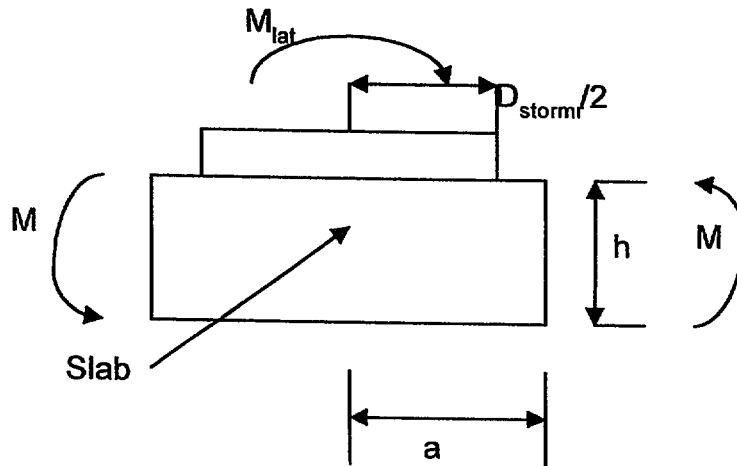
The calculation above does not consider the additional bending moment induced by the shear load acting at the surface of the slab. The computation of this bending moment is site dependent in that it depends on the frictional characteristics of the underlying foundation. Here, we provide a bounding computation that assumes the underlying foundation can support a shear load equal to the net horizontal surface load provided. Therefore, the surface shear load multiplied by the slab thickness is an additional moment that is resisted by slab bending

$$H := 2.58 \cdot 360000 \cdot \text{lbf} \quad h = 54 \cdot \text{in}$$

H is the net horizontal load computed as the peak horizontal acceleration computed from the dynamic analysis multiplied by the cask weight. Then the additional moment to be resisted by slab bending as a plate is

$$M_{lat} := H \cdot h \quad M_{lat} = 5.016 \cdot 10^7 \cdot \text{in} \cdot \text{lbf}$$

To estimate the additional moment in the slab, we consider the plate solution from [11.2.4] to apply. The figure below shows the configuration analyzed:



The figure represents a circular plate (thickness h and radius a) that is clamped at its outer extremity and subject to a specified moment over a radius equal to the contact diameter of the cask. For calculation purposes, we assume that a is 25% larger than the radius over which the moment is applied. Table 64 in the cited reference provides the maximum radial stress in the slab as a function of the geometry and loading.

From the table cited, the maximum radial stress in the slab is

$$a := .5 \cdot D_{storm} \cdot 1.25 \quad a = 82.812 \cdot \text{in}$$

$$s_r := 82.26 \cdot \frac{h}{a} \cdot \frac{M_{lat}}{314 \cdot h^3} \quad s_r = 54.412 \cdot \text{psi}$$

The bending moment corresponding to this stress, over a circumferential length "b" is:

$$M := s_r \cdot \frac{b \cdot h^2}{6} \quad M = 3.173 \cdot 10^5 \cdot \text{in} \cdot \text{lbf}$$

The safety factor, adjusted to account for this additional moment is:

$$r_{LC1} := \frac{M_u}{M_{LC1} + M} \quad r_{LC1} = 1.687 \quad > 1 \text{ OK}$$

The factored vertical shear load for this load case is

$$F_{\text{Shear}} := Wt_{\text{storm}} \cdot (\text{AMP1}) \quad F_{\text{Shear}} = 2.344 \cdot 10^6 \cdot \text{lbf}$$

$$r_{sLC1} := \frac{V_{c1}}{F_{\text{Shear}}} \quad r_{sLC1} = 3.062 \quad > 1$$

L.7.3.2.2 Local Calculation

We neglect the dead load of the concrete under the sector lug for this calculation. We first assume that the local load is computed based on the peak sector lug tension load from the dynamic analyses.

$$\text{AMP2} := \frac{2.355300 \cdot \text{lbf}}{Wt_{\text{storm}}} \quad \text{AMP2} = 1.974 \quad \text{Table 10.6}$$

$$M_{LC2} := \text{AMP2} \cdot M_{c2} \quad M_{LC2} = 2.619 \cdot 10^6 \cdot \text{lbf} \cdot \text{in}$$

$$r_{LC2} := \frac{M_u}{M_{LC2}} \quad r_{LC2} = 2.339 \quad > 1 \text{ OK}$$

This safety factor is also corrected for the effect of local surface shear in the same manner as performed for the global calculation.

Using the maximum local shear force on a clevis as reported in Appendix H (use the net shear from a single bolt x 5 bolts per sector lug):

$$H := 5.52070 \cdot \text{lbf}$$

H is the net horizontal load computed as the peak horizontal acceleration computed from the dynamic analysis multiplied by the cask weight. Then the additional moment to be resisted by slab bending as a plate is

$$M_{\text{lat}} := H \cdot h \quad M_{\text{lat}} = 1.406 \cdot 10^7 \cdot \text{in} \cdot \text{lbf}$$

From the table cited, the maximum radial stress in the slab is

$$a := .5 \cdot D_{\text{storm}} \cdot 1.25 \quad a = 82.812 \cdot \text{in}$$

$$s_r := 82.26 \cdot \frac{h}{a} \cdot \frac{M_{\text{lat}}}{314 \cdot h^3} \quad s_r = 15.252 \cdot \text{psi}$$

The bending moment corresponding to this stress, averaged over a circumferential length "b", is:

$$M := s_r \cdot \frac{b \cdot h^2}{6} \quad M = 8.895 \cdot 10^4 \cdot \text{in} \cdot \text{lbf}$$

The safety factor, adjusted to account for this additional moment is:

$$r_{\text{LC1}} := \frac{M_u}{M_{\text{LC1}} + M} \quad r_{\text{LC1}} = 1.8 \quad > 1 \text{ OK}$$

The calculated shear force for this local load case is

$$F_{\text{Shear}} := W_{\text{t storm}} \cdot (\text{AMP2}) \quad F_{\text{Shear}} = 7.106 \cdot 10^5 \cdot \text{lbf}$$

$$r_{\text{LC2}} := \frac{V_{\text{c2}}}{F_{\text{Shear}}} \quad r_{\text{LC2}} = 3.67 \quad > 1$$

L.7.4 Slab and Soil Bearing Loads

L.7.4.1 Average Bearing Pressure at Subgrade Under Dead Load

First compute load due to pad weight, W_{conc} . The weight density of concrete is

$$W_{\text{conc}} := \gamma_c \cdot h \cdot \text{pitch}^2 \quad W_{\text{conc}} = 1.148 \cdot 10^5 \cdot \text{lbf}$$

Next compute the total average pressure due to the pad plus the cask

$$P_{\text{average}} := \frac{W_{\text{t storm}} + W_{\text{conc}}}{\text{pitch}^2} \quad P_{\text{average}} = 19.386 \cdot \text{psi}$$

The soil allowable bearing pressure must exceed this value to insure against long term creep of the soil under the pad.

L.7.4.2 Average Global Bearing Pressure Under Normal Conditions Under the Cask Using Factored Global Load and Constrained Concrete

$$P_{if} := \frac{1.7 \cdot Wt_{storm}}{2 \cdot \left(\pi \cdot \frac{D_{storm}^2}{4} \right)} \quad P_{if} = 22.192 \cdot \text{psi}$$

Note that we have computed the bearing pressure based on 2 times the pad area to reflect the constraint afforded by the adjacent concrete.

$$P_{allowc} := .7 \cdot .85 \cdot f_c \quad P_{allowc} = 2.38 \cdot 10^3 \cdot \text{psi} \quad [11.1.1, \text{Sec. 10.15}]$$

$$\frac{P_{allowc}}{P_{if}} = 107.245 \quad > 1 \text{ OK}$$

L.7.4.3 Average Global Bearing Pressure Under Accident Conditions Under the Cask Using Accident Load and Constrained Concrete

$$P_{if} := \frac{6.51 \cdot Wt_{storm}}{2 \cdot \left(\pi \cdot \frac{D_{storm}^2}{4} \right)} \quad P_{if} = 84.983 \cdot \text{psi}$$

Note that we have computed the bearing pressure based on 2 times the pad area to reflect the constraint afforded by the adjacent concrete.

$$\frac{P_{allowc}}{P_{if}} = 28.006 \quad > 1 \text{ OK}$$

L.7.4.4 Average Local Bearing Pressure Under Accident Conditions Under a Clevis Assembly Using Accident Load and Constrained Concrete

$$AMP2 := \frac{110900 \cdot \text{lbf}}{Wt_{storm}} \quad AMP2 = 0.308 \quad \text{Table 10.6}$$

$$P_{if} := \frac{AMP2 \cdot Wt_{storm}}{2 \cdot \left(\pi \cdot \frac{D_{eff}^2}{4} \right)} \quad P_{if} = 256.601 \cdot \text{psi}$$

$$\frac{P_{allowc}}{P_{if}} = 9.275 > 1 \text{ OK}$$

L.7.4.5 Average Soil Bearing Pressure Under Accident Conditions at the Bottom Surface of the ISFSI Pad

Here we estimate the soil pressure at the interface with the concrete under accident conditions. For this calculation, we assume that the average compressive load includes the amplified load from the cask (which includes the cask dead load) plus twice the dead load of the pad associated with the cask.

$$P_{if} := \frac{(6.51 \cdot Wt_{storm} + 2 \cdot W_{conc})}{1 \cdot (\text{pitch}^2)} \quad P_{if} = 1.513 \cdot 10^4 \cdot \frac{\text{lb}}{\text{ft}^2}$$

L.8 COMPUTER FILES

This Mathcad created document is archived on server directory \projects\971178\ais\hi982004. No other files are used for this document.

L.9 RESULTS

All results obtained during the course of the analyses are contained within Section 7.0. No additional evaluations are required to demonstrate that the acceptance requirements are satisfied.

L.10 CONCLUSIONS

L.10.1 An acceptable slab thickness and reinforcement pattern is:

Slab thickness = $h = 4.5 \text{ ft}$

Reinforcement #11 bars top and bottom @ 8"; 3" cover for bottom reinforcement, 2" cover for top reinforcement.

L.10.2 All load combination limits are met as required by the ACI Reinforced Concrete design codes.

L.10.3 Concrete Bearing pressure limits are satisfied.

L.10.4 The minimum subgrade modulus of 200 pci is acceptable.

L.11 REFERENCES

L.11.1 Governing Documents

11.1.1 ACI-349-97, Code for Nuclear Safety Related Concrete Structures, American Concrete Institute, 1997.

L.11.2 Other Documents

11.2.1 Designing Floor Slabs on Grade, B.C. Ringo and R.B. Anderson, The Aberdeen Group, Addison Ill., 1992.

11.2.2 HI-951312, HI-STORM 100 TSAR, Rev. 4.

11.2.3 Foundation Analysis, R.F. Scott, Prentice Hall, 1981, p.157.

11.2.4 Theory of Plates and Shells, Timoshenko and Woinowsky-Krieger, McGraw-Hill, 2nd Edition, 1959, Section 63.

L.11.3 Applicable Computer Codes

11.3.1 MATHCAD 7.0, Mathsoft, Inc., 1997.

The computer environment where these codes are applied is Windows 95 using a Pentium Processor

APPENDIX M - Clevis-to-Baseplate Weld Qualification for HI-STAR 100 High Seismic Attachment

M.1 INTRODUCTION

This appendix provides the weld structural analysis for the connection between the Clevis Blocks and the Baseplate in the High Seismic Attachment Structure for HI-STAR 100. The results from these calculations are summarized in Section 11.

M.2 METHODOLOGY

The input loads are developed from the seismic analyses reported in Section 10 of this topical report. The load components on each clevis block segment form the input to the analysis with the weld geometry as specified in the Figures associated with Section 7 of this report. The maximum shear stress in the weld is computed and compared with the allowable shear stress permitted. The accident load combination is the only case considered since the welds are not structurally active under conditions of normal operation.

M.3 ACCEPTANCE CRITERIA

The maximum combined shear stress in the weld must not exceed 42 % of the ultimate strength of the weld material.

M.4 ASSUMPTIONS

M.4.1 Weld are treated as line elements in the calculation of section properties. This is standard engineering practice.

M.4.2 Compressive reactions from clevis-to-baseplate contact are neglected from the clevis f in the computation of resistance to bending moments. This is conservative.

M.4.3 Vertically oriented compression loads from the clevis pins are assumed to transfer directly by compression contact and do not load the welds.

M.5 INPUT DATA

Allowable weld shear stress (See Sub-section 11.1.4)

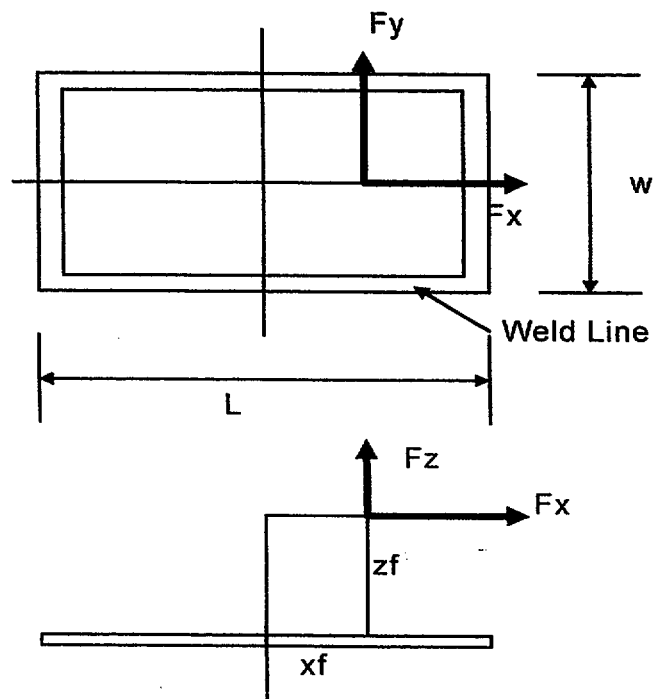
$$\tau_{all} := 29400\text{-psi}$$

Bounding Input Loads (see Table 10.2 in Sub-section 10.1.1)

Vertical Load (z direction)	FZ := 356300-lbf	Total loads from Clevis Stud
Radial Load (x direction)	FX := 99000-lbf	
Lateral Load (y direction)	FY := 99000-lbf	

Weld Geometry and Load Orientation

The following figure shows the loaded configuration for either portion of the clevis blocks. Dimensions are obtained from the Figures in Subsection 7 of this topical report.



From Figure 7.4, the following dimensions are given:

OUTBOARD CLEVIS BLOCK

$$L_o := 12.625 \cdot \text{in}$$

$$w_o := 6.5 \cdot \text{in}$$

$$t_{wo} := 0.75 \cdot \text{in}$$

INBOARD CLEVIS BLOCK

$$L_i := 6 \cdot \text{in}$$

$$w_i := 6.5 \cdot \text{in}$$

$$t_{wi} := 0.75 \cdot \text{in}$$

For the purpose of weld qualification, we apply the loads from the pin at the centerline of the pin and at the mid-length of the contact length between the clevis pin and the clevis hole. Therefore, the following load location points are assumed relative to the centroid of the weld region in each clevis block.

$$x_{fo} := .5 \cdot 5.5 \cdot \text{in}$$

$$x_{fi} := .5 \cdot L_i - 1 \cdot \text{in} \quad x_{fi} = 2 \cdot \text{in}$$

$$y_{f0} := 0 \cdot \text{in}$$

$$y_{f1} := 0 \cdot \text{in}$$

$$z_{f0} := 3.25 \cdot \text{in}$$

$$z_{f1} := 3.25 \cdot \text{in}$$

Calculations for Inboard Clevis Block

Compute the following weld section properties:

$$L_w := L_i + 2 \cdot 375 \cdot t_{wi}$$

$$L_w = 6.562 \cdot \text{in}$$

$$z_f := z_{f1}$$

$$x_f := x_{f1}$$

$$w_w := w_i + 2 \cdot 375 \cdot t_{wi}$$

$$w_w = 7.063 \cdot \text{in}$$

$$A_3 := 2 \cdot (L_w + w_w) \cdot 0.707 \cdot t_{wi}$$

$$A_3 = 14.449 \cdot \text{in}^2$$

$$I_{11} := \frac{L_w \cdot w_w^3}{12}$$

$$I_{11} = 192.648 \cdot \text{in}^4$$

$$I_{22} := \frac{w_w \cdot L_w^3}{12}$$

$$I_{22} = 166.336 \cdot \text{in}^4$$

$$A_{\text{internal}} := L_i \cdot w_i$$

$$A_{\text{internal}} = 39 \cdot \text{in}^2$$

The absolute values of the input loads to this clevis are

$$F_x := 0.5 \cdot F_X$$

$$F_x = 4.95 \cdot 10^4 \cdot \text{lbf}$$

$$F_y := F_x$$

$$F_z := 0.5 \cdot F_Z$$

$$F_z = 1.782 \cdot 10^5 \cdot \text{lbf}$$

Due to the offset of the loads from the centroid, the following moments develop:

$$M_x := F_y \cdot z_f$$

$$M_x = 1.609 \cdot 10^5 \cdot \text{in} \cdot \text{lbf}$$

$$M_{y1} := F_x \cdot z_f$$

$$M_{y1} = 1.609 \cdot 10^5 \cdot \text{in} \cdot \text{lbf}$$

$$M_{y2} := F_z \cdot x_f$$

$$M_{y2} = 3.563 \cdot 10^5 \cdot \text{in} \cdot \text{lbf}$$

$$M_z := F_y \cdot x_f$$

$$M_z = 9.9 \cdot 10^4 \cdot \text{in} \cdot \text{lbf}$$

The following stresses develop:

$$\sigma_1 := \frac{F_z}{A_3}$$

$$\sigma_1 = 1.233 \cdot 10^4 \cdot \text{psi}$$

$$\sigma_2 := \frac{M_x \cdot w_w}{2 \cdot I_{11}}$$

$$\sigma_2 = 2.949 \cdot 10^3 \cdot \text{psi}$$

$$\sigma_3 := \frac{(M_{y1} + M_{y2}) \cdot L_w}{2 \cdot I_{22}} \quad \sigma_3 = 1.02 \cdot 10^4 \text{ psi}$$

$$\tau_1 := \frac{F_x}{A_3} \quad \tau_1 = 3.426 \cdot 10^3 \text{ psi}$$

$$\tau_2 := \frac{F_y}{A_3} \quad \tau_2 = 3.426 \cdot 10^3 \text{ psi}$$

$$\tau_z := \frac{M_z}{2 \cdot A_{\text{internal}} \cdot t_{wi}} \quad \tau_z = 1.692 \cdot 10^3 \text{ psi}$$

The maximum shear stress at any point in the weld group is

$$\tau_{\text{max}} := \sqrt{(\sigma_1 + \sigma_2 + \sigma_3)^2 + (\tau_1 + \tau_z)^2 + (\tau_2 + \tau_z)^2}$$

$$\tau_{\text{max}} = 2.649 \cdot 10^4 \text{ psi} \quad SF_i := \frac{\tau_{\text{all}}}{\tau_{\text{max}}} \quad SF_i = 1.11$$

Calculations for Outboard Clevis Block

Compute the following weld section properties:

$$L_w := L_o + 2 \cdot 375 \cdot t_{wo} \quad L_w = 13.187 \text{ in} \quad z_f := z_{fo} \quad x_f := x_{fo}$$

$$w_w := w_o + 2 \cdot 375 \cdot t_{wo} \quad w_w = 7.063 \text{ in}$$

$$A_3 := 2 \cdot (L_w + w_w) \cdot 0.707 \cdot t_{wo} \quad A_3 = 21.475 \text{ in}^2$$

$$I_{11} := \frac{L_w \cdot w_w^3}{12} \quad I_{11} = 387.13 \text{ in}^4$$

$$I_{22} := \frac{w_w \cdot L_w^3}{12} \quad I_{22} = 1.35 \cdot 10^3 \text{ in}^4$$

$$A_{\text{internal}} := L_o \cdot w_o \quad A_{\text{internal}} = 82.062 \text{ in}^2$$

The absolute values of the input loads to this clevis are

$$F_x := 0.5 \cdot F_X \quad F_x = 4.95 \cdot 10^4 \text{ lbf}$$

$$F_y := F_x$$

$$F_z := 0.5 \cdot F_Z \quad F_z = 1.782 \cdot 10^5 \text{ lbf}$$

Due to the offset of the loads from the centroid, the following moments develop:

$$M_x := Fy \cdot zf \quad M_x = 1.609 \cdot 10^5 \text{ in} \cdot \text{lbf}$$

$$M_{y1} := Fx \cdot zf \quad M_{y1} = 1.609 \cdot 10^5 \text{ in} \cdot \text{lbf}$$

$$M_{y2} := Fz \cdot xf \quad M_{y2} = 4.899 \cdot 10^5 \text{ in} \cdot \text{lbf}$$

$$M_z := Fy \cdot xf \quad M_z = 1.361 \cdot 10^5 \text{ in} \cdot \text{lbf}$$

The following stresses develop:

$$\sigma_1 := \frac{Fz}{A_3} \quad \sigma_1 = 8.296 \cdot 10^3 \text{ psi}$$

$$\sigma_2 := \frac{M_x \cdot w_w}{2 \cdot I_{11}} \quad \sigma_2 = 1.467 \cdot 10^3 \text{ psi}$$

$$\sigma_3 := \frac{(M_{y1} + M_{y2}) \cdot L_w}{2 \cdot I_{22}} \quad \sigma_3 = 3.179 \cdot 10^3 \text{ psi}$$

$$\tau_1 := \frac{Fx}{A_3} \quad \tau_1 = 2.305 \cdot 10^3 \text{ psi}$$

$$\tau_2 := \frac{Fy}{A_3} \quad \tau_2 = 2.305 \cdot 10^3 \text{ psi}$$

$$\tau_z := \frac{M_z}{2 \cdot A_{\text{internal}} \cdot t_{wo}} \quad \tau_z = 1.106 \cdot 10^3 \text{ psi}$$

The maximum shear stress at any point in the weld group is

$$\tau_{\max} := \sqrt{(\sigma_1 + \sigma_2 + \sigma_3)^2 + (\tau_1 + \tau_z)^2 + (\tau_2 + \tau_z)^2}$$

$$\tau_{\max} = 1.381 \cdot 10^4 \text{ psi}$$

$$SF_o := \frac{\tau_{\text{all}}}{\tau_{\max}}$$

$$SF_o = 2.129$$